The Dissertation Committee for Theresa Helene Baumgartner Certifies that this is the approved version of the following dissertation:

Maximizing the Value of Information from Downhole High-Frequency Drilling Dynamics Data

Committee:

Eric van Oort, Supervisor

David Nicolas Espinoza

Masa Prodanovic

Sanjay Shakkottai

Ahmed H Tewfik

Carlos Torres-Verdin

Maximizing the Value of Information from High-Frequency Downhole Dynamics Data

by

Theresa Helene Baumgartner, B.S.; M.S.; M.S.

Dissertation

Presented to the Faculty of the Graduate School of

The University of Texas at Austin

in Partial Fulfillment

of the Requirements

for the Degree of

DOCTOR OF PHILOSOPHY

The University of Texas at Austin

May 2017

Dedication

Zwei Dinge sollten Kinder von ihren Eltern bekommen: Wurzeln und Flügel". Johann Wolfgang von Goethe.

Für meine Eltern, die mir Wurzeln und Flügel gegeben haben.

"There are only two lasting bequests we can hope to give our children. One of these is roots, the other, wings." Johann Wolfgang von Goethe.

To my parents, who gave me roots and wings.

Acknowledgements

I would like to express my appreciation and gratitude to my advisor, Dr. Eric van Oort. He strikes the right balance between providing guidance and freedom to pursue new or unorthodox ideas. His ability to make everyone believe in his visions - of drilling automation and beyond - has motivated me immensely over the past years.

I would especially like to thank Dr. Pradeep Ashok, who has given me a lot of support and important input. I am grateful for the interactions and the multi-facetted exchange of ideas with all my remarkable research colleagues.

During my internships, I learned, got inspired and stayed in touch with reality – they enabled me to do research that is aiming at solving real problems. I highly appreciate the various people in the industry that made it possible:

My work at NOV has sparked my interest in the topic of this work. NOV's supply of data and continuous collaboration were vital to my research. QRI has provided an immense learning experience and exposure during the course of two summer internships. I've never seen such a high density of intelligence and I appreciate the variety of characters in the company. I thank Shell and the people of Shell's drilling mechanics technology group for another superb internship opportunity.

I greatly appreciate the exchange of data and ideas with various companies, most notably ConocoPhillips, who have also financially supported my research.

Maximizing the Value of Information from High-Frequency Downhole Dynamics Data

Theresa Helene Baumgartner, PhD

The University of Texas at Austin, 2017

Supervisor: Eric van Oort

Downhole drilling dynamics are poorly understood. Neither models nor experiments seem capable of fully describing the movements and forces of the drillstring during drilling. Downhole measurements could potentially hold the key to those missing insights, however data is not yet used to its full potential. This work addresses the barriers to obtaining value from downhole dynamics data and offers solutions to overcome them.

A novel kinematic model was developed that fully accounts for sensor position and measurement design. It supports the hypothesis that lateral vibrations cause high-frequency fluctuations of tangential accelerations. Hence, against currently prevailing scientific opinion, "high-frequency torsional oscillations" (HFTO) are not actually a torsional phenomenon, but the consequence of a lateral vibration. A downhole measurement tool under off-center rotation captures particular high-frequency data patterns that can be considered a sensor artifact. If ignored, these artifacts can impact the calculations of RPM and other derived measurements from downhole data.

An extensive set of downhole data was analyzed to improve downhole dynamics data collection schemes for detecting drilling dysfunctions. For each prominent type of dysfunction, minimum data collection frequencies are specified. Such guidelines assist in

collecting downhole data at sampling rates that are high enough to draw meaningful conclusions, but low enough to not flood limited available bandwidth and memory capacities. Even though a sensor is set up to measure only a single parameter along a single axis, it captures a variety of downhole events, which may lead to misinterpretations. These events can still be differentiated based on their typical frequency ranges. It is further shown how 'noisy' frequency ranges can be detected and selectively removed by combining multiple downhole measurements.

A lack of transparency and inefficient processes around sensor design, data collection, processing, and transfer cause misinterpretation and under-utilization of drilling downhole data. A review of tool design and sensor identifies sources of bad data quality. Eventually, defined data quality requirements will offer sustainable sensor data improvement. To work with downhole data generated under current circumstances, data processing techniques are developed and demonstrated. Algorithms that combine data, drilling processes, and physics automatically correct sensor errors. Further, a machine learning approach for automated vibration classification based on patterns is developed.

A standardized structure to transfer downhole data from the service provider to the end user is suggested. The structure does not only define *how* the data should be shared, but also *what* additional data (metadata) is required. Specifications of such informational requirements improve transparency and comparability of measurements. Therefore, the proposed data format is a prerequisite for automated drilling data analysis.

Table of Contents

List of Figures

Introduction

Drilling is a process that removes soil and rock to gain access to a subsurface target: usually a reservoir containing hydrocarbons in the form of oil or natural gas. The drilling process creates a wellbore that ensures a connection between the reservoir and the surface. In its simplest form, the well construction process requires a rotating bit that breaks the rock, a rotating mechanism, and a string that transfers weight and rotation from the surface to the bit. In addition, a drilling fluid in the wellbore counteracts the downhole pressure and transports rock cuttings to surface. In the early days, wells were drilled vertically in the ground. Since the 19th century, technology has evolved towards creating complex drilling paths, including horizontal drilling. Nowadays, wellbores can reach thousands of feet in length, take a variety of shapes and while still reaching narrowly defined targets. Much of this success can be attributed to novel downhole measurements during the drilling process (e.g. Belaskie et al., 1993; Schen et al., 2003; Raap et al., 2011; Trichel et al., 2016).

Drilling is governed by *uncertainties*. Unknown geological structures, rock properties and pressure regimes, and uncertainties about hydraulic as well as mechanical behavior of the interplay of the drillstring, rock and the formation make the well construction process vastly different from constructing cars, airplanes, or buildings. In addition, the downhole processes usually cannot be directly observed, but need to be indirectly inferred by simplified physical models or measurements. All of this limits our ability to establish clear cause and effect relationships between our actions and their impact on the entire system.

Wells can be drilled with different purposes. Some are drilled to discover new petroleum reservoirs (exploration wells), others are drilled to maximize the production in relatively well-known fields (development wells) (Mitchell and Miska, 2010). Most of the data used in this work was collected from development wells. For such wells, the objective is not only to optimize operational time and cost to drill the well; it is also to create a high-quality wellbore which ensures production over its entire active lifetime as well as integrity long after it has been shut-in.

Decisions in drilling cover a spectrum of timelines, from long-term strategies to adjustments within less than a second. A drilling engineer decides on a variety of design factors before drilling commences. Such design factors include the structure, shape, and path of the wellbore, as well as surface equipment, components of the drillstring or the type of drilling mud used. During operations, parameters such as the amount of weight on bit (WOB) or the speed of rotation (RPM, revolutions per minute) need to be adjusted at every point in time. In some cases, for instance managed pressure drilling (MPD)[1] or top drive torque[2], control systems are already available to automatically controlling real-time adjustments in milliseconds. All these decisions are based on estimates of a variety of uncertain parameters. In reality, until today, prior experience of the people in charge is probably the most important factor for decision making.

The research presented in this work is conducted on the premise of working towards *drilling automation*. Reducing human interactions through automation promises to not only improve the safety but also standardize and thus improve all processes of well construction.

[1] Managed pressure drilling (MPD) is a process where the pressure in a wellbore is controlled from surface using chokes.

[2] Top drive is a device that rotates the pipe at surface. Top drive torque is controlled to mitigate stick-slip, a form of torsional vibration of the drillstring, where usually uniform rotational speed becomes erratic.

Before drilling automation can be achieved, many prerequisites must be in place: automated processes are carried out by control systems, which are orchestrated by algorithms. However, these algorithms can only be developed after scrupulously defining procedures for every process at the rig (Jamieson et al., 2008). For many, drilling is still considered an art. Art does not follow physical principles nor equations. The first challenge in this multi-step chain of procedures followed by algorithms followed by controls is to "take the art out of drilling" and turn it into a more predictable science. One of the inevitable and favorable "side-effects" of making drilling more scientific are drilling performance improvements. Such *drilling optimization* aims at two areas: first, to make the right decisions in the planning phase, and second, to remove all waste (in time and/or cost) during operations.

In many other industries, physical relations are well established or experimental data has delivered meaningful insights. In drilling, the availability of *data* from surface and downhole is the basis for all drilling automation and optimization efforts. Downhole data traditionally has been immensely valuable for formation evaluation and wellbore positioning. The focus of this work is on *drilling dynamics data*, which concerns itself with the motions of the drilling system under the presence of forces. Such data offers a glimpse at the complex downhole environment and helps to define processes without solely relying on a human's possibly biased descriptions. Due to the potentially high risks and even higher consequences (i.e. well blow-outs) critical models need to be thoroughly tested with field data before they can be employed in enhanced systems. The need for accurate real-time measurement is currently driving the development of downhole sensor technology and higher bandwidth data transmission technologies, such as wired drillpipe (e.g. Ali et al., 2008).

Within the last years, exponential changes in processing power and data science provided a basis for *big data analytics*, which many industries are profiting from (e.g. Whitfield, 2017). Although large scale deployment of artificial intelligence (AI) in drilling has been predicted to be at the verge of breakthrough for many years, the barrier of entry in the drilling domain seems to be higher than elsewhere. While modern drilling rigs produce many gigabytes of data per well already, data is not yet used to its full potential. Many people working with drilling data may argue that there is no *big data* problem; instead, there is a *messy data* problem. A complicating factor is that tools, sensors, measurements, derived values, or data structures are still far from any standardization; such that data collected from one well does not compare to other wells. Oftentimes there is a complete lack of descriptive metadata to make sense out of the actual data. The type of tool and the process of data collection may be just as important as the data itself, but these factors are largely undocumented. Unplanned human actions can greatly impact measurements[3] and lead to invalid interpretations or bad data. Merging data science with an understanding of engineering and operations thus becomes essential to make sense of data. Since actions are still carried out by humans, it is important to bear in mind that any suggested solution is currently only as effective as the willingness of the driller or engineer to implement it.

OBJECTIVES

This work aims at improving the *value of information* of downhole data in the most effective way possible. On the one hand, this means solving problems of data interpretation. This is complicated by the fact that the drilling process cannot be visually inspected by an outside observer: sensors move together with the system that they are

[3] For instance, manually adding multiple barrels of water into a tank whose volume gets recorded.

measuring. On the other hand, it means developing strategies to systematically removing barriers for large scale data analytics and appropriately preparing drilling data for data scientists from outside this industry.

In a larger context, this research aimed towards facilitating automation and performance improvements in the well construction process. The vision is to develop drilling systems with automated diagnostics and even decision-making capabilities. Such systems will be beneficial in an environment where humans are either physically excluded from decision making (e.g. smart downhole control) or where computational systems will prove to outperform humans (e.g. parameter adjustments to optimize the drilling penetration rate). Data is an enabler of automation. To confidently make decisions and take actions, data fidelity and reliability that data needs to be established first. Thus, this research is improving the value of downhole data through the following objectives:

- Correct interpretation of downhole high-frequency data, i.e. providing an answer to the question: "What are the motions of the drillstring and sensors to produce the available measurements?"
- Differentiation between valuable signals and noise or sensor artifacts, i.e. the segregation of effects that are simultaneous contributors to a downhole measurement.
- Identification and removal of the technical root causes of bad data and data misinterpretations, by analyzing sensor design and operational errors.
- Optimization of the data collection process by defining sampling rate requirements, e.g. for efficiently detecting drilling dysfunction in the data.
- Development of effective data analysis methods with short term remedies for frequent data errors.

- Removing inefficiencies of data and knowledge transfer from service provider to end user by improving standardization and transparency.
- Sustainably creating an environment that enables automation in companies and equips equipping current students with a "digital mindset".

CONTRIBUTIONS

Drilling data analysis and automation applications are technological game changers in the drilling industry. The productivity of a single rig in the Bakken region is 8 times higher in 2017 than it was in 2007 for oil and more than 15 times higher for natural gas (EIA Drilling Productivity Report, 2017). Aside from fracking and horizontal drilling, part of this success can be attributed to improvements in surface and downhole measurements during drilling (e.g. Trichel et al., 2016). Despite these benefits, drilling data is not yet used to its full potential. *The contributions of this work are removing important barriers to drilling data analysis and automation applications.* Better utilization of data and sensors then ultimately leads to increases in the rate of penetration (ROP), tool life, reduced non-productive time (NPT), faster learning curves, etc. and helps delivering better quality wells saver and cheaper. Detailed contributions will be listed in Chapter 7.

OUTLINE

Chapter 1 will provide the reader with the technical basics of drilling process data collection and drilling dysfunctions that should be detected and mitigated. The background given in this chapter is essential to the other chapters.

Chapter 2 shows how a seemingly trivial off-center rotation of the drillstring can affect downhole measurements. Kinematic modeling using a tensor calculus approach is employed to simulate downhole acceleration data. It supports an alternative and simpler

explanation than the one currently prevailing in the drilling industry. This work initially has been published as a paper titled "*Pure and Coupled Drill String Vibration Pattern Recognition in High Frequency Downhole Data*" at the ATCE 2014 in Amsterdam, the Netherlands. Another paper titled "*Interpretation of High-Frequency Vibration Patterns using a Kinematic Model*" has been submitted to the *Journal of Petroleum Science and Engineering* and is currently under review.

To shed light on the limitations of data collection, storage and transfer, *Chapter 3* describes a data collection system that is optimized under downhole circumstances. Based on the analysis of collected field data, optimum sample rates per sensor are suggested. The analysis offers solutions for differentiating meaningful measurements from noise and sensor artifacts. The work in this chapter was presented at the 2015 ATCE in Houston, TX, with a paper titled "*Maximizing Drilling Sensor Value through Optimized Frequency Selection and Data Processing*".

Chapter 4 addresses data errors. Root causes of data errors and misinterpretations often lie in the sensors and the collection process. Therefore, downhole sensors, intricacies of tool designs, calibrations and sensor errors are described in the introduction of this chapter. This work is based on inputs from *Nii Ahele Nunoo* and *Alemzeb Khan*, both affiliated with *National Oilwell Varco (NOV)*, a manufacturer of downhole tools. A paper titled "*What is Wrong with my Drilling Data? Current State and Developments of Downhole Dynamics Measurement Tools*." will be submitted for a drilling conference. In addition, short term solutions for automated error correction and data processing are presented in this chapter. These methods have been developed and tested using field data provided by *ConocoPhillips* and *Hess*. This work titled "*Automated Downhole Drilling Data Correction and Cleaning Methodologies*" will be submitted as a conference paper.

Along the lines of the importance of sensor design, deployment and processing for a meaningful analysis, *Chapter 5* is an attempt at improving the transparency of data and sharing better information faster with data analysts. Therefore, a new memory data transfer standard has been developed and shared with the industry at the 2016 SPE IADC Drilling Conference in Fort Worth, TX. The paper "*Efficiently Transferring and Sharing Drilling Data from Downhole Sensors*." has been conducted in collaboration with *Yang "Alex" Zhou* at the University of Texas at Austin.

Chapter 6 summarizes the work, lists contributions, and identifies areas for future work.

Appendices A, B, C, and D complement the chapters. In addition, *Appendix E* then takes a broader perspective and examines how universities can prepare their engineering students for future data driven jobs. It describes the approaches and findings of helping groups of undergraduate students analyze "messy" drilling data. *Yang "Alex" Zhou* and *Gurtej Saini*, *Dr. Pradeepkumar Ashok*, at the University of Texas at Austin, and *Matt Isbell* affiliated with *Hess*, as well as many undergraduate students collaborated in the project. In addition, it describes some of the basic data curation and visualization processes that proceeded any in-depth analysis described in this work. A paper titled "*Future Workforce Education through Big Data Analysis for Drilling Optimization*" was presented at the 2017 SPE IADC Drilling Conference in The Hague, the Netherlands.

The chapters follow a sequence that gradually takes the reader from an in-depth mathematical topic, across engineering and process optimization, all the way to educational efforts. This range of topics is in line with the variety of necessary requirements to improve drilling data analysis.

Chapter 1: Background and Previous Work

1.1 DRILLING DYSFUNCTIONS

Drilling dysfunctions are unplanned and undesirable downhole circumstances during the well construction process. Dysfunctions may involve the mechanical system of drillstring, the hydraulics system, the rock formation, or a combination of these. Downhole sensors play a vital role in diagnosing dysfunctions, because some cannot be unambiguously detected from surface sensors alone, while others show critical latencies between downhole occurrence and surface detection. Oftentimes, models are used to infer downhole conditions based on simplified assumptions. Direct information from downhole sensors eliminates some of these uncertainties and latencies. The following section gives an overview of the most prominent dysfunctions and provides background information on drilling terminology.

Downhole sensors and data processing are beginning to provide novel solutions to old problems. In most cases, however, formal methodologies (e.g. how to extract key performance indicators from data, established thresholds for dysfunction measurements) have not been established yet. This chapter should help the reader understand how and in which areas this "drilling data revolution" will be potentially most valuable.

1.1.1 Drillstring Vibrations

Drillstring vibrations are undesired oscillating movements of the drillstring. They are the most rigorously studied and modeled downhole dynamics events. They are known to cause high-frequency dynamic responses and are of high priority for the analysis of downhole high-frequency data. In addition, these vibrations are frequent and persistent

drilling performance limiters. Severe levels of vibrations might lead to potential damage of downhole tools with costly unintended trips for the bit, while mild levels of vibrations can already significantly slow down drilling progress (Ertas et al., 2013). The occurrence of vibrations has been correlated with wellbores full of "twists and turns", i.e. wellbore tortuosity. Over the past 50 years, the drilling industry has used vibration models to represent downhole kinematics and dynamics to understand, detect and eventually mitigate them (Shor et al., 2014). Some of the models are used to control surface torque and RPM to mitigate low frequency torsional oscillations of the drillstring. These have shown considerable success and are currently widely implemented in drilling operations. Early models were often not capable of reproducing the complexities of real drilling dysfunctions, such as multiple vibrational modes acting together, the impact of unknown and constantly changing parameters such as formation properties, or the geometry of a flexible drillstring thousands of feet in length. More sophisticated finite element models are starting to take such complexities into account, but they often have the disadvantage of requiring significant calculation times. This limits their application in real-time, for instance when comparing modeled results with real-time high-frequency data. Vibrations have been detected in any part along the drillstring, from the bit to surface. The oscillations can be classified into three different basic types or modes: torsional, lateral, and axial.

Stick Slip

Stick-slip is a *torsional vibration* where the rotational speed varies periodically with time: in severe cases the bit can come to a complete stop, or even turn into the opposite direction, then ramp up in speed to several times the original rotational velocity, followed by a slow-down and another stop of rotation (**Fig. 1**).

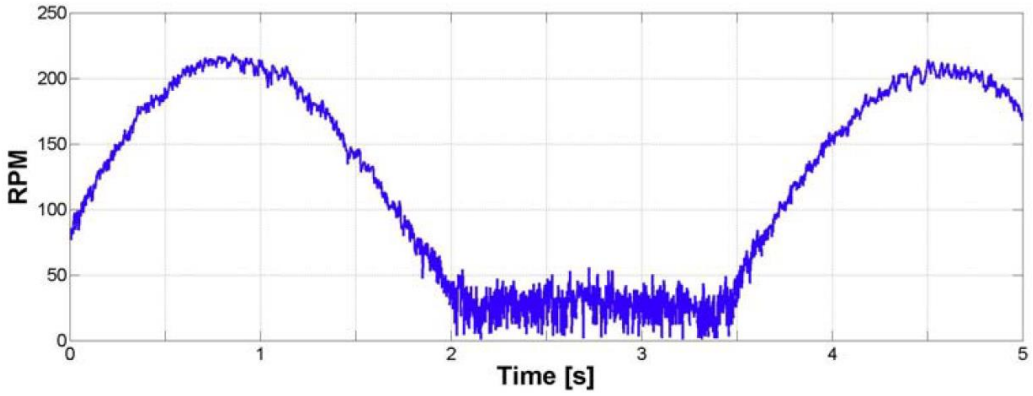

Fig. 1—Example of downhole stick slip vibration observation as reported by Ledgerwood et al. (2010): "Downhole rotary speed of typical stick-slip event in the research well."

The most common theory on the causes of stick-slip is that torsional strength of the string is too low to overcome high frictional forces between the cutters and the formation and/or stabilizers and the borehole wall. During the "stick" cycle, the bit stops rotating, despite constant RPM input from surface. The drillstring then winds up until enough torsional force is applied to overcome the frictional forces, resulting in the "slip" cycle. Another hypothesis on the causes of stick-slip vibrations focuses on the oscillatory pendulum effect. Laboratory experiments (e.g. Shor, 2016) have shown fluctuations in rotational speed even without frictional forces.

Stick-slip is a distinctly low-frequency phenomenon, with its period ranging from less than 1 to up to more than 20 seconds. In most cases, stick-slip can be detected from surface measurements, mainly from periodic fluctuations of the surface torque signal. A common mitigation action, following the theory of high friction, is to increase the revolutions per minute and decrease the weight on bit, to "reduce the depth of cut" and therefore the drag at the bit (Davis et al., 2012). In the late 1980s, companies like Shell and

NOV independently developed “soft torque” or “soft speed” rotary systems to mitigate torsional vibrations (Halsey et al., 1988; Runia et al., 2013). These are rotary drive control systems that adjust both torque and rotational speed to cancel out the first order vibrational mode of stick-slip. The original systems were developed for DC drilling drives using analog torque feedback. Due to changing control systems on modern drilling rig motors, these active stick-slip mitigation systems were no longer functioning properly. Currently the technology is revitalized and new algorithms are being developed (Harris et al., 2014). In addition, vibration simulations are now being integrated with real-time downhole measurements and add to the effectiveness and success of the control system.

Whirl

Whirl is a *lateral vibration*, where the rotational axis of the bit does not align with the center of the borehole, and the bit center performs additional rotations around the borehole. Brett et al. (1989) were one of the first to describe and show this phenomenon using both high-frequency downhole data and bottom-hole patterns. Just like a spirograph, the cutters leave patterns of hypotrochoid curves at the bottom of a hole. Equations for cutter positions during whirl and whirl angular speed show similarities to the parametric equations for a hypotrochoid. Whirl is a high-frequency phenomenon, with dominant frequencies in the range of 20 to 60 Hz, corresponding to the whirl angular speed, as shown in **Fig. 2**.

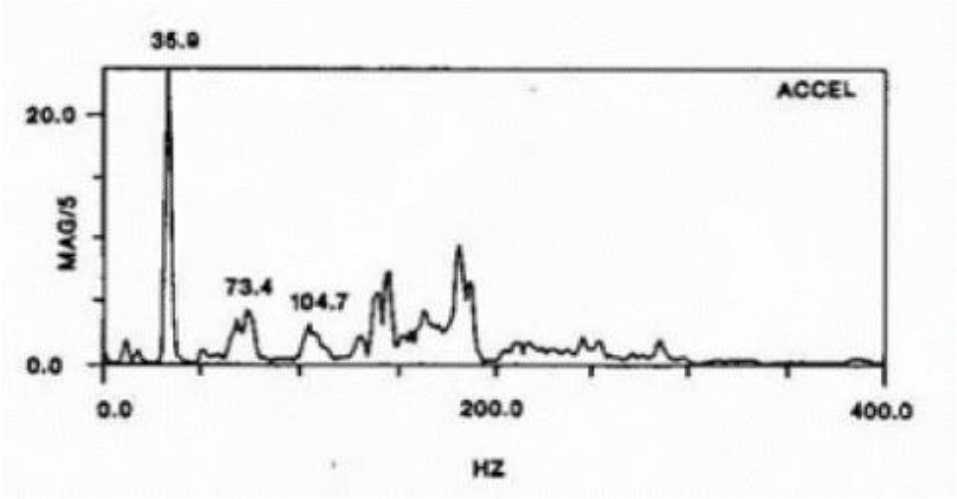

Fig. 2—Whirl frequency and high-frequency overtones as measured by Brett et al. (1989): "Typical lab frequency response of whirling bit."

Whirl can occur in two distinct forms: backward whirl (where the drillstring rotates clockwise and the center of the string rotates counter-clockwise around the borehole) and forward whirl, where both drillstring and drillstring center rotate clockwise but with different rotational speeds. Jansen (1992) also mentions chaotic whirl: a form of whirl where the drillstring center does not follow a particular direction, but moves in a random and highly unstable fashion. Whirl can hardly be directly measured from surface with data acquisition rates of 1 Hz or lower. In field practice, indirect methods are being used, such as the mechanical specific energy (MSE) approach, where the total energy input is compared with the rock penetration rate. If the same amount of energy input yields lower drilling progress, this could be indicative of losing energy to vibrations rather than rock-cutting action (Dupriest et al., 2005). If a severe case of whirl is detected, a typical field recommendation is as follows: "Stop drilling, take the bit off bottom and wait a few minutes until the whirling motion of the bit has terminated. Then resume drilling with higher weight on bit, to prevent the bit from moving once more into an eccentric position." Jogi et al.

(2002) link the occurrence of destructive whirl to excitements of resonance frequencies of the BHA (bottom hole assembly). Based on this theory, commercial software allows companies to test their BHA design against interference between natural frequencies of the BHA and input RPM values. The software then recommends the avoidance of certain ranges of surface rotational speeds during drilling.

Bit Bounce

Bit bounce is an axial vibration that is excited through bit-rock interaction, and are particularly prevalent when using tri-cone bits. The rise of preferential application of PDC (polycrystalline diamond compact) bits over tri-cone bits has caused a shift of focus away from axial vibrations towards lateral and torsional vibrations. Axial vibrations can also be artificially introduced by downhole tools, such as agitators or jars (Shor et al., 2014).

1.1.2 Buckling

The drillstring assembles pipes of different weights. In vertical wells, heavier pipes, such as drill collars and heavy weight drill pipes (HWDP), are located closer to the bit and provide the weight on bit required for crushing the rock. A drillstring assembly ensures that the upper part of the drillstring is kept under tension, and only a small portion under compression. Buckling occurs when compressive forces exceed the pipe's buckling resistance. Under buckling, the string acts like a spring and inhibits the transfer of weight to the bit. In addition, RPM becomes erratic, thus almost impossible to predict (Lund and Martel, 2013). This dysfunction thereby significantly reduces drilling performance. Downhole sensors allow the detection of buckling and the adaptation of drilling parameters.

1.1.3 Tool Failure

Mechanical tool failure is a major source of non-productive time. The process of pulling out the entire drillstring (tripping out), replacing tools and running back into the hole (tripping in) may result in significant costs and time delays. A parting of the BHA or drillstring (twist-off) can cause lost tools in the borehole, resulting in significant efforts for regaining the lower part of the string (fishing) and even abandoning parts of the well and re-drilling from a higher location (sidetracking). Vibrations subject the tools to extreme cyclic stresses. During stick slip vibrations, RPM values can by far exceed technical RPM limitations of motors and rotary steerable systems. Unintended rotation in the opposite direction under severe stick slip will have damaging effects on the bit. While there exists footage of destructive vibration during drilling, Close et al. (1988) studying some of the first downhole vibration measurements already pointed out that often the highest levels of vibrations are recorded while the bit is off bottom. They specifically identified reaming operations and pumping and rotating while off bottom as major sources of vibration. Other causes for fatigue failure of tools are drillstring bending due to hole tortuosity, unfavorable weight transfer or poor BHA design (Raap et al., 2011).

1.1.4 Tortuosity

Tortuosity is the deviation from a planned, straight wellbore and is one of the most important indicators for wellbore quality. Twists, abrupt turns, short radius curves and kinks (doglegs) in the wellbore bend the pipe, increase friction, and reduce the effective wellbore diameter. This can lead to tool failure due to high cyclic stresses and an inability to run casing and other tools to bottom. In addition, it can jeopardize cementing quality, zonal isolation, and production. Traditionally, the level of wellbore tortuosity has been reported as dogleg severity, a degree of curvature measured about every 90 ft. Wellbore

position is indirectly inferred from wellbore length (measured depth, MD), recorded inclination (slope) and azimuth (deviation from northern direction). Stockhausen and Lesso (2003) raised awareness about the negative impacts of smaller scale tortuosity that is undetectable with measurement intervals of 90 ft. Mud motors, in particular, can cause undesired and largely undetected deviations from the planned well path. Continuous measurements of position along the wellbore has in recent years led to better descriptions of wellbore shape. Along with new measurements, researchers are developing new ways to quantify wellbore tortuosity and offer KPIs (Key Performance Indicators) for wellbore quality (Zhou et al., 2016, Bang et al., 2016).

1.1.5 Hydraulic Dysfunctions

The fluids system is vital to the drilling process. In conventional drilling operations, the hydraulic pressure of the mud balances formation pressures and prevents influx of gas (kick) or excessive reservoir fluids into the wellbore (well control). Mud pressures must reside within a window of pore pressure (lower limit) and formation fracture pressures (upper limit). This mud-weight window is also called the “drilling margin”.

Formation strength tests, such as a formation integrity test (FIT) or a leakoff test (LOT), determine the integrity of the formation and are usually conducted after drilling out a casing shoe. Pressure responses are usually monitored using surface data. For formation strength tests, the use of downhole data would remove uncertainties related to fluid compressibility and latencies of the pressure signal on surface (van Oort and Vargo, 2008).

During drilling, surface pressures are monitored to recognize a sudden pressure increase, indicating a potential kick. Well control is an area that would greatly benefit from the availability of downhole data. Downhole pressure sensors distributed along the string

and real-time data transfer could enable an instant and reliable kick detection (Gravdal, 2009).

Staying within the mud-weight window is not only critical during drilling. Surge and swab pressures during tripping operations can exceed these limits if the axial velocity and acceleration of the string are too high. Models (e.g. Iversen et al., 2006; Cayeux et al., 2011) are used to estimate the effect of pipe movements on downhole pressures; this enables the optimization and automation of tripping procedures.

Mud transports rock cuttings to surface, which is a vital function of the drilling process. The blocking of the annulus between drillpipe and borehole with solids (cuttings and cavings, i.e. a pack-off, and not being able to move the pipe out of the borehole (stuck pipe) are dysfunctions caused by inadequate hole cleaning or cuttings transport.

Insufficient bit hydraulic horsepower is considered another drilling dysfunction that limits ROP and may lead to bit balling. Kendall and Goins (1960) first studied the distribution of surface pump pressures to maximize the jet impact force at the bit.

Cayeux et al. (2013) stated that measurements for drilling automation should be taken as close as possible to the real boundary of the problem. Downhole measurements of annular pressure minimize inaccuracies in comparison to surface measurements and can indicate insufficient hydraulic horse power, solids transport and hole cleaning (e.g. Coley and Edwards, 2013).

1.1.6 Drilling Performance Limiters

The rate of penetration (ROP) or drilling speed has a significant impact on time and cost of operations. Low ROP can have a variety of causes, including directional steering, hard formations, bit wear or failure, vibrations and buckling. To achieve high ROP under normal circumstances, there are basically only three operational parameters that can be

adjusted for high drilling performance: WOB, RPM and flow rate. Design choices, such as bit selection, mud properties, etc. can have a significant impact on performance, but these factors can usually only be adapted in between bit runs. Many theoretical models on ROP optimization exist; they usually rely on the correct input of such design choices (Bataee et al., 2010). ROP optimization using data and machine learning algorithms is becoming an increasingly active area of research (e.g. Jiang and Samuel, 2016, Gidh et al., 2012, Evangelatos and Payne, 2016). Despite these efforts, attempts at ROP optimization currently are mostly done using experience and data from nearby wells (offset wells), without the use of machine learning techniques.

It is common drilling wisdom that an unfavorable combination of RPM and WOB parameters leads to lateral or torsional downhole vibrations. A low ROP could be indicative of losing energy to vibrations rather than rock-cutting action (Dupriest et al., 2005). Downhole WOB is generally lower than surface WOB for a variety of reasons, including friction and wellbore tortuosity. Inadequate weight transfer from surface to downhole is another major limiter of drilling performance. As detailed in Chapter 3, insights from downhole data can be used to systematically eliminate performance limiters.

1.2 DATA AND MEASUREMENTS

1.2.1 Rig Data and Performance

Data has always been used in one way or another to improve drilling performance for decades. With the development of the "technical limit concept" in the late 1990s, the use of data has become more methodical (Bond et al. 1998). The technical limit describes the absolute minimum time in which a single operation can be conducted using currently available technology. The difference between actual drilling time and the technical limit is

lost time and should be eliminated if possible. To find the technical limit from data, well time records are broken down into single operations, the fastest of which are pieced together to form a theoretically "perfect well". Such a breakdown of operational procedures and their respective times are included in daily drilling report since their introduction (Quay, 1986). In the beginning, operational time recordings were done manually. Thonhauser (2004) presented automated activity monitoring of wells to achieve unbiased, more accurate and more granular breakdowns of rig activities. Rule based algorithms and data of existing measurements such as block height, hook load, pump rates, rotary speed was used to identify rig activities like drilling, tripping, making connections, etc. Monitoring and evaluating time-based activities of different crews soon became the key to drilling performance. Today, time still is the number one performance indicator in drilling. New measurement technology might allow for a more differentiated perspective on drilling performance. Other factors, such as wellbore placement, low wellbore tortuosity (Zhou et al., 2016), strong cement bonding beyond the active well life (Liu et al., 2015) may become part of a future drilling performance evaluation.

1.2.2 Drilling Data and Quality

Bad data is data of insufficient quality characteristics for specific applications. Usually, first a new technology is developed, for which data is required. Then data is found to limit the performance of that technology. Only then calls for data quality improvements are starting to emerge. After Thonhauser et al. (2004, 2005) used rig data for activity monitoring, data quality was found to be inadequate. In 2007, Mathis and Thonhauser suggested solutions for data standardization, quality control and quality reporting, data compression, and visualization. In 2013, Arnaout et. al. defined real-time rig data quality KPIs as: completeness, continuity, timeliness, validity, accuracy, consistency, and

integrity. With the increased use of rig data for automation application, the need for reliable data quality became urgent (Zenero et al., 2016; Ashok et al., 2016; Otalvora et al., 2016).

For surface measurements, the drilling industry is just beginning to consider sensor calibration critical to job execution. An increased awareness of the value of data preceded an increased awareness of the quality of data. A special task force has been formed amongst more than 20 operator companies. This operator's group to promote standards to enable optimization and advanced analytics. They realized that advances in data quality do not start at the rig, but much earlier in the supply chain, at the manufacturers of sensors and tools. The group therefore is also working on standardized calibration devices and calibration procedures (Zenero and Behounek, 2016).

Incorrect well position (MWD) or logging while drilling (LWD) information can result in collisions with other wells or lost production opportunities. Because of such obvious downsides of bad data, industry bodies, such as the *Industry Steering Committee on Wellbore Survey Accuracy (ISCWSA)* or *the SPE - Well Positioning Technical Session* are continuously working towards improving the quality of survey data. Conventions and standards on measurements have already been successfully implemented in these areas. The logging community is very well aware that knowing about data is just as important as knowing about the tools and processes of data collection. Therefore, courses on log analysis include in-depth knowledge of tools' working principles, deployment methods, and data processing. A similar mindset towards downhole dynamics data would also improve drilling data analysis.

For downhole measurements, shock, and vibration data from MWD tools has traditionally been collected to monitor and predict the life of downhole tools. Now downhole dynamics data receives more interest and is collected at increasingly high sample

rates. It is more commonly used for insights in downhole forces and motions, which are critical to drilling performance (e.g. Trichel et al., 2016). Bad drilling dynamics data can stem from many processes, including sensor technology, tool design, manufacturing, tool deployment, data collection, processing, and transfer. The calibration of downhole sensors, however, is even more challenging than the calibration of surface sensors.

1.2.3 Surface Measurements

Real-time information from the rig has been collected and streamed since the 1980s (e.g. Isaac and Bobo, 1984; Guidry and Scego, 1986). Numerous sensors continuously produce a variety of data from the rig site. Some sensors are concerned with the monitoring of tool conditions (e.g. sensors in the top drive), while others measure operational parameters. The most basic measurements are torque, tension or hookload, mud pressure, flow rates and rotational speed. From these parameters alone, rig activities (drilling, tripping, making connection, etc.) can be easily detected. For this reason, downhole data analysis always requires additional surface parameters. The sampling frequencies range from 1 to 15 Hz, but data is often stored and/or transmitted at lower rates (Lesso et al., 2011). The data may be displayed on a simple gauge or viewed on an electronic human machine interface (HMI) with visualization capabilities. In addition to direct measurements, certain parameters are inferred from other measurement. MSE (mechanical specific energy) is an important parameter for drilling optimization and calculated from WOB, torque, RPM, ROP and bit size. With the inclusion of such calculated values, data sets of continuous surface data can have more than 500 “channels” (column or single value over time).

Recent developments attempt to improve access to information at surface involve more accurate and higher frequency measurements at the top drive. Instrumented surface

subs contain sensors for bending, vibrations, pressures, temperatures, rotational speeds, etc. and can record at frequencies above 100 Hz (Wiley et al., 2015).

1.2.4 Downhole Dynamic Sensors

Downhole sensors have been used to gain insights in downhole dynamics phenomena and detect and mitigate drilling dysfunctions. The Esso Production Research Company used downhole high-frequency data to study forces and motions of the drillstring as early as 1968 (Cunningham, 1968; Deily et al., 1968). A step-change in sensor application and adoption came in the 1980's, when MWD (measurement while drilling) tools started to be implemented for well logging and wellbore positioning purposes (Wolf et al., 1985; Ramsey, 1983). Most downhole dynamics sensors run today are still part of MWD tool suites, with ever-increasing downhole processing capabilities and real-time data transmission rates. In addition, stand-alone dynamic measurement subs have also been developed, in variable sizes and comprising a variety of sensor types.

In its simplest setup, a dynamics measurement sub may comprise only a single sensor, for instance a radial accelerometer. Subs may be placed just behind the bit or at multiple locations along the drillstring. Larger tools typically contain an array of sensors, such as accelerometers, gyroscopes, magnetometers, strain gauges and pressure and temperature sensors. These tools often contain more than one sensor of one kind. For instance, combining measurements from multiple multi-axes accelerometers allows, in contrast to single sensors, "the separation of measurements in three orthogonal directions as well as decoupling of rotational and translational movement" (Hoffmann et al., 2012).

In downhole dynamic subs, accelerometers are primarily used for measurements of vibrations. In most MWD tools, three orthogonally mounted accelerometers measure the strength of the Earth's gravitational field. Combined with measurement of the magnetic

North using magnetometers, wellbore azimuth and inclination can be determined. These measurements are then used to determine the position of the wellbore in a Cartesian coordinate system. Gyroscopes and magnetometers are used to infer the downhole rotational speed. Strain gauges measure a change in resistance based on deformation of the material. They are used to determine downhole WOB (weight on bit) or more precisely weight on tool, downhole torque, or torque on bit (TOB), and bending forces. Orientation of the strain gauge determines the type of measurement. Orientation along the axis of the drillstring measures a proxy for WOB, while a layout with a certain angle to the drillstring axis indicates torque. Strain gauges are particularly susceptible to changes in temperature and can show significant offsets that need to be corrected for.

Pressure transducers can record downhole pressures both inside the drillstring and in the annulus. The measurements can be used to monitor pressure conditions downhole and infer undesirable drilling states related to hydraulics. Pressure while drilling (PWD) is particularly valuable in managing ECD (equivalent circulating density), monitoring cuttings transport and hole cleaning (Mallary et al., 1999; Coley et al., 2013). Using more than one downhole pressure sensor even allows for the determination of mud rheology in real-time and under downhole conditions. The wellbore then becomes an instrument itself, the equivalent of a large pipe viscometer (Karimi Vajargah et al., 2015).

1.2.5 Downhole Data Transmission

For many years, the state of the art technology for downhole data transfer in near real-time has been mud pulse telemetry. In mud pulse telemetry, a downhole valve can restrict the flow in certain intervals and therefore send binary pressure pulses to surface, which are recorded by pressure sensors. Downhole information can be reconstructed from these digital pressure pulses. Data can also be pulsed down to a tool from surface and

trigger changes in parameters through the same process. Data transfer rates of mud pulse telemetry typically reach about 10 bits/seconds; this is usually too low to transfer measurements with high sample rates to surface. Also, these systems are susceptible to the drilling environment and face high error rates under challenging conditions, such as extended reach wells, high pressure high temperature wells, change in mud properties and interferences by vibrations (Emmerich, 2015).

To overcome these limitations, high broadband connections between the downhole tools and the surface have been established. Wired drillpipe technologies, such as NOV's IntelliServ, open new possibilities with regards to downhole monitoring, control, and rig automation. Networked drillstring telemetry allows having real-time bi-directional broadband communication with downhole tools in rates of 57,600 bits/seconds. Because the broadband telemetry works independently of the medium present, the networked drillstring can transmit data regardless of the fluid environment or during situations of total fluid losses (Craig et al., 2013).

The network telemetry system consists of 1) a stainless steel, armored coaxial cable that runs between the pin and box of each tubular, 2) induction coils at the pin and the box of each connection, and 3) electronic elements known as booster assemblies that enhance the data signal as it travels the length of the drillpipe to prevent signal degradation, and additionally allow measurements to be taken along the length of the drillstring. An electromagnetic field associated with the alternating current signal transmitted through the cable is responsible for transmitting data. As the alternating electromagnetic field from one coil induces an alternating current signal in the nearby coil, data is transmitted from one tubular to the next.

Veeningen et al. (2011) point out the advantages of high-frequency and high resolution data transmission via wired drillpipe, especially for downhole dynamic events. Sensors for pressure, temperature and vibrations are placed along the entire drillstring and continuously transmit data to surface, giving more comprehensive insights into the drillstring system than with measurements at a single point (e.g. Cardy et al., 2016).

1.2.6 Limits of Data Availability

The physical disconnect between the bit (target of actions) and the surface (initiation of actions) together with insufficient data transfer between bit and surface is the cause of most challenges in drilling.

Wired drillpipe was developed to overcome these limiters with high bandwidth bi-directional communication. Such new technologies constitute significant improvements, but do not fully solve the issues of access to downhole information. The broadband capacity of wired drillpipe is currently limited to 57,600 bits/seconds (Craig et al., 2013), which is equivalent to 1800 32-bit numbers per second. 5 sensors each sending data at 400 Hz can already exceed the broadband capacities of wired communication. Improved data transfer systems open up technological improvements for sensors. New subs, equipped with more sensors, measuring, and transferring data at higher frequencies are currently under development and will quickly swamp available bandwidths and downhole memories.

Drilling operations already produce gigabytes of data every day from a multitude of sources and in a variety of data formats, such as real-time data streams from surface or downhole, unstructured text from reports, static well, rig, or formation information, etc. To gain important knowledge on drilling dysfunctions, data must be aggregated and integrated at some point during its way from source to end usage. Even if downhole data could reach

surface in all attempted granularity, current data processing tools and capabilities wouldn't yet be capable of properly analyzing it.

1.2.7 Downhole Data

Following the Nyquist frequency theorem (Poletto et al., 2004), the sampling rate should generally be at least twice as high as the highest frequency of interest. Frequencies of the measured signal that are higher than this Nyquist frequency are aliased (folded, mixed with lower frequencies) in the sampled output. If downhole vibration recorders are designed to detect characteristic frequencies and their overtones for lateral vibrations, sensors should have sampling rates of hundreds of Hz. While bit runs can last for several days, continuous sampling at such high frequencies would require data capacities far beyond current technological and economic limits. Due to limitations in data storage capacities, tool manufacturers have traditionally applied a different approach, collecting both *continuous data* (statistics) and *burst data* (raw measurements) with the following characteristics.

- *Continuous data:* Most downhole vibration tools sample data at high-frequency rates and process it immediately downhole. Key statistical parameters, such as the root mean square (RMS) value (which is a measure for the variance of the signal (D'Ambrosio et al., 2012)) and minimum and maximum values within a time window of several seconds are calculated instantly and stored, while the bulk of the high-frequency data gets dismissed. The algorithms and type of extracted parameters vary across different tools.
- *Burst data:* At certain points throughout the bit run, high-frequency snapshots, so-called "burst" sequences, are recorded and stored in the tool's memory. These snapshots can be taken at periodic time sequences or initiated through triggers, such

as high acceleration levels. These burst sequences or research sequences typically show sampling rates of hundreds of Hz (e.g. 800) and cover periods of several seconds.

Nomenclature, exact sampling rates and window lengths vary by companies and projects. **Fig. 3** illustrates a downhole data processing diagram as used by a particular company (Bowler et al., 2016).

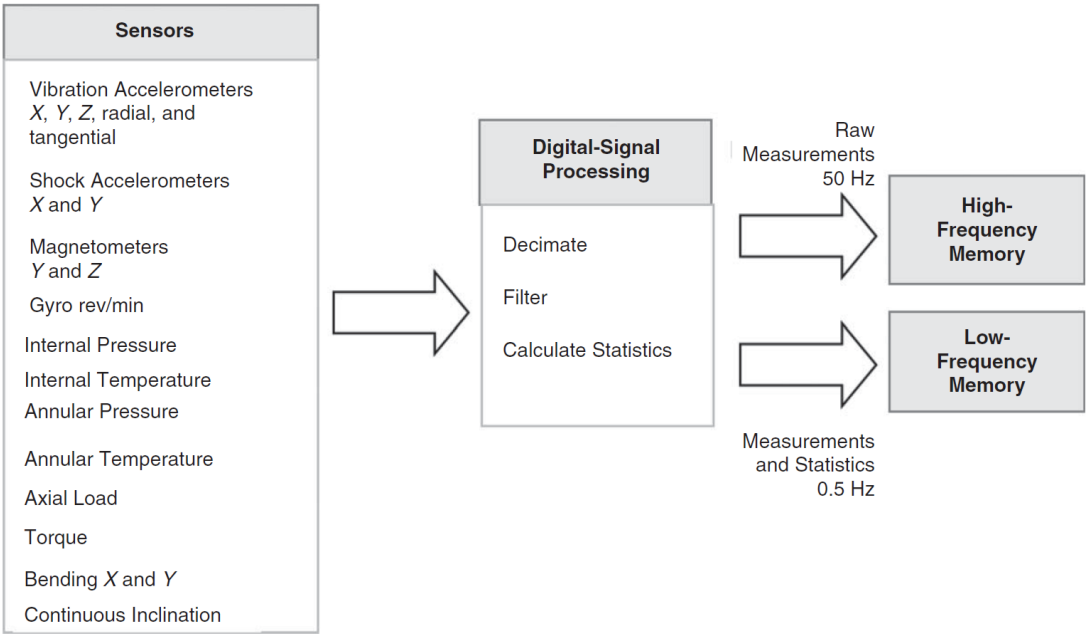

Fig. 3—Data processing diagram provided by Bowler et al. (2016): "Block diagram of the sensors, digital signal processing, and recording within the tool."

1.2.8 Vibration Models and Data

Vibration modeling has been one of the most prominent areas of academic research in drilling for decades. To date, researchers develop new or better views on the underlying

physics of drillstring vibrations (e.g. Ledgerwood, 2010). It has become possible to simulate buckling and drillstring behavior in great detail.

Still, there seems to exist a large gap between a purely research/analytical perspective and a practical/operational perspective. Despite the availability of hundreds of models, and possibly millions of invested research hours, drillstring vibrations are still mostly unpredictable and sometimes even stay undetected. Even the causes and main influence factors of vibrations leave room for disagreements and disputes.

The importance of physical models to understand the underlying principles cannot be overstated. However, in field applications most of these models reach limits in the complexity-accuracy tradeoff. Predominant factors, like the heterogeneity of rock formations are typically neglected and modeled with simplifying assumptions (e.g. as homogeneous material with a uniform friction factor). A straight or slightly bent cylinder usually approximates the borehole shape. In reality, the shape shows differences in diameter (washouts), spirals, ledges, and doglegs. The shape determines the contact points throughout the well and thus the boundary conditions of the models (Sumrall, 2013). Regardless of how accurate models might be, the industry still lacks tools to describe these extremely relevant details with enough precision.

Many different systems in drilling act together in known or unknown ways. With data, it is only possible to capture a fraction of the influence factors of the system and significant variables may be missed. As shown later in this work, a variety of different and sometimes unknown phenomena compound a single measurement. Well understood physics help to separate important measurements from noise. Sigura et al. (2016) note that high-bandwidth data availability will be a game changer for drilling models and simulation, but that such systems still pose significant challenges. Increased availability of downhole

measurements and a better understanding of such data could help to eventually close the gap between theoretical models and field applications.

Chapter 2: High-Frequency Downhole Data Interpretation: An Alternative View on High-Frequency Torsional Oscillations (HFTO)[4]

2.1 INTRODUCTION

New high-frequency downhole recorders and high-bandwidth real-time data transmission tools (such as wired drillpipe) are heralding the era of big data in drilling. Nevertheless, high-frequency data is not yet used to its full potential, as the industry is only just beginning to make sense out of the many gigabytes of recorded data. Analysis of high-frequency data appears to be particularly useful to better characterize and understand vibration events, which are prominent technical limiters of drilling performance.

A kinematic model was developed to study the expected high-frequency acceleration measurement output under a whirling motion of the drillstring. Two different modeling approaches were found to yield the same results. A numerical vector approach provides a clear geometric interpretation, while tensor calculus analysis yields an explicit mathematical formulation of sensor kinematics. The vibration patterns predicted by the model matched the patterns observed in high-frequency field data very well, both in the time and frequency domain. The comparison reveals essential details of the downhole kinematics of vibrational modes, particularly regarding interpretation of patterns, which allows a better classification of vibrational dysfunctions in field data. High-frequency

[4] Chapter based on: Baumgartner, T., & van Oort, E. (2014, October 27). Pure and Coupled Drill String Vibration Pattern Recognition in High Frequency Downhole Data. Society of Petroleum Engineers. doi:10.2118/170955-MS. Contributions: Baumgartner, T.: Author, van Oort, E.: Supervisor.

fluctuations in downhole measurements previously attributed to a phenomenon called high-frequency torsional oscillations (HFTO) can be explained purely by considering the effect of the whirling motion of the string on downhole accelerometers. This alternative explanation is much simpler than the HFTO hypothesis, which requires multiple assumptions.

This novel interpretation of high-frequency downhole sensor data allows differentiation of measurements of downhole dynamics into sensor artifacts and harmful vibrational dysfunctions that require attention and mitigation actions and sensor artifacts, which do not require such action. Thus, the wealth of information provided by high-frequency vibration patterns, which is unavailable in low-frequency surface data, offers the possibility to significantly improve vibration mitigation methods. This, in turn, provides opportunities for step-changes in drilling performance improvement.

2.1.1 Previous Work

Mathematical representation of drillstring dynamics began in the 1960s. Models had few degrees of freedom and simplifying assumptions such as circular boreholes, vertical wells, and independence of vibration modes (for a comprehensive overview, see Shor et al., 2014). Brett et al. (1989) were the first to describe the path of a single cutter of a PDC bit under bit whirling. With this, Brett could explain “star” or “weave basket” shaped patterns in the bottom hole produced by whirling PDC bits. Later, drillstring vibrations were represented using three dimensional dynamic models. In 1992, Jansen published analytical solutions for periodic forward whirl and backward whirl as well as a chaotic motion of a drillstring. He used a mass-spring system with two degrees of freedom to apply non-linear rotor dynamics. In 1994, Guo and Hareland created a dynamic model of the BHA and bit to assess the cyclic impact loads caused by bit “wobbling”. These loads

act on PDC bits and eventually lead to cutter failure. Leine et al. (2002) presented a model that incorporated both stick-slip and whirl. He used the model to support the theory that fluid forces are the cause for a sudden change from stick-slip to whirl, with both vibrational modes coexisting only for a very small range of drillpipe rotational speed.

In 2011, Stroud et al. developed an analytical model to simulate backward whirl. Numerical approximation methods were used to solve equations of motions in real-time, which allows the observation of the effects of clearance and friction factors on borehole friction and whirl frequency. The model could reproduce frequencies observed in previous work (Vandiver et al., 1990) and in laboratory tests. In 2014, Makkar et al. studied the coupling between lateral and torsional vibrations in laboratory tests and dynamic simulations, which incorporated cutter kinematics during whirl.

2.1.2 Purpose

Downhole vibration sensors are used to get an indication of the type and magnitude of dysfunctions during the drilling process. High-frequency snapshots of downhole accelerations show distinct patterns (re)occurring throughout different bit runs. Examples of high frequency downhole burst windows can be found in Appendix A.1. These patterns offer a wealth of information on downhole dysfunctions that will help to better distinguish and characterize different modes of vibration for tailored mitigation techniques. A simple kinematic representation of a string in a borehole as a planar disk is used in the following to study the displacements, velocities, and accelerations, which an accelerometer experiences during off-center rotation. Both RPM values and whirl rotational speeds are model inputs, not model results.

For the purpose of analyzing patterns in high-frequency vibration data, kinematic models are advantageous over more complex dynamic models: calculations and

assumptions are very transparent and reproducible. Computation times are furthermore low. Variables can therefore be changed in real-time and their effect on the outcomes can be studied efficiently.

2.2 INTERPRETATION OF HIGH-FREQUENCY DOWNHOLE DATA

This introductory chapter presents an issue at the core of a misunderstanding of measurements and data, with profound impact on the drilling industry. The issue is related to the fact that the process of sensor design, data collection, calculations, and processing is still disconnected from data analysis.

In downhole data recorded during drilling, tangential accelerometers measure non-zero values with high-frequency fluctuations often in access of 100 Hz and multiple overtones in the frequency spectrum. These observations led to the discovery of a new vibrational phenomenon and the coining of the term “high-frequency torsional oscillations”. HFTOs have been reported in numerous publications (e.g. Warren and Oster, 1998; Pastusek et al., 2007; Oueslati et al., 2013; Tikhonov and Bukashkina, 2014; Hohl et al., 2016) and have recently received increasing attention with the commercialization of services to detect and prevent HFTOs. The phenomenon observed in tangential accelerometer data has been attributed to torsional fluctuations of the drillstring, i.e. a high-frequency form of stick-slip vibrations. Root causes are either attributed to bit rock interactions (e.g. Jain et al., 2014) or torsional resonances of the collar or drillstring (e.g. Warren and Oster, 1998 or Lines et al., 2013). In these publications, HFTOs were postulated based on field data observations and were verified by comparing the frequency spectra resulting from dynamic modeling to frequency spectra of field data. An important assumption underlying these modeling efforts is that the instantaneous center of rotation is in line with the centerline of the pipe (Macpherson et al., 2015).

A measurement of lateral vibration usually refers to the resulting acceleration vector of two orthogonal measurements, while a stick slip index is calculated from variations in RPM. Under an on-center rotation assumption, accelerations in tangential and radial direction of a sensor on a disc with constant distance r to the center of rotation and with angular speed $\dot{\alpha}$ (e.g. in revolutions per minute, RPM) can be described as:

$$r = r \cdot e_r \tag{1}$$

$$\dot{r} = v = \dot{r}e_r + r\dot{e_\alpha} = \dot{r}e_r + r\dot{\theta}e_\theta \tag{2}$$

$$\ddot{r} = \dot{v} = a = \ddot{r}e_r + 2\dot{r}e_r + 2\dot{r}\dot{e_\theta} + r\ddot{e}_\theta = \left(\ddot{r} - r\dot{\theta^2}\right)e_r + \left(r\ddot{\theta} + 2\dot{r}\dot{\theta}\right)e_\theta \tag{3}$$

Since r = constant, $\dot{r} = \ddot{r} = 0$, and the equation simplifies to:

$$a = \left(-r\dot{\theta^2}\right)e_r + \left(r\ddot{\theta}\right)e_\theta. \tag{4}$$

For uniform circular motion (rotation around the string's center), radial acceleration is directed towards the center of rotation, which for on-center rotation is the center of the string:

$$a_r = -r\dot{\theta^2} = -\frac{v^2}{r} \text{ with } v = r\dot{\theta}. \tag{5}$$

Tangential acceleration is perpendicular to radial acceleration and is positive in the direction of velocity. For uniform circular motion, tangential acceleration is zero:

$$\mathrm{a_t} = \mathrm{r\ddot{\theta}} = \frac{\mathrm{dv}}{\mathrm{dt}} = 0 \tag{6}$$

Under the assumption of a constant center of rotation, fluctuations of tangential accelerations can only be explained by a non-constant rotational angular velocity of the pipe. Yet, as soon as the pipe centerline moves about in the wellbore, the path of the sensor is not circular and *Eq. 5 and Eq. 6 do not apply*. In a whirling string scenario, fluctuations of both radial and tangential accelerations are expected, because the sensor undergoes a non-circular path, first described for cutters on a bit by Brett et al. in 1989.

It is important to correctly interpret these high-frequency fluctuations. Hohl et al., for instance, point out in 2016: “Since it is not always possible to avoid HFTO with operational parameters the dynamic stresses must be considered in tool design to prevent severe damage to tools in the BHA.”, hinting at the destructive nature of HFTOs and at requirements of new downhole tool designs, measurements and software that can limit the “damages caused by this phenomenon”.

The following section will introduce a kinematic whirl model that helps to interpret these accelerations and offers an alternative and simpler explanation for the phenomenon of HFTOs.

2.3 MODEL

The model represents borehole kinematics in two dimensions as a planar disk rotating in a confining, perfectly round circle. Effects of gravity, contact forces between the borehole and the drillstring, viscous damping forces, friction forces, more complex bit or stabilizer geometries, interactions between inner and outer string (e.g. cutting actions) and any other dynamic effects are ignored in this model. In the context of the presented model, forward and backward whirl only refer to the direction of whirl rotation in relation to the drillstring rotation, with the same direction for the former and the opposite direction for the latter.

Fig. 4 illustrates a smaller circle of radius r (representing bit, BHA or drillstring) that rotates eccentrically in a larger circle of radius R (representing the borehole). Borehole and drillstring are viewed from above. The drillstring always rotates clockwise with angular velocity ω, while the string center rotates with angular velocity $\dot{\Theta}$ in clockwise direction for forward whirl and in counter-clockwise direction for backward whirl. The center of the drillstring follows a circle of radius $\delta = R - r$ with angular velocity ω, while

the drillstring of radius r rotates around its center with angular velocity Θ. The position of the string center is a model input and can be varied anywhere from δ = R – r (fully eccentric, eccentricity = 100%) to δ = 0 (fully concentric, with coinciding borehole and drillstring center). A velocity or accelerometer sensor is represented as a point S at a distance p from the center of the drillstring. The distance is a model input and can be varied anywhere from the wall of the string to the center of the string.

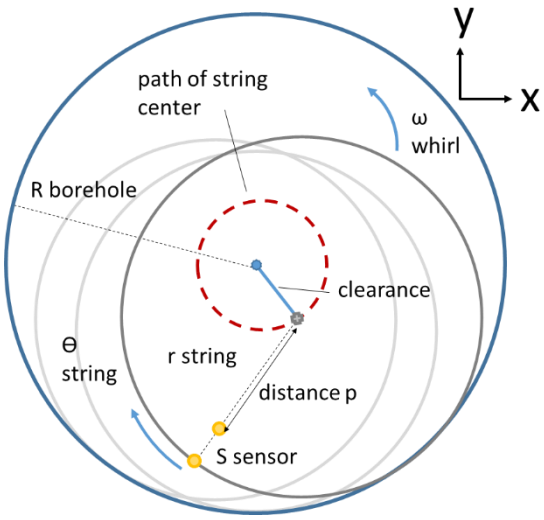

R = Borehole radius [m]

r = Drillpipe radius [m]

p = Distance of sensor from borehole center [m]

ω = Whirl angular velocity [rad/s]

Θ = Drillpipe rotation velocity [rad/s]

δ = Eccentricity of drillpipe [m]

Fig. 4—2D model of a drillstring in a borehole as a planar disk. The string rotates around its center with velocity Θ, while that center itself rotates around the borehole center with angular velocity ω.

The coordinates of the sensor point S are given by superposition of drillstring rotation and whirl movements: x_f and y_f for forward whirl, and x_b and y_b for backward whirl as stated below. First and second time derivatives yield velocities and accelerations in x and y directions in a Cartesian coordinate system as follows:

For forward whirl:

$$x_f(t) = +\delta\, cos(\omega t) + r\, cos(\Theta t) \tag{7}$$

$$y_f(t) = -\delta\, sin(\omega t) - r\, sin(\Theta t) \quad (8)$$

$$x_f'(t) = v_{xf}(t) = -\delta\, \omega sin(\omega t) - r\, \Theta\ sin(\Theta t) \quad (9)$$

$$y_f'(t) = v_{yf}(t) = -\delta\, \omega\, cos(\omega t) - r\, \Theta\ cos(\Theta t) \quad (10)$$

$$x_f''(t) = a_{xf}(t) = -\delta\, \omega^2\, cos(\omega t) - r\, \Theta^2\, cos(\Theta t) \quad (11)$$

$$y_f''(t) = a_{yf}(t) = +\delta\, \omega^2\, sin(\omega t) + r\, \Theta^2\, sin(\Theta t) \quad (12)$$

For backward whirl:

$$x_b(t) = +\delta\, cos(\omega t) + r\, cos(\Theta t) \quad (13)$$

$$y_b(t) = +\delta\, sin(\omega t) - r\, sin(\Theta t) \quad (14)$$

$$x_b'(t) = v_{xb}(t) = -\delta\, \omega\, sin(\omega t) - r\, \Theta\ sin(\Theta t) \quad (15)$$

$$y_b'(t) = v_{yb}(t) = +\delta\, \omega\, cos(\omega t) - r\, \Theta\, cos(\Theta t) \quad (16)$$

$$x_b''(t) = a_{xb}(t) = -\delta\, \omega^2\, cos(\omega t) - r\, \Theta^2\, cos(\Theta t) \quad (17)$$

$$y_b''(t) = a_{yb}(t) = -\delta\, \omega^2\, sin(\omega t) + r\, \Theta^2\, sin(\Theta t) \quad (18)$$

In previous kinematic models, authors have used $\delta \cdot \cos(\omega t)$ for the whirl rotation and $r \cdot \sin(\omega t + \Theta t)$ for the drillstring rotation, replicating the whirl rotation within the drillstring rotation (e.g. Brett et al., 1989; Stroud et al., 2011). However, the movement of the point S with regards to whirl angular velocity ω is entirely covered by the term $\delta \cdot \cos(\omega t)$ and the model currently allows for whirl rotation while the drillstring does not rotate around its axis. Whirl and drillstring rotation therefore can be treated independently.

2.4 Accelerations "As Seen" by the Sensor

Newton's law applies in the inertial frame of reference, i.e. any forces experienced by a sensor need to be described in a fixed system. Here, the center of the inertial frame of reference is the center of the borehole circle, which is static relative to the earth's frame of reference. The total movement of the sensor is therefore a superposition of the rotation of

the drillstring center around the borehole and a rotation of the sensor around the drillstring center.

To represent the location, velocity, and accelerations in the coordinates of the borehole, superposition and first and second derivatives are sufficient. To compare the model to the sensor measurements, accelerations need to be expressed in the sensor's coordinate system, described by unit vectors in tangential and radial directions of the sensor at any point along the curve it follows. Using a standard engineering approach, kinematic equations (positions, velocities, and accelerations) are described in the inertial frame of reference and are then successively transferred into the required coordinate system. The model requires at least 3 different coordinate systems, i.e. frames of reference to fully describe kinematic equations: the origin of the first frame (inertial) is the borehole center, the origin of the second frame is the pipe center that rotates around the borehole, and the third origin is the sensor center that rotates around the pipe.

Previous work (e.g. Vandiver, 2011 and Dykstra, 1996) have used the methodology of rotational matrices to transfer accelerations described with the inertial coordinates to coordinates that travel with the sensor. A rotation matrix performs a rotation operation and can only be applied in Euclidian spaces, which is a world of straight lines. In his work on special and general relativity, Albert Einstein (1915) points out that Kugelgeschöpfe (spherical inhabitants) do not have to go on a Weltreise (world tour) to perceive that they are not living in a Euclidian universe and provides a simple geometric example, linking smaller circles with the radius of the inhabited sphere. In other words, principles of the Euclidean geometry do not hold on a sphere, circle, or other non-flat surfaces. For spheres of large radii, such as the earth, the difference between a Euclidian and a non-Euclidian space can oftentimes be negligible. This does not apply in our situation, however. The first

radius in the described whirl model, the distance between the center of the borehole and the center of the drillpipe, can be extremely short. When the rotation matrix is applied a second time, from the center of the drillpipe to the sensor itself, we are on a curve with extremely large curvature, thus in a highly non-Euclidian space. The rotation matrix approach is therefore no longer valid. Based on this insight, two novel approaches are presented that describe the kinematics of such a sensor in all their complexity.

The first approach is numerically transforming the accelerations expressed in the x and y coordinates of the inertial reference frame into tangential and radial components, using geometric insights. The second approach uses tensor calculus to find explicit analytical expressions of a sensor's accelerations when moving along any given curve. These expressions describe tangential and radial accelerations "as seen" by the sensor, but described in inertial x and y coordinates.

2.4.1 Numerical Approach

After all calculations are performed in the borehole (inertial) frame of reference accelerations are expressed in instantaneous tangential and radial coordinates of the sensor's frame of reference in a separate step. The latter frame is moving together with the sensor, but the direction of the orthogonal unit vectors can be derived from the velocity and acceleration vectors at each time step. In a vector representation, β is the angle between the direction of the acceleration and velocity. Tangential and radial acceleration components $a_{tan}(t)$ and $a_{rad}(t)$ are orthogonal, and the tangential acceleration vector per definition points in the direction of the velocity (**Fig. 5**).

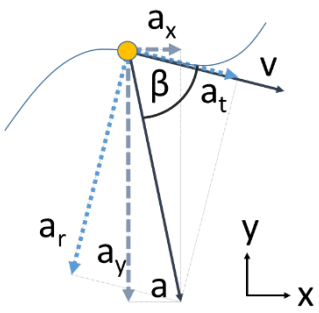

Fig. 5—Orthogonal components of the acceleration vector.

Multiplication by the orthogonal components of β separates tangential and radial components of the total acceleration vector:

$$a_{\tan}(\mathrm{t}) = a(\mathrm{t})\, cos\, \beta\, (t) \tag{19}$$

$$a_{rad}(t) = a(t)\, sin\, \beta\, (t) \tag{20}$$

where β is the angle between velocity and acceleration vectors, given by

$$\beta(t) = \cos^{-1}\left(\frac{\begin{bmatrix} a_x(t) \\ a_y(t) \end{bmatrix} \cdot \begin{bmatrix} v_x(t) \\ v_y(t) \end{bmatrix}}{|a(t)| \cdot |v(t)|}\right) \tag{21}$$

2.4.2 Analytical Approach

In addition to the geometric approach, the authors present a tensor analysis approach, which was employed to explicitly express the anticipated accelerations in tangential and radial directions of the sensor. Tensor analysis is a specific type of language within mathematics. Albert Einstein once championed Riemannian tensor analysis and made significant contributions, most notably in the formulation of the Theory of General Relativity. For instance, he achieved notational brevity of equations by introducing a concept that is still termed *Einstein summation*. Tensor analysis aims at a geometric description that is independent of a coordinate system, an application very well suited for

the given problem. Using tensors, one can develop equations without the requiring a specific choice of coordinate system beforehand. Detailed derivations, notation conventions, and further explanations can be found in Appendix A.2.

A sensor moving about a drillpipe that whirls in a borehole is best represented by a surface embedded in an ambient (inertial) space. Tensor calculus is an excellent choice to describe the geometry of an arbitrary surface, a 2D object in a 3D ambient space. Tangent vectors and normal vectors to the plane can be described explicitly for any point on such a surface.

In general, the acceleration vector **A** of the sensor moving along a curve that is confined to a surface is given by

$$\boldsymbol{A} = \frac{\delta V^{\alpha}}{\delta t}\boldsymbol{S}_{\alpha} + \boldsymbol{N}B_{\alpha\beta}V^{\alpha}V^{\beta}, \tag{22}$$

where $\frac{\delta V^{\alpha}}{\delta t}\boldsymbol{S}_{\alpha}$ is the *tangential acceleration* and the term $\boldsymbol{N}B_{\alpha\beta}V^{\alpha}V^{\beta}$ constitutes the *centripetal or radial acceleration.*

The application to the above described 2D sensor path yields the following expression:

$$\boldsymbol{A} = \frac{x'(t)\cdot x''(t)+y'(t)\cdot y''(t)}{x'(t)^2 + y'(t)^2}\cdot\begin{bmatrix}x'(t)\\y'(t)\end{bmatrix} + \frac{y'(t)\cdot x''(t) - x'(t)\cdot y''(t)}{x'(t)^2+y'(t)^2}\cdot\begin{bmatrix}y'(t)\\-x'(t)\end{bmatrix}, \tag{23}$$

where $x'(t), x''(t), y'(t)$ and $y''(t)$ are the above-described time derivatives of the position vector in the borehole frame of reference. The first part in Eq. 23 constitutes the *tangential acceleration vector*, the second part the *radial acceleration vector*.

2.4.3 Approach Comparison

The results of the numerical and the tensor analysis approach are identical. Both approaches have fit-for-purpose applications. The numerical approach is simple and evident to the reader. Calculations can be performed very quickly, and enabled the

development of a user interface to study the effects of changes in the input parameters on the output in real-time and compare them to existing field data patterns.

The derivation using tensors provides an explicit mathematical expression and an understanding of how the curvature of the sensor path causes the fluctuations in accelerations. Different frames of reference and conversions between them previously have led to confusion in kinematic modeling. These equations are derived without pre-defining any frame of reference, making this approach fundamental and universally applicable. The equations are also valid in higher dimensions; thus, they provide a basis for adding axial vibrations to the kinematic model of a sensor and the accelerations it experiences.

2.5 RESULTS

The above-mentioned equations were used to calculate velocity and acceleration vectors during forward whirl and backward whirl (**Fig. 6**). Velocity and acceleration vectors in both cases change their magnitude and direction in each of the small lobes between the outer and the inner circle.

Fig. 7 illustrates the simulated radial and tangential acceleration component in time and frequency domains. Pipe rotational speed and whirl speed are constant. The simulated sensor readings exhibit high-frequency fluctuations, which can be attributed to the non-circular motion the sensor undertakes during off-center rotation.

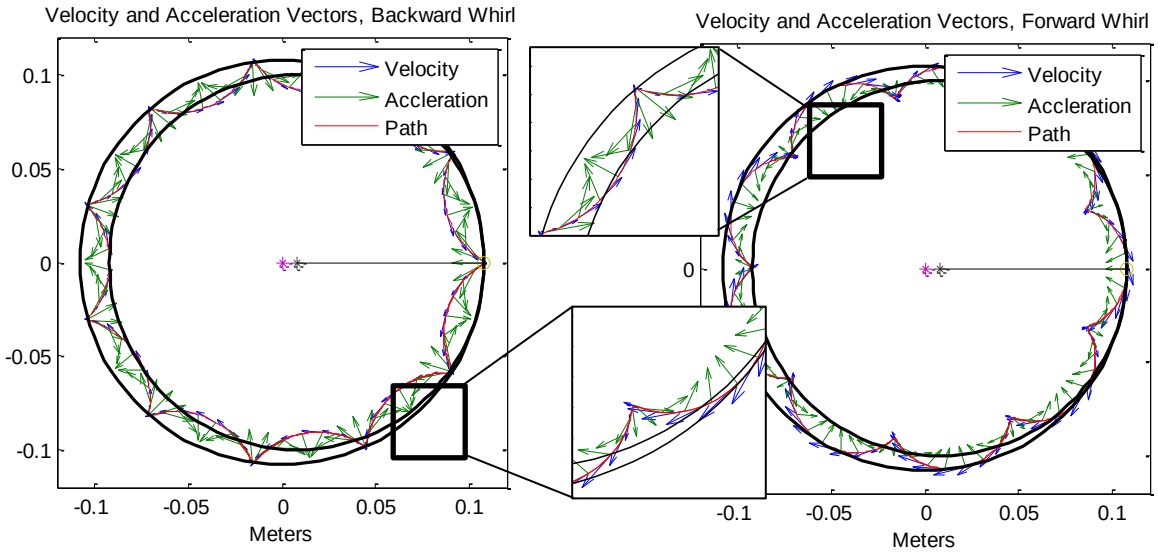

Fig. 6—Velocity and acceleration vectors during forward whirl (left) and backward whirl (right).

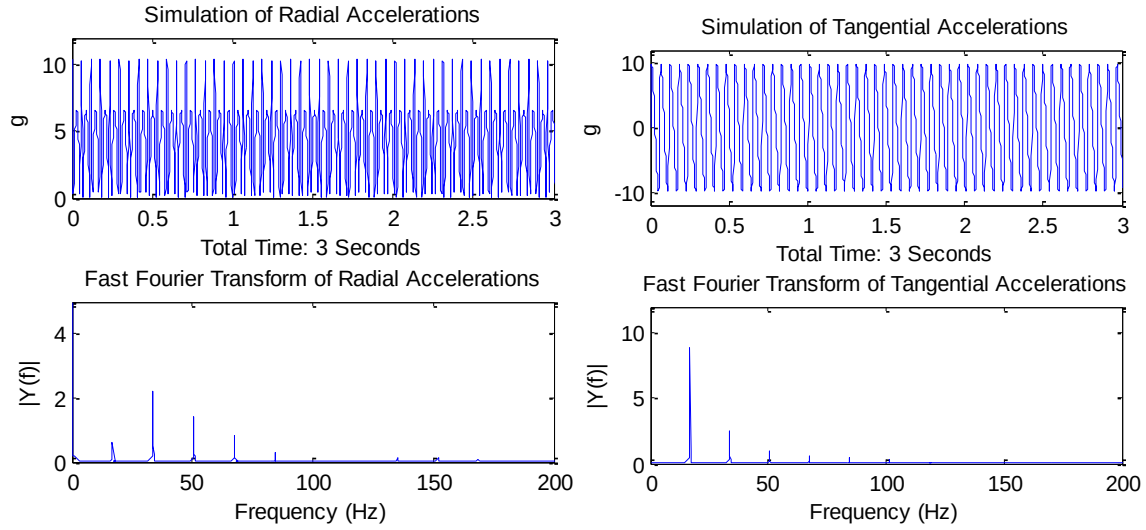

Fig. 7—Model results of simulated radial and tangential accelerations, displayed in time domain (top) and frequency domain (bottom) with the following parameters: Borehole diameter: 8.5 in, pipe diameter: 7.73 in, pipe rotational speed: 134 RPM, whirl frequency: 14.7 Hz (backward whirl), eccentricity and sensor location: 100%. |Y(f)| in g is the absolute magnitude of the signal.

2.5.1 Model Verification

The output of the simple kinematic model is compared to field data that was recorded during actual drilling operations using stand-alone vibration measurement devices with data recording capabilities. The field data sampling rate was either 400 Hz or 800 Hz.

Fig. 8 shows that field data of radial accelerations (left) and model outputs (right) correspond surprisingly well. Both time domain patterns and frequency peaks could be almost perfectly reproduced by adjusting pipe and whirl rotational speeds alone. A Fast Fourier Transform (FFT)[5] was used to characterize the frequency response of the system. The sampling frequency of the model matches the sampling frequency of the field data. For the comparison of model results and field data, known parameters were unchangeable model inputs, such as a bit size of 8.5 in. or an RPM (revolutions per minute of the drillstring) value of 112. The peak of characteristic frequency and its approximately equidistant overtones depend mainly on the whirl speed. Other parameters such as type of whirl (forward/backward), clearance and eccentricity can be used as fitting parameters for acceleration amplitudes. Forward whirl and backward whirl showed similar responses in time and frequency domain.

The simulation in Fig. 8 uses the backward whirl case for representation of the field data to better match the field data patterns. The field data shows an offset of 3 g from the 0-g-line. This offset could originate from potential downhole sensor calibration or sensor

[5] Fast Fourier transform (FFT) is a fast implementation of the discrete Fourier transform (DFT), for samples sized 2n (where n is a positive integer). The function transforms time domain signals into the frequency domain. The size of the data sets usually is not 2n, and can lead to distortions at the low end of the frequency spectrum. The MATLAB FFT implementation calculates the length closest to 2n and pads the data with zeros at the end, to improve the performance of the algorithm.

drift issues and was ignored. It is, however, an excellent example of the many data quality issues complicating high-frequency data analysis.

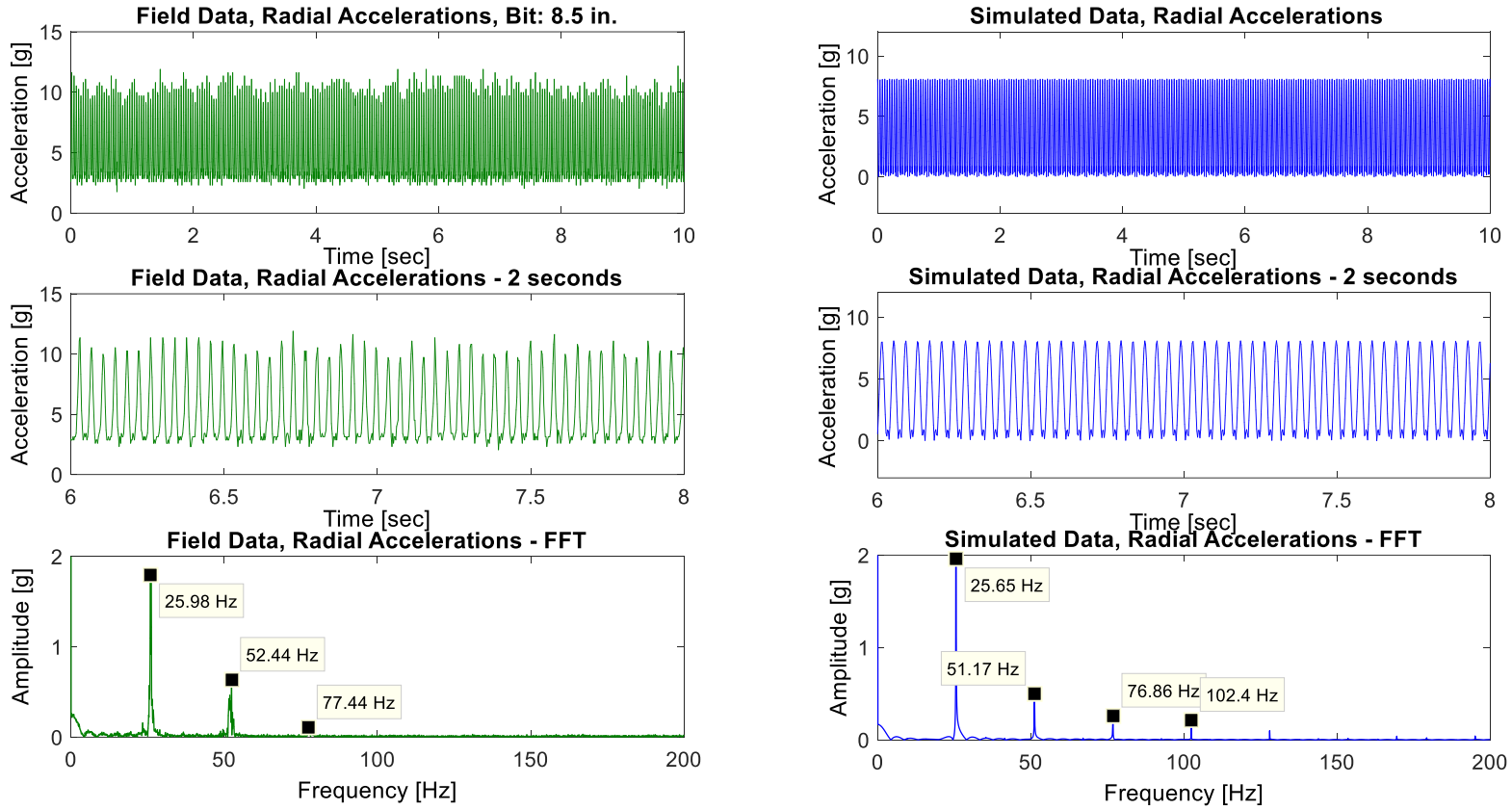

Fig. 8—Field Data (left), radial accelerations, bit size: 8.5 in. Simulated data (right): backward whirl, radial accelerations. 10 seconds burst window on the top with 2 second zoom in the middle. Fast Fourier transform (FFT) of the data on the bottom shows characteristic frequency peaks of field and simulated data. Parameters for simulation: whirl: 151 rad/s, 112 RPM, borehole diameter: 8.5 in., clearance: 0.162 in., pipe eccentricity: 65%.

Fig. 9 displays measured and simulated tangential accelerations for a different set of field data. The data was collected from a downhole memory tool with multiple tangential accelerometers. No post-processing was performed on the selected signal that was recorded from one of the accelerometers. Again, the model was able to match the patterns, both in time and frequency domains. The dominant frequency of tangential acceleration (66.41 Hz) results from the subtraction of the drillpipe angular speed (1.59 Hz) from the whirl angular speed (68 Hz).

Pipe eccentricity as an input factor can hardly be verified with actual field data. It varies with time during the drilling process and may depend on the axial location of the measurement tool, the presence of stabilizers in vicinity of the sensor, the borehole shape, etc. In the model, pipe eccentricity influences the amplitude of the accelerations, but not the patterns. Other effects that may influence the overall vibration amplitudes include damping/cushioning of fluids, forces due to interactions between drillstring and borehole wall (lateral bit bounces) or bit-rock interactions.

Any additional noise in the signal broadens the base of individual frequency peaks in the spectrum. Such noise could stem from ab uneven shape of the borehole, bit cutters or from various other sources such as the downhole motor or surface equipment. Additional frequencies could be excited through interference with axial modes of vibrations that a two-dimensional model does not account for. Rotational effects in combination with stabilizer or bit geometries may have effects on the measurements. Quantification of the gap between real values and simulated values should be studied in future work.

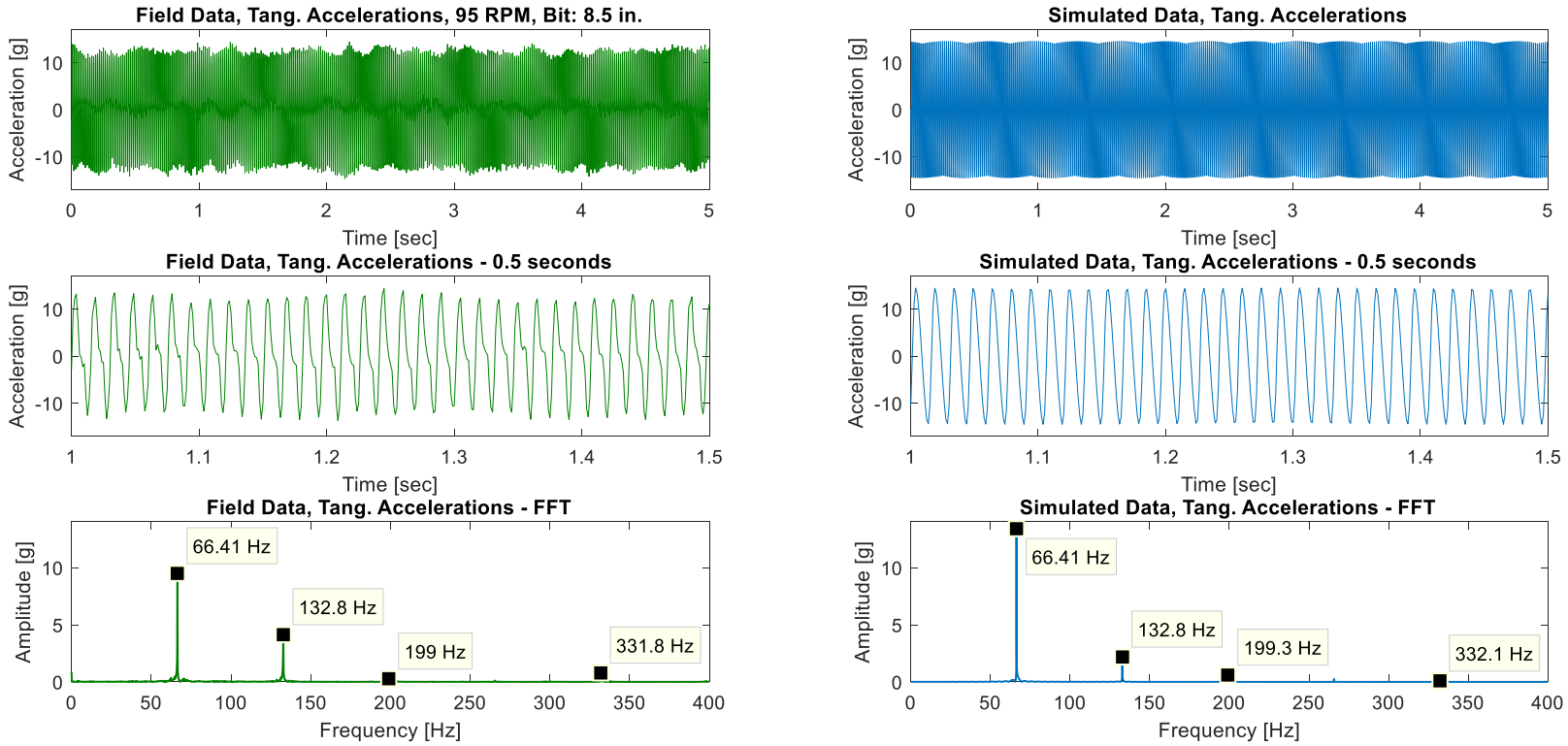

Fig. 9—Field Data (left), tangential accelerations. Simulated data (right), forward whirl tangential accelerations. 10 seconds burst window on the top with 0.5 second zoom in the middle. Fast Fourier transform (FFT) of the data on the bottom shows characteristic frequency peaks. Parameters for simulation: forward whirl: 68 Hz, 95 RPM, borehole diameter: 8.5 in., drillpipe diameter: 8.422 in., clearance: 0.04 in., pipe eccentricity: 80%, sensor position: 80% of drillpipe radius.

2.5.2 Coupling of Stick Slip and Whirl Vibrations

In addition to lateral vibrations, the model can represent stick-slip to investigate patterns of coupled vibration. The relationship between whirl frequency and rotational speed of the drillstring for pure rolling motion without slip can be calculated from borehole geometry and pipe speed (Brett et al., 1989, or equations for curves of hypotrochoid):

$$\omega = \frac{r}{(R-r)}\theta \tag{24}$$

Varying friction factors between borehole and pipe in reality could allow for varying amounts of tangential slippage, and the relationship of drillstring angular speed and whirl speed could vary significantly from the given ratio (Vandiver et al., 1989). In this kinematic model, whirl angular speed and pipe angular speed can be varied either using the given ratio or varied independently from each other.

Whirl and Stick Slip Frequency Variations

The sticking and slipping periods are modeled by introducing a time dependent *sinusoidal function* for drillstring and whirl angular velocities. In field data, a great variety of RPM shape functions during stick slip can be observed (cf. Baumgartner et al., 2015 or Chapter 3). A sinusoidal function is an oversimplification of the vibrational complexity. Nonetheless, for modeling purposes, the advantages of using a differentiable function outweighs severe disadvantages of this simplification. The period p_t of the stick-slip cycle is variable.

Instead of a constant rotational speed θ, the position vectors x(t) and y(t) can be calculated by introducing a time-dependent drillpipe rotational speed $\dot{\vartheta}(t)$. $\dot{\vartheta}(t)$ is a sinusoidal function that depends on average pipe rotational speed RPM_{avg}, oscillation amplitude A_{mpl} (when $RPM_{avg} = A_{mpl}$ the string reaches a momentary full stop) and a torsional oscillation period p_t in [rad/sec]:

$$\dot{\vartheta}(t) = RPM_{avg} - A_{mpl} \cdot sin(p_t t) \tag{25}$$

Integration yields the time dependent rotation angle $\vartheta(t)$ of the drillpipe, given by:

$$\vartheta(t) = -\int \left(RPM_{avg} - A_{mpl} \cdot sin(p_t t)\right) dt \tag{26}$$

$$\vartheta(\mathrm{t}) = -\mathrm{RPM_{avg}t} - \frac{\mathrm{A_{mpl}}}{\mathrm{p_t}} \cos(\mathrm{p_t t}) \tag{27}$$

If whirl variations are coupled with RPM variations, Eq. 24 applies:

$$\Omega(\mathrm{t}) = \frac{r}{(R-r)} \vartheta(t) \tag{28}$$

For independent whirl variations, we again introduce a time-dependent whirl rotational speed $\dot{\Omega}(\mathrm{t})$, described by an average whirl rotational speed Wrl_{avg}, whirl amplitude WA_{mpl}, and the same period of torsional oscillation p_t as above. Integration yields the time-dependent angle $\Omega(t)$

for forward whirl: $$\Omega_f(t) = -Wrl_{avg} t - \frac{WA_{mpl}}{p_t} cos(p_t t) \tag{29}$$

for backward whirl: $$\Omega_b(t) = +Wrl_{avg} t + \frac{WA_{mpl}}{p_t} cos(p_t t) \tag{30}$$

The resulting position vectors with both variable pipe and whirl angular velocity are

for forward whirl: $$x_f(t) = \delta\, cos(\omega_f(t)) + r\, cos(\theta(t)),$$

$$y_f(t) = -\delta\, sin(\omega_f(t)) - r\, sin(\theta(t)), \tag{31}$$

for backward whirl: $$x_b(t) = +\delta\, cos(\omega_b(t)) + r\, cos(\theta(t)),$$

$$y_b(t) = +\delta\, sin(\omega_b(t)) - r\, sin(\theta(t)), \tag{32}$$

and the respective time derivatives yield velocity and acceleration vectors expressed in inertial x and y coordinates. These can be used as input for calculations of

tangential and radial accelerations, using either the numerical or the tensor calculus approach described in Chapter 2.3.

2.5.3 Results of Coupled Vibrations Modeling

Field accelerometer data reveals examples of coupling of high-frequency with low-frequency variations. **Fig. 10** shows tangential accelerations with low frequency variations of about 0.3 Hz and high-frequency variations of about 41, 67 and 131 Hz. Studying RPM variations by comparing field data to model outputs allows for interpretation of this pattern as stick slip phenomenon coupled with whirl. The discrepancy between modeled and field data can be attributed to many factors. The choice of modeled RPM(t) shape function is considered most important, i.e. a triangle or step function would show different results than this sinusoidal function. Another factor could be the coupling between stick slip and whirl amplitudes, i.e. the whirl rotational speed may or may not be directly correlated with the RPM fluctuations.

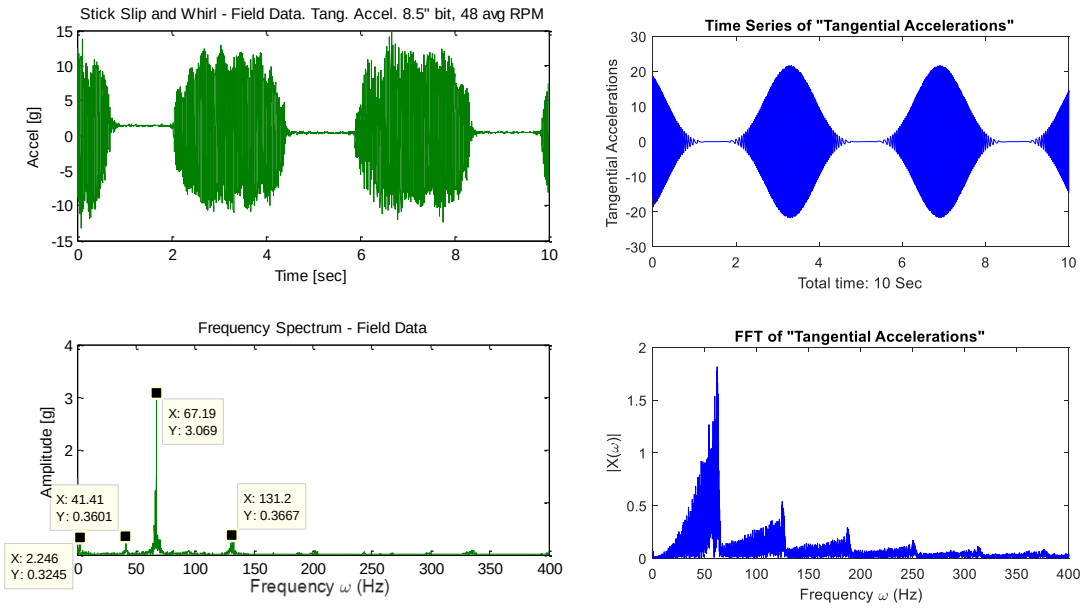

Fig. 10—Tangential accelerations, field data on the left and simulation on the right, of coupled whirl and stick-slip vibrations. 10 second windows of 800 Hz data on top, Fast Fourier Transform of the data on the bottom. Parameters for simulation: Borehole diameter: 8.5 in., clearance: 0.18 in., 48 RPM (average), stick slip period: 3.6 seconds, average whirl frequency: 45 Hz.

Fig. 11 shows radial accelerations during a long stick-slip cycle with a period p_t of 8.5 seconds. Just as RPM picks up, typical whirl patterns appear. The fluctuations show a lower amplitude when a certain speed is reached and increase again at the end of the slip cycle with low RPM. Again, the field data shows an offset of about 4 g, which is attributed to a sensor drift and/or calibration issue. This particular pattern occurred throughout the bit run. Field data suggests that one or more parameters change within the stick-slip cycle and thus cause the change in whirl amplitude. One possible hypothesis is that the whirl stops at the peak of the RPM cycle, and picks up once the pipe speed slows down again. The model output on the right side is not capable of replicating this sudden decoupling of whirl and stick slip within the slip cycle.

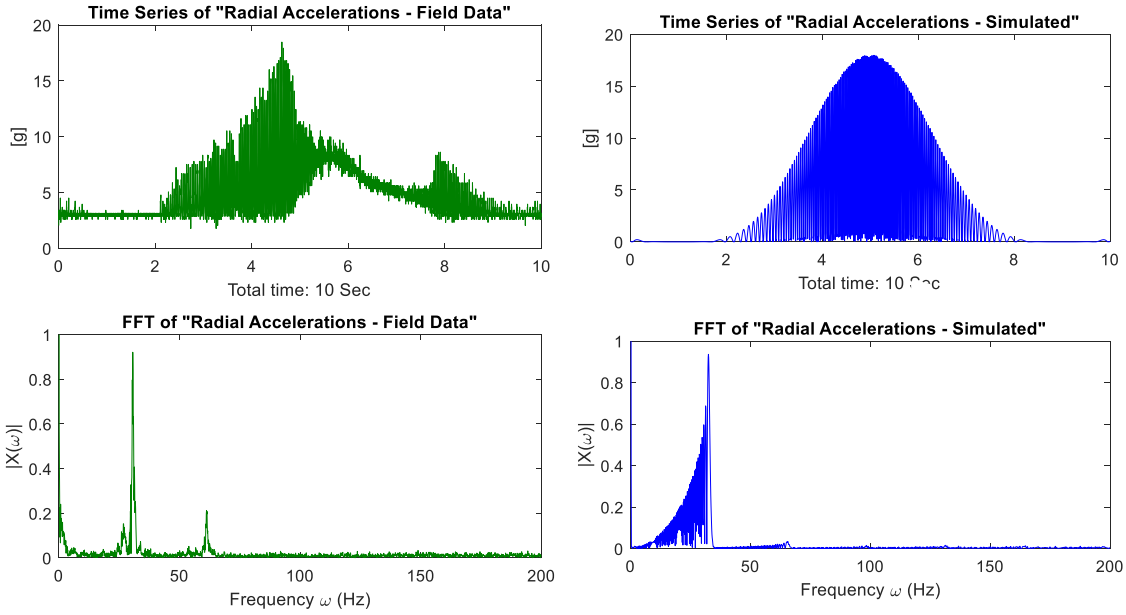

Fig. 11—Radial accelerations, field data on the left and simulation on the right, of coupled whirl and stick-slip vibrations. 10 second windows of 400 Hz data on top, Fast Fourier Transform of the data on the bottom. Parameters for simulation: Borehole diameter: 7 in., clearance: 0.13 in., 150 RPM (average), stick slip period: 8.5 seconds, average whirl frequency: 19 Hz.

Investigations using a kinematic model with variable parameters in real-time allow relating sensor data to actual pipe movements. This helps to create a better understanding of the physics of vibrations in pure or coupled forms, producing more accurate and faster predictive models, and eventually finding better mitigation strategies for drilling dysfunctions. Detailed studies and simulation of coupled effects will be part of future work.

2.5.4 Kinematic Model Limitations

Fig. 12 presents field data of radial accelerations. It shows periodic patterns of 2.6 Hz and typical whirl frequencies with 75 and 95 Hz. The measured radial accelerations reached the highest values of the entire run whenever this pattern was present in the data.

Interestingly, the radial accelerations vary in both positive and negative directions. These patterns may not be related to stick-slip, since radial accelerations would never be negative in that case. In laboratory experiments, Minett-Smith et al. (2010) observed a transition phase before backward whirl gets fully developed (**Fig. 13**). At that stage, the BHA experiences strong lateral shocks. The relatively elevated levels of positive and negative radial accelerations therefore could show up if the bit laterally "bounces from one wall to another". The periodicity of patterns in this data suggests an interpretation as backward whirl, rather than chaotic whirl.

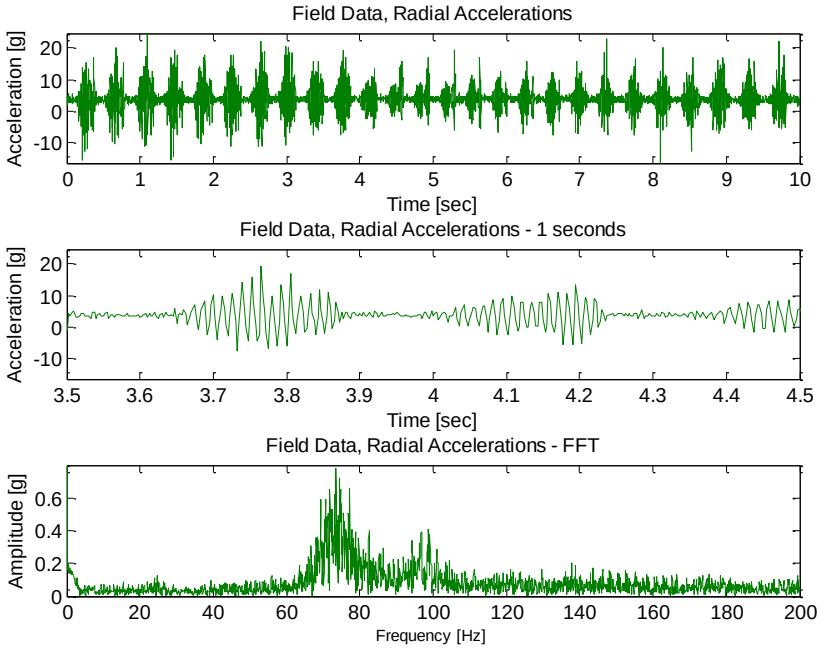

Fig. 12—Field data, radial accelerations showing periodic patterns with negative values.

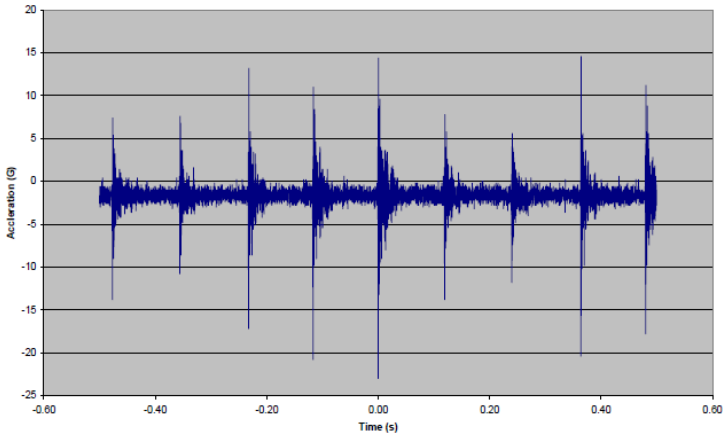

Fig. 13—Recorded data of impact between BHA and borehole wall for partial backward whirl with 5 impacts per second at 100 RPM (Minett-Smith et al. 2010).

As mentioned in the model description, in the context of the presented model, forward and backward whirl only refer to the direction of whirl rotation in relation to the drillstring rotation. In literature, forward whirl may refer to a special case of forward synchronous whirl, where whirl and pipe rotational speed are exactly the same. Backward whirl has been described as a high impact force and thereby destructive phenomenon. The kinematic whirl model can be used to demonstrate expected accelerations for the general case. If field data measurements exceed expected forces, explanations of such special cases require the presence of additional driving forces and could indicate more severe vibrational dysfunctions.

2.5.5 Input Variable Sensitivities

Characteristics of the output signals are levels of accelerations or velocities, frequency peaks, periodicity of overtones (peak distances) and relative amplitudes of frequency peaks. The effect of changing model input variable on these characteristics of the simulated data output is not straight forward. A reduction of pipe eccentricity, for

example, results in lower acceleration levels, while other input variables have more complex effects. In particular, the interaction of whirl and changing RPM values requires further investigation by comparison of model outputs and field data.

In **Fig. 14**, the clearance between borehole and drillstring is varied while all other parameters are kept constant. Radial, tangential, and combined accelerations are displayed in the frequency domain, by performing a Fast Fourier Transform of the signal for each of the incremental changes in clearance. Radial acceleration levels of the dominant frequency increase with increased clearance while tangential levels decrease. The resulting acceleration vector remains constant for any clearance value. When the drillstring radius is exactly half the borehole radius, the frequency overtones disappear in the radial acceleration signal, while they reach peak levels in the tangential acceleration case.

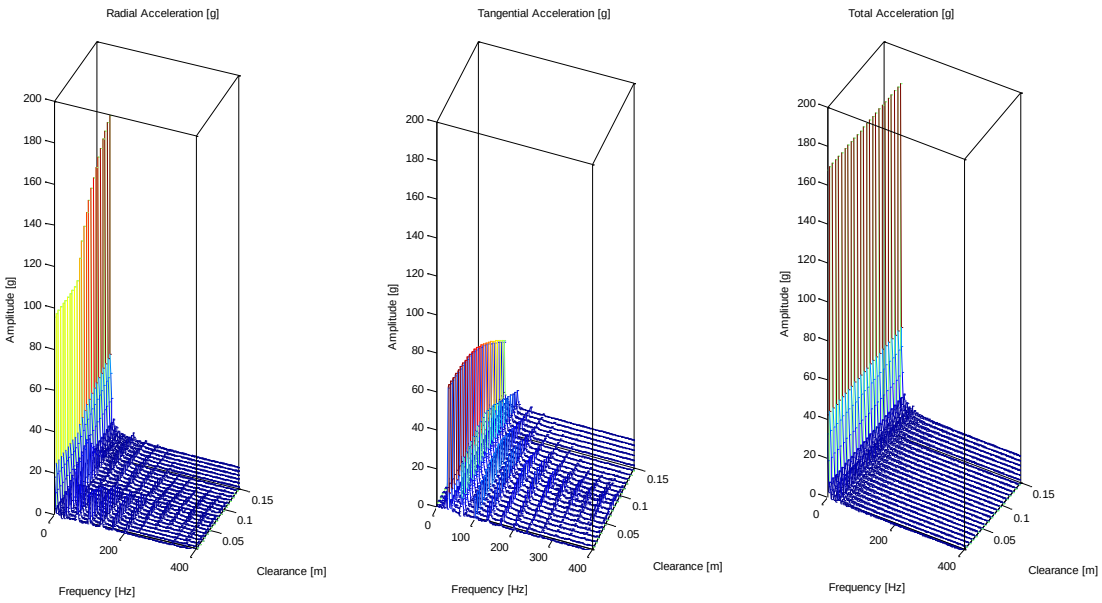

Fig. 14—Simulated data. Influence of variance in clearance on radial, tangential, and combined accelerations.

2.6 DISCUSSION

2.6.1 Pipe Rotational Fluctuations vs. Whirl

Appendix A.3 illustrates the expected measurements in time and frequency domain for a hypothetical HFTO pipe movement, i.e. high-frequency fluctuations of RPM(t) modeled as a sinusoidal function with a period of 0.05 (20 Hz). As predicted by Eq. 4, the tangential acceleration shows the exact same frequency content as the input signal (20 Hz) and radial accelerations have one additional "overtone" of twice the input signal (40 Hz). Unless the input signal RPM(t) is modified to a more complex function, the HFTO assumption is not capable of replicating the field data with its complex frequency spectrum.

The comparison of model output and real-time data shows that this whirl model with constant pipe and whirl rotational speed in contrast can explain high-frequency fluctuations of both radial and tangential accelerations solely by the effect of eccentric rotation of the drillstring. The model in this work does not require any three-dimensional geometries or dynamic effects that attribute these simulated frequencies to natural frequencies of the drillstring or any other dynamic system.

Occam's razor states that "among competing hypotheses, the one with the fewest assumptions should be selected". Whirl is a proven and observed physical effect during drilling and thereby presents a logical candidate for the origin of "HFTOs". Under field conditions with well explored phenomena such as buckling, pipe sag, well paths with micro-doglegs, etc. the assumption of "no whirl" (constant instantaneous center of rotation) is actually unrealistic.

By contrast, explaining the same measurements using the concept of real high-frequency torsional oscillations requires a very different set of assumptions. First, the existence of high-frequency variations needs to be postulated. Note that the phenomenon

was “discovered” only based on observations in downhole high-frequency data (Evangelatos and Payne, 2016). Second, the kinematic model (Eq. 5 and 6) for radial and tangential components depends on the choice of function RPM = RPM(t). These functions are unknown and further assumptions of their characteristics are required. Previous work (Dykstra, 1996) simplifies the problem assuming a sinusoidal function, even though, in the case of lower frequency RPM fluctuations during stick slip, field data shows a large variety of shapes. We use the same sinusoidal function here to show coupling effects of stick slip and whirl vibrations, but our alternative theory of the origin of high-frequency tangential fluctuations being a sensor artifact does not require any such assumption.

Comparing the assumptions required for the two explanations of the same phenomena, it is concluded that Occam’s razor favors the whirl alternative, as the simplest, most logical explanation for the HFTO observations. The model therefore offers an alternative explanation of the phenomenon of “high-frequency torsional oscillations” as a sensor artifact caused by off-center rotation during whirl events.

In addition, providers of vibration monitoring services claim that the whirling motion can be accounted for using opposite accelerometers and adding or subtracting the measurements. As demonstrated using the whirl model in Appendix A.4, this approach, however, does not eliminate the high-frequency fluctuations in the data.

This work demonstrates that as soon as the drillpipe rotates off-center, sensors placed on the side of the drillstring no longer represent the string as a whole. Sensors undergo a different path than the center of the pipe. Equations that apply for uniform circular motions no longer apply under whirl motion. This is not only true for accelerometers, but also for gyros and magnetometers that show similar high-frequency fluctuations under whirl. However, these exact sensors are used to infer the rotational speed

of the drillpipe (RPM). Hohl et al. (2016) claim that the occurrence of fluctuations in RPM is the causation of tangential accelerations. They thereby they neglect the possibility that the fluctuations in both cases are correlated and have similar root causes (**Fig. 15**).

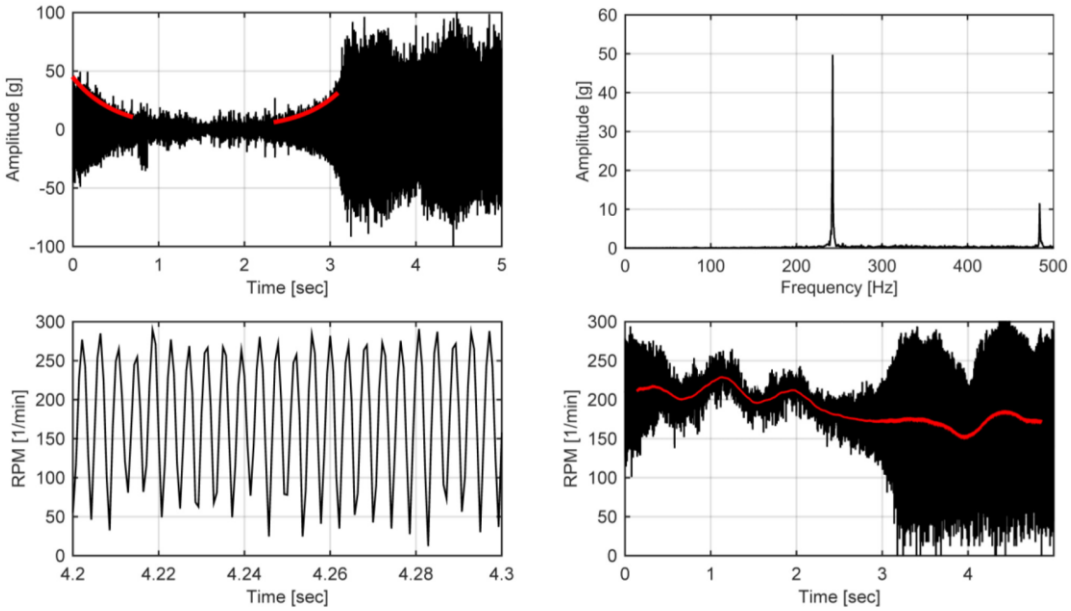

Figure 1—Tangential accelerations measured at the bit at a radius of 0.036 m in time and frequency domain (upper left, upper right). Rotary speed measured in revolutions per minute (rev/min) for one set of high-frequency data and zoomed in (lower left, lower right).

Fig. 15—Hohl et al. (2016) use calculated RPM values to claim a causation of high-frequency torsional oscillations in the tangential acceleration signal by fluctuations in rotary speed.

Fig. 16 compares the magnetometer reading with calculated RPM values for data recorded at a sampling rate of 800 Hz. Note that the time scales are 5, 10 and 3 seconds for normal, stick slip vibrations and whirl vibration respectively. For the case of normal drilling and stick slip, the calculated RPM values do not show significant high-frequency fluctuations. For the whirl case, calculated RPM values show fluctuations in accordance with whirl frequencies. RPM values are calculated from gyro or magnetometer data. Equations for RPM calculations, again, assume that assume uniform rotation (Meyer,

2007). Hence the high-frequency fluctuations in RPM values are again a sensor artifact that needs to be accounted for.

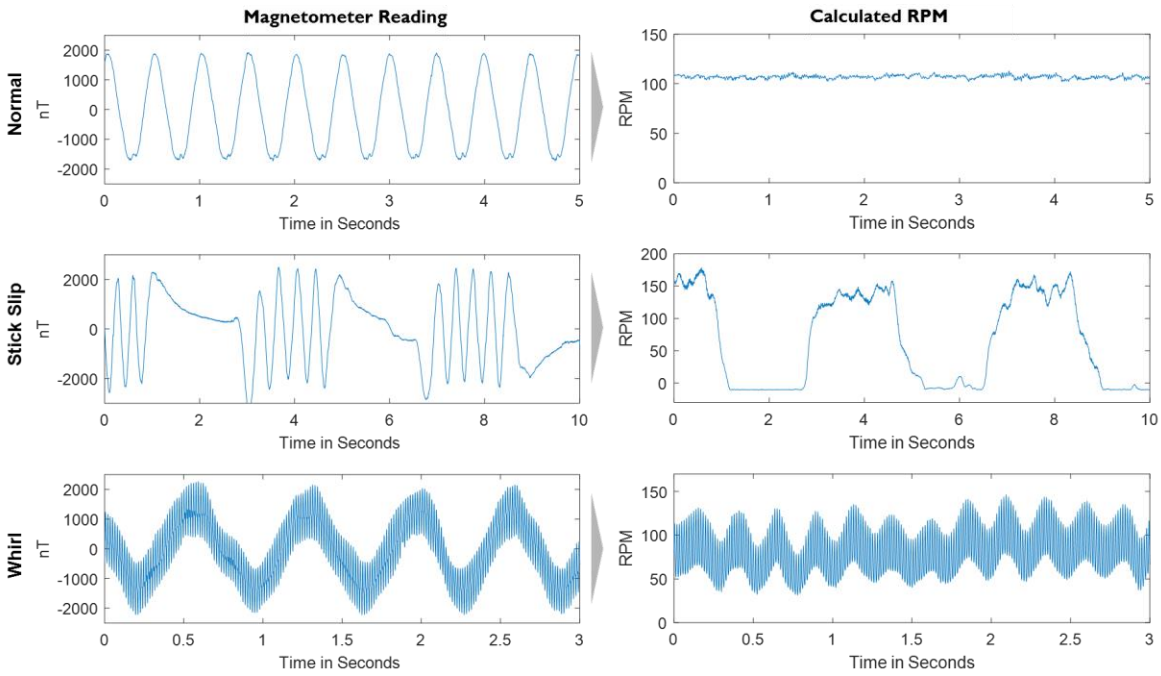

Fig. 16—Comparison of magnetometer data and calculated RPM values for normal drilling (upper), stick slip (middle) and whirl vibrations (lower). Note that the time scales are different for each of the three cases.

2.6.2 Experimental Proof for Future Work

The following section describes a possible controlled experiment that could provide a proof for the described whirl hypothesis and will be subject to future work:

The setup is a drillstring simulator that consists of a series of lumped masses mounted on a slender steel rod (Fig. 15). A motor provides rotary motion at defined rotational speeds. Such an experimental setup, for instance, has been developed at the Shell Research Center in Rijswijk (Shor, 2016).

In contrast to field operations, in this setup it is possible to add ‘outside observers’ to the drillstring system. These outside observers are high speed cameras that detect the rotational speed of individual elements. Vertical stripes on the string elements allow a visual analysis of the generated images. The cameras need to capture enough images to identify possible high frequency fluctuations in the rotational speeds (at least 500 frames per second). In addition, the cameras also capture any lateral movement of the individual lumped masses. To compare data from the experiment with available field data, radial and tangential accelerometers should be placed on string elements at an off-center position.

During the experiment, the drillstring is rotated by the motor at the top with a constant rotational speed. Additional sensors are required to ensure such a constant RPM input. The drillstring needs to be brought into a whirling motion. This could be achieved by a mechanical lateral displacement at a certain point along the string or by implementing a bent section into the steel rod.

For the analysis, data from the accelerometers on the string is compared with data from the RPM input and the high-speed cameras. The cameras can detect either whirling motions or torsional fluctuations of the drillstring. Data from the accelerometers then provides expected measurements for each type of pipe movement.

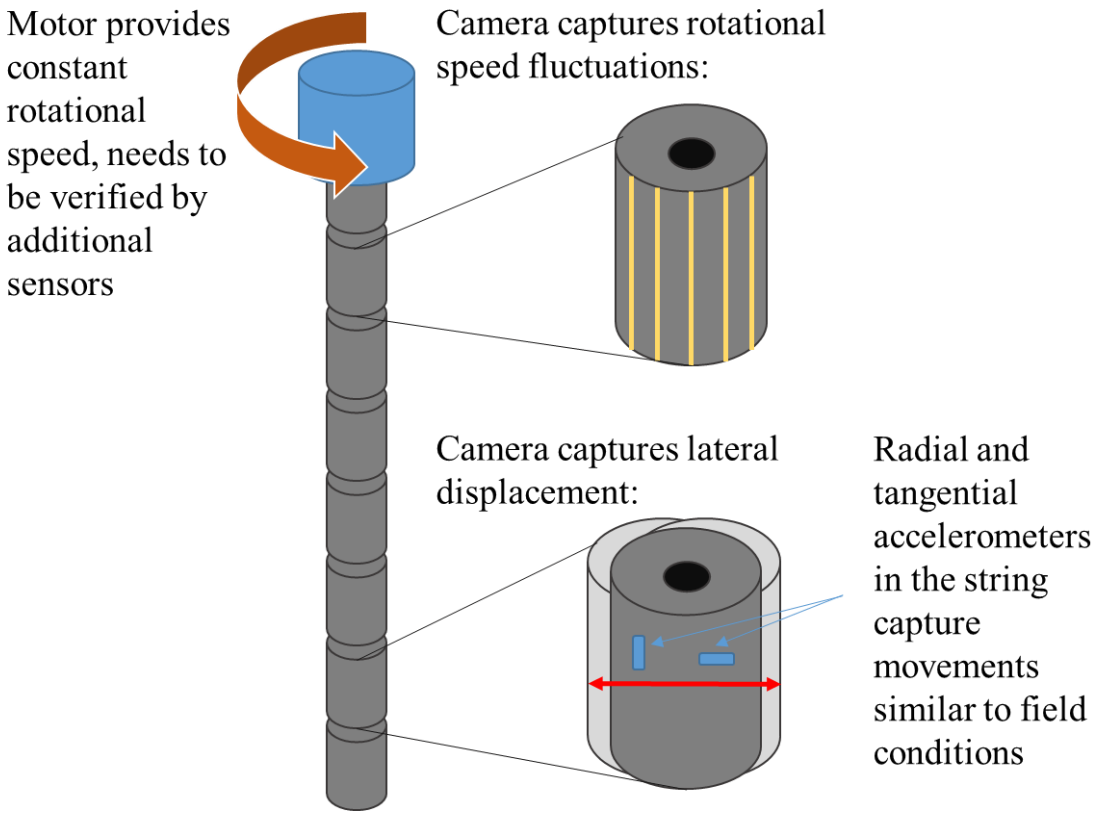

Fig. 17—Possible experimental setup to verify sensor artefact vs. high frequency torsional oscillations.

2.6.3 Comparable Application

A tangible analogy to the forces that apply to a sensor located on the side of a wobbling drillstring, exists in a very different context, the readers might have experienced firsthand: visitors in several theme parks around the world can enjoy a spinning tea cup ride. In Disney parks, these installations are named Mad Hatter Tea Party, inspired by a scene from Alice in Wonderland. A rider sits inside a tea cup that spins around its own center. Several groups of such tea cups are mounted on a larger turntable, sometimes rotating within even another turntable. Although individual rotations are smooth, their combination exerts rather strong “fictitious” forces on the riders.

2.6.4 Implications of Findings

In state-of-the-art MWD tools, multiple multi-axis accelerometers are deployed to accurately separate lateral from torsional measurements. Although Zanonni et al. in 1993 pointed out sensitivities of the radial accelerometer response to changes in RPM, a current perception is that accelerations in radial directions correspond only to lateral vibrations and tangential accelerations are indicators for torsional fluctuations and stick-slip. The kinematic model clearly demonstrates that as soon as the rotational axis does not align 100% with the center of the borehole, these signals cannot - and should not - be looked at independently. Whirl affects the measured rotational speeds and accelerations, while stick-slip also affects lateral measurements. Using the results of this whirl model, we can interpret high-frequency fluctuations as whirl and differentiate them from stick slip by their frequency content (Baumgartner and van Oort, 2015; see also Chapter 3), not by measurements of sensors oriented in different orthogonal directions.

The current practice of only studying statistics (such as RMS, minimum or maximum values) of the data over certain time windows results in the loss of valuable information. High or low frequency signals can generate the same statistical values, despite their inherently different high-frequency patterns. In addition, measurements are not (yet) standardized (Osnes et al., 2009). They depend on the setup of the tool, on the placement of the tool in the drillstring, on the position of the sensor within the tool, on the type of accelerometer, on the number of sensors, on the number of measurement axes and so forth. In Chapter 4, we demonstrate the effectiveness of automated pattern recognition methodology when classifying large amounts of high-frequency data, an approach that takes overall acceleration levels and signal frequencies into account.

2.7 CONCLUSIONS

A 2D kinematic model for whirl vibrations is proposed in this chapter. It represents the drillstring as a rotating disk within a larger circle of the borehole. The inner disk was prescribed an off-center rotational movement (whirling motion) that allowed the calculation of the velocities and accelerations experienced by a sensor placed at any point of the inner disk. Expected tangential and radial accelerations of a sensor are derived using a numerical as well as an explicit approach. Considering the sensor location, the kinematic equations of bit whirl closely reproduced whirl vibration patterns observed in multiple field data sets, both in time and frequency domains.

The simulated responses demonstrate that high-frequency fluctuations of tangential and radial accelerations can be attributed to a whirling motion of the drillstring. The frequency of these fluctuations can reach hundreds of Hertz. Thus, this work offers an alternative explanation of fluctuations in tangential acceleration measurements, previously attributed to a phenomenon termed high-frequency torsional oscillations (HFTOs).

The current work illustrates that the location of the sensor within the measurement sub must be considered when processing or analyzing downhole drilling high-frequency data. The path of the sensor is different from the path of the center of the string. Additional accelerations are recorded that do not represent the motions of the drillstring as a whole. For this reason, perfectly valid models of vibrations may not match up with measurements, unless sensor artifacts, such as the one described here, are considered. Eccentric rotation of the bit, BHA and/or drillstring affects the measurements of rotational speeds. To distinguish these vibration types from accelerometer measurements, the patterns should be investigated explicitly. Current practices of averaging accelerations or deriving only RMS

and maximum/minimum accelerations over a certain time window are insufficient to fully resolve downhole dysfunction behavior geared at taking the right mitigation actions.

Chapter 3: Optimization of Downhole Dynamics Measurement Systems[6]

3.1 INTRODUCTION

Downhole data transmitted in real-time can be used to optimally select parameters during drilling and optimize off-bottom operations. The wealth of information from retrieved memory data gives immediate insights in well specific performance limiters. Nevertheless, downhole data is not yet used to its full potential, as the industry is only just beginning to make sense out of the many gigabytes of recorded data. Often, measurements cannot be unambiguously linked to specific downhole dynamics and their respective dysfunction. Most valuable information is lost directly at the sensor when processing (e.g. averaging) is not done appropriately. In other cases, vast amounts of high-frequency data are transmitted and stored without providing much useful information. Large data volumes quickly reach the limits of transmission broadband and memory capacities of downhole tools. At surface, they pose huge challenges to drilling data analysis and data integration.

As a solution to handling the rapidly increasing amounts of drilling data, this chapter proposes a value of information based approach to downhole sensors, data processing and analysis. An extensive set of field data from multiple operations is used to demonstrate the interrelation of dynamic effects and their impact on downhole sensor measurements. Different requirements on sensor type and sample frequency apply to

[6] Chapter based on: Baumgartner, T., & van Oort, E. (2015, September 28). Maximizing Drilling Sensor Value through Optimized Frequency Selection and Data Processing. Society of Petroleum Engineers. doi:10.2118/174986-MS. Contributions: Baumgartner, T.: Author, van Oort, E.: Supervisor.

identify several types of drilling performance limiting dysfunctions, such as vibrations, well tortuosity or cutting accumulations due to poor hole cleaning.

It is shown that the analysis of frequencies is key to separate multiple downhole effects wrapped into one measurement. For each prominent type of dysfunction, minimum data collection frequencies are specified. This approach allows for the differentiation of unimportant noise from valuable drilling performance insights. These insights are used to describe more effective methods of data processing, by cross-linking information from multiple sensors.

3.1.1 Data and Performance

Data can either be an enabler or performance limiter in drilling. Without transparency on surface actions and resulting downhole reactions, drilling is essentially a black box that limits its practitioners to trial and error. With direct access to comprehensive information on the downhole environment, drilling mechanics can be fully understood, procedures can be optimized and risks largely eliminated.

Sensors are only capable of capturing a low dimensional snapshot of the complexity of the dynamics they are exposed to in a downhole environment. With increased data transfer capabilities, there is a tendency to simply increase the number of sensors downhole and collectively increase sampling rates. But more is not necessarily better. First, even the large transfer bandwidths of wired drillpipe can be exceeded with a few high-frequency sensors. Second, the amount of data produced by each drilling rig already cannot be fully analyzed in all its granularity at surface with current data processing technology. Third, not all data is equally valuable and useful.

Insightful information on downhole dysfunctions and mechanical correlations is already present in current downhole data sets. In this work, we show how the value of

massive amounts of "confusing" and ambiguous downhole data can be increased and how a separation of valuable information from unimportant noise and sensor artifacts can be achieved. By answering the question "*what specific information is required to identify and mitigate performance limiters?*", this chapter provides guidance on maximizing the value of current downhole sensors. At the same time, it shows how current and future downhole sensor data loads can be rationalized and managed.

3.1.2 Value of Information

Inadequate information on drilling dysfunctions is a real drilling performance limiter. The physical disconnect between the bit and surface, as well as additional barriers to data transfer are the main obstacles to exploit opportunities for drilling optimization and more efficient well delivery. Wired drillpipe was developed to overcome these limiters with high bandwidth bi-directional communication. Such recent technologies constitute significant improvements, but do not fully solve the issues of access to downhole information. New subs, equipped with more sensors, measuring, and transferring data at higher sample rates are currently under development and will quickly swamp bandwidths and downhole memories.

Streaming data from surface or downhole fulfills a variety of current or future purposes. For the detection of drilling dysfunction from downhole data, different types of dysfunctions require different datasets. To optimize the system of data capturing, transfer, analysis, and implementation it is essential to consider the end usage of the data. How many magnetometers are required to record downhole RPM for the purpose of stick slip alarms? What is the required sampling and data transfer rate? What data sensors and sample rates are required for automated surface adjustment of WOB and RPM parameters?

A piece of information is considered valuable if - and only if - it reveals new insight on the occurrence or state of drilling dysfunctions, and this insight can be used to make drilling improvements. Every sensor incrementally adds transparency and knowledge on downhole environment and dysfunctions. But at some point, the user knows enough, such that any additional data becomes of rapidly diminishing value. Under data transfer and budget limitations, what is the minimum set of measurements that allows the driller to be sufficiently informed to cope with most - if not all - of the drilling performance limiters and achieve optimized drilling conditions?

3.1.3 Sample Rate Requirements

In a system with bandwidth and memory limitations, the number of channels (signal outputs), measurement sample rate and measurement duration (for memory only) can be adjusted to optimize the information gain from downhole sensors. Sensors transfer an analog signal into discrete samples and later reconstruct a continuous function of the measurement. If the sampling rate is too low, the reconstruction will exhibit imperfection. The Nyquist criterion states that for a perfect transfer of an analog to a digital signal and vice versa, the sampling rate should be at least twice as high as the frequency of interest in the recorded signal. On the other hand, to delineate the dynamic effects of interest, phenomena do not have to be measured at a sampling rate much higher than this Nyquist frequency. Thus, a direct rationalization of sampling rate, data-storage and transmission can be achieved by characterizing phenomena of interest at their Nyquist frequency, and only at their Nyquist frequency. What those frequencies should be is discussed in more detail for various phenomena associated with the previously discussed drilling performance limiters in the next section.

3.1.4 Datasets

Data sets used in this work were collected from different drilling projects. High frequency data was captured during land operations in Oklahoma and in the Middle East. No postprocessing had been done on these data sets, so they were ideal to study patterns of high frequency from these data sets.

An operator conducted a drilling data study gathering data from 2 wells and 5 wells in two separate phases of the project. In phase 1, data was captured using continuous data (sampling periods of 2.56 seconds). In phase 2, all downhole data was collected using a sampling rate of 50 Hz for all available measurements. These measurements included annular pressures, axial vibrations, gravity, RPM (derived value), torque (corrected, derived), torque (uncorrected), weight on bit (corrected, derived), weight on bit (uncorrected). Surface data (1 Hz sampling rate) and other information such as daily drilling reports (DDR) and survey files were also available.

3.1.5 Approach

The downhole data sets were visually inspected to identify captured downhole dysfunctions. A comparison to literature, surface data sets and amongst multiple downhole measurements helped to identify data patterns and link them to their root causes. The data patterns are grouped by dysfunction type and into low/medium/high frequency ranges. The suggested sampling rates in this work are at least twice as high as the highest frequencies per dysfunction found in this dataset or shown in literature.

- *Literature review:* listing commonly observed drilling dysfunctions and expected frequency ranges. For some dysfunctions, especially vibrations, frequency ranges are common drilling knowledge and are available in literature (see Chapter 1.1.1

Drillstring Vibrations). These literature observations could be verified with the available data in our study.

- *Data processing:* data processing involves several steps to transfer data from the file format it was delivered into data sets that allow data analysis; including re-organizing files into an appropriate structure; understanding the content of the data, quality checking, and cleaning data.7
- *General visualization of data:* plotting downhole data together with available surface data. This step enables an overview over individual bit runs, hole depths, rig activities, etc. Additional general data can be found in daily drilling reports and needs to be studies to identify "unusual" operations and operational problems that may affect the data.
- *Visualization of data of interest:* to identify coupled effects of dysfunctions in downhole data, multiple data streams (WOB, TOB, RPM, Vibrations, etc.) are visualized on the same graph. Together with available rig activity information (drilling/tripping/connection, etc.) the data is screened for relevant patterns. A combination of measurements helps to identify the root cause: e.g. for bit bounce, WOB fluctuates while TOB stays relatively constant. Flexible display options, zoom functions and programmable plots are required to efficiently screen large data sets.
- *Signal processing:* for high frequency data, a discrete Fourier transform is performed to identify frequency spectra. An adequate selection of individual data windows has an outcome on the clarity of the results in the frequency domain. Since

[7] Details on the specific steps required can be found in Chapter 5.1.3 Transfer of Downhole Data – A Case Study, as well as in Appendix D.3.2 Data Curation

associated frequency peaks tend to change over time, the spectra get noisy for large data sets.

3.2 Downhole Measurements and their Interpretation

The interpretation of downhole measurements is everything but trivial. Using sensors, the phenomenon causing a measurement can only be inferred but in most cases not directly measured. Movement and loads acting on sensor are unknown and one sensor usually can only observe variables associated with one particular axis at a time. The direction of that axis changes as the sensor moves within the system. Direct calibration of sensors in the downhole environment is generally not possible, and verification of sensor measurements through other sensors is generally limited (although considerable progress has been made in this area, cf. Ambrus et al., 2013).

Despite these challenges, this section illustrates observable phenomena in field data and how the interpretation of measurements can be facilitated through differentiation by frequencies, comparisons of patterns and correlations of multiple signals.

3.2.1 Vibrations

The three basic types of oscillatory movements (vibrations) are differentiated into movements in lateral, torsional, or axial direction. In theory, vibrational types can be separated using orthogonally oriented accelerometers. In real measurements, we often see a variety of different phenomena captured by the same sensor and signal. These phenomena originate from a variety of root causes and a differentiation is essential for detection and mitigation of problems and for maximizing the information gain from a signal.

Lateral, tangential and axial vibrations are associated with reduced ROP, tool failures and lead to measurement errors in other downhole sensors. Close et al. (1988)

studying some of the first downhole vibration measurements already pointed out that often the highest levels of vibrations are recorded during off bottom operations, such as reaming or pumping and rotating while off bottom.

Lateral vibrations are responsible for the highest frequency dynamics (50 Hz and above, or periods of below 0.02 seconds). The results of Chapter 2 are again summarized here, because they are essential for the correct interpretation of the featured high-frequency data. **Fig. 18** shows a 5-second sequence of field data (800 Hz sampling rate) from a tangential accelerometer recorded during off-center rotation (left). A fast Fourier transform (FFT) of the data reveals frequency peaks of 66 Hz and above. These high-frequency fluctuations in the tangential acceleration data can be solely attributed to a whirling motion of the drillstring in the borehole. A simple kinematic whirl model was able to reproduce the sensor output in a simulation (right) both in time and frequency domain (see Chapter 2). In this case, the frequency responses are artifacts of the sensor movement within the drillstring, and do not represent the changes of acceleration the drillstring undergoes as a whole. The dominant frequency of such whirling movement ranges from 15 to 100 Hz, with overtones that can reach up to multiple hundreds of Hz, often exceeding the Nyquist frequency limits of the sample rate (Oueslati et al., 2013).

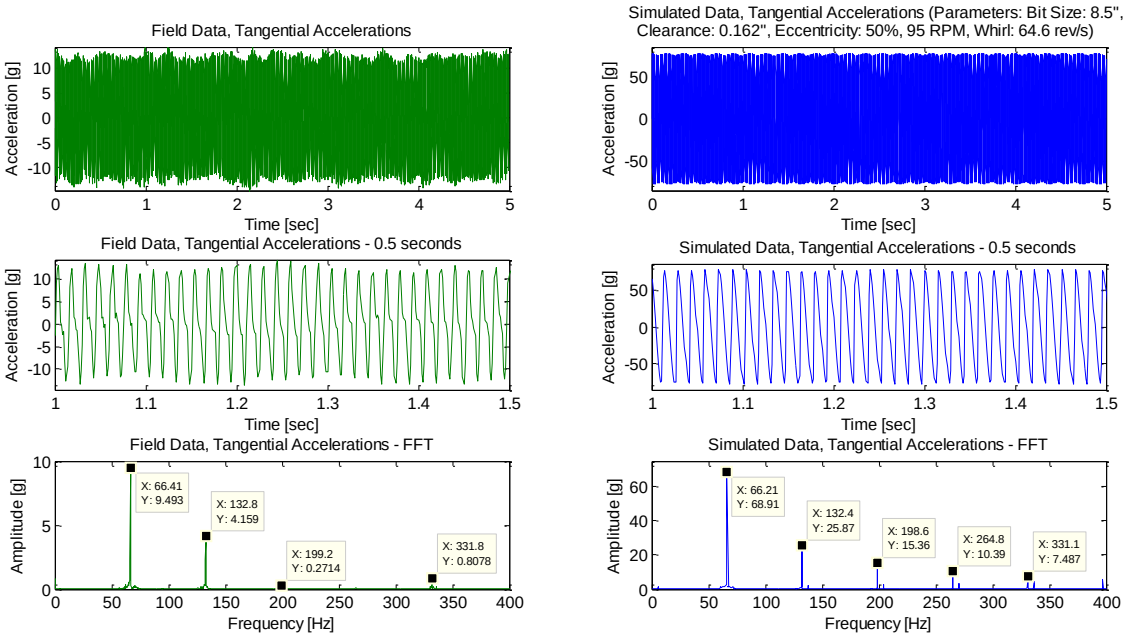

Fig. 18—Comparison of tangential accelerations for field data (left) and simulated forward whirl (right).

Fig. 19 shows radial accelerations with high amplitudes. Its motions and dynamics most likely can be accredited to a backward whirl phenomenon. In the case of pure rotation (despite off-center rotation, RPM fluctuations or both), radial accelerations are always positive. In this data set, radial measurements are both positive and negative. The negative accelerations could indicate the presence of additional forces, such as a bit laterally bouncing off from one wall to another. In laboratory experiments, Minett-Smith et al. (2010) observed a transition phase before backward whirl gets fully developed. Their data is comparable to data in Fig. 19**.** At this stage, bit, BHA or string experience strong lateral shocks. The frequencies observed with this type of whirl pattern are typically in the order of 60 – 120 Hz, with very high vibration amplitudes.

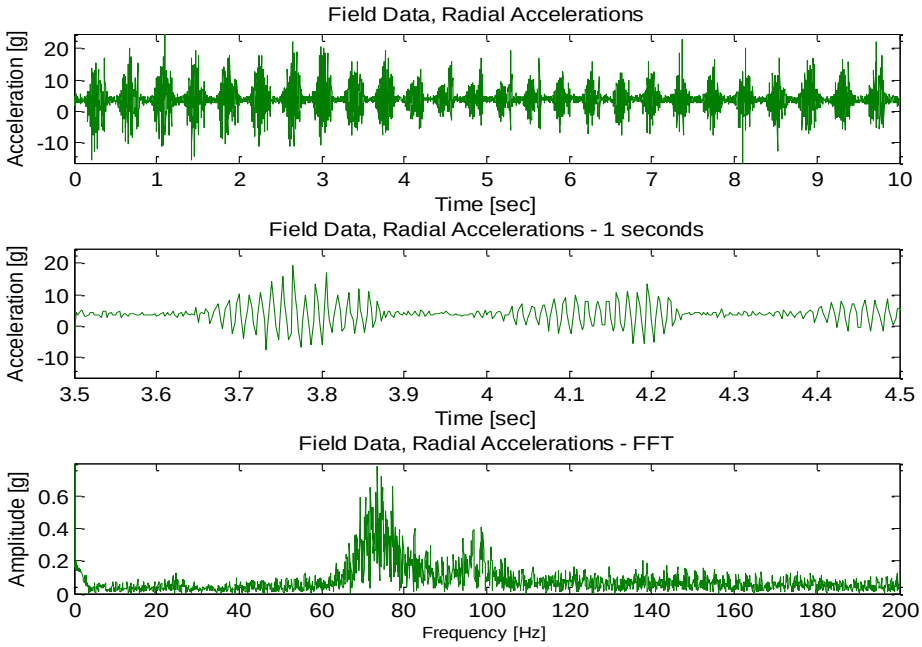

Fig. 19—Destructive whirl with dynamic forces causing negative radial accelerations of high amplitudes. Fast Fourier transform (FFT) of the data on the bottom shows characteristic frequency peaks at 74 and 92 Hz.

Torsional or stick-slip vibrations are visible in all downhole measurements. During the stick phase, radial and axial accelerations are reduced or close to zero or even negative, torque builds up and WOB decreases slightly. **Fig**. 20, **Fig. 21** and **Fig. 22** show periodic stick slip phenomena recorded at 50 Hz, with the periods of stick slip of about 5-6 seconds in each case. Downhole RPM values (blue line) are calculated from gyroscopes, with the measurement sub located right above the motor. RPM values in this data set had to be manually corrected for offsets (i.e. calibration/measurement errors). In these cases, it is easy to spot a zero RPM line from the stick slip patterns. In Fig. 20, stick slip periods are about 6 seconds. WOB, TOB and axial accelerations show patterns that are governed by stick slip behavior. Notably, TOB peaks just before the release from the stick period.

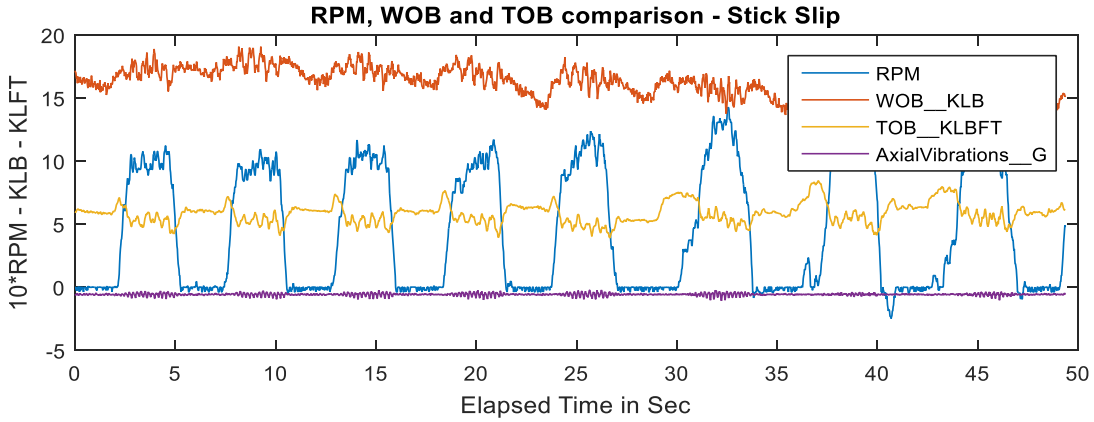

Fig. 20—RPM, WOB, TOB and axial accelerations under fully developed stick slip with periods of about 6 seconds.

In Fig. 21, severe stick slip (1st minute) is followed by lower level torsional oscillations and then again by fully developed stick slip (6th minute). The severe stick slip is characterized by periods of 1 seconds and negative RPM values that indicate a counter-clockwise rotation of measurement tool. A reduction of stick slip severity (minute 1 and minute 6.5) is correlated with a reduction of WOB.

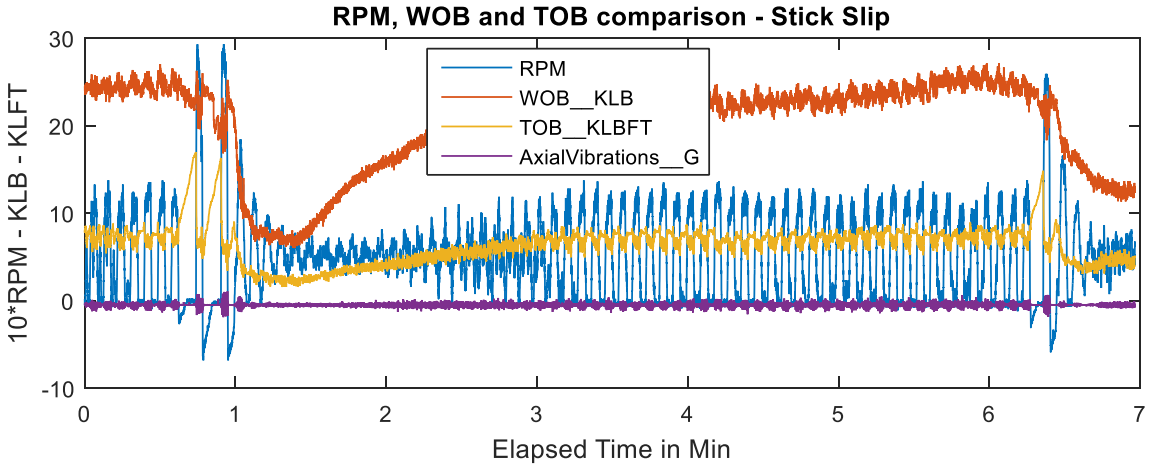

Fig. 21—Two severe stick slip events about 5 minutes apart.

Fig. 22 shows prolonged severe vibrations with counter-clockwise rotations. The stick slip periods are about 5-6 seconds long. RPM values are calculated from gyroscopes or magnetometers. In some cases, the derived values might be unreliable. Are the negative RPM values real? To eliminate the possibility of certain measurement or data processing errors when calculating RPM, downhole RPM data can be verified using surface RPM data: the total number of rotations during a given period of time must be the same for downhole and surface RPM data, when effects of "torqueing up" the string are neglected. These calculations were performed and verified the counter-clockwise rotation.

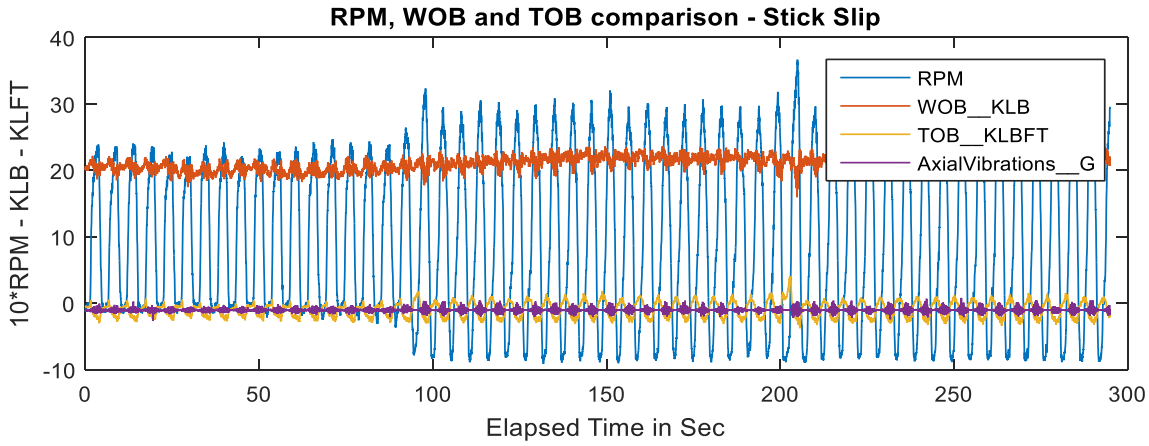

Fig. 22—Stick slip with significant negative rotational speeds, stick slip period about 5-6 seconds.

Axial vibrations (**Fig. 23**) have been a major subject of research for roller cone bits, but are scarcely observed in data sets with PDC bits. Axial vibrational frequencies are found to be in the range of 3 – 20 Hz. **Fig. 24** shows fluctuations of axial accelerations with two characteristic frequency peaks of about 0.25 and 7.5 Hz. A differentiator for axial vibrations are high fluctuations of WOB values, while TOB values are comparatively stable.

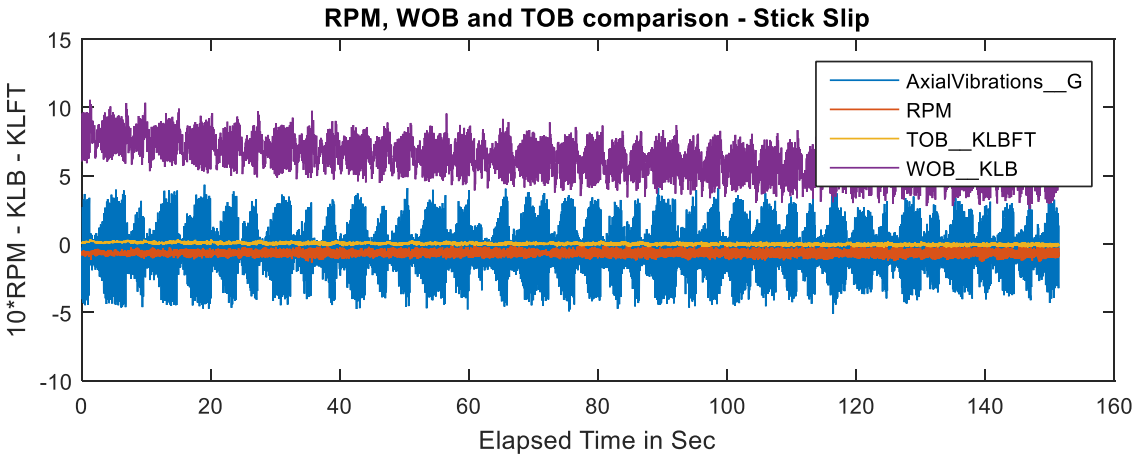

Fig. 23—Axial accelerations (blue) and corresponding WOB and TOB values.

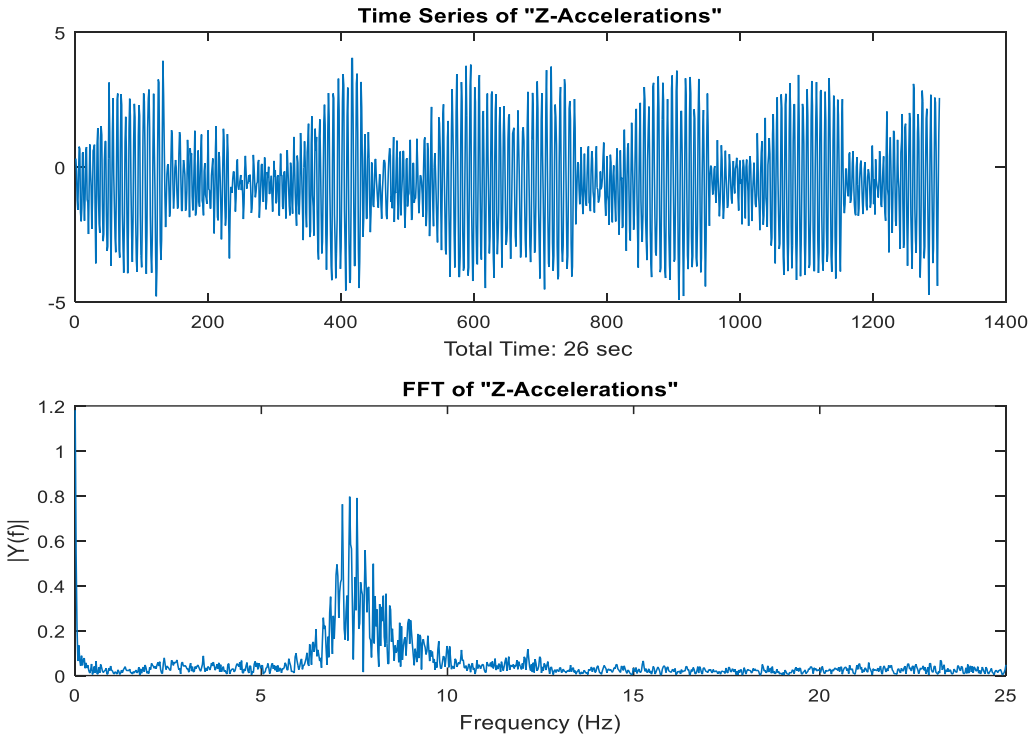

Fig. 24—Frequency response of axial vibration with a high-frequency peak of 7.5 Hz.

3.2.2 Strain Measurements

Weight on Bit is regarded as one of the key factors for optimizing the rate of penetration. Downhole WOB values are usually significantly less than surface WOB values, weight is "lost" through friction, trajectory, and hang-ups in the wellbore. Buckling, a dysfunction, where the string acts like a spring, can greatly reduce the effective downhole weight. As a rule of thumb for normal operations, 30% of the applied surface WOB gets lost. This ratio, however, can be much higher or lower, and can be highly non-linear. The ability to more effectively apply WOB based on downhole limits rather than surface restrictions holds great potential ROP performance gains for oil and gas companies. Reliable absolute WOB measurements and low frequency changes and trends are essential for using this downhole information appropriately. However, the WOB measurement is a composition of a variety of downhole dynamics, such as all three forms of harmonic vibrations. **Fig. 25** shows that under stick slip vibrations, WOB can fluctuate up to 10 klb, which in this case is 30 % of its maximum value of 30 klb. If, in a post-processing step, this 50 Hz data is averaged, these peaks might be removed from the data. Unable to observe the maximum loads in data displayed to e.g. a driller, unsuitable data could lead to exerting too high WOB during the slip phase. In addition, the data in Fig. 25 seems to demonstrate that stick slip vibrations are not affected by changes in WOB. Surface WOB is greatly reduced to almost zero within a period of 6 minutes, downhole WOB decreases simultaneously, but neither the amplitude, nor the period of stick slip seems to change.

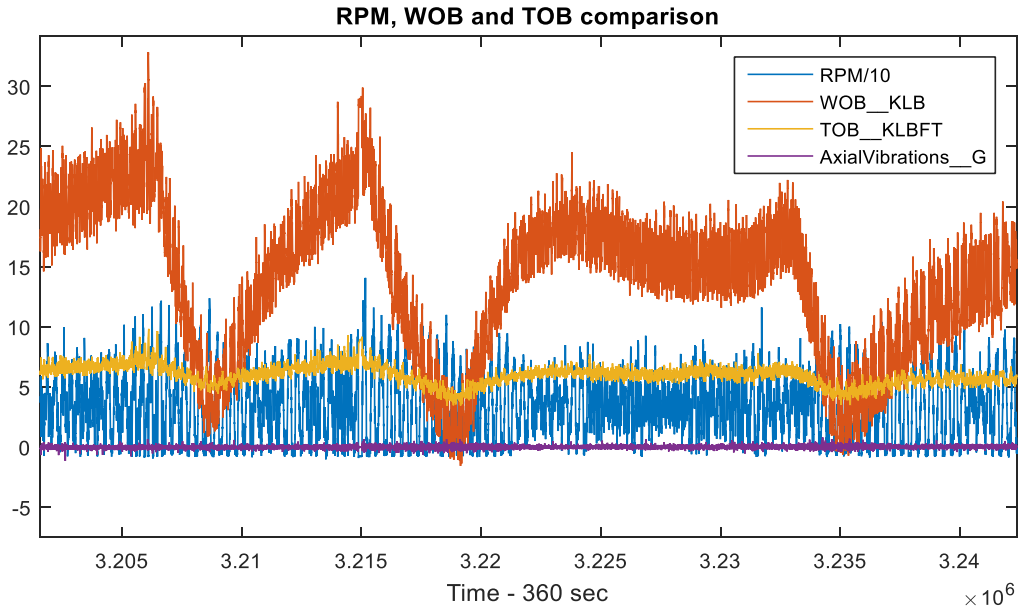

Fig. 25—Comparison of WOB and TOB under stick slip.

WOB measurements tend to oscillate in accordance with every rotation of the drillpipe despite relatively stable axial vibration levels. This can be explained by changes in the stress regime and bending of the pipe with every rotation, if there is a misalignment of the center of the drillpipe and the center of the borehole. **Fig. 26** compares these WOB fluctuations with magnetometer data. Magnetometers measure the earth's magnetic north and thus capture rotations in the inertial reference frame of the borehole. The stick slip pattern is clearly observable. In the slip phase, the pipe rotates 5 times, in the stick phase, the pipe rests at a certain angle from north and the data shows constant values. WOB measurements show a perfect alignment with magnetometer data throughout the entire run. This allows attributing WOB fluctuations to cyclic stress changes during each rotation. Changes in sensor design or post-processing techniques could remove such artifacts. Note that also the absolute WOB values in Fig. 26 are out of range. As detailed in Chapter 4, their offset is attributed to downhole pressures and temperatures acting on the strain

gauges.

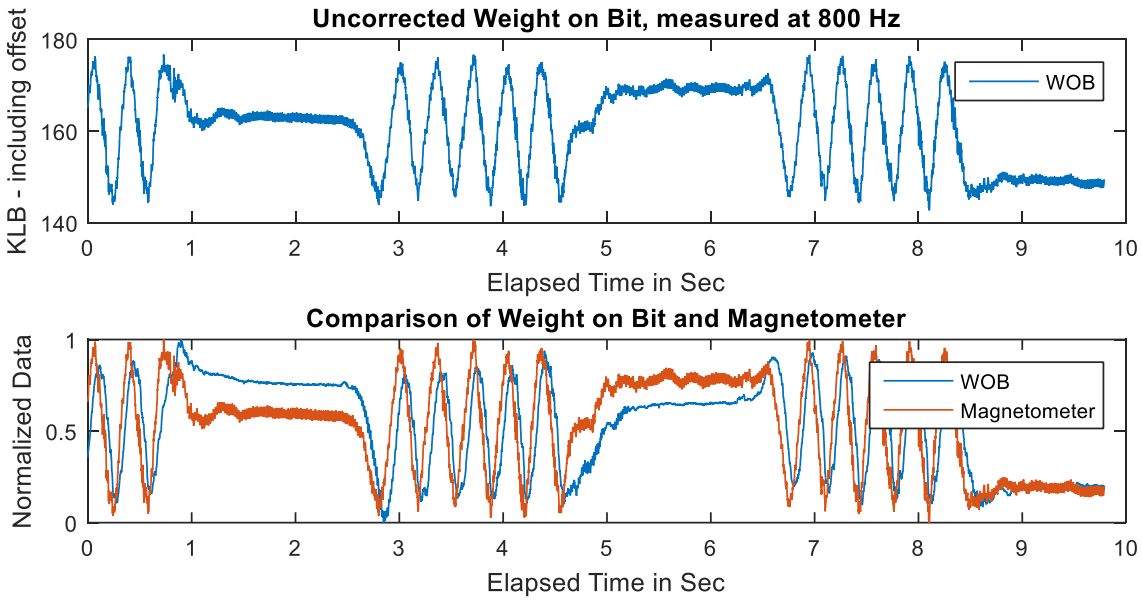

Fig. 26—Downhole WOB measurements (top) shows fluctuations of 30 klb that are correlated to rotations of the drillpipe.

Downhole torque (also referred to as TOB (torque on bit) or torque on tool) is obtained using strain gauges. In contrast to WOB, the strain gauges are offset by a certain angle to the axial axis of the drillstring. Downhole torque measurements are affected by pipe rotations as shown in **Fig. 27**.

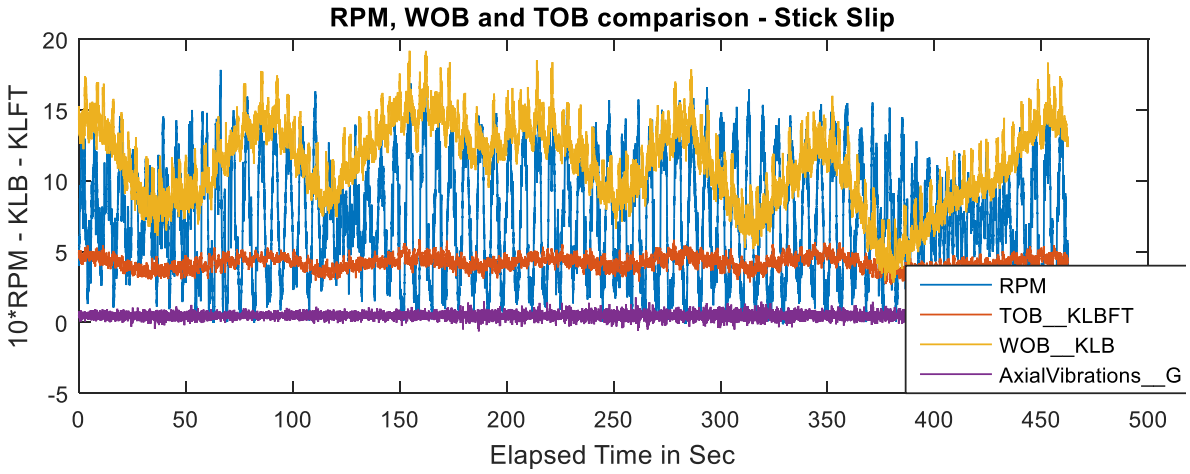

Fig. 27—Comparison of RPM, WOB and TOB shows the strong correlation of these three measurements with respect to their frequencies.

Bending information can be related to wellbore tortuosity. Dogleg severity as a measure of tortuosity is calculated from inclination and azimuth information. These surveys are usually taken every stand (90 ft) and do not capture wellbore tortuosity in its required granularity. Heisig et al. (2004) showed that downhole bending information from dynamics and MWD tools closely matched survey data.

3.2.3 Pressure

Sensors can record downhole pressures both inside the drillstring and in the annulus. Pressure data is used to infer slower response phenomena, such as hole cleaning efficiencies (e.g. Coley and Edwards 2013), downhole formation integrity tests (FIT) and equivalent circulating density (ECD) monitoring (e.g. van Oort and Vargo, 2008) or kick detection (e.g. Gravdal, 2009).

Still, high-frequency pressure data shows effects of lateral, torsional, and possibly axial dynamics. In **Fig. 28** a comparison of 800 Hz burst sequences reveals the effects of

lateral vibrations on the pressure recordings. Tangential acceleration shows a dominant frequency peak of 72 Hz. This frequency range, together with the pattern and rather low amplitudes of +/- 15 G indicate off center rotation, or whirl vibration. The same frequency peak of 72 Hz can be found for the internal drillpipe pressure. This indicates that the root cause of these high-frequency pressure fluctuations is related to whirl dysfunctions. One hypothesis is that these pressure fluctuations of 1000 psi could be caused by the off-center pipe movements. Another possible explanation are mechanical effects on the sensor itself, making them sensor artifacts.

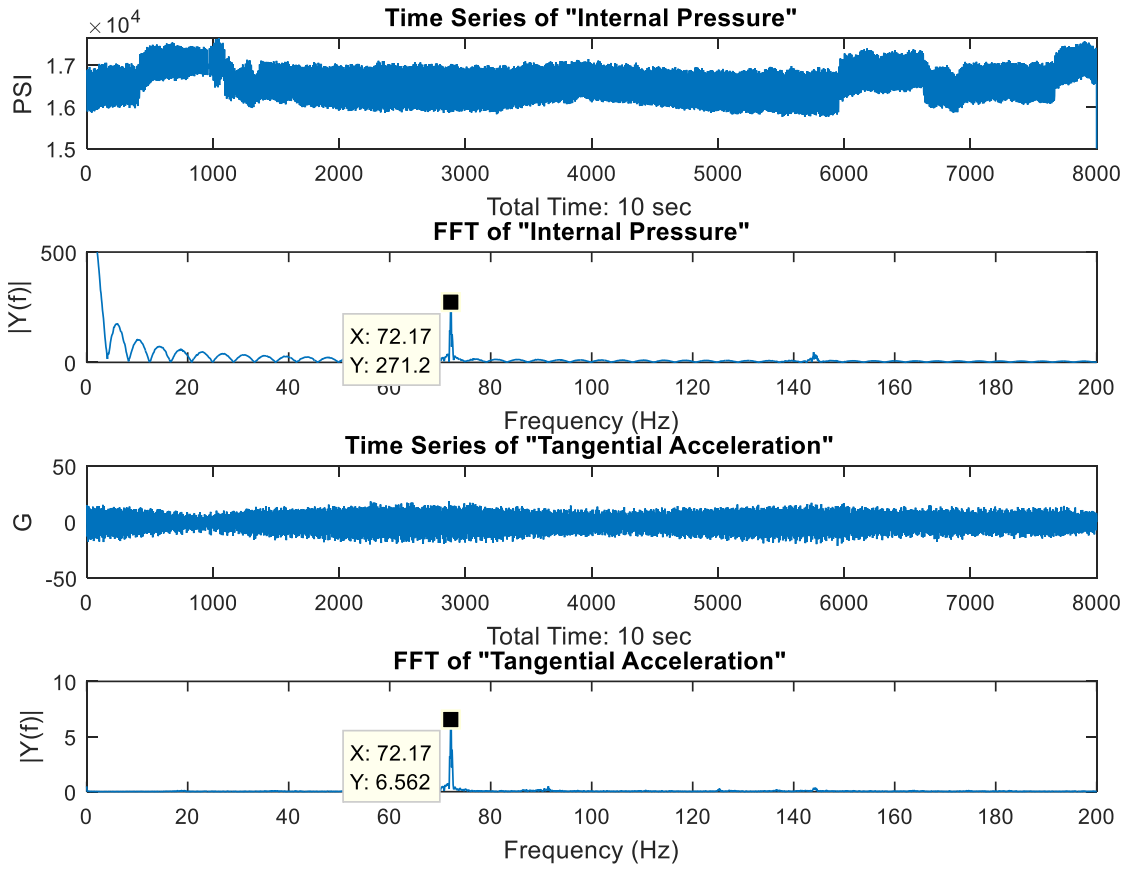

Fig. 28—Pressure fluctuations show exactly the same frequency peaks as tangential accelerations. These vibrations cause pressure fluctuations of 1000 psi.

Fig. 29 compares internal drillpipe and annular pressure. The pressure scales are quite different, still some fluctuations show a clear negative correlation of the two signals (see arrows in Fig. 29). Temporary restrictions of the bit nozzles, for instance, could simultaneously increase the internal pressure and reduce the annular pressure. Other effects appear only in annular pressure. A comparison of the two signals could help to differentiate pressure effects by their location of occurrence. For instance, flow restrictions in the nozzles could possibly have effects on both pressure readings, while annular cuttings accumulations will not be visible inside the drillstring.

Pressure data is typically monitored with a resolution of minutes to hours. Even formation integrity tests are conducted observing changes in pressure within a couple of minutes. The study of higher frequency pressure data could be beneficial for well control purposes. Hydraulic kick detection models suggest pressure responses to formation influxes within a couple of seconds (Gravdal, 2009).

Hardly any literature has been published on investigation of high-frequency pressure data. The Nyquist frequency principle should only be applied after thorough investigation of the highest possible phenomena in the data. Burst samples of 400 or 800 Hz are valuable for research on high-frequency pressure phenomena. These fluctuations may or may not influence drilling performance, however, it will be worthwhile to investigate. Just like in studies of patterns of vibration (Chapter 2), patterns in high-frequency pressure data could reveal a wealth of information on flow regimes and downhole dysfunctions.

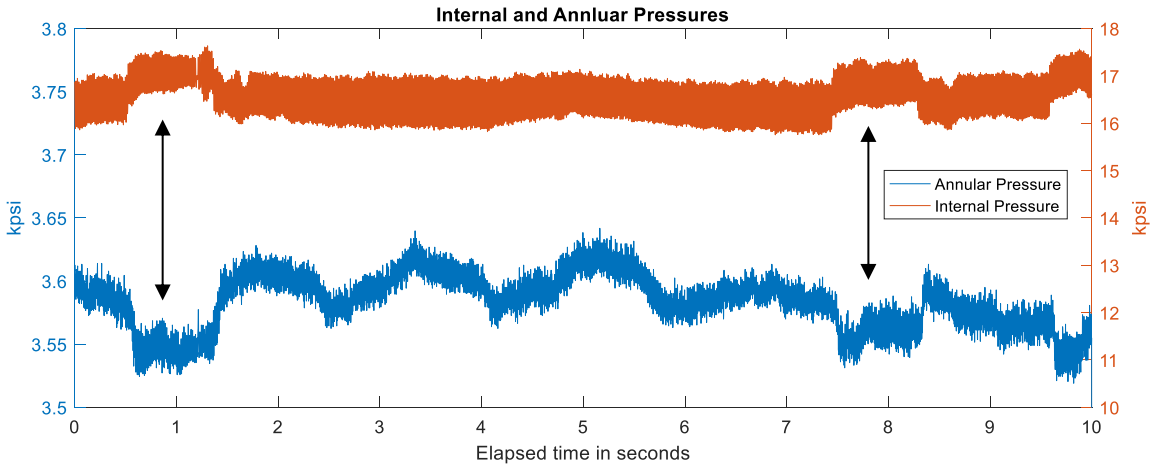

Fig. 29—Despite vastly different absolute pressures, high-frequency internal pressure and annular pressure show correlating pressure fluctuations.

3.2.4 Sample Rate Requirements

Fig. 30 summarizes downhole dynamics phenomena and frequencies observed in field data using commonly available downhole sensors. It specifies the required frequency to capture these phenomena with downhole sensors, based on the Nyquist frequency rule. This list can be used to greatly rationalize and optimize downhole data storage and transfer.

Type	Sub-Category	Comments	Observed Typical Frequency/Periods	Data Sampling and Processing Rate
Lateral Vibrations				
	Backward Whirl	Additional dynamic component, high amplitudes, negative radial accelerations	Up to 120 Hz +	250 Hz +
	Forward Synchronous Whirl	Identified from bit wear, whirl speed equals rotational speed, low frequencies	< 3 Hz	10 Hz
	Off Center Rotation	Only movement of the sensor without dynamical forces, very high frequency spectra of overtones (500 Hz+)	First mode up to 70 Hz + overtones	250 Hz +
	Chaotic Whirl	Described in literature, not (yet) identified in data		
Torsional Vibrations				
	Harmonic Stick Slip	Period depends on length of drill string, negative rotation can occur	<0.1 – 2 Hz	5 Hz
	Torsional Fluctuations	Frequencies related to RPM, Different sources, e.g. stabilizers, doglegs, buckling,	0.5 Hz – 10 Hz	20 Hz
	Lithology changes	Correlation with tangential acceleration, depth based	< 1 Hz	< 2 Hz
Axial Vibrations				
	Bit Bounce	Harmonic axial fluctuation of high amplitude	5-20 of Hz	50 Hz
	Vibrational Dynamics	Effects of lateral and torsional vibrations on axial vibration measurements	Up to 120 Hz	250 Hz +
	RPM Fluctuations	Stress and strain changes for each rotation, especially in curve section	0.5 Hz – 10 Hz	30 Hz
Downhole Weight on Bit				
	Weight transfer	Low frequencies	< 1 Hz	< 2 Hz
	Dynamics (Vibrations)	Whirl and stick slip frequencies	Up to 120 Hz	250 Hz +
	Bit Bounce	Harmonic fluctuation, medium frequency	5-20 of Hz	50 Hz
Downhole Torque				
	Torque Transfer	Due to friction, buckling	0.5 Hz – 10 Hz	20 Hz
	Torque Fluctuations	RPM related	0.5 Hz – 10 Hz	20 Hz
	Dynamics (Vibrations)	Whirl and stick slip frequencies	Up to 120 Hz	250 Hz +
Pressure				
	Kick detection	Pressure increase due to influx	< 1 Hz*	< 2 Hz
	ECD monitoring	Cuttings transport, surge and swap	< 1 Hz*	< 2 Hz
	Changes in DH pressure regime	Depending on DH pressures, ECD, pump rates, etc.	< 1 Hz*	< 2 Hz
	Dynamics (Vibrations)	Pressure fluctuations based on pipe movements	Up to 120 Hz	250 Hz +
Temperature				
	Temperatures	Low frequencies	< 1 Hz	< 2 Hz

… frequencies that reveal valuable information

….* currently reported in literature, high frequency pressure data may reveal higher frequency phenomena

Fig. 30—Summary of downhole dynamics observed in high-frequency downhole data.

3.3 SENSOR-SYSTEM REPRESENTATION

The dynamic environment that sensors are subjected to poses a major challenge on downhole measurements. A sensor is collecting data from a system which the sensor itself

is part of. Under such conditions, it is impossible to isolate measurements and solely capture dynamics in one particular direction. This becomes most effectual when the drillstring starts to rotate off-center or "wobble" around the borehole. A sensor positioned within the wall of the pipe then follows the path of a spirograph or hypotrochoid curves (Brett et al., 1989). The nature of this path forces the sensor to constantly change direction, velocity, and acceleration of its movement, while the drillstring itself performs a rather smooth rotation. A sensor that is not located in the center of the drillstring thus does cannot represent the entire drillstring.

In larger tools, often two or more measurements are combined to account for these effects from a purely mathematical perspective. Data sets often contain calculated values, such as "lateral vibration values" from multiple accelerometers. Most of these algorithms simply add, subtract, or average the outputs of two or more sensors (Mayer, 2007). This methodology is not sufficient to account for all the complexities in the movement of the pipe and these calculated values still contain high-frequency noise.

The kinematic model in Chapter 2 shows that under whirl, tangential and radial accelerations are not independently indicated different modes of vibrations. Similar effects can be observed with other downhole measurements: torsional phenomena like stick-slip exhibit effects on strain measurements. Downhole RPM calculated from magnetometer outputs show whirl fluctuations. Similarly, all movements of the drillstring dynamically impact downhole pressures and cause stress effect in pipes.

3.3.1 Differentiation by Frequency

In addition to possible sensing errors (see Chapter 4), downhole sensors correctly measure different phenomena aliased in the signal. Stick-slip vibrations, mud motor rotations, fluctuations in pump pressure, automated surface WOB and RPM adjustments,

etc. could all happen at the same time and affect the measurements. These phenomena often can be differentiated by their individual frequencies. These frequencies may vary significantly, but they can be broadly categorized in low, medium, and high-frequency dynamics:

Low frequency dynamics can be linked to change of surface parameters, such as surface WOB or RPM adjustments, changes in formation properties or other changes of the drilling system with no or low periodicity. Switching from sliding to rotating mode and back for directional drilling is another example of a low frequency dynamic phenomena that is visible in almost all data downhole streams. These lower frequency dynamics are in the order of minutes and can be studied using continuous low frequency downhole or sometimes even surface data.

Medium frequency dynamics show periodicities of several seconds. They can be linked to rotational movements of the drillstring, BHA or bit, mud motor or rotary-steerable system (RSS), low frequency vibration phenomena (e.g. stick slip) and other known or unknown effects of similar periodicity.

High-frequency dynamics in this work are considered phenomena with frequencies above 1 Hz up to several hundreds of Hz. To study these dynamics, high-frequency data is required. Traditional continuous data generally does not have sufficient sampling rates to capture these effects. Using high-frequency burst data allows for an appropriate analysis, but this type of data is subject to availability. As to current knowledge, lateral vibrations or whirl is the only effect that has been proven to cause very high-frequency responses in the measurements. **Fig. 31** shows low, medium, and high-frequency dynamics of the WOB measurement.

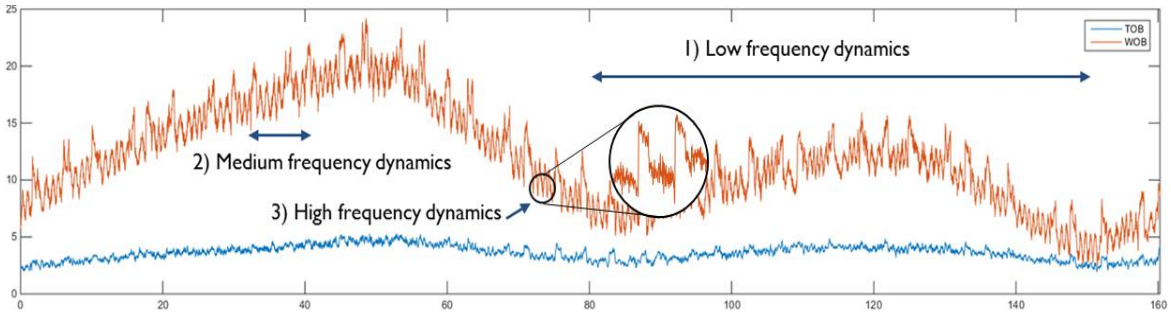

Fig. 31—TOB and WOB measured with 50 Hz sampling rate show dynamics that can be related to a variety of effects.

3.4 SELECTIVE FILTERING

3.4.1 Theory

Making use of insights from the field data examples demonstrated here, data can be aggregated and more valuable information can be extracted from a signal. The following is an illustration of a data processing strategy for WOB data, yielding a high value of information and yet achieving significant data reduction:

As an initial step, WOB data must be corrected for linear and non-linear offsets and time shifts in relation to surface data and other downhole measurements (details in Chapter 4). Highest frequency dynamics can be associated with lateral vibrations of the drillstring. A frequency analysis of torsional or radial acceleration data reveals frequencies associated with whirl, low pass filters are adjusted instantaneously to filter these from the WOB signal. A similar process is valid if axial vibrations occur.

The data reveals two kinds of medium frequency dynamics: stick slip vibrations (or less severe torsional oscillations) and cyclic loads due to bending at each rotation. Stick slip frequencies and downhole rotational frequencies are closely linked and can be obtained from magnetometers or gyroscopes. Note that within one slip cycle, the drillstring can perform multiple rotations. Again, associated frequencies can be filtered from the WOB

signal. Low frequency changes of surface WOB input values can be filtered from the signal using surface measurements. What is left in the signal is the actual information of interest: for instance, decreasing downhole WOB despite constant surface WOB could indicate increased friction factors due to accumulations of cuttings, or a more tortuous trajectory.

3.4.2 Case Study

This case study features data recorded during drilling operations in 2012. The burst data sequences studied here are recorded at a sample rate of 800 Hz and each sequence is 10 seconds long. Multiple burst windows were captured at the curved section of a well, in a depth of 7000 – 9000 ft. A drilling dynamics measurement sub was located above an RSS (rotary-steerable system), used instead of a mud motor to provide directional control.

Fig. 32 compares recorded downhole weight on bit values (blue), torque (yellow) and tangential accelerations (red). The top graph is 10 seconds long, while the bottom graph highlights details in a 1-second window. This time-based view already reveals multiple effects at different frequencies: high fluctuation levels for about 2.5 seconds, followed by low fluctuation levels for about 1.3 seconds, clearly indicate stick slip vibrations. In addition, the slip phase shows high-frequency fluctuations in all data streams. In the following, filtering techniques are applied to this snapshot of data to offer more insights.

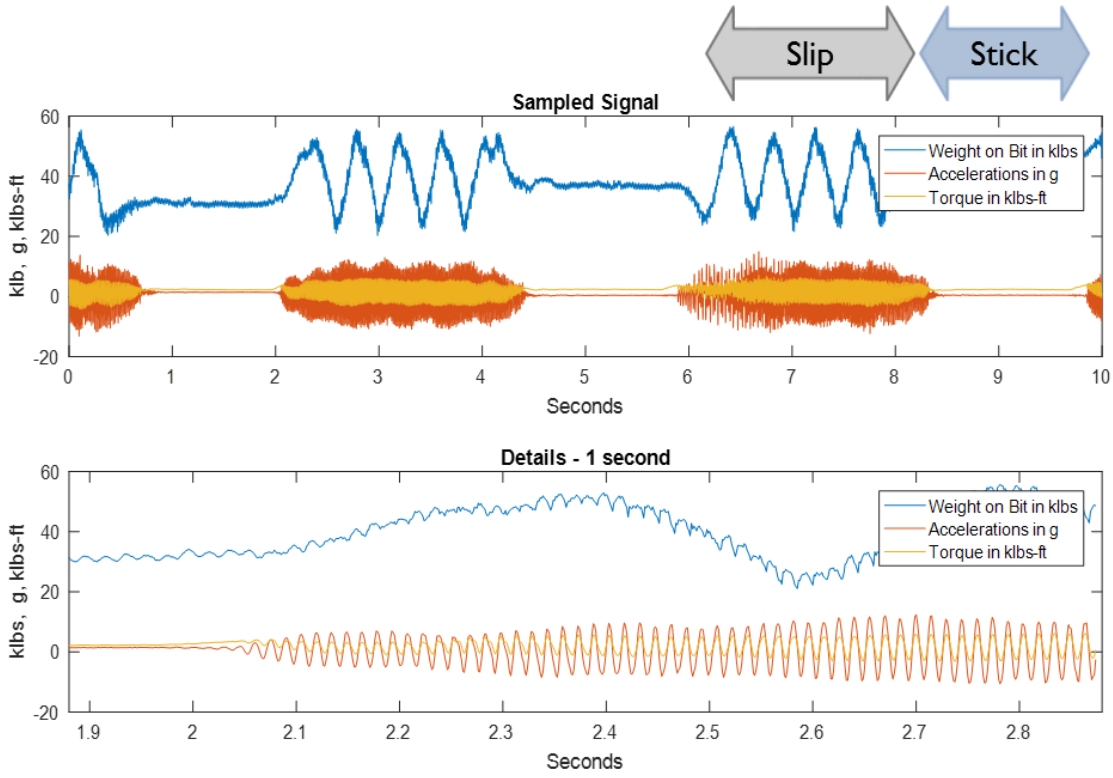

Fig. 32—Downhole WOB, TOB and tangential acceleration measurements over 10 seconds (top) and details (bottom).

Fig. 32 displays the data described above after low pass filters have been applied to each time series. A lower frequency variance of about 0.4 Hz within the slip cycles is now clearly visible in acceleration and torque data. This signal component can be attributed to pipe rotations, as verified by comparison with magnetometer data (Fig. 26 in Chapter 3). Average stick and slip cycle RPM values add up to about 120 RPM, which is the surface RPM set point.

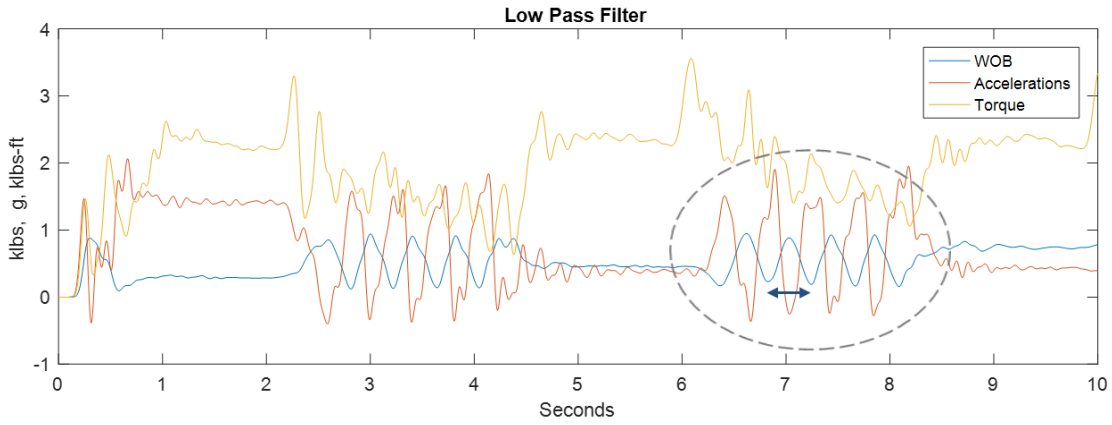

Fig. 33—Downhole WOB, TOB and tangential acceleration after a low pass filter had been applied to the data.

Fig. 33, **Fig. 34**, and **Fig. 35** show the results of a low pass filter applied to the data in time domain (top) and in frequency domain (bottom). The low pass filter amplifies the higher frequencies. The tangential accelerations (Fig. 33) have dominant frequencies of about 67 Hz and overtones of about 131 Hz and higher. Based on the analysis in Chapter 2, these can be attributed to whirl vibrations.

Torque measurements (Fig. 34) show the same frequencies as the acceleration data. The most likely explanation for this phenomenon is that whirl vibrations cause high-frequency changes of pipe stress and strain, captured by strain gauges. Thus, the measurements can be considered noise.

As expected, downhole WOB measurements (Fig. 35) also show the same known signal components. The same explanation applies here: strain gauges capture slight changes in pipe movements due to vibrations, even though the direction of measurement is orthogonal to the lateral vibrations. In addition, WOB has a prominent frequency peak at exactly 50 Hz.

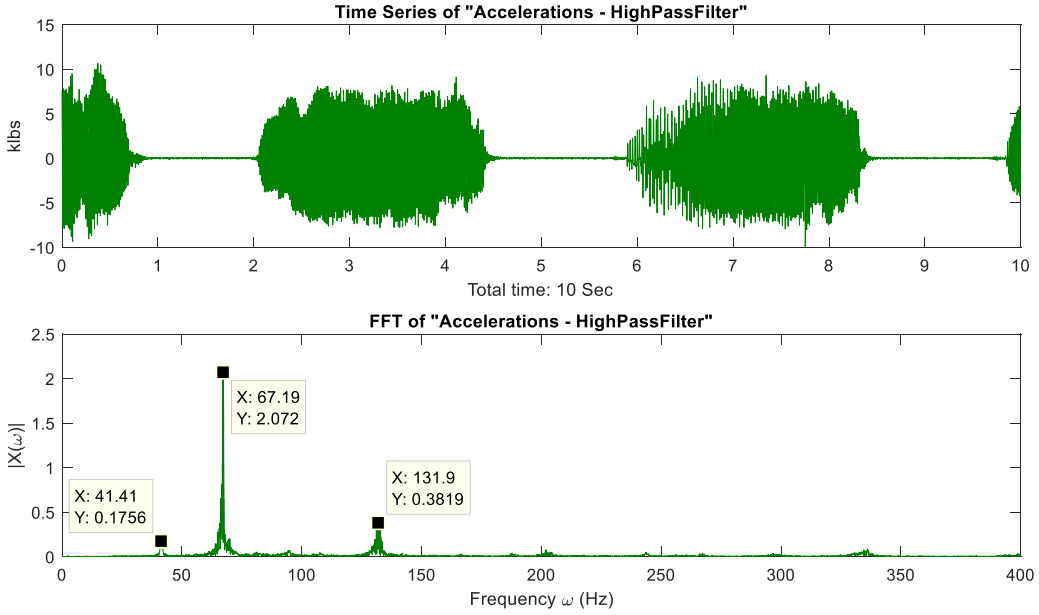

Fig. 34—High pass filter applied to acceleration data (top) with resulting FFT (bottom).

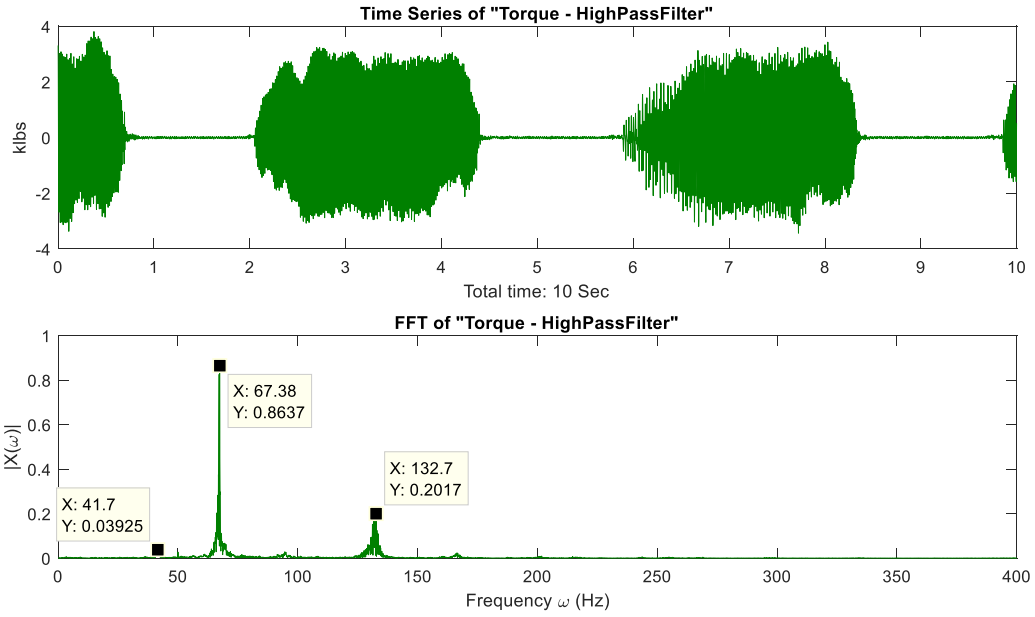

Fig. 35—High pass filter applied to torque data (top) with resulting FFT (bottom).

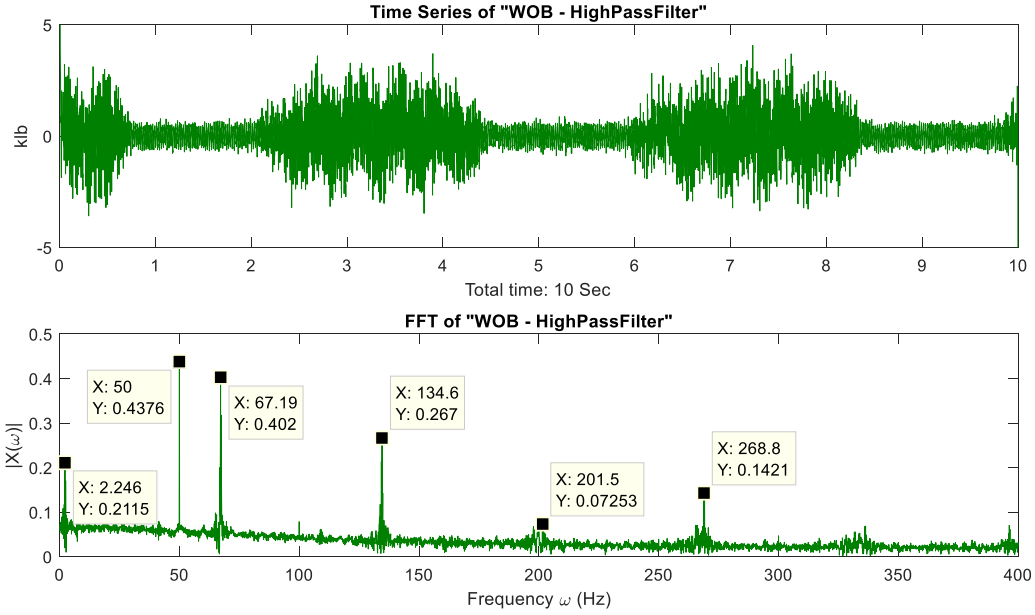

Fig. 36—High pass filter applied to WOB data (top) with resulting FFT (bottom).

Additional filters help to find the root cause of the frequency peaks in Fig. 35. Fig. 37 compares the results after a band pass filter was applied to the WOB data. A band pass filter only allows a narrow frequency spectrum to pass, the other data is discarded. When frequencies around 67 Hz are singled out (left side), most of these fluctuations occur during the slip phase when the pipe moves, as expected. In contrast to this observation, when frequencies of the 50 Hz peak are singled out (right side), these occur throughout the data snippet. This means a 50 Hz background noise is prevalent even during the stick phase. Accordingly, the root cause of the 50 Hz peak can be attributed to effects independent from pipe movement. Since pressure measurement also do not show a frequency peak at 50 Hz, hydraulics is another unlikely source. This extraordinarily “clean” peak may be attributed to noise inherent to the sensor or data processing.

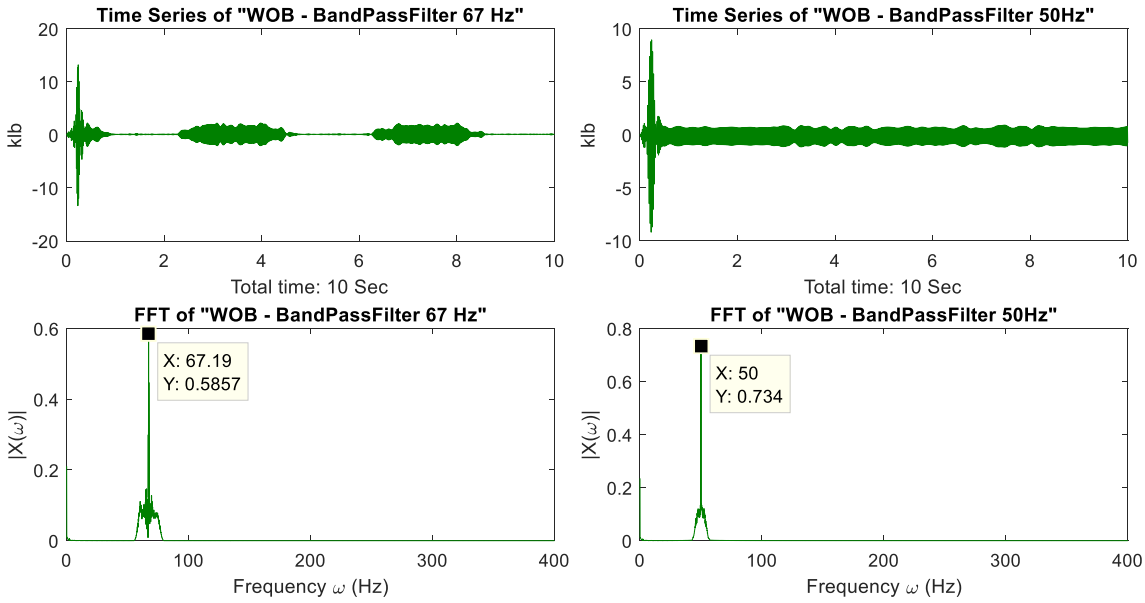

Fig. 37—Band pass filters applied to WOB data (top), with the allowed frequency band (bottom): 65 – 70 Hz on the left and 47 – 53 Hz on the right.

Annular pressure data also has frequency components associated with lateral vibrations. A high pass filter helps to make them visible in a plot of the frequency spectrum (Fig. 38). These frequencies can be removed to focus on periodic events that only occur in the pressure data (Fig. 39). For instance, periodic negative spikes occurring approximately every 0.9 seconds are not observed in any other measurement of the given data set and may be related to RSS tool activities.

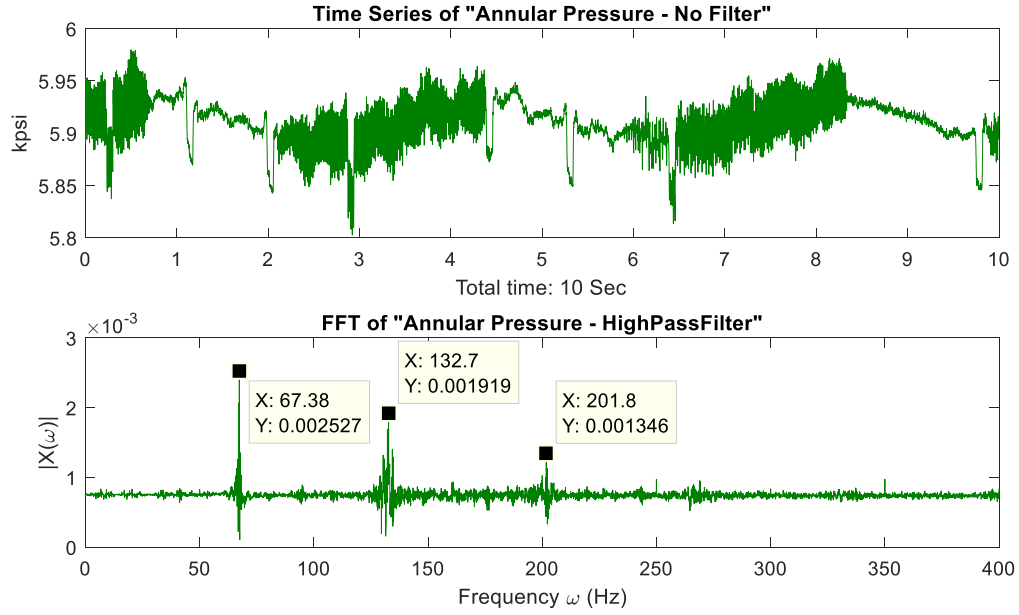

Fig. 38—Annular pressure data, original measurements (top) with the frequency spectrum (bottom) after passing data through a high pass filter to amplify higher frequency ranges.

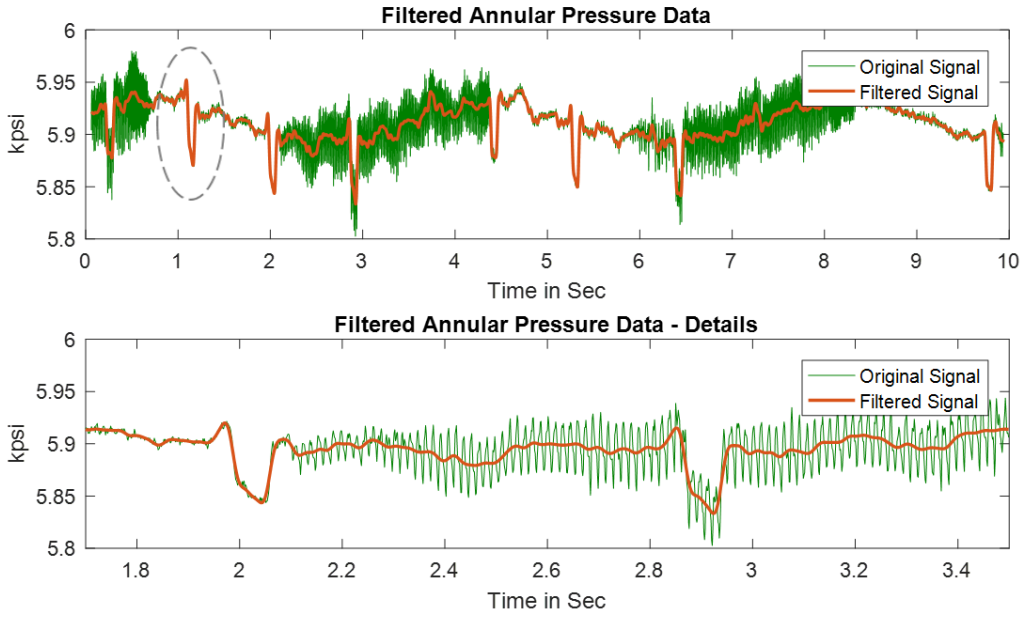

Fig. 39—Low pass filter (cutoff at 30 Hz) applied to annular pressure data.

3.5 CONCLUSIONS

Inadequate information on downhole drilling dysfunction is a real drilling performance limiter. Measurements recorded and transferred at insufficient sampling rates will miss important dynamical effects. At the same time, signals obtained at too high sampling rates may not add additional insights and instead clog up the data acquisition, storage, and transfer system. High sampling rates may also cover essential information by "high-frequency noise", thus overloading systems and limiting analysis capabilities. The result is the same: opportunities for meaningful drilling performance optimization will be missed.

Despite innovative technologies for data transfer becoming available, the bandwidths, downhole memories and analysis capabilities are still limited. Moreover, any time memory gets expanded it will quickly be used to the maximum of its capacity – rationalization of data is therefore essential. To stay within the bandwidths of the system while maximizing the value of information from downhole sensors, the frequency of captured data needs to be customized to the type of measurement and type of downhole dysfunction of interest. Guidelines for achieving this are provided in this chapter.

Field data examples in this work show that downhole measurements are highly interlinked. For instance, drillstring vibrations influence all other measurements, including weight, torque and even pressure readings. To optimize the usage of downhole data, sensor outputs from different sensor types need to be combined during data processing. Some sensors can be used to detect the occurrence of downhole dynamics and their respective frequencies directly and instantaneously. Then these frequencies can be selectively filtered from other sensors. A differentiation of downhole dynamics by its characteristic

frequencies allows accurate drilling dysfunction root cause analysis with filtering of important signals from unimportant noise.

Even though it is very important to rationalize sensor data and optimize sampling frequencies as argued in this chapter, it is important to occasionally go “out of the box” and capture high-frequency dynamics for research purposes to obtain new and improved insights. An example is given in this chapter for high-frequency pressure data, which may be either real or a sensor artifact – more work is necessary to determine this. Note that this phenomenon would not have shown itself if pressure data-sampling would only have been restricted to “optimum” low frequency sampling rates.

Chapter 4: Sensor Errors and Correction Methods

4.1 INTRODUCTION

A higher interest in downhole information will inevitably be followed by a higher interest in good quality data. For wellbore positioning surveys, awareness of data errors and sensor calibration techniques are well established (e.g. Jamieson, 2012). For surface data, operators have realized that the data quality doesn't only start when data is captured, it starts at the design and manufacturing of sensors (Zenero and Behounek, 2016). For downhole data, which is currently not part of standard drilling analysis, the awareness of data quality will come with a more frequent use of the data.

An introductory chapter describes the process of sensor selection, tool design and calibration and lists major constraints for each process. Expected sensor errors due to downhole conditions are described. Processing techniques that can significantly shape the data are detailed. These insights establish a relation between sensor selection/calibration techniques and good downhole measurements. In the long run, only adequate sensors and calibrations will deliver sustained data quality.

In the short-run, downhole data can demonstrate its benefits if it can be used in a timely and efficient manner. Despite sensor design efforts, downhole dynamics measurements show errors that are currently inevitable. The second part of this chapter addresses these challenges and offers short-term solutions. It describes a variety of commonly observed measurement errors and demonstrates their negative impact on drilling data analysis. Then, methodologies for automated corrections of such errors are

presented. All approaches are tested on medium to high-frequency downhole data from multiple drilling projects.

4.1.1 Sensor Selection and Design

Sensor selection and design is governed by a variety of factors that each impose technical limits. Power availability, tool size, software, ability to calibrate a sensor and tool life are amongst the most important design considerations for downhole measurement tools.

Electrical Power

In traditional wireline logging applications, almost infinite power can be supplied through the cable and a sensor's power draw is not a design consideration. In MWD tools and other measurement subs, batteries generally provide power to sensors and processing units. The tool's batteries must supply enough electricity for at least an entire bit run. Therefore, sensor power becomes the "number one" commodity of a downhole tool. Sensors that consume less power are favored over the ones that consume more power, despite possible performance tradeoffs. Sensors with very low power draw can become unstable or "flakey" and are easily influenced by the environment. Power considerations also play a role in selecting self-calibrating features, more advanced processing techniques, or extracting additional data streams from a measurement, since these further increase the downhole power consumption.

Size

The maximum diameter of a tool is governed by the hole and BHA diameter, thus space for sensors and wiring is also a limited commodity. The hollow tubular shape adds additional constraints for mounting box shaped sensors; additional sleeves and pockets may

be required. Adequate pressure and temperature resistant sensors or self-calibrating sensors often are simply too big for the available tool space.

Lately, microelectromechanical devices (MEMS) and even nanoelectromechanical devices (NEMS) are becoming available; these developments allow the compression of traditionally larger sensor designs into a much smaller scale. The size benefits, however, are often contrasted by showing reduced reliability and uncertain behavior. Also, additional protection material around such small-scale sensors can offset the size benefits.

Mounting

The type of mounting is an important consideration in the tool's design phase and influences the sensor outputs. Some sensor bodies can have mounting holes or brackets integrated into the sensor. Other smaller sensors are integrated into a "package" that can be mounted in a pocket inside the tool. Sensors may require to be hard mounted to the tool (not cushioned), while others are soft mounted (cushioned) and more protected against impacts. For instance, shock recordings will be dampened for cushioned sensors and record much lower values than hard mounted ones.

Data Transmission

Downhole data can either be transmitted to surface in real-time (using mud pulse, wired drillpipe, etc.) or stored in memory and retrieved only after the bit run. Sensors, calibration, and post-processing systems must be tailored to the type of data display and the software applications. Real-time systems utilize different viewing platforms with specific processing requirements.

Calibration

Calibration is the process of configuring a sensor to ensure that a measured data point lies within a predefined range. Calibration often requires specific calibration equipment and manual procedures; sensors and housing tools need to be designed to facilitate the testing process. Off-the-shelf calibration equipment is often unsuitable for testing downhole measurement subs, which can be many 10s of feet in length. Tool manufacturers need to develop their own calibration equipment and methods, whereby ideally, the downhole conditions are simulated during the calibration process. To facilitate the calibration process, the tool is may be separated into smaller parts; thus, the mechanics of the calibration process become an important variable in designing the tool.

In-tool calibration (auto-correction) is required for real-time streaming of data. Calibration through software can remove errors from cross-talk of sensors, wiring between sensors and other tool components or inaccuracies of the sensor itself. For this technique, auxiliary systems, such as a memory chip or the central processing unit, must be capable of conducting the correction. Working memory, processing capacity, power draw, etc. can limit the software calibration techniques. If there is no immediate need for corrected data, raw values may be stored in the tool's memory and retrieved after the bit run. Advanced correction techniques can then be applied at surface, where more computational power is available.

4.1.2 Sources of Errors

Despite careful sensor selection and design, some errors in the data are still inevitable. Downhole temperature, pressure, and shocks (high impact forces) are considered the main sources of error; details and error mitigating techniques are described in the following section:

Temperature

Temperature carries the biggest potential for sensor error. Standard downhole temperatures range around 75-125°C; some high-temperature wells heat up to more than 200°C. Sensors show various temperature-based characteristics, which need to be considered before the sensors are embedded in the tool. They may expand or "behave" differently, depending on the type of mounting. Calibrated sensors can become unreliable under high-temperature conditions; several effects are differentiated:

1. *Physical damage*: Thermally resistant material may expand under heat, but these changes are usually reversible. If the sensor or sensor parts are not thermally resistant, they can experience physical deformation or melting. This type of damage is usually irreparable.
2. *Railing*: "Railing" is a term used when the sensor incorrectly is outputting the maximum or minimum value of its range, which renders it unusable. Sensor manufacturers provide recommended temperature ratings; railing is a common phenomenon if a sensor is exposed to temperatures outside that range.
3. *Temperature drift:* A commonly observed problem (also for data used in this chapter) is sensor drift, where a measured value varies from its zero level. The magnitude of the drift is a function of temperature. The functions can be *linear* or *non-linear* with change in temperature. Drift factors are determined from sensor data sheets and/or testing procedures. Such inputs can then be used for automated downhole corrections.
4. *Sensitivity changes*: A change of sensor sensitivity leads to a change in the scale of the measurement. This is an important error to detect and correct, as it may change the measurements significantly and is not easily detected as sensor error.

Pressure

Just like high temperatures, pressures of sometimes more than 20,000 psi are a common source of error for downhole sensors. Sensors have recommended operating ranges for pressures. The resulting sensor errors are comparable to temperature errors: irreparable damages, drifts, and sensitivity changes. Even if recommended pressure ranges are exceeded in downhole applications, there are multiple methods for compensation:

- Sensors can be *shielded off* by being embedded into a pressure resistant case. However, this method adds complexity to the manufacturing process and is limited by space restrictions in the tool.
- Mechanical *pressure compensation* is a more commonly used method to correct for errors caused by high pressures. It involves intricate machining and carefully balancing dissimilar materials, adding to manufacturing costs.
- Pressure induced errors can also be *compensated by computational methods*, analogous to temperature corrections.

Shocks

Downhole forces induced through vibration or rough tool handling expose sensors to high impact loads, or shocks. Newer smaller sized sensor technology usually is even more susceptible to shocks. Shocks can not only cause spikes and noise in a measurement, it can physically damage a sensor. Sensor manufacturers may specify the accumulated number of shocks it can withstand. However, such shock numbers are unreliable for practical applications, because shocks cannot be accurately counted in the downhole environment. Additionally, downhole conditions may change the robustness of the sensor. High shock environments greatly affect sensor calibration. If it is possible to “soft-mount” the sensor, such cushioning reduces the exposure to shocks.

4.1.3 Data Processing

Data Rates

Sensors measure an analog (continuous) physical phenomenon at a certain sample rate and an analog to digital converter (ADC) turns this continuous signal into a discrete (digital) signal. The sampling rate of a sensor depends on multiple factors: the sensor design and its built-in processing (filtering) capacities, the ADC, the recording scheme and the data transfer or storage process. In some cases, sensors already have a digital output i.e. they have an ADC built into them. The output data rate of such digital sensors cannot be changed. An attempt to output higher data rates only provides more data points along an interpolated curve between actual data recordings. More commonly, a sensor outputs an analog signal and a separate ADC converts it into a digital signal. In this set up, the data sampling rate depends on the capabilities of the ADC. "Fast" ADCs with high sample rates consume a lot of power compared to "slower" ones. The system clock of an ADC ensures that the digital samples are taken uniformly (at the same time intervals). Currently, there is no standardized process available to calibrate these clocks.

Digital Resolution

Digital resolution is the smallest difference between two distinguishable numbers. It is a property of the sensor's sensibility, thus the hardware. If the digital resolution is not high enough, measurements appear to be constant for certain time intervals, as shown in **Fig. 40**. More sensitive sensors can deliver a higher digital resolution, but thereby increase the data volumes per measurement. Downhole measurements typically have a 12 or 16-bit resolution; a higher resolution can be available if needed. Because of data storage and transmission limitations, there usually is a tradeoff between sample rates and resolution per

sample. These choices depend on the specific data requirements and should be carefully considered for different applications.

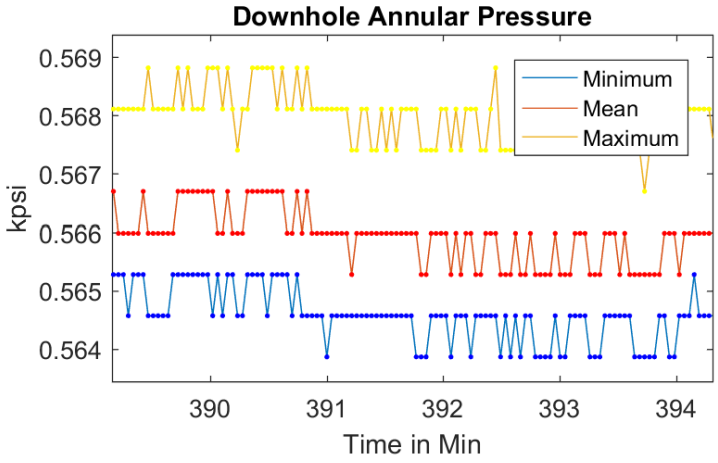

Fig. 40—Example of a signal output with a digital resolution that is too low.

Filtering

Filtering is a standard procedure in digital signal processing. It is important if the measurement not only contains the expected variations, but also captures unwanted signals. Filtering then removes certain frequency variation and keeps others.

Hardware filtering requires additional electrical components to be placed in the path of the sensor and the master devices, which control and coordinate all the sensors. Most sensors have built-in hardware filters to remove high-frequency noise. The setup of these filters can be tailored to specific applications.

Software filtering can be implemented at the downhole sensor or in a post processing step. In both cases the filters need to be applied to raw data and not any derived or truncated data.

Filters are essential tools to clean a signal from unwanted noise or errors and focus on the important measurements. However, the filtering process can greatly modify the data

and is usually irreversible. The exact same measurement with two different filters could be completely different, so filters need to be chosen wisely. Information on applied filters should be made available to the end user of the data.

4.2 AUTOMATIC OFFSET CORRECTION

Despite the above described efforts in sensor design, sensor errors sometimes are inevitable. Drifts of accelerometer data can be observed in most of the analyzed field data and were mentioned in literature (e.g. Shor et al., 2015). To effectively compare vibration levels throughout a run or amongst multiple wells, data needs to be corrected for drifts and other offsets. This chapter presents an algorithm that can automatically detect static components in the data and, based on those, shift data to zero levels. Only then, vibration severity levels should be determined and areas of high vibration flagged for further analysis.

4.2.1 Static and Dynamic Acceleration Components

For vibration analysis, it is beneficial to introduce a differentiation of acceleration data into 2 components: a static and a dynamic component.

The static component depends on the angle of the sensor axis to the earth's surface. An accelerometer resting parallel to the earth's surface will read 1 g (or -1 g). Tilting the accelerometer will result in a reduced static component (**Fig. 41**).

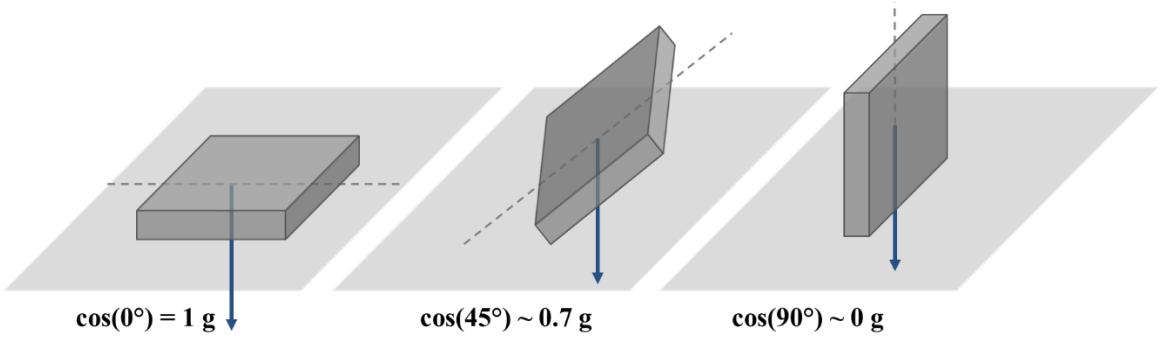

Fig. 41—Measurements of a single accelerometer axis relative to its position.

Movements in drilling are almost never uniform and smooth. While the drillstring is rotating and the bit is crushing the rock, the dynamic component oscillates around the static component. The dynamic component indicates vibrations or other pipe movements.

Severe vibrations can cause acceleration peaks of more than 50 g. If the static value of vibration would range between 0 and 1 g, it wouldn't have much impact on a severity classification and could potentially be ignored. However, sensors can drift significantly. As described in the introduction of this chapter, techniques exist to correct for drifts that follow functions with known parameters, but those corrections are often omitted or are inaccurate.

4.2.2 Observations in Accelerometer Data

Fig. 42 shows data from a downhole axial accelerometer. The data was recorded over 7 days and some of the data (day 2 and 3) is missing. **Fig. 43** gives a detailed view of the first 5 hours. The dotted lines indicate -1, 0 and 1 g values. At the start of the data set, the static component of the acceleration data has a value of 0, as it can be expected while the tool lays flat on surface. The value quickly approaches -1, while the tool is turned into a vertical position and is "running in hole". In hours 1.5-2 a slight drift from its expected value can be observed. From hour 2 onwards, the drilling process starts, observable through

higher levels of vibrations and less frequent connection patterns. As the tool changes its inclination in the curve section, the static component gradually increases to 0 g. For a correctly measuring device, the static component is expected to reside around 0 g as the horizontal section is drilled. Instead, the base value of the acceleration slowly rises to more than +3 g (Fig. 42**,** hour 60). At the end of the bit run (hour 66), the tool is "pulled out of hole", and the static component falls back to almost -1g. When the BHA finally is laid down at surface, the accelerometer reads a correct value of 0 g. Surface calibration cannot prevent this type of sensor error, because it is only prevalent under downhole conditions.

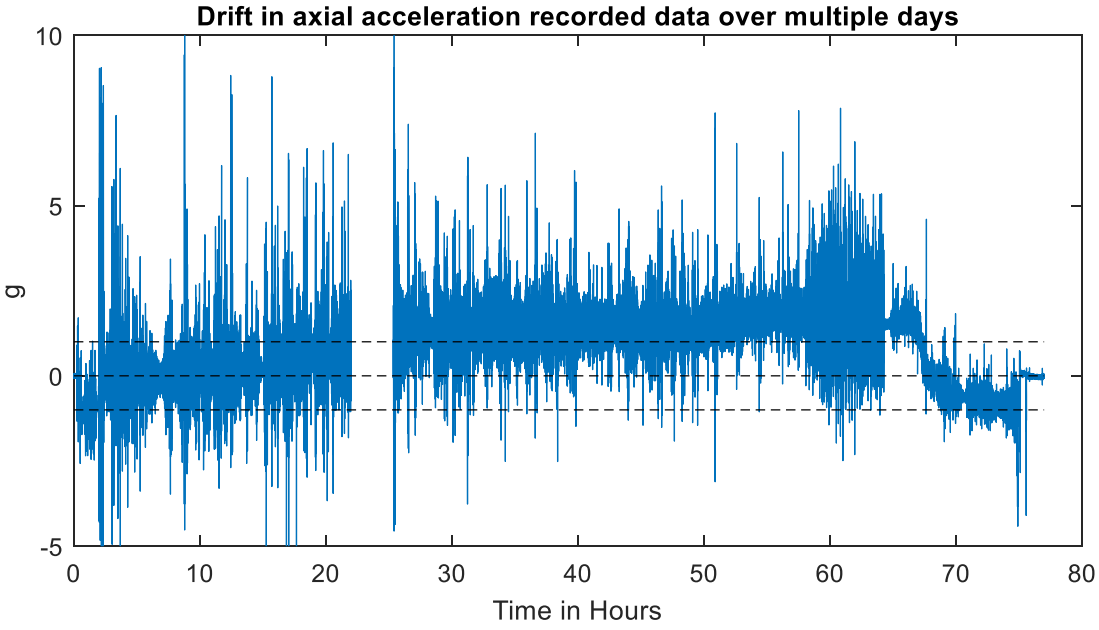

Fig. 42—Data from a downhole accelerometer (axial) recorded for one bit run over 5 days (2 days are missing).

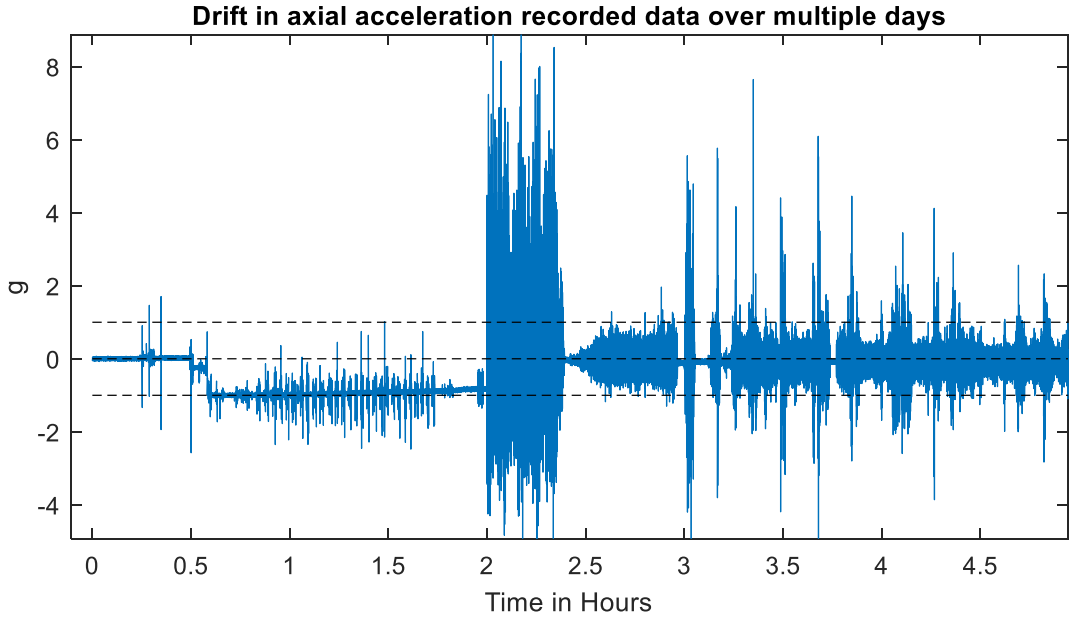

Fig. 43— Data from a downhole accelerometer (axial) recorded for one bit run over 5 days (2 days are missing), details of the first 5 hours of the bit run.

4.2.3 Acceleration Correction

Only the dynamic component should be considered when comparing and classifying acceleration levels. The static component includes the drifts and effects of the sensor's direction or setup (e.g. a horizontal tool can either show values of +1 g or –1 g).

One may suggest finding the static component by simply calculating a running average of the data. Yet, when the sensor is in motion, the instantaneous mean of the data may not necessarily match the static component. For instance, an axial sensor measures additional accelerations as the tool moves along its axis, or a radial acceleration sensor measures a centrifugal component. High impacts from a particular direction may also skew the mean.

However, during a connection, the drillpipe hangs "in slips", and is therefore relatively stable for a short time (about 1.8 minutes in **Fig. 44)**. During this period, the

variance is insignificant compared to the rest of the drilling process, so the mean of the data is reliably close resembling the static component.

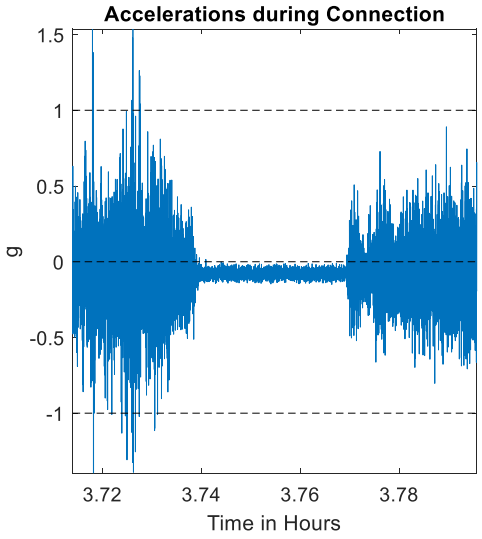

Fig. 44—Axial accelerations during a connection procedure.

These no-movement sequences are characterized by a significantly lower standard deviation than all other data periods. For lower frequency data (e.g. data with sampling rates of about 0.4 Hz), standard deviation values can often be directly retrieved from "continuous data". The data in Fig. 44 has a sampling rate of 50 Hz. Here the standard deviation is calculated for windows of 10 seconds (500 data points). **Fig. 45** displays the distribution of standard deviation values calculated from the data shown above. In this case, about 9% of the standard deviation values are below 0.025 g – these are the times when the string hangs in the slips. After 9% there is as steep increase of variations in the data. Using this information, a cutoff of the lowest 7% or 0.020 g of standard deviation clearly identifies no-movement sequences of this bit run.

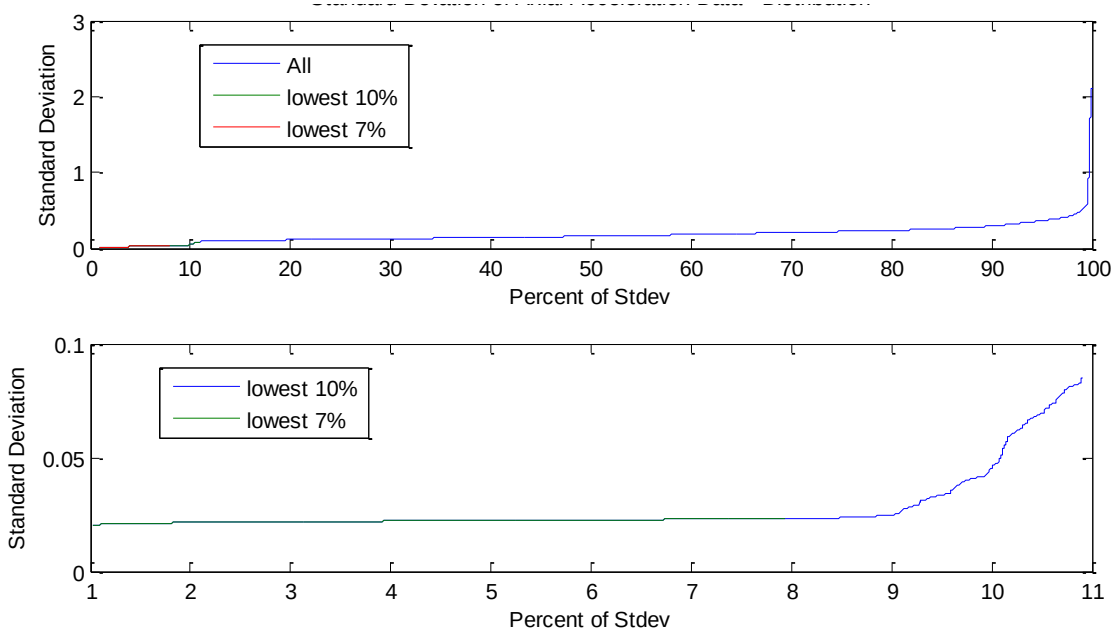

Fig. 45—Cumulative distribution for standard deviation values calculated from accelerometer data, all values (top) and details (bottom).

In a next step, the "baseline points" for each low-variance window (here each window is 10 seconds long) are calculated. For axial and tangential accelerometers, these are the mean values, for radial accelerometers these are the minimum values.

Finally, individual baseline points are connected through interpolation. In most cases, a linear interpolation is sufficient, because the baseline points occur relatively frequently (during connections) and are evenly spread out through the run. For highly non-linear shifts, a different method of interpolation can fit the data better.

The resulting interpolated curve (offset) constitutes the static component of the data. Subtracting the offset from the original data yields the "cleaned" dynamic component of acceleration data. **Fig. 46** shows the original data (blue), the offset curve (yellow), indicators for low standard deviation (stars) and the "cleaned" dynamic component

(orange) of axial acceleration data. A flow chart of the above-described algorithm can be found in Appendix B.1.

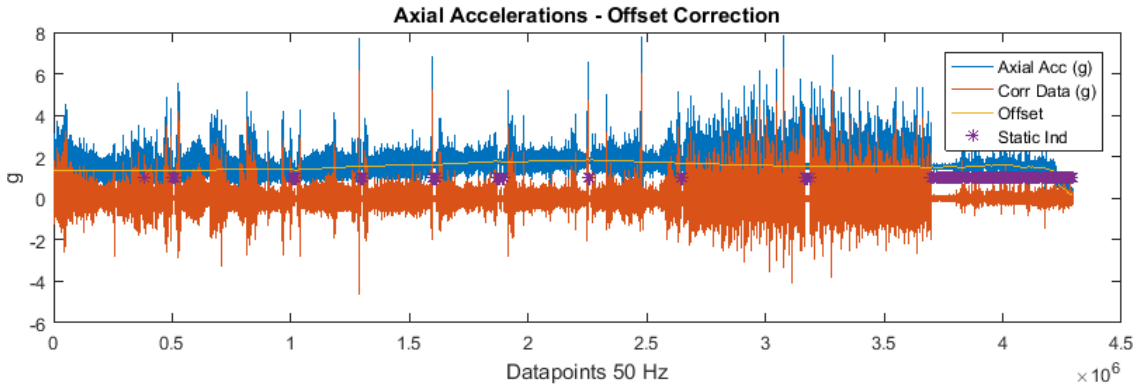

Fig. 46—Corrected (orange) and uncorrected (blue) acceleration data.

4.2.4 Accelerometer Data for Velocity and Position

Rate of penetration (ROP) is usually inferred from surface data, e.g. using the movement of the block as an approximation for the progress of the bit. Even though the measurement of the change in block height may be fairly accurate, huge uncertainties lie in the transfer of movement within the string. The drillpipe could buckle, which interferes with transferring the movement and weight on bit. The stretch of steel along thousands of feet and under varying temperature and pressure conditions can be modeled, but is still subject to uncertainties.

An obvious remedy would be to directly measure the movement along the drillstring axis downhole. In theory, an axial accelerometer should give an indication of the instantaneous velocity of the tool and thus the ROP of the bit. If it was possible to clean accelerometer data from noise (e.g. vibrations, drifts, gravity effects), accelerations could be numerically integrated to yield relative velocity and measured depth.

This process, known as “dead reckoning” is already difficult for surface applications with higher quality sensors in a stable environment (e.g. Randell et al., 2003). Despite several attempts of inferring velocities from accelerometer data, we have not achieved any meaningful results. For the given data quality, it is not possible to differentiate movements of drilling progress from noise, especially since the movements are insignificant compared to vibrational oscillations. We must conclude that it is not possible to derive bit position or velocity from acceleration data alone.

4.3 AUTOMATED WOB AND TOB CORRECTION

Weight on bit (WOB) is not directly measured at surface, instead it is inferred from a hook load sensor located at the deadline anchor. WOB is then calculated by subtracting that hook load measurement from the estimated buoyant weight of the string (Saputelli et al., 2003). Imperfect weight and torque transfer causes estimates based on surface data to be much higher than downhole measurements (Pink et al., 2013). Analytical or finite element models can provide better estimates for downhole values (e.g. Wu and Hareland, 2012), but they are not generally used in drilling operations. Because of such inaccuracies, several authors could demonstrate the benefits of direct downhole weight and torque information on drilling performance (e.g. Belaskie et al., 1993; Pink et al., 2013).

4.3.1 WOB and TOB Measurements

Grosso et al. (1983) describe details on WOB and torque on bit (TOB) sensors of an MWD tool: “WOB is measured by a temperature and flexure-compensated strain-gauge bridge mounted on the drill collar. By taking a measurement with the bit off bottom, the system compensates for the drill-collar weight below the tool. The TOB measurement is

identical to the WOB measurement except that the gauges are oriented to be sensitive to the torsional shear strains in the drill collar".

Strain gauges are susceptible to high-pressure and high-temperature environments and show significant drifts. The above-mentioned off bottom measurement not only adjusts for the collar weight below the tool, but is also supposed to compensate for possible sensor drifts.

Fig. 47 shows a typical downhole WOB profile during a connection procedure. The data has been recorded at 50 Hz. WOB is not yet corrected and has a negative offset of about 100 klb. Actions on surface, such as turning the mud pumps off and on, pulling the pipe up to remove the slips, tagging bottom, etc. cause reactions in the downhole WOB data. Circulating fluid exerts higher pressure than fluid at rest. When the pumps are on, the equivalent circulating density (ECD) of the fluid leads to a stronger buoyancy effect – the string is lighter. In the example shown in Fig. 47, the pump pressure induced buoyancy decreases the weight of the string by about 15,000 lb.

Taring is a procedure carried out during a connection to calibrate MWD and surface torque and weight measurements (Sutcliffe and Sim, 1991). During rotary drilling (entire drillstring is rotated from surface) the bit is off bottom, rotary speed and flow rate are comparable to the parameters used during drilling. For taring while steering (mud motor turns only the lower portion of the BHA), the bit does not rotate. The taring procedure takes about 2 minutes and is usually conducted after the survey[8].

At the beginning of the connection, there is another chance to get a taring value from the data: the string is pulled off bottom, but the mud is still in circulation (minute

[8] A survey is a measurement of inclination and azimuth of the MWD tool, which bit position is inferred from.

1040 in Fig. 47). If these points are not chosen carefully, downhole WOB data can potentially be off by more than 10 klb despite correction attempts.

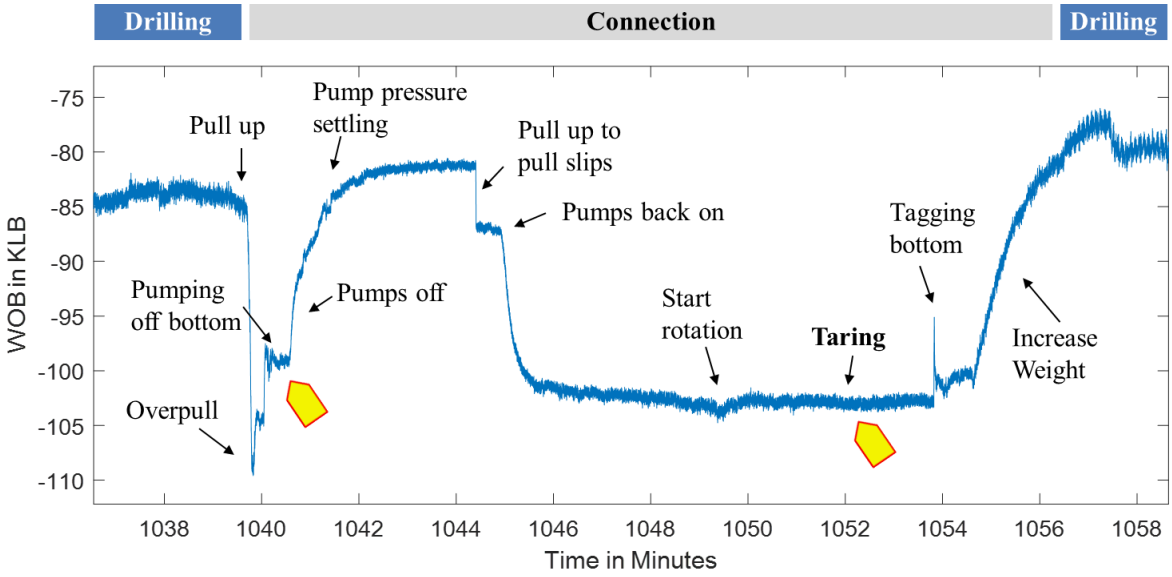

Fig. 47—Typical downhole WOB profile during a connection procedure; two pentagon arrows are indicating the theoretical zero WOB points. Note that the data is not yet calibrated and the values are off by about -100 klb.

These taring values are used to correct real-time data, which is streamed or pulsed to surface while the tool is downhole. Oftentimes, tools do not automatically correct for the offset. Uncorrected or unreliably corrected data is then calibrated in a manual post-drilling analysis process: an analyst hand-picks the above-described zero-WOB points from the data patterns. This process is error prone and time consuming. Manual post-processing and data cleaning, such as WOB and TOB correction, are among the main reasons for delays in data delivery from the service company to the end user (see Chapter 5).

4.3.2 Automated Zero-WOB Detection

The process of picking correct zero-WOB values can be automated, and the tedious manual process eliminated. The proposed algorithm combines physics and downhole data to find the first of the two indicated zero-WOB moments: right when the pumps are shut off to make the connection. The algorithm consists of multiple steps:

1. Selecting points with low pressure variance
2. Finding connections from low variance clusters
3. Selecting the beginning of each cluster as zero-WOB points
4. Interpolating the selected zero-WOB points to produce an offset curve

A flow chart of the algorithm can be found in Appendix B.1.

Selecting Low Variance Pressure Points

The variance distribution in the data helps to differentiate static (pumps off) from dynamic (pumps on) data. Just as demonstrated for the automatic correction of acceleration data, downhole pressure measurements (internal or annular) can be used to find connection operations in the data, i.e. clusters of low variance in pump pressure.

Depending on the data set, pressure variance information may be directly available. Otherwise, the difference between the maximum and the minimum pressure over a short time window can serve as a proxy for variance values. In **Fig. 48** this delta value is calculated for every available data point (here data points were available every 2.56 seconds). Low absolute pressure values may also indicate connections. However, the static pressure values change with TVD (total vertical depth) and may be “out of calibration”. Therefore, using relative pressure values is advantageous over cutoffs based on absolute values.

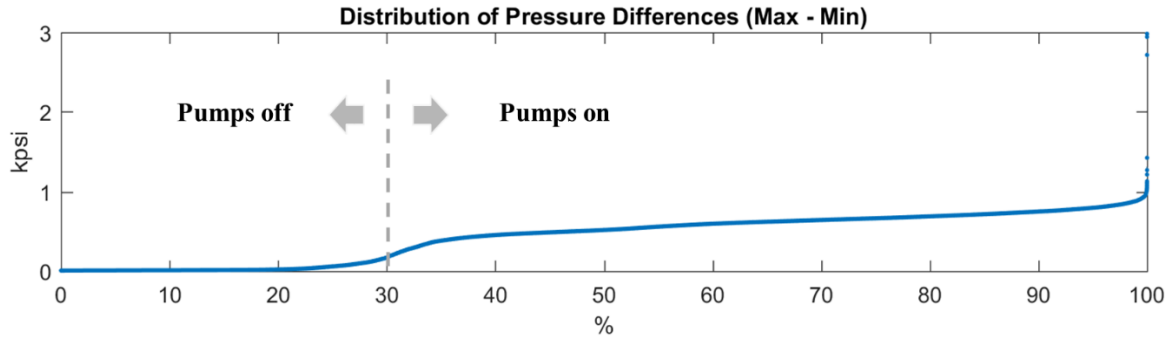

Fig. 48—Distribution of differences between the minimum and maximum pressure values from an internal downhole pressure sensor.

Defining Connections by Clustering Points

Real data is noisy. The selected thresholds do not perfectly indicate pump-off times. Some random low pressure variance indicators may show during drilling, while pressure fluctuations may occur even when the pumps are off. Data processing techniques remove random points (e.g. indicators without other indicators nearby), connects adjacent indicator clusters into one cluster, and removes clusters that are too short to indicate a connection. All these steps can be done automatically, although they may require adjustments based on the sample rate of the available data.

Finding Zero-WOB Times

The moment where WOB or TOB should be zero is right at the start of a "pump-off-cluster". **Fig. 49** shows the results of the automated WOB correction algorithm. The WOB data shown here has already been manually corrected. Most of the time, the automated procedure picked points close to the manual selection. In comparison to the performance of the human correction, the automated system picks very consistently. The automated taring points still can be off, especially at the end of a section, when the bit has reached TD (total depth). The performance of the automated system is sensitive to the

choice of pump-on-pump-off-threshold: if it is too low, the taring point is picked too late and WOB measurements appear lower than the real values; whereas if the threshold is too high, WOB measurements appear higher than they really are.

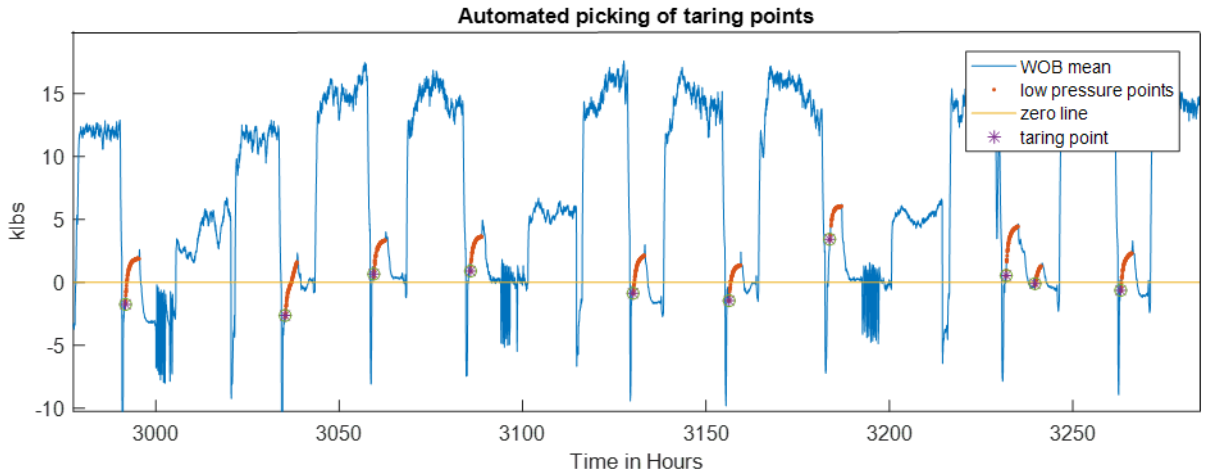

Fig. 49—Results of automated WOB/TOB correction algorithm. The WOB data has already been corrected, the automatically picked points, by enlarge, coincide with the manually picked ones (zero line).

Defining an Offset Curve

The taring points can be used to correct both WOB and TOB data. Usually, the offset of the data follows a certain trend and taring points can be interpolated using linear or non-linear functions.

4.3.3 Alternative Approach – SAX Algorithm

In a search for WOB correction methods, it has been attempted to automatically replicate the human process by the application of a pattern recognition approach. We have implemented a SAX (Symbolic Aggregate approXimation) algorithm. SAX (e.g. Keogh et al., 2005 or Lin et al., 2012) can transform time series into strings. The algorithm consists of 2 steps, first the original time series is transformed into a Piecewise Aggregate

Approximation (PAA) and second, PAA data is turned into strings. PAA divides the time-based data into equidistant sequences and stores the mean of each sequence.

The SAX algorithm was applied to identify the zero-WOB point in the connection patterns. The algorithm is supposed to identify the overpull as the lowest point and then capture the zero-WOB point shortly thereafter. Based on the sequence of letters, these points may be identified throughout the entire dataset (e.g. through a letter combination A followed by an E). In **Fig. 50**, the algorithm could successfully identify the lowest WOB point, it fell short however, to identify the point of interest thereafter.

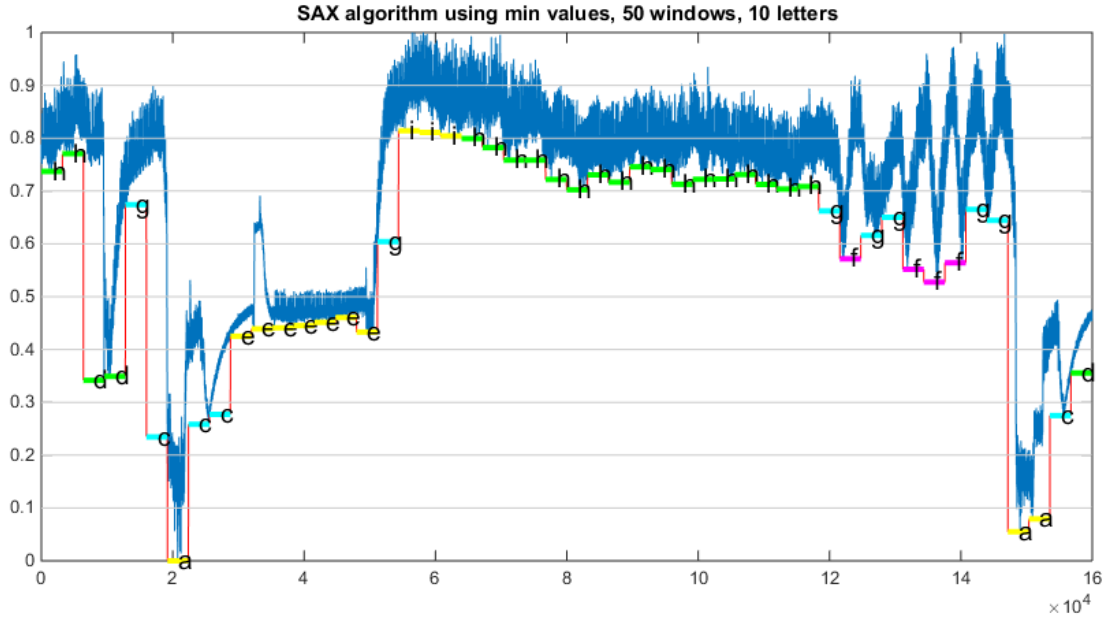

Fig. 50—Application of SAX algorithm to identify zero WOB point in connection patters. WOB data is normalized in this example.

In **Fig. 51** the SAX algorithm does not even identify the lowest point of the connection.

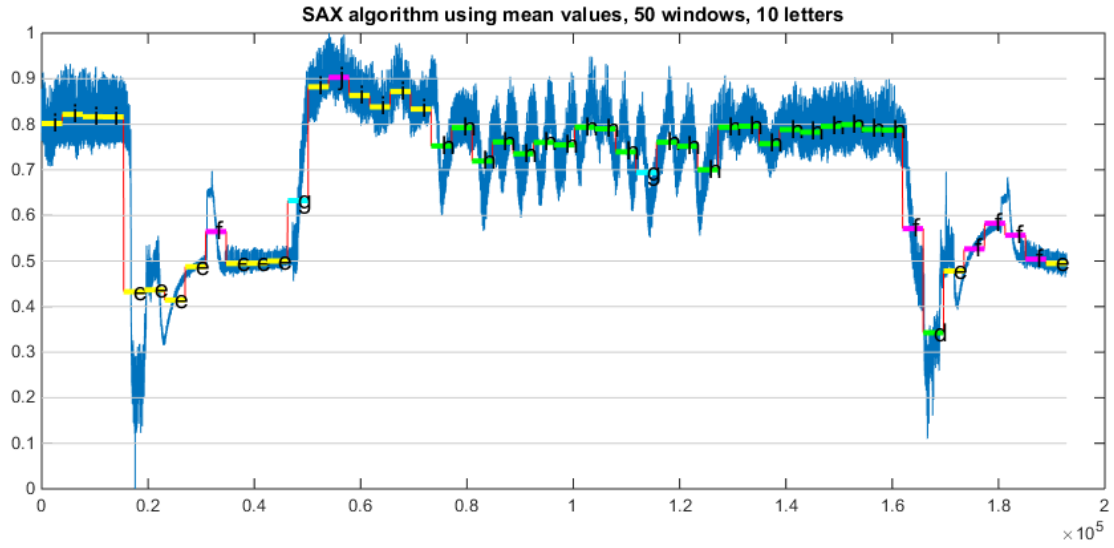

Fig. 51—Sax algorithm misses the "a" letter required for the identification of the connection.

The application of the SAX algorithm on connection patterns in WOB data didn't yield satisfying results. Purely time series data based approaches, such as SAX, may face the following challenges:

- The connection patterns are dissimilar, so it is even difficult for a trained human eye to pick the right point.
- Techniques that apply averages are inaccurate due to unforeseeable and significant spikes in pressure data.
- Even if the right letters were picked, the averaging techniques may have made the methodology inaccurate, since the correct WOB point is limited to a very small time interval.

- Normalization of data is required, because the data can drift out of physically possible values.
- Event detection could improve the proposed SAX approach, but it adds another layer of complication to the problem.

4.4 AUTOMATED DOWNHOLE AND SURFACE ALIGNMENT

Downhole data does not include parameters such as surface values for WOB, RPM and flow rates, or other parameters that allow to determine the rig activity at a certain point in time. Therefore, the alignment of surface and downhole data is necessary to add context to downhole data. Downhole data sets usually contain "time stamps", i.e. a date and time indicator for every row in the data set. However, these downhole times often are not well aligned with surface times. As described in more detail in Chapter 5, the time discrepancies can be seconds (e.g. latencies, clock errors), minutes (e.g. processing errors), hours (e.g. time zone errors) or even days and years (human errors).

Correctly aligning surface and downhole data is currently a tedious manual process. It can be achieved by finding distinct spikes in both data sets, or comparing patterns of connection and drilling sequences.

4.4.1 Alignment Algorithm

The proposed automated alignment algorithm is based on detecting similar patterns in connection times and the distances between connections. Mud pumps must be shut off during each connection. Pressure data is a very reliable indicator of turned off pumps, both on surface and downhole. In short, binary pump-on/off patterns for downhole and surface data sets are compared at every instance, the best match indicates the right time alignment.

Fig. 52 is an illustration of the alignment algorithm. First, binary pump-off indicators are extracted from the data, both for surface and downhole. For surface data, a threshold for pump pressure (e.g. lower than 200 psi) is used to determine that the pumps are shut off. Other parameters, such as flow rate or pump strokes could be used interchangeably. For downhole data, absolute thresholds are not suitable, since pressure changes with TVD. Instead, turned off pumps are indicated by a low variance in pressure (see WOB correction algorithm).

Next, basic data processing techniques are applied to the binary indicators for both downhole and surface data: scattered points are removed, clusters in close proximity are connected (they likely belong to the same connection activity) and short clusters are deleted (just low pressure, not a real connection). In addition, surface data is resampled at the same sample rate as the downhole data.

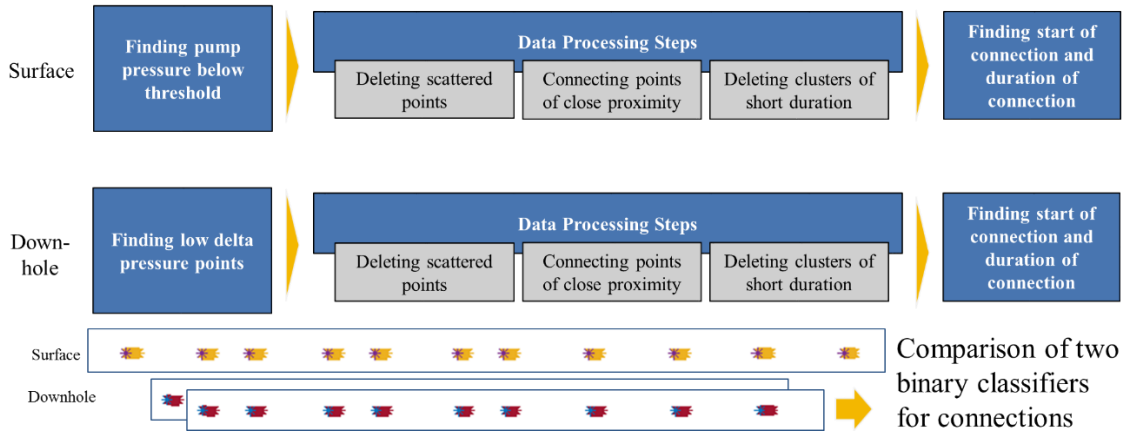

Fig. 52—Illustration of algorithm for surface and downhole alignment.

As shown in **Fig. 53**, the binary surface and downhole pump off indicators are compared at each time step, while the shorter set (most often downhole) is moved along the longer sequence (most often surface). For each time step n, the match number may be

calculated as the sum of instances, where the subtraction of surface and downhole indicators i yields zero. The highest match number indicates the best alignment.

$$match_n = \sum_i [(SF\_Ind_i - DH\_Ind_i) = 0] \tag{33}$$

$$shift = \max(match_n) \tag{34}$$

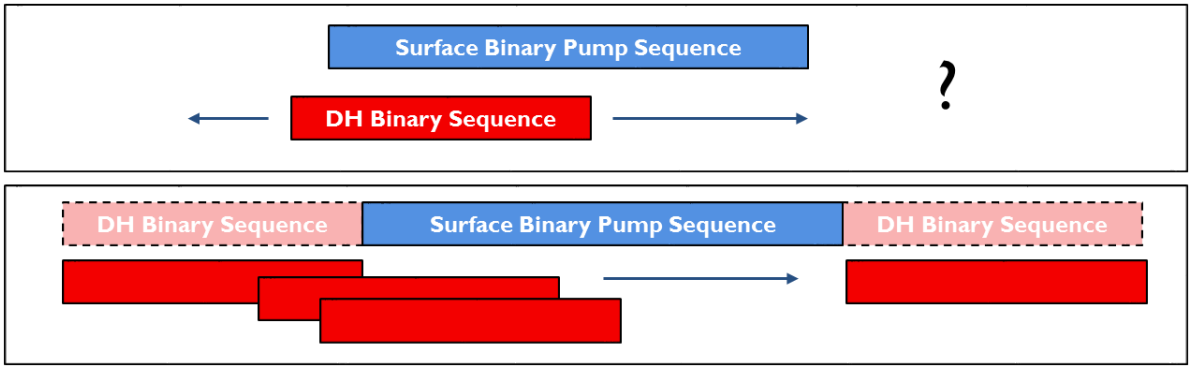

Fig. 53—The shorter sequence is moved along all time steps of the longer sequence to find the right match.

In **Fig. 54** a single maximum point for best alignment clearly stands out.

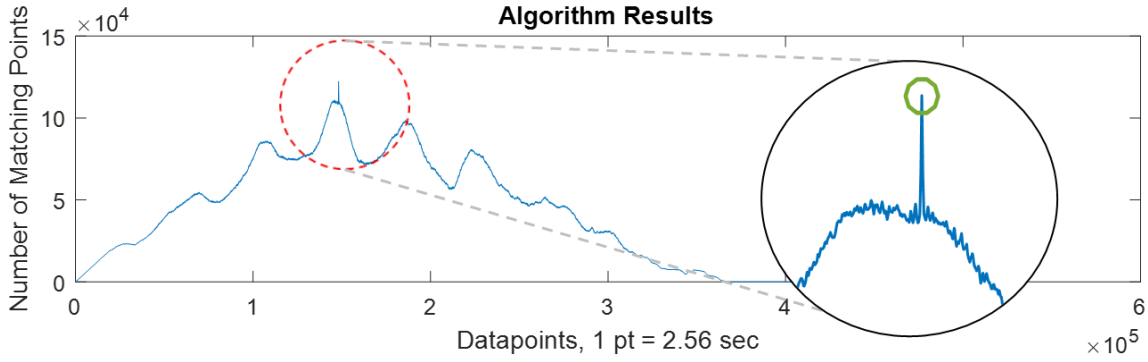

Fig. 54—Results of match number n for all surface data points.

Fig. 55 shows two matching sequences of real data. The algorithm was still able to identify the correct alignment, although both sequences do not perfectly match (which is expected using field data).

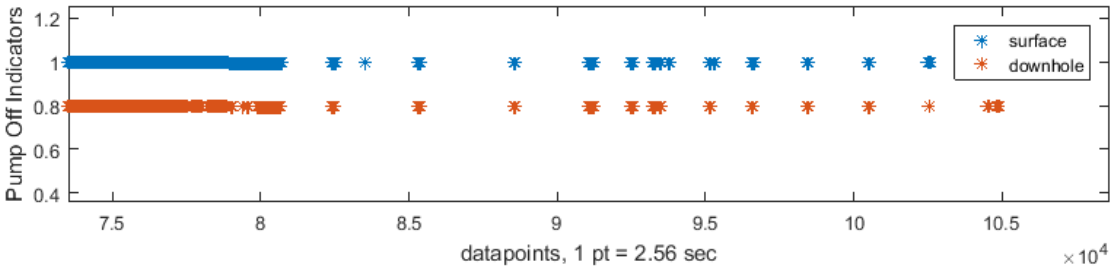

Fig. 55—Matching binary sequences in surface and downhole data, downhole data indicators are 0.8 instead of 1 for better illustration.

4.4.2 Latencies

Theory

The proposed algorithm matches the two time series by aligning changes in pressure responses to pump activities. It thereby neglects any latencies that inevitably occur as the distance between downhole and surface measurements advances. The term "water hammer" is describing the generation and propagation of a pressure wave through liquids in pipes. Shutting off or making changes to the pump rate produces a pressure wave traveling in the borehole. The more rapid the change, the larger the pressure wave. These pressure waves have been studied in the context of drilling for shut-in strategies of the blow-out-preventer (BOP) (Jardine et al., 1993) or pump pressure transients for long wellbores (Skalle et al., 2014).

In rigid pipes, the acoustic velocity c of a pressure pulse is

$$c = \sqrt{K/\rho}\,, \tag{35}$$

where K is the fluid's bulk modulus and ρ is its density. Both, Jardine et al. (1993) and Skalle et al. (2014), adjust Eq. 35 for elasticities of the wellbore and pipe, because a fraction of the energy is absorbed by expanding walls. Skalle et al. (2014) additionally account for suspended solid particles in the mud by adjusting the bulk modulus and mud density. Based on their assumptions, Jardine et al. (1993) use a constant wave speed of c = 1,350 m/s, whereas Skalle et al. (2014) use c = 1,400 m/s for subsequent calculations.

For our purposes, it is legitimate to assume a constant wave speed (e.g. of 1,350 m/s), so the time delay is only proportional to the borehole length. For a hypothetical enhanced-reach well of 10,000 meters, the latency at the last connection for c = 1,350 m/s is 7.41 seconds, for c = 1,400 m/s is 7.14 seconds. Even if neglected parameters cause the assumed wave speed to be off by 200 m/s, the largest latency uncertainty spans about 1 second. With sampling rate periods of about 2.5 seconds, this difference cannot be noticed in the data.

Application of Latencies

To improve the above-mentioned technique despite latencies, data can be corrected before running the algorithm. A flow chart of the matching algorithm under consideration of latencies can be found in Appendix B.1.

Let's say latency effects are "stretching" downhole data in comparison to surface data (**Fig. 56**). The downhole time t' then is

$$t_i' = t_i + \Delta t_i. \tag{36}$$

Making use of the relationship of latency and measured depth (MD) and wave speed c we get

$$t_i' = t_i + \frac{MD_i}{c}. \tag{37}$$

Note that downhole dynamics data is usually time based, while latency effects depend on the hole depth, so the "stretch" is not constant over time.

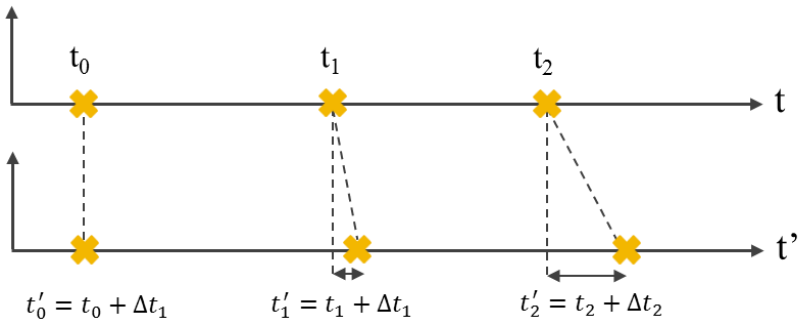

Fig. 56—Latencies "stretch" downhole time t' compared to surface time t.

Since hole depth information is usually present in the surface data sets, the surface data needs to be "stretched" to resemble the downhole time using Eq. 37 before running the algorithm.

If hole depth information is available in the downhole data set and not in the surface set, the time of the downhole set needs to be corrected using

$$t_i = t_i' - \frac{MD_i}{c}. \tag{38}$$

Because this procedure changes the sampling rate (e.g. from periods of 1 second to periods of 1.0007 seconds), the surface data then needs to be resampled in the sampling periods of the downhole data.

After adjusting for expected latencies, the matching algorithm can be run on the data. After the matching algorithm indicated the correct alignment of the data, the latency at the start of the downhole data set needs to be added to the matched time. Then, the original (unchanged) downhole data should be used for further analysis. Physics based latencies, as opposed to drifting clocks in sensors, should not be eliminated from the data.

If, in future studies, the correlation of surface and downhole data effects is investigated with high-frequency data, such latencies must be modeled and the properties of the mud and wellbore considered. Another option for more accurately aligned data is to carefully calibrate the clock located in the downhole tool. Such techniques for clock calibration are yet to be developed. In addition, data processing times in the downhole tool then need to be accounted for.

Discussion

Theoretically, latencies could be tackled using data based approaches such as time warping. In the case of determining latencies, a physical approach by nature is preferable over a data approach. Downhole data sets are usually based on individual runs while surface data sets contain data for the entire well. Therefore, the latency at the start of a downhole data set is not 0, but it is determined by physics (i.e. pressure latencies are determined by the pressure wave propagation speed and the length of the wellbore). A purely data based algorithm wouldn't recognize this difference and the initial latency at the start of the data would be 0 by default.

In addition, the duration of the latency depends on the type of data that is used for alignment. For pressures, latencies are determined by water hammer physics. For vibration data, latencies are determined by the vibrational wave propagation through the string. For WOB, latencies are determined by the properties of the string (elasticity, stretch, etc.).

4.5 AUTOMATED VIBRATION CLASSIFICATION

Current vibration classification methods usually differentiate type of measurement (radial, tangential, axial) and absolute vibration levels (Macpherson et al., 2015). With this alone, it is difficult to satisfactorily classify vibrations and their levels, because of coupling

effects, offsets, drifts, etc. Also, measurements are not (yet) standardized, they depend on the setup of the tool, on the placement of the tool in the drillstring, on the position of the sensor within the tool, on the type of accelerometer, on the number of sensors, on the number of measurement axes and so forth (Baumgartner et al., 2016; or see Chapter 5). Sometimes sensitive MWD tools are deliberately dampened to increase the tool life. This, however, will affect accelerometer measurements. Even if all these factors are accounted for, accelerometer outputs show a certain offset that varies over time in the same bit run.

The current practice of only studying statistics (such as RMS, minimum or maximum values) of the data over certain time windows results in the loss of valuable information (Baumgartner, van Oort, 2015; or see Chapter 3). High or low frequency signals are capable of generating the same statistical values, despite their inherently different high-frequency patterns. Service companies usually have fixed thresholds for acceptable RMS acceleration levels, and sometimes these levels are different for torsional, lateral, and axial directions (Osnes et al., 2009). All these factors complicate quick identification of the type of vibration and the appropriate mitigation strategy, which is quite different for e.g. stick-slip and whirl. In the following, we propose an effective approach to identify vibrations based on their data patterns rather than absolute acceleration or torque values.

4.5.1 Approach

The approach to automated vibration classification revolves around the basic idea that patterns in acceleration data are more important for its distinction than absolute values. It employs statistical methods to automatically recognize the type of vibration in high-frequency data sequences. Pattern recognition is a technique in machine learning concerned with assigning a given pattern to one of a finite set of known classes. The goal is to replicate

human recognition and classification techniques by an automated algorithm. The described pattern recognition approach is using supervised machine learning techniques that require labeled data for training an algorithm, as opposed to unsupervised learning techniques where the algorithm provides a classification automatically.

First, the downhole high-frequency data set is spit into time windows of equivalent length. Each of the data sets is given a classification regarding the type of vibration that can be observed. The classification is done manually using the author's prior knowledge and insights gained from the whirl model described in this work. While humans can recognize patterns naturally in a variety of representations (image, sound, data graphs, etc.), for machine processing the data input needs to be in a digitized and tabulated format. The process of describing the high-frequency patterns with a few characteristics is called "feature extraction". These features, not the entire data set, function as predictive variables for the machine learning algorithm. The algorithm learns how features (characteristics) of a dataset relate to a particular classification. The algorithm then can reapply the learned relations to new data and perform the classification automatically.

Only a certain portion of the pre-classified datasets are used for training the algorithm, the other part is used for testing it. In the testing phase the trained algorithm us run on the "unseen" test data. A comparison of the automated classification and the existing classification indicates the effectiveness of the algorithm.

4.5.2 Validation

In a test study, we demonstrate the effectiveness of the described approach for automated vibration classification. A set of field data recorded during an actual drilling operation was selected for this study. The particular data set included a variety of vibration types of different severities. Like other downhole data sets, in addition to continuous data,

it contained burst data sequences with sampling rates of 400 Hz in 10-second windows, recorded approximately every 20 minutes in a 90-hour bit run. The signal was recorded using one radially oriented accelerometer located close to the bit. **Fig. 57** displays four examples of downhole vibration events in time windows of 10 seconds. The vibration patterns of interest are stick-slip and lateral vibrations.

The data set includes 250 of the 10-second windows described above. Each burst sequence consists 4000 data points of acceleration measurements. We manually classified all 250 burst sequences after visual inspection as stick-slip/no-stick-slip or whirl/no-whirl. For the feature extraction step we defined several features (predictive variables) and automatically extracted these features from each burst set.

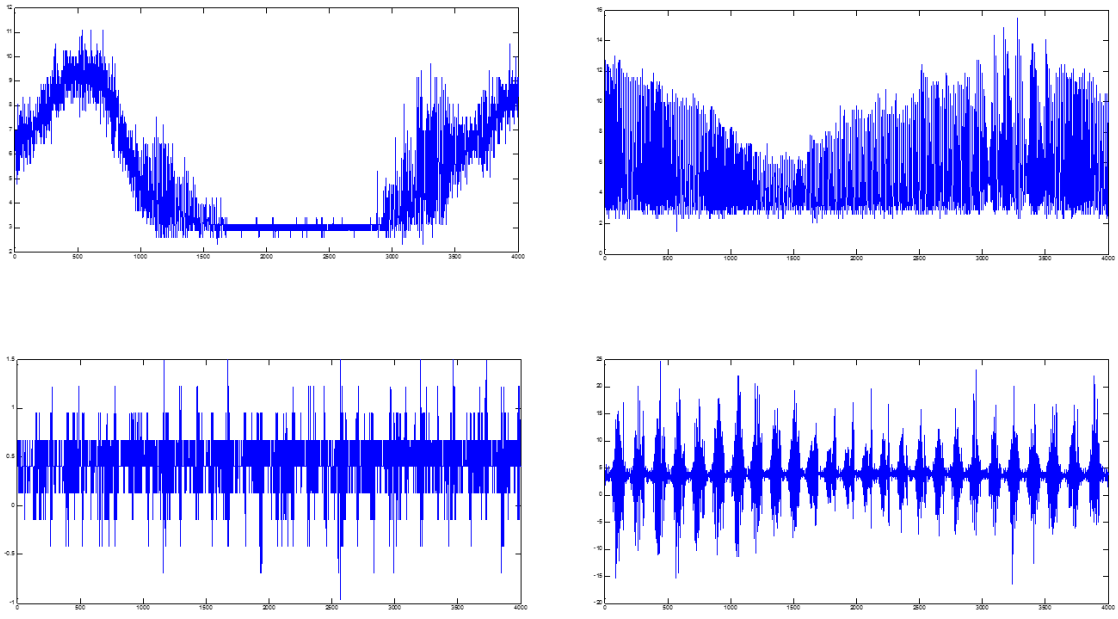

Fig. 57—Examples for vibrational patterns from a radially oriented accelerometer, each being 10 seconds long. The top left window captured low frequency stick-slip, the top right shows the same low frequency stick-slip coupled with whirl; the bottom left window was recorded while the bit was off bottom; the bottom right window most probably indicates a severe form of lateral vibration.

The final feature set included 250 observations with the following 15 predictive variables (an illustration of the feature set can be found in the Appendix B.2):

- **Time**: Time stamp of the data recording is included in the data to account for time dependent phenomena.
- **Statistical Data**: Statistical data includes absolute maximum and minimum values, the difference between them, standard deviation, and variance.
- **Smoothed Data**: Since stick-slip is overlaid by higher frequency events, a running average algorithm has been used to calculate a smooth curve following low-frequency fluctuations. Extracted from this smooth curve are the maximum, minimum and difference between those two.
- **Frequency Data**: A Fast Fourier Transform (FFT) has been performed on the data and for the two highest peaks in the frequency spectrum, both frequency and amplitudes and their distance have been recorded.

The data set with 250 observations was split into a training data set and a test data set with a ratio of 70% to 30%, i.e. 150 observations for training and 100 for testing. A Naïve Bayes Classifier was run on the set. Further information on the algorithm and parameters can be found in Appendix B.2. In this particular data set, the bit was on bottom and drilling in 93 out of the 250 observations, hence 37%. Stick-slip was present in 50% out of these 37% on-bottom-observations, lateral vibrations were present 30% of the time spent on drilling. The automated classification of stick-slip and whirl was performed independently with two separate algorithms, one for each class.

4.5.3 Results

The naïve Bayes classifier was able to correctly identify stick-slip in approximately 90% of the cases and whirl in approximately 92% of the cases. The algorithm was more likely to create false alarms, i.e. indicate a vibrational dysfunction event when there was none rather than failing to recognize it from the data. Many of the wrongly predicted classes were in fact also visually hard to distinguish from normal drilling or coupled forms of stick-slip and whirl. Typical confusion matrices for stick-slip (left) and whirl (right) are shown in **Fig. 58**.

		Visual/Manual Classification	
		No Stick Slip	Stick Slip
Model Classifi-cation	No Stick Slip	51	4
	Stick Slip	6	39

		Visual/Manual Classification	
		No Whirl	Whirl
Model Classifi-cation	No Whirl	54	0
	Whirl	6	15

Fig. 58—Example confusion matrix for a Naïve Bayes classifier, with a failure rate of 10%, showing false negative and false positive classifications for 100 sample burst sequences.

The machine learning approach demonstrated to be effective in detecting stick-slip and whirl in a particular data set. Applications of this work could be an automated classification (tagging) system for new data sets for improved post drilling analysis or the development of algorithms for immediate classification, implemented downhole or at surface.

With this approach, real-time classification of downhole data could be performed directly at the downhole sensor, offering opportunities for significant data reduction while essential information is provided. Only two numbers, one indicating the type of vibration and the other indicating its severity need to be sent to surface through either wired pipe or mud pulse telemetry. Post processing of gigabytes of data could be performed in minutes,

after an algorithm has been trained with a sufficient amount of data. The analysts could immediately identify downhole dysfunctions and easily link them to operational parameters, formations, and other drilling conditions. Heisig et al. (1998) describe the process of advanced feature extraction from downhole data using fixed thresholds in absolute values to classify vibrations. The novelty of the current method presented here is the application of supervised learning techniques for automated classification based on these features.

4.6 DISCUSSION

As mentioned throughout this work, the user is provided with downhole data in a variety of forms. Type of measurement (e.g. internal vs. annular pressure), data rates and types of recorded statistics (e.g. minimum, maximum, variance) usually solely depend on the settings chosen by the data provider and changes with every data set. The success and parameters for the shown algorithms in this chapter depend on these factors and need to be tailored to the characteristics of the data set.

Downhole time series data shows an elevated level of complexity. First, as shown in Chapter 3, most downhole effects have a potential to influence a particular measurement. Thus, patterns are not always predictable and unexpected high or low frequency noises can interfere with the signal. For instance, periodicity of the signal can depend on operations (e.g. the distance between 2 connections), which varies significantly. Traditional signal processing approaches may fail under rapidly changing and unpredictable patterns. Therefore, the above described methods are tailored to the specifics of the drilling process (e.g. finding connections as ‘static points’) and, for the first time, achieve results that can replace manual input and improve performance (in comparison to the manual correction).

For offset correction of accelerometer data, the average of the data over a short window may not coincide with the expected zero level. Therefore, first, time windows without additional disturbances need to be found: during connections when the string is 'in slips'.

For example, a pattern recognition technique, the SAX (Symbolic Aggregate approximation) algorithm, was applied for the identification of the zero-WOB point during a connection. In our experience, such algorithms seemed to be less successful than the methods described above. The connection patterns may change significantly, because the actions on surface are not strictly standardized. Even if the data is normalized, high or low spikes cause the patterns to take different shapes each time. Often, the points of interest are difficult or impossible to spot for even a trained human eye. Thus, so far, the application of physics (e.g. finding low pressure variance) combined with data has been more successful than a purely data based technique.

4.7 CONCLUSIONS

Downhole sensors for measuring drilling dynamics are promising to positively impact drilling performance and enable drilling automation. Downhole data is currently underused. Many drilling engineers are facing difficulties making decisions based on downhole real-time data or analyzing such data after drilling. Better data quality will result in higher utilization of such data and positively impact drilling performance. However, sensors and the process of data collection, processing, and transmission need to be improved to deliver more useful and reliable data to the end users.

4.7.1 Long-Term Solutions

Most importantly, operators and other users of data must define and enforce data quality according to their needs. The design of downhole sensors needs to be based on the requirements of the end users. Higher costs of better sensors that deliver more accurate data can then be justified by operational savings. Such efforts require interdisciplinary initiatives and collaborations across different types of companies. Tool manufacturers need to better involve suppliers of sensors, so they are adequately designed for applications in harsh downhole environments. This supply chain improvement process has been successfully implemented for many other services and products, and in many other industries.

Wellbore positioning and well logging efforts have shown successes of standardization and transparency of calibration, corrections, and data formats that lead to more reliable data for decision making. Similarly, for downhole dynamics data, transparent and standardized calibration procedures could hold the key for improved data quality. Calibration periods should be subject to contracts between operators and service companies. The need for additional calibration methods, especially during operations, should be identified and new techniques developed.

4.7.2 Short-Term Solutions

Analysis of downhole data requires skills and experiences that every individual analyst currently needs to re-develop from scratch. This work summarizes commonly encountered obstacles and offers solutions to them. Novel data correction and classification techniques are developed and applied to recorded field data in this work. Drilling dynamics data that was previously completely out of range and thus unusable became valuable.

For downhole data, it is difficult to use absolute values (e.g. for identification of shut-off pumps) because the data can drift significantly out of physically possible values. Relative values, such as variance, are more reliable identifiers, despite bad data quality.

For classification of vibrations, using the absolute values to differentiate severities is inaccurate for two reasons: first, accelerometers also record a gravity component and they usually drift significantly; second, as detailed in Chapter 2 and 3, movements cannot be recorded in isolation with single axis sensors. This work demonstrates how offsets can be removed from accelerometer data and how a naïve Bayes classifier can successfully detect vibration types, even for coupled events.

A methodology to automatically identify zero-WOB/TOB points and thus calibrate data was developed and demonstrated using field data. This can make tedious manual processes that are currently delaying the transfer of data to the end users obsolete. It also could offer a solution to replace lengthy and error prone taring procedures at the rig.

A simple but effective algorithm can automatically align downhole and surface data. Downhole latencies in pump pressure responses are also taken into account.

The suggested techniques include applications of machine learning, as well as basic data processing, using a combination of data and process knowledge. Even though signal processing techniques were less successful in some of the tested applications, this work does not reject their usefulness in general. For future work, the application of conventional signal processing should be explored further.

The presented methods in this work are a small selection of many possibilities. The same objectives can be achieved using different approaches and there is a need to develop additional methods to further improve the quality of analysis. Nonetheless, we hope that

the shown techniques are only short term fixes of a problem that, in the long run, can be solved by better sensor technology.

Chapter 5: A Data Transfer Format for Transparency and Standardization[9]

5.1 INTRODUCTION

The drilling industry has begun to cherish the value of data collected from downhole sensors, often gathered at high frequencies. Moreover, it has started to capitalize on the availability, analyses, and credibility of this data through step-changing knowledge gains that have enabled meaningful drilling performance improvements. As a result, topics like data quality, data ownership, and data integration are now routinely being discussed among stakeholders as data from downhole memory tools slowly starts to integrate into routine well planning, optimization, and automation workflows.

The collectors of data usually are not the sole owners and main beneficiaries of such data. Large amounts of data are transferred from service providers to various collaborators within and across companies. The process of agreeing on a data format, relevant accessory information and means of transfer, is currently laboriously repeated on a project-by-project basis. This practice not only unnecessarily consumes resources on both ends, but also carries the risk of losing crucial contextual information. WITSML (Wellsite Information Transfer Standard Markup Language), a current standard for transmission of technical data, is often unsuitable for large high-frequency data files and do not provide enough flexibility for certain contextual information.

[9] Chapter based on: Baumgartner, T., Zhou, Y., & van Oort, E. (2016, March 1). Efficiently Transferring and Sharing Drilling Data from Downhole Sensors. Society of Petroleum Engineers. doi:10.2118/178900-MS. Contributions: Baumgartner, T.: Concept, methodology and sample MDTS structure; Zhou, Y.: Literature and file formats; van Oort, E.: Supervision.

This work proposes a file format suitable for securely storing downhole data and sharing it across all stakeholders, providing both flexibility and simplicity. The developed file format implements a set of specialized horizontal and vertical dividers to structure contextual information on the well, the run, and the sensors, and to store them in the same file as the measurements. Among other things, well and section information, responsible personnel, equipment and sensor properties, time calibration, and operational parameters may be specified. The inclusion of both required and optional inputs ensures both flexibility and essential context, and allows the coverage of a variety of applications. It is comparable to the Log ACSII Standard (LAS) file that quickly found wide acceptance in the well logging community and beyond after its introduction in 1990.

The implemented dividers enable the data files to be easily accessed by variety of programs and comfortably viewed by the human eye using any standard spreadsheet or text file application. Importing and exporting applications can be provided to the users, who can then easily produce these files from raw data for transfer, or integrate them into existing data management systems.

Stakeholders, such as operators, service companies, and tool manufacturers are involved with the creation of this standard file format to ensure consent among all users. The standardization of downhole sensor data files proposed in this work marks a key step towards automated analysis of downhole data, reduction of data loads, and data integration. Our approach is illustrated using examples of how the new standard can be applied on actual field data.

5.1.2 Problem Statement

In recent years, the emergence of downhole sensor data has helped the industry to gain a better understanding of the drilling dynamics. However, analysis of such data has

been difficult mainly due to the incompleteness of contextual data. Unlike its more standardized off-shelf counterparts, the surface sensors, downhole sensors can be vastly different from one another. The same downhole sensor measurement (i.e. measurement of lateral drillstring vibration) can generate very different values depending on the sensor orientation, sensor location, processing technique, etc. Lately, the industry has started to recognize the importance of providing such information to avoid confusion in downhole memory data (Macpherson et al., 2015). They proposed to use an open measurement framework in an attempt to standardize the measurement. However, it stopped short from offering a solution for transferring such important data.

Sharing data among stakeholders is of essential importance in the oil and gas industry. Vital measurements of the downhole environment are usually carried out by multiple service providers, which are later reported back to the operator (who are the main beneficiaries of the data). To extract value, data is frequently analyzed by internal personnel from different segments within the operator company, by external consultants, and by third party collaborators. Often as the data owner, the operator company has a strong incentive to thoroughly collect, properly store, and effectively share a complete set of data. Data acquisition and exploitation are usually done by separate groups of people with little overlap. This makes metadata (or contextual information) an even more essential part of such a data set, without which sophisticated analyses by different parties becomes very labor-intensive. In addition, vendor neutrality in the data structure allows effective use of it by all parties equally.

At this time, the transfer of the downhole memory data lacks a standardized protocol. Downhole measurements have traditionally been saved in a spreadsheet; minimal to no contextual information is usually provided, typically only through a short name of a

measurement, the file name itself, or in a dump of unstructured separate files. When analyzing such data, the end user must reach out to multiple parties to acquire the needed contextual data, making the process inefficient and painfully slow. There is an urgent need for a standardized format for transferring memory data with a minimal set of essential metadata to enable an efficient, user friendly way of sharing data.

This work proposes a LAS-style data format specifically to address this issue. LAS is a remarkable success story for sharing well logging data, and could be similarly helpful for downhole dynamics data. It provides an easy to adopt, simplistic solution that can facilitate the effective sharing of downhole data until it can be integrated with more advanced standards supporting all ranges of data in the drilling industry.

Other industries that use data to explore complex relationship have had similar struggles and came up with similar mitigation strategies. For instance, the Genomics Standard Consortium (GSG) was founded in 2005 and helps promoting standards to make genomic data discoverable, by international standards. They too, defined a framework for standardized minimum information about gene sequences, described in a commentary in *Nature Chemical Biology*[10].

5.1.2 Approaches for Sharing Data

Sharing and transferring of data is of immense importance for the entire oil and gas industry. Compared to the drilling industry, the well logging community has done an excellent job in developing specific formats for data transferring and sharing, supporting the need for data collaboration among a diverse group of end users. They, too, had to go through a process of defining and managing data quality in their data (e.g. Al-Farisi et al.,

[10] http://www.nature.com/nchembio/journal/v11/n9/pdf/nchembio.1890.pdf

2002). A case study on the well logging data usage for the Belridge field by Area Energy provided a detailed breakdown in **Fig. 59** below (Allan et. al., 2012).

End-User	Needs, Uses, and Customers
Geologists	Geologists are not 'power users' of petrophysical data. They generally need enough log curves to pick the key geologic markers and any fault cuts via visual correlation using nearby wells. The geologists for the Tulare reservoirs rely on the field's petrophysicist to calculate porosity and saturation curves. The calculated curves are then used in their 3D reservoir models to monitor the growth of the steam chests and plan new wells. The geologists for the diatomite reservoir rely on algorithms to calculate curves for porosity and saturations. The raw and calculated curves are then used to improve the existing reservoir characterization and to build 3D models. The 3D models are used for pore volume and oil-in-place as well as to generate the pseudo-logs needed by the development engineers to plan future wells.
Petrophysicists	The petrophysicist for the Tulare reservoirs reviews the triple combo curves for each open-hole log. The sand beds are given a constant density porosity in wash-out sections and the saturation depends upon a mix of water, oil and steam depending upon where the well is structurally and whether any steam-chests have developed. However, most of the workload is from the reviews of the GR and neutron curves from each of the many cased hole observation wells that are relogged every two years. The porosity and saturation curves are then exported to the geological databases for use by the geologists. Petrophysical work for the diatomite reservoir is currently limited to detailed evaluation of the few fully logged wells and special core analysis in order to confirm existing petrophysical algorithms or show the need for new ones. Because so many wells are logged each year, it is not feasible to evaluate each well individually. Instead an Archie-based algorithm is run routinely to get the 95% solution.
Reservoir Engineers	The engineers for the diatomite reservoir need pressure data from the open-hole RFT surveys to measure waterflood conformance and then adjust water injection. They also use temperature data from DTS surveys to monitor water injection by zone.
External Customers	Government regulatory agencies, joint venture partners, and some royalty owners have a right to receive the raw petrophysical data. Paper prints and Adobe PDF copies of the logs are normally sufficient. Distribution of these mandatory copies is typically done automatically by the Petrophysical Data Management Center and is invisible to the other end-users. The government regulatory agencies normally place copies of the logs in the public domain either soon after receipt or at the end of two years if the well is confidential.

Fig. 59—The use of well logging data by different parties (after Allan et al., 2012).

Propelled by the need, several different data transfer standards have been developed over the years. They are the general ASCII format used for temperature logs and profile surveys, the Log Information Standard (LIS) by Schlumberger, the LOG ASCII Standard (LAS) by Canadian Well Logging Society, the Digital Log Interchange Standard (DLIS)

forma by API (American Petroleum Institute), and the WellLogML format by Energistics (Allan et al., 2012).

Among them, WellLogML is the most technically advanced data format. It was designed to be a web based exchange standard for well log data, with the intent to replace the LAS format in the 2000s (Schultz et al., 2000). However, it has yet to gain popularity. The LAS format is still the "work horse" of well logging community and beyond, mainly because of its simple, easily readable layout (Schultz et al., 2000).

On the drilling front, the quest for a data transferring format catering to real-time surface sensor data has led to WITSML (Wellsite Information Transfer Standard Markup Language). It has become the de-facto transfer standard for surface sensor data exchange and real-time data streaming. However, the current WITSML version 1.4, is inadequate for downhole memory data use because of its limited capabilities for metadata specification. The addition of comprehensive downhole data support in future releases will give WITSML extended capabilities. Even then, downhole data will require metadata of much greater detail and complexity than surface data.

Recently, the SPE Drilling System Automation Technical Section (DSATS) selected OPC-UA (Open Platform Communications Unified Architecture) as a communication framework for drilling automation. It has benefits over WITSML, because of its wide acceptance in industrial automation, security model, extensibility, scalability (Florence et al., 2015). While those are all desirable characteristics, OPC-UA does not specifically address the issues in downhole data transfer and certain added features make it inefficient to use for this purpose.

As mentioned previously, the transferring of downhole memory data frequently involves the use of USB sticks or hard drives. Many end users also prefer manual

inspection, and for some measurements, manual or semi-automated manipulation after retrieving the data is required. Simplicity and human readability, along with machine readability and data completeness, are the most desirable features. The *memory data transfer standard* (MDTS) proposed in this chapter provides a ready-to-use solution for the transferring of downhole memory data until it can be integrated with more advanced standards supporting all ranges of data in the drilling industry. A detailed case study that inspired the development of the proposed memory data transfer standard is described in the next section.

5.1.3 Transfer of Downhole Data – A Case Study

The transferring of downhole dynamics data from vendors to a client (operator) for analysis is just starting to become more common. Traditional drilling data transfer methods (e.g. WITSML) are currently not used for such downhole dynamics data; an efficient transaction process has yet to be developed.

This illustrative case study describes difficulties during data analysis of a pilot project for drilling optimization using downhole data. The lack of an appropriate data transfer method caused significant delays and reduced potential value of the data. During the case study, multiple wells were drilled using a variety of measurement devices from multiple vendors, both at surface and downhole. Quick and reliable analysis of vibration data usually allows a drilling engineer to adjust the designs of bits and BHAs for future runs and wells, or optimize drilling parameters (weight on bit, rotary speed etc.) while drilling for improved drilling performance. Vibration data from various locations in the drilling system also has value for research purposes. It allows for the study of propagation of vibrations through the string, to find vibration sources (e.g. bit, BHA or drillstring for lateral vibration), to verify vibration models with actual data, to determine the optimum

placement for measurement tools, etc. Some of these goals were set back by a variety of issues, most notably related to inefficiencies in the data transfer process.

Time Delay in Data Delivery

It can be generally stated that the value of downhole data decreases rapidly with time. Real-time information from the downhole system has the highest potential for instant mitigation of drilling performance limiters, risks, and identification of improvement opportunities. From post-run analysis, new runs and wells can be improved. Months after the well construction operation, historical data will have only indirect impact through research, identification of bad drilling practices, etc. In this example, it took up to several months for the complete datasets to reach the operator. By that time, momentum and incentives for operation engineers to analyze these datasets had nearly vanished.

Lack of Standardization and Definitions

In 2009, Osnes et al. outlined the lack of standardization of MWD vibration measurements. Until today no significant progress seems to have been made. The industry has yet to come up with a satisfying, but simple vibration classification, i.e. a single, well defined number that triggers the right mitigation action. Tool set up, sampling rates, data processing (such as filtering or combining multiple sensors), axial and lateral distances, etc. all influence the measurements. For vibrations, some companies calculate an RMS (root mean square) value, where the severity of vibrational dysfunctions is defined by threshold per type (Macpherson et al., 2015). These thresholds, however, are not universal. Two different tools deployed under the exact same circumstances would measure different levels of vibrations. In addition, thresholds for vibration severity classifications, if there are any, are not based on certain rules, but are chosen more or less arbitrarily (Osnes et al.,

2009). Thus, measurement data alone carries little value, metadata on thresholds is provided.

Data Corrections Requirements

Downhole sensors are susceptible to pressure and temperature conditions and experience a significant drift with time. One way these drifts can be corrected is to use defined off-bottom conditions as zero lines. This process, if done manually, is labor intensive and prone to errors. Physically impossible values (e.g. WOB is significantly higher downhole than on surface) can then be attributed to measurement errors either downhole, at surface, or both, or they are due to data processing errors. Such corrections need to be properly recorded in the metadata.

Another form of data correction is the synchronization of surface and downhole time stamps. Clocks do not only suffer from time shifts, but also exhibit systematic errors (for one clock, time passes faster than for another). These frequency errors can originate from downhole pressure and temperature conditions and are hard to detect. Considerable time shifts can occur due to processing errors, where a manually entered date is off by years or a tool gets calibrated at the shop and then deployed at a well in a different time zone. These factors make it difficult and labor intensive to align downhole and surface data.

Chapter 4 offers background information and automated solutions to some of the measurement errors. A standardized format for downhole memory data does not solve the issue of data synchronization, but properly recorded time synchronization information prevents this labor-intensive effort from being carried out multiple times.

High-Frequency Sequences

High-frequency sequences (also referred to as “burst” or “snapshot”) are very particular to downhole data sensors, and file sharing structures must account for them. Due to memory limitations, not all the recorded data is stored at its sampling frequency but at a much lower output rate. Downhole tools commonly are set up to record short windows of typically 5 or 10 seconds of data of frequencies in the range of 400 to 1000 Hz. These sequences are usually shared in individual files for each sequence. In this case study, these windows were recorded every 20 minutes. It proved impossible to analyze these sequences in context of continuous data (i.e. aligning “slow” and “fast” data from the same sensor), since no information to assist time alignment was shared. Even the automated alignment algorithm would fail in this case, because the sequences are non-continuous and usually too short to pinpoint connections or other spikes in data.

Lack of Metadata

In general, metadata is data that describes other data. In the context of this work we define metadata very broadly. Metadata can be any additional data assisting the usage of the actual time-based values in the datasets. In current convention, information necessary to relate downhole dynamics data to other data of the same well or run is only captured in the structure of how the file is stored. For instance, the only reference to the well name could be the name of the folder containing all the data for a certain well. Furthermore, subfolders might be named after the run number or called “lateral section” or “curve section”. If the datasets are taken out of their original structures, issues with unclear identification of datasets and subsets will arise. Information provided through data headers does not sufficiently indicate the nature of the measurement, e.g. if it was directly recorded or derived from multiple measurements. In exceptional cases, metadata is provided through

separate data files, such as specification sheets or daily drilling reports. Even then, the unstructured nature of those separate files and possible information overload prevent an efficient and automated usage of those metadata.

No Basis for Automation of Analysis

The volumes of downhole data collected per well was in the order of several gigabytes. These volumes per se do not constitute a "big data problem", however, under current circumstances, there is a high amount of manual labor required to convert the data into digestible information (e.g. into key performance indicators (KPI) or summary reports). Ideally, data should reside in the operator's database, which then enables automated analysis. Such a transfer from current spreadsheets, however, would require a tedious mapping process for each individual file type and would need to involve engineers and as well as IT personnel. Then, new vendors with different data formats would require a repetition of this process each time.

Case Study Conclusions

Barriers for the correct interpretation of data from downhole sensors are high. Because hiring a new service from a new company involve resources on both sides, operators will naturally tend to settle with a small number of tools and thus file types. This eliminates them from the potential benefit of competition or trying out innovative technology. The oil and gas industry in general - and the drilling industry in particular - significantly lags innovative developments in other industries. Latest technological developments show potential of handling data efficiently without requiring relational databases and semi-standardized structures. New machine learning techniques possibly have the potential to make the definition of structures, features and algorithms, obsolete

(e.g. Hinton et al., 2013). Yet, until these technologies can be proven to be effective solutions for complex drilling data problems, standardization is the way to go.

5.2 STANDARDIZED FORMAT

The suggested approach of agreeing upon a standard for transferring downhole high-frequency data constitutes a solution to most of the problems in the case study. As mentioned previously, there is a great diversity of file formats for the purpose of data transfer currently available. The selection of an appropriate file format for transferring downhole dynamics data should foster the widespread use and acceptance. Highest benefits for users should be achieved through the following principles:

1. *Simplicity and User Friendliness:*

Downhole dynamics data could become the ideal drilling optimization playground for data scientists and drilling engineers. The proposed data format should facilitate opening this field to professionals outside the major operating and service companies, as well as players in the disciplines outside the oil and gas industry. To avoid any barriers to data access, these files must be both human- and machine-readable, and accessible with any standard spreadsheet or text application. Moreover, the files should be easy on the eyes of the users and open to direct manipulation.

2. *Flexibility:*

Similar to the transfer of well log data, some metadata is absolutely required for its use (e.g. unique well name) and other data is “nice to have”, i.e. optional (e.g. well coordinates). The suggested MDTS supports this differentiation in required and optional metadata. As soon as such a choice of metadata becomes available to the industry, the exchange of metadata for each operation can be implemented through contractual agreements between data collectors and their clients.

The comprehensive analysis of downhole dynamics data is not (yet) part of the standard drilling engineering workflow. As sharing of such data becomes more popular, the specifications of required and optional metadata will be subject to an iterative process. The file format and related applications need to support these iterations in a flexible way.

3. *Data Integration, Completeness, and Quality:*

Companies still face many issues with data storage and data management. Many files are still stored and shared outside of standardized data management systems. This is especially true for one-off data sets and non-routine projects. To ensure the ease of integration of data contained in a file, metadata that is essential for the identification of an operation, should be stored within the file itself. A human readable header section ensures that measurements can be traced back to the respective run and integrated with other data.

4. *Standardization:*

With more and more data generated from every well, standardization is a prerequisite for an efficient and automated data analysis. After going through a mapping process once, data and corresponding metadata can flow seamlessly into a database. MDTS does not restrict or standardize what kind of measurement is being transferred, it is only concerned with the standardization of format and corresponding metadata.

From a variety of different transfer standards, LAS type ASCII (or Unicode) text files seem to be most suitable for the given objectives. It promises the alluring benefit of quick and widespread adaptation, both within and beyond the drilling industry. Standardizing the transfer of downhole data and setting metadata requirements will need to go through several iterations with small improvements. Those changes can be best

implemented and tested making use of the flexibility of a stand-alone MDTS file. Once accepted, it can later be integrated with other transfer standards.

5.3 METADATA SPECIFICATIONS

The drilling industry would greatly benefit from established and agreed upon measurements. Under current circumstances, standardization of measurements can only be pursued as a long-term goal. Cultivating transparency of measurements therefore is the best first step towards that goal. Metadata on the measurement, processing techniques and sensor specifications aims to achieve this transparency for the end user and has been addressed by a recent cross-industry effort (Macpherson et al., 2015).

The metadata header contains 5 basic blocks: file, well, run, sensor and measurement information. While file, well and run information ensure the "integrability" of the data, sensor and measurement information enable the required transparency of the measurements. One of the advantages of a LAS type file format is the ability to store a description of a "tag" (i.e. a piece of metadata with a unique name) together with the tag itself. This minimizes the misinterpretation of what a tag means. It therefore improves both the quality of the metadata during file creation and the interpretation of the end user. One file typically reports the output of one measurement tool, which can contain more than one sensor and multiple measurements. In Appendix C, an exemplary *memory data transfer standard* (.mdts) file for downhole dynamics measurements is provided.

File information features details on the version of the standard and the creation of the file, allowing end users to trace errors and ambiguities back to their origin.

File Information Block	
Tag	*Description*
Version	Memory Data Transfer Standard Version
Wrap	No wrap: One Line per time step
FileGenDate	Date this MDTS file was generated
FileGenName	Person who generated this MDTS file
FileGenAffil	Affiliation of person who generated this MDTS file

Fig. 60—File information block.

Well information includes descriptions that allow to link the file to related well information, such as a unique well identifier, geographical information and companies involved.

Well Information Block	
Tag	*Description*
WellName	Descriptive name of well
WellUID	Unique well identifier (country specific: API in US, NPD in Norway, etc.)
Wellbore	Identification of borehole
OperatorName	Operating company
ContractorName	Drilling contractor company
ServiceCompanyName	Data collection service company
SpudDate	Spud date
Field	Name of field
State	State
Country	Country
Latitude	Wellhead position latitude (north is positive)
Longitude	Wellhead position longitude (east is positive)

Fig. 61—Well information block.

Run information details parameters specific to the setup of the bit and BHA and includes time synchronization, sensor calibration and operational details. Downhole dynamics data is typically reported separately for each drilling run. Unlike depth based

logging data, drilling dynamics data is time-based and there are no overlaps between different runs, so the files can be treated separately.

Run Information Block

Tag	*Description*
BitRunNumber	Bit run number
StringRunNumber	The BHA (drilling string) run number
RunStartTime	Date and time that activities started
RunEndTime	Date and time that activities stopped
StartDepth	Depth of data recording start
EndDepth	Depth of data recording end
WellType	Wellbore trajectory shape (vertical, curve, horizontal, tangent,...)
BitSize	Diameter of drilled hole
BitType	Type of bit
SurfaceDataReference	Surface data collection system/company (e.g. Amphion, Pason,…)
TimeCorrection	Time lag to surface reference data reference, both shift and stretch
OperationsComments	Irregular operational event occurring in this run

Fig. 62—Run information block.

Device information describes the measurement sub (MWD, near-bit measurement system, etc.) that can contain one or more sensors. Details on device vendor, location and data transmission are specified in this block.

Device Information Block

Tag	*Description*
DeviceName	Commercial name of device
DeviceVendor	Unique identifier for data service company (e.g. stock code)
VendorContactName	Contact person within data service company
NullValue	Invalid number indicator
Transmission	Type of data transmission system (memory, mud pulse, wired drillpipe)
MemorySize	Size of downhole data storage (if applicable)
RealTimeRate	Data rate for real time submission (if applicable)
NoofSensors	Number of sensors in device
DeviceLocation	BIT, BHA, ASM, SUB, RIG, BSL - descriptive location
Axial Position	Distance from bit (ref: lower end of device)

Fig. 63—Device information block.

Sensor information specifies technical details on the sensors in a tool. The suggested list of metadata is repeated for each sensor in a device. This information does not change for the same sensor and should therefore be easy to compile by respective vendors. A sensor is any device that produces an individual measurement, e.g. if a multi-axis accelerometer produces 3 different data streams (axial, radial, and tangential), these 3 sensors should be described separately.

Sensor Information Block (repeated for each sensor)	
Tag	*Description*
~S1	Sensor number (S1,S2,S3,…)
SensorName	Commonly used sensor description or name
SensorType	Technical sensor name
SensorCategory	Acceleration, Velocity, Displacement, Force, Bending Moment, Torque, Pressure, Temperature, Angle, Frequency, Power
relAxialPosition	Distance from lower end of device
relLateralPosition	Distance from device axial center
SamplingRate	Sensor sampling rate
LastCalibrationDate	Date and time of last sensor calibration
LastCalibrationType	Offsite, onsite manual, onsite semi-automatic, onsite automatic
MinValueRange	Lower limit of sensor measurement
MaxValueRange	Upper limit of sensor measurement
Accuracy	Estimated field accuracy
Precision	Repeatability of measurement
DigitalResolution	Measurement increments
Filter	Signal goes through filtering process
High Cut-Off Amplitude	Filter description details
High Cut-Off Frequency	Filter description details
High Roll-Off Amplitude	Filter description details
High Roll-Off Frequency	Filter description details
Low Cut-Off Amplitude	Filter description details
Low Cut-Off Frequency	Filter description details
Low Roll-Off Amplitude	Filter description details
Low Roll-Off Frequency	Filter description details

Fig. 64—Sensor information block.

Measurement information specifies each of the data channels (columns) in the data section, it constitutes the data headers. **Fig. 65** illustrates such header information, where each row describes one column of data. Downhole dynamics data is often derived from one or more sensor measurements, so additional metadata is required for transparency. One sensor can produce a variety of sensor outputs, so each channel (time based data stream) requires a separate description. The measurement information block contains the very basic but essential information for each channel.

Measurement Information Block	
Tag	***Description***
Time	Time and date in standard format
Elapsed Time	Zero value = start of bitrun
Acceleration	Radial acceleration
RPM	Calculated value from radial acceleration
RMS	Root mean square value – measurement statistics

Fig. 65—Measurement information block.

For *sophisticated analysis*, the end user needs to know more than just basic data. In the *Channel Details Block*, details on each measurement need to be disclosed (**Fig. 66**). Since the details may differ for each sensor, they are differentiated in required and optional measurement metadata. These include details on the measurement sequences (if not continuous), calculated statistics, corrections, and data classification information.

Channel Details Block (repeated for each data column)	
Tag	*Description*
~C1	Channel number (C1, C2, C3,…)
Sensor	Sensor or sensors used for this measurement
OutputRate	Channel data rate
MeasurementCharacter	None, average, standard deviation, minimum, maximum, RMS, etc.
MovingAverage	Average calculated in moving window vs. fixed number of data points
WindowLength	Window length of statistics
DerivedValue	Output other than direct measurement or statistics
DerivationDetails	Description of derivation
Continous	Continuous data stream over the entire run vs sequences
SequenceLength	Window length of one high frequency sequence
SequenceGap	Time distance between two windows
SequenceTriggering	Start of data collection after triggering measurement value
Correction	Post retrieval data correction
CorrectionProcedure	Description of algorithm or procedure for data correction
Classification	Classification of measurement into severities or types
Class1	Name of classification type and upper and lower limits in respective units
Class2	Name of classification type and upper and lower limits in respective units
Channel comments	Irregular measurement observations

Fig. 66—Channel details block (per channel).

The data service company are capable of collecting all the above information. As described in the next section, MDTS generation software (writers) can be set up to largely automate the process of data collection, by extracting metadata from the vendor's databases. The LAS type format facilitates quality and completeness checks for metadata.

5.4 Workflow, Benefits, and Implementation

The memory data transfer format is intended to provide a vendor-neutral, simplistic solution for the effective transferring of downhole data for different parties. It specifies a minimal requirement for metadata that is provided along with measurements themselves. This ensures the completeness and usefulness of the measured data. The introduced format enables effective and efficient transfer of this data. Vendor-neutrality frees operators and

end users from the service provider's proprietary data architecture. As a standard format, it also functions as a point of reference for all parties to define data completeness. The simplicity of the format promotes an easy and direct access of the data by all parties, including universities, individuals, and small companies without sophisticated data infrastructures. It promotes wider adoption and utilization of valuable downhole data for deep analysis and drilling optimization.

Along with MDTS, readers and writers supporting popular data managing system will also need to become available for use. The service provider will then use a supported writer application to output all required data (and metadata) into the proposed MDTS file automatically. On the other end, end users can either uses the transferred data directly with a text editor, spreadsheet software, or can incorporate the transferred data with suitable readers into their data managing system.

Currently, several service providers, sensor manufacturers, and operators have expressed their interest, and have provided their input in finalizing the memory data transfer standard. Future collaboration towards reader and writer development catering to specific data managing systems is also being planned. We welcome interested parties to join the conversation.

5.5 CONCLUSIONS

This work outlines issues that are currently experienced with the transfer of downhole data from vendor to client and offers a solution. Recognizing that measurements cannot be fully standardized, it is suggested to define a standardized structure for sharing downhole data that can be easily adopted by all parties involved. In addition, by defining not only *how* the data should be shared, but also *what* additional data (metadata) needs to be shared, this solution ensures transparency of measurements. Such transparency will

increase the confidence in downhole dynamics measurements, and therefore enable and stimulate the development of applications building upon these measurements. These applications, not the measurements or tools themselves, are the true value creators.

Transparency and standardized data structures are not limiting to innovation, they are the first and necessary steps towards building a strong business case for the use of downhole data, captured either in real-time or in memory. Only then a true innovation process can be initiated to help the industry drill safer, faster, and better wells.

Chapter 6: Conclusions

6.1 CONCLUSIONS

This work shows that many areas in the field of high-frequency downhole data analysis are still terra incognita. For downhole dynamics data, the disconnect between tool technology, data collection and data analysis is larger than in other related areas, such as petrophysics. This disconnect can lead to misinterpretations of downhole data. Before such data can feed into rig controls and decision support systems, it needs to be fully understood, trusted and be of well-defined quality.

In Chapter 2 a 2D kinematic whirl model could demonstrate that high frequency fluctuations of tangential accelerometer data can be attributed to a whirling motion of the drillstring, not a high frequency change in rotational speed as the prevailing industry belief suggests. This work therefore offers an alternative explanation for the phenomenon of high frequency torsional oscillations (HFTOs). A novel tensor calculus approach to transferring the accelerations into the sensor's frame of reference reveals the nature of discrepancies with previous approaches: additional derivatives stemming from the transfer of coordinate systems had been neglected using rotational matrices.

It is consequently demonstrated that sensors under off-center rotation capture artifacts due to their eccentric sensor position within the drillstring. For comparison of results of vibration modeling and field data, these artifacts need to be accounted for. In addition, eccentric rotation of the bit, BHA and/or drillstring affects the calculation of rotational speeds from other measurements.

Chapter 3 provides an observational study of drilling dysfunctions using downhole data from a 5-well dataset. It is demonstrated that under bandwidth and memory limitations, the sampling rate of captured data needs to be customized to the type of measurement and type of downhole dysfunction of interest. Guidelines for optimized sampling rates are provided in the chapter. In addition, it is shown that downhole measurements are closely interlinked. Still, downhole dynamics can be differentiated by their characteristic frequency ranges. For adequate data interpretation and dysfunction detection, data from multiple measurements need to be combined during data processing. It is further shown how frequency ranges associated with a specific type of dysfunction can be selectively removed from other measurements in an instantaneous fashion.

Chapter 4 investigates design aspects of downhole sensors and reveals limitations and the source of sensor errors. To improve the quality of data from downhole sensors, tool design needs to be optimized for respective applications. Eventually, sensor and data quality requirements need to be specified by the end users.

To improve data quality in the short run, Chapter 4 demonstrates commonly observed obstacles to automated drilling data analysis and offers solutions to them. Automated solutions for accelerometer and weight/torque sensor error corrections are demonstrated. An algorithm is suggested that can automatically align surface and downhole data using pressure data patterns. For correct alignment, latencies due to traveling speeds of pressure wave propagation are considered. Based on the insights of previous chapters, a new method of vibration classification is demonstrated. The new approach is based on detecting patterns in high frequency data, as opposed to using hard thresholds of either lateral or torsional measurements.

The introduced techniques combine physics, drilling processes, and data. Signal processing approaches alone may be insufficient: data patterns may be non-repetitive, sensors may drift out of physically possible values, and data may not fully reveal phenomena such as latencies without a physical assessment.

Chapter 5 offers solutions to currently inadequate processes when transferring data from a data service provider to the end users. A data structure for sharing downhole data is specified. In addition to *how* data is shared, this work also specified what *metadata* needs to be shared with the data. The specification of such requirements of additional information improves transparency and is a prerequisite for downhole dynamics data analysis. Such standardized data structures do not limit sensor innovation as they are adaptive to new developments.

6.2 MAJOR CONTRIBUTIONS

The contributions include:

- *Re-interpretation of high-frequency downhole accelerometer data using tensor analysis methods.* The correct interpretation of such high-frequency variations of accelerometer readings as sensor artifacts will save companies millions of dollars in research, service, and unnecessary vibration mitigation cost. This finding underlines the importance of having an in-depth understanding of data acquisition as well as the physics underlying the data before a meaningful and appropriate response can be formulated.
- *Provision of guidelines for optimized sampling rates for detecting drilling dysfunctions.* Bandwidth and memory space usually pose limits on downhole data collection. The suggested approach optimizes the data collection scheme by maximizing the informational content from the sensors.

- *Demonstration of coupled downhole dynamics effects, its impacts on data analysis and its mitigation*. Sensors capture not only the intended phenomena, but also other downhole forces and motions. This awareness is a prerequisite for a meaningful comparison of downhole dynamics models with actual field data.
- *Suggestions for short and long term strategies to improve downhole data quality*. Demonstrated automated processing techniques improve processes significantly and enable valuable applications. In addition, a novel strategy for feature extraction of time series data was developed that enables the application of automated classification algorithms.
- *Development of a new data transfer format that specifies meta data for faster transfer and better usage of downhole data.* This basic but useful work was well-received in the industry and its implementation and wide-scale adoption is currently in preparation.
- *Supporting the education of undergraduate students in data analysis.* The job of a drilling engineer is currently migrating from being experienced-based to being analysis based. Such efforts are helping a new generation being optimally prepared a career in a "digital" drilling industry.

6.3 FUTURE WORK

Data from downhole sensors is just beginning to gain attention from researchers and engineers in the drilling industry. With current trends in automation, having a more scientific understanding of the drilling process and better models that can incorporate measurements, downhole data will become ever more important. The following guidelines and suggestions for further word are concerned with prerequisites and enablers for a truly automated and optimized drilling process.

Comprehensive Tool Model

A downhole measurement tool within a drillstring is exposed to certain forces and undergoes certain movements. A sensor located in this tool then captures these dynamics. What we can study as measurements are mere hints at the original processes that created the data. This work sheds light on other influencing factors from data generation to data analysis. A comprehensive model can now be developed that combines the physics of multiple sensors and their locations along the string with the data they capture. The output of the model then is a replication of the motions and forces that led to the measurements. Such a system could then automatically correct for sensor error (in the presence of other measurements), analogous to the sensor fusion approach previously demonstrated by Ambrus et al. (2013) for surface data.

Big Data Drilling Sets

Drilling data is complicated to analyze, mostly because of its unstructured and non-repetitive nature. At this moment, it is nearly impossible to collect a comprehensive data set for a single well, while carrying out effective comparisons of a large number of wells is unthinkable. The presented work attempts to start a process of digitization and standardization of drilling data to make this possible in the future. These data sets would have a classification of impact factors (rotating vs. sliding, motor vs. RSS, stabilizer placement, human interventions etc.). Classification algorithms can then be applied on all data sets. Such big data sets would finally open up the drilling industry to machine learning applications that have shown tremendous success in other industries.

Appendices

APPENDIX A

A.1 Patterns of High Frequency Acceleration Data

The following section shows examples of burst windows measured with downhole accelerometers. These burst windows are captured about every 20 minutes throughout the bit run. **Fig. 67**, **Fig. 68** and **Fig. 69** were recorded with a radial accelerometer and a sampling rate of 400 Hz from a vertical well. Each plot shows 4 patterns recorded for 10 seconds each at separate times. **Fig. 70** and **Fig. 71** were recorded from a different well with a tangential accelerometer and a sampling rate of 800 Hz. Here each figure shows 2 separate patterns, 10 second windows on the top and an additional detailed view of 2 seconds on the bottom.

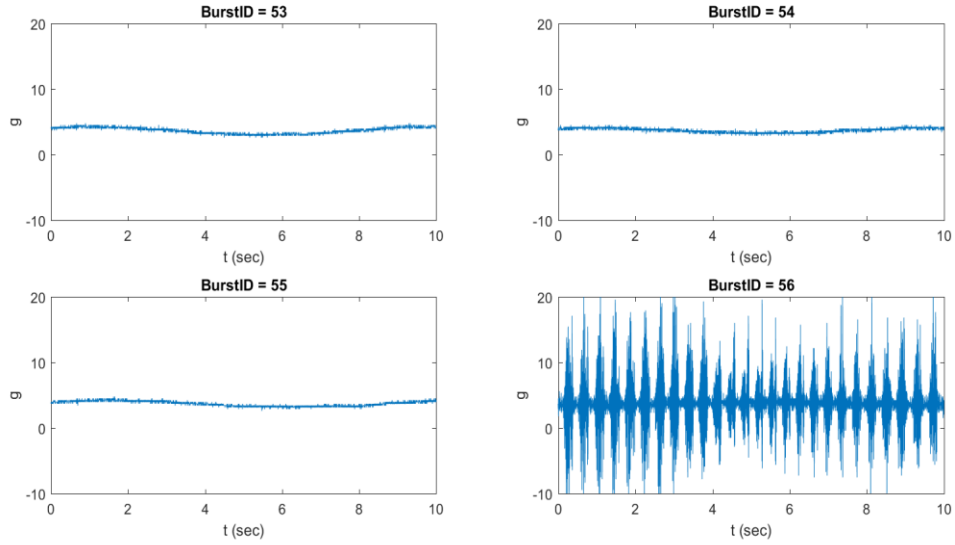

Fig. 67—Normal drilling (Burst ID = 53, 54, 55) and distinct pattern with negative radial accelerations (discussion of this particular pattern can be found in Chapter 2.5.4)

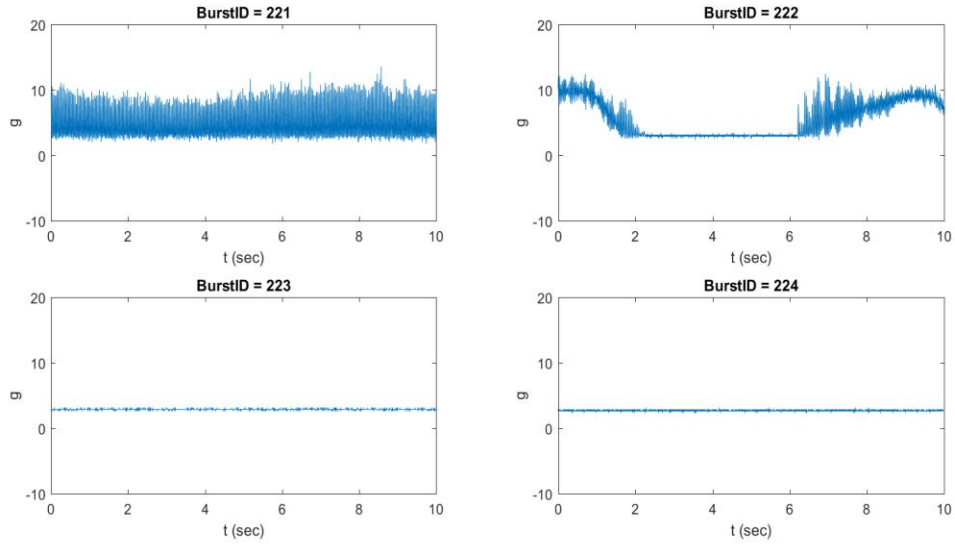

Fig. 68—Pattern examples for whirl (Burst ID = 221), fully developed stick slip (Burst ID = 222) and no drilling (Burst ID = 223 and 224). 'No drilling' can occur during a connection or during tripping.

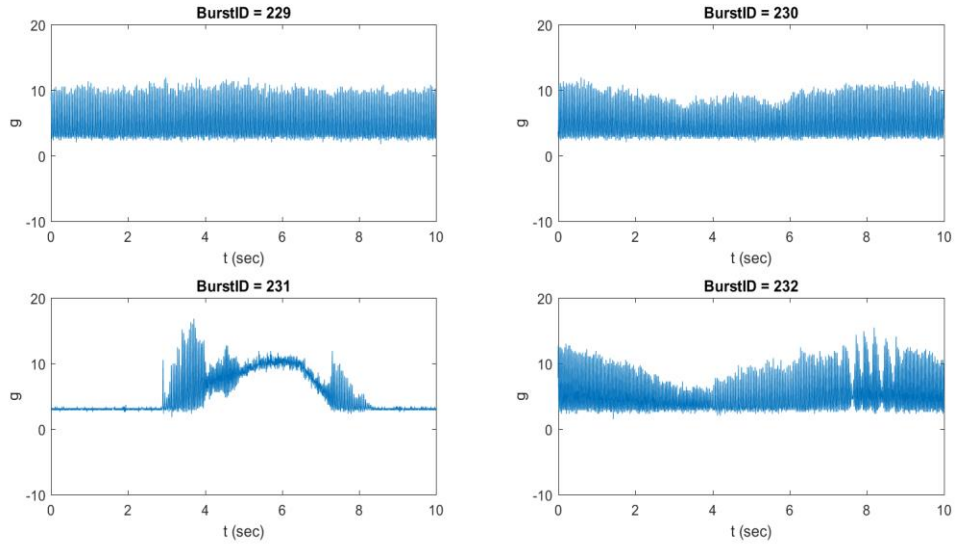

Fig. 69—Pattern examples for whirl (Burst ID = 229), whirl with slower RPM in the middle (Burst ID = 230), fully developed stick slip (Burst ID = 231) and whirl and RPM fluctuation (Burst ID = 232)

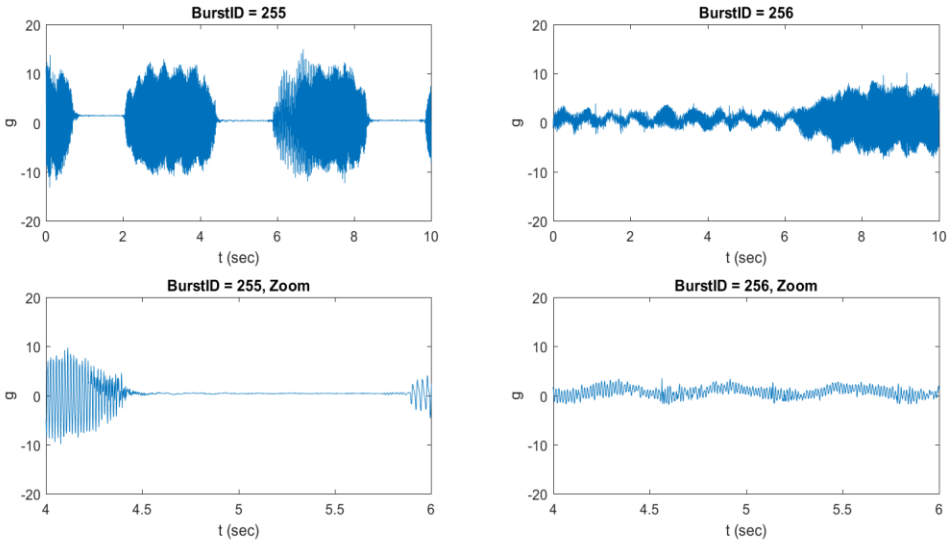

Fig. 70—Fully developed stick slip pattern (Burst ID = 255) and normal drilling with an onset of whirl (Burst ID = 256).

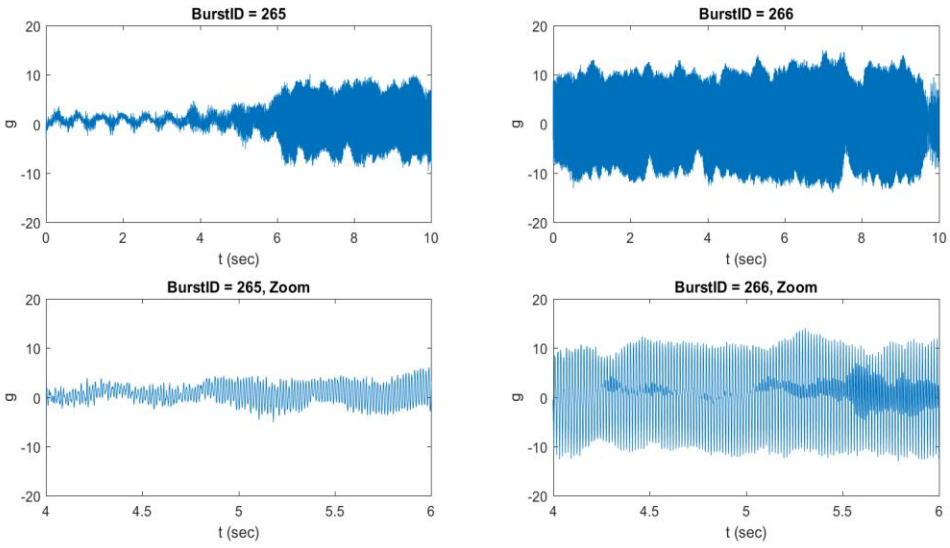

Fig. 71—Normal drilling with an onset of whirl (Burst ID = 265) and whirl (Burst ID = 266).

A.2 Radial and Tangential Accelerations with Tensor Analysis

General Derivation

The following equations are derived for the general case and are valid for n ambient coordinates and (n-1) surface coordinates (**Fig. 72**). The equations are then specified for a 2D ambient space (x, y) and a 1D surface, i.e. the curve that the sensor is confined to. The acceleration of the sensor thus depends on the curvature of its trajectory. Vectors are represented by bold capital letters with a single index, while tensors are represented by a capital letter with two indices. The following derivation presupposes a basic understanding of the basics of tensor calculus, such as tensor notation, vectors, coordinate systems, index juggling, Einstein summation or surface descriptions. Nomenclature and most definitions are borrowed from Grinfeld, 2013 and Collier, 2012.

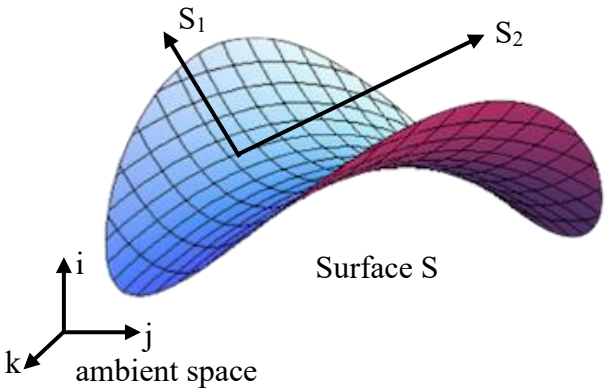

Fig. 72—Illustration of a surface and its covariant basis S_1 and S_2 embedded in an ambient Cartesian coordinate system i, j, k.

A sensor is moving along a trajectory confined to a surface. The trajectory $\gamma(t)$ is given by

$$S^{\alpha} = S^{\alpha}(t). \tag{A.1}$$

The position vector of the sensor is given by $\mathbf{R} = \mathbf{R}(\mathrm{S}(\mathrm{t}))$ and velocity vector **V** is derived by

$$V = \frac{d\boldsymbol{R}(S(t))}{dt} \tag{A.2}$$

$$= \frac{\partial \boldsymbol{R}}{\partial S^{\alpha}} \frac{dS^{\alpha}}{dt} \tag{A.3}$$

$$= \boldsymbol{S}_{\alpha} V^{\alpha} \tag{A.4}$$

$$= V^{\alpha} \boldsymbol{S}_{\alpha}\,, \tag{A.5}$$

with velocity component V^{α}

$$V^{\alpha} = \frac{d\boldsymbol{S}_{\alpha}}{dt}. \tag{A.6}$$

Acceleration **A** can be derived by

$$\boldsymbol{A} = \frac{d\boldsymbol{V}}{dt} \tag{A.7}$$

$$= \frac{d}{dt}[V^{\alpha} \boldsymbol{S}_{\alpha}] \tag{A.8}$$

$$= \frac{dV^{\alpha}}{dt} \boldsymbol{S}_{\alpha} + V^{\alpha} \frac{d\boldsymbol{S}_{\alpha}(S(t))}{dt} \tag{A.9}$$

$$= \frac{dV^{\alpha}}{dt} \boldsymbol{S}_{\alpha} + V^{\alpha} \frac{\partial \boldsymbol{S}_{\alpha}}{\partial S^{\beta}} \frac{dS^{\beta}}{dt} \tag{A.10}$$

$$= \frac{dV^{\alpha}}{dt} \boldsymbol{S}_{\alpha} + V^{\alpha} V^{\beta} \frac{\partial \boldsymbol{S}_{\alpha}}{\partial S^{\beta}} \tag{A.11}$$

$$= \frac{dV^{\alpha}}{dt} \boldsymbol{S}_{\alpha} + V^{\alpha} V^{\beta} (\nabla_{\beta} \boldsymbol{S}_{\alpha} + \Gamma_{\alpha\beta}^{\gamma} \boldsymbol{S}_{\gamma}) \tag{A.12}$$

$$= \frac{dV^{\alpha}}{dt} \boldsymbol{S}_{\alpha} + V^{\alpha} V^{\beta} \Gamma_{\alpha\beta}^{\gamma} \boldsymbol{S}_{\gamma} + V^{\alpha} V^{\beta} \nabla_{\beta} \boldsymbol{S}_{\alpha} \tag{A.13}$$

$$= \frac{\delta V^{\alpha}}{\delta t} \boldsymbol{S}_{\alpha} + V^{\alpha} V^{\beta} \nabla_{\beta} \boldsymbol{S}_{\alpha} \tag{A.14}$$

$$= \frac{\delta V^{\alpha}}{\delta t} \boldsymbol{S}_{\alpha} + \boldsymbol{N} B_{\alpha\beta} V^{\alpha} V^{\beta} \tag{A.15}$$

Finally, the acceleration vector **A** of the sensor is given by

$$\boldsymbol{A} = \frac{\delta V^{\alpha}}{\delta t} \boldsymbol{S}_{\alpha} + \boldsymbol{N} B_{\alpha\beta} V^{\alpha} V^{\beta}, \tag{A.16}$$

where the term $\frac{\delta V^{\alpha}}{\delta t} \boldsymbol{S}_{\alpha}$ is called *tangential acceleration* and the term $\boldsymbol{N} B_{\alpha\beta} V^{\alpha} V^{\beta}$ is called *centripetal or radial acceleration*. The *total derivative of velocity* $\frac{\delta V^{\alpha}}{\delta t}$ is defined as

$$\frac{\delta V^{\alpha}}{\delta t} = \frac{dV^{\alpha}}{dt} + \Gamma^{\alpha}_{\beta\gamma} V^{\beta} V^{\gamma}, \tag{A.17}$$

resulting in

$$\boldsymbol{A} = \left(\frac{dV^{\alpha}}{dt} + \Gamma^{\alpha}_{\beta\gamma} V^{\beta} V^{\gamma}\right) \boldsymbol{S}_{\alpha} + \boldsymbol{N} B_{\alpha\beta} V^{\alpha} V^{\beta}. \tag{A.18}$$

The covariant basis of the surface $\boldsymbol{S}_{\alpha}$ is defined by partial differentiation. For a 2D surface in a 3D ambient space, $\boldsymbol{S}_{\alpha}$ are two vectors tangential to the coordinate lines S^1 and S^2:

$$\boldsymbol{S}_{\alpha} = \frac{\partial \boldsymbol{R}}{\partial S^{\alpha}} \tag{A.19}$$

The covariant metric tensor is defined by

$$S_{\alpha\beta} = \boldsymbol{S}_{\alpha} \cdot \boldsymbol{S}_{\alpha} \tag{A.20}$$

The contravariant metric tensor $S^{\alpha\beta}$ is defined as the matrix inverse of $S_{\alpha\beta}$:

$$S^{\alpha\beta} S_{\beta\gamma} = \delta^{\alpha}_{\gamma} \tag{A.21}$$

Finally, the *contravariant basis* S^{α} of a surface is defined by

$$\boldsymbol{S}^{\alpha} = S^{\alpha\beta} \cdot \boldsymbol{S}_{\beta} \tag{A.22}$$

The *shift tensor* Z^{i}_{α} relates the surface (Greek letters) and the ambient basis (Latin letters). The entries of this tensor are the components of the *covariant basis* $\boldsymbol{S}_{\alpha}$ of the surface with respect to the ambient basis $\mathbf{Z}_{\mathrm{i}}$. The shift tensor is given by

$$Z^{i}_{\alpha} = \frac{\partial Z^{i}}{\partial S^{\alpha}} = \boldsymbol{Z}^{i} \cdot \boldsymbol{S}_{\alpha} \tag{A.23}$$

In the ambient space, the *Christoffel symbol* Γ^{k}_{ij} measures the rate of change of the covariant basis with respect to the coordinate variables. For embedded surfaces, the covariant basis $\boldsymbol{S}_{\alpha}$ is only capable of representing vectors that lie in the tangent plane of the surface. In a curved surface, at least some of the vectors of the Christoffel symbol will have components in the normal direction. The *Christoffel symbol* $\Gamma^{\alpha}_{\beta\gamma}$ is defined by

$$\Gamma_{\beta\gamma}^{\alpha} = \boldsymbol{S}^{\alpha} \cdot \frac{\partial \boldsymbol{S}_{\beta}}{\partial S^{\gamma}} \tag{A.24}$$

The normal vector **N** with components N^i represents the direction orthogonal to the covariant basis $\mathbf{S}_\alpha$. It is implicitly defined by stating orthogonality to the tangent plane and unit length:

$$\boldsymbol{N} \cdot \boldsymbol{S}_{\alpha} = 0 \tag{A.25}$$

$$\boldsymbol{N} \cdot \boldsymbol{N} = 1 \tag{A.26}$$

For the subsequent calculations, the explicit expression of N^i given in 3 and 2 dimensions, respectively, will be used:

$$N^i = \frac{1}{2} \varepsilon_{ijk} \varepsilon^{\alpha\beta} Z_{\alpha}^{j} Z_{\beta}^{k} \ \text{(3D)} \tag{A.27}$$

$$N^i = \varepsilon_{ij} \varepsilon^{\alpha} Z_{\alpha}^{j} \ \text{(2D)}, \tag{A.28}$$

where ε_{ijk} or $\varepsilon^{ijk}$and $\varepsilon^{\alpha\beta}$ or $\varepsilon_{\alpha\beta}$ are the *Levi-Civita symbols*. They are absolute tensors and are used to define the curl operator and the cross product of vectors. The absolute property with respect to orientation-preserving coordinate changes can be achieved by scaling the *permutation symbols* e_{ijk} or $e^{ijk}$and $e^{\alpha\beta}$ or $e_{\alpha\beta}$ by a volume element (3D) or length element (2D) $\sqrt{Z}$ for ambient space and $\sqrt{S}$ for surfaces. The permutation symbols are defined by

$$e_{ijk} = e^{ijk} = \begin{cases} 1 & if\ ijk\ is\ an\ even\ permutation\ of\ 1,2,3 \\ -1 & if\ ijk\ is\ an\ odd\ permutation\ of\ 1,2,3 \\ 0 & otherwise \end{cases} \tag{A.29}$$

The Levi-Civita symbols can be calculated by

$$\varepsilon_{ijk} = \sqrt{Z}\, e_{ijk}, \qquad \varepsilon_{\alpha\beta} = \sqrt{S}\, e_{\alpha\beta}$$

$$\varepsilon^{ijk} = \frac{e^{ijk}}{\sqrt{Z}}, \qquad \varepsilon^{\alpha\beta} = \frac{e^{\alpha\beta}}{\sqrt{S}},$$

where $\sqrt{Z}$ and $\sqrt{S}$ are the square roots of the determinants of the covariant metric tensors Z_{ij} and $S_{\alpha\beta}$, respectively:

$$\sqrt{Z} = \sqrt{|Z_{ij}|} \text{ and } \sqrt{S} = \sqrt{|S_{\alpha\beta}|}\,.$$

In Cartesian coordinate systems $\sqrt{Z} = 1$.

Tensor calculus is especially valuable to create a proper description of physically meaningful derivatives of vectors. However, differentiations of vectors in tensor notation is not trivial. The core of tensor calculus is the fact that only tensors are invariant to changes of coordinates. Thus, differentiation in a tensor calculus sense is not only required to satisfy familiar sum and product rules, but also to produce tensors out of tensors during differentiation. To satisfy the latter rule, a new differential operator, the *covariant derivative* ∇_i had to be developed. In affine coordinates (skewed but otherwise regular grid of coordinates, e.g. Cartesian coordinates are affine coordinates), the covariant derivative ∇_i coincides with the partial derivative $\partial/\partial Z^i$. In non-affine coordinate systems (e.g. polar coordinates) covariant differentiation, the Christoffel symbol arises, accounting for time derivatives of the coordinate system itself. While for ambient coordinates the *covariant derivative of the covariant basis* $\nabla_i \boldsymbol{Z}_j$ vanishes, the quantity $\nabla_\alpha \boldsymbol{S}_\beta$ (covariant derivative of the covariant surface basis) does not vanish due to the curvature of the surface. This lack of the *metrilinic* property for surface tensors gives rise to the *curvature tensor* $B_{\alpha\beta}$ *defined by*

$$B_{\alpha\beta} = \boldsymbol{N} \cdot \nabla_\alpha \boldsymbol{S}_\beta \tag{A.30}$$

The curvature tensor is an extrinsic property of a surface and depends on how the surface is embedded in the ambient space. The acceleration of a particle (or sensor) that moves along a surface depends on the curvature tensor.

Application

The above equations are applied to the problem described in Chapter 2. The sensor follows a trajectory that is confined to a planar surface. The ambient space is described by a two-dimensional Cartesian coordinate system with coordinates Z^i, with $Z^1 = x$ and $Z^2 = y$. A single variable describes the surface coordinate system $S^\alpha = S^1 = t$, i.e. it is a curve embedded in a 2D ambient system.

The position vector R is given by

$$\boldsymbol{R} = \boldsymbol{R}(x(t), y(t))$$

Velocity:

$$\boldsymbol{V}^\alpha = \frac{d\boldsymbol{S}^\alpha}{dt} = \frac{dt}{dt} = 1$$

Covariant basis:

$$\mathbf{S}_\alpha = \frac{\partial \mathbf{R}}{\partial \mathrm{S}^\alpha} = \begin{bmatrix} \mathrm{x}'(\mathrm{t}) \\ \mathrm{y}'(\mathrm{t}) \end{bmatrix}$$

Covariant metric tensor:

$$S_{\alpha\beta} = \boldsymbol{S}_\alpha \cdot \boldsymbol{S}_\alpha = \begin{bmatrix} x'(t) \\ y'(t) \end{bmatrix} \cdot \begin{bmatrix} x'(t) \\ y'(t) \end{bmatrix} = x'(t)^2 + y'(t)^2$$

Contravariant metric tensor given by:

$$S^{\alpha\beta} = \frac{1}{S_{\alpha\beta}} = \frac{1}{x'(t)^2 + y'(t)^2}$$

Contravariant basis:

$$\boldsymbol{S}^\alpha = S^{\alpha\beta} \cdot \boldsymbol{S}_\beta = \frac{1}{x'(t)^2 + y'(t)^2} \cdot \begin{bmatrix} x'(t) \\ y'(t) \end{bmatrix}$$

Shift tensor:

$$Z^i_\alpha = \frac{\partial Z^i}{\partial S^\alpha} = \begin{bmatrix} x'(t) \\ y'(t) \end{bmatrix}$$

The Christoffel symbol $\Gamma^\alpha_{\beta\gamma}$ has a single entry $\tilde{\Gamma}$:

$$\Gamma_{tt}^{t} = \tilde{\Gamma} = \frac{1}{x'(t)^2 + y'(t)^2} \cdot \begin{bmatrix} x'(t) \\ y'(t) \end{bmatrix} \cdot \begin{bmatrix} x''(t) \\ y''(t) \end{bmatrix} = \frac{x'(t) \cdot x''(t) + y'(t) \cdot y''(t)}{x'(t)^2 + y'(t)^2}$$

Permutation symbols:

$$e_{ij} = \begin{bmatrix} 0 & 1 \\ -1 & 0 \end{bmatrix}, \text{ and}$$

$$e^{\alpha} = 1$$

With $\sqrt{Z} = 1$ and $\sqrt{S} = \sqrt{x'(t)^2 + y'(t)^2}$, the Levi-Civita Symbols are:

$$\varepsilon_{ij} = \frac{e_{ij}}{\sqrt{Z}} = \begin{bmatrix} 0 & 1 \\ -1 & 0 \end{bmatrix} \text{ and}$$

$$\varepsilon^{\alpha} = \frac{e^{\alpha}}{\sqrt{S}} = \frac{1}{\sqrt{x'(t)^2 + y'(t)^2}}$$

Normal vector:

$$\boldsymbol{N} = \varepsilon_{ij}\varepsilon^{\alpha}Z_{\alpha}^{j} = \begin{bmatrix} 0 & 1 \\ -1 & 0 \end{bmatrix} \cdot \frac{1}{\sqrt{S}} \cdot \begin{bmatrix} x'(t) \\ y'(t) \end{bmatrix} = \frac{1}{\sqrt{S}} \cdot \begin{bmatrix} y'(t) \\ -x'(t) \end{bmatrix} = \begin{bmatrix} \frac{y'(t)}{\sqrt{x'(t)^2 + y'(t)^2}} \\ \frac{-x'(t)}{\sqrt{x'(t)^2 + y'(t)^2}} \end{bmatrix}$$

The curvature tensor:

$$B_{\alpha\beta} = \boldsymbol{N} \cdot \nabla_{\alpha}\boldsymbol{S}_{\beta} = \frac{1}{\sqrt{S}} \cdot \begin{bmatrix} y'(t) \\ -x'(t) \end{bmatrix} \cdot \begin{bmatrix} x''(t) \\ y''(t) \end{bmatrix} = \frac{y'(t) \cdot x''(t) - x'(t) \cdot y''(t)}{\sqrt{x'(t)^2 + y'(t)^2}}$$

The above results yield the final acceleration given by Eq. A.16:

$$\boldsymbol{A} = \left(0 + \frac{x'(t) \cdot x''(t) + y'(t) \cdot y''(t)}{x'(t)^2 + y'(t)^2} \cdot 1 \cdot 1\right) \begin{bmatrix} x'(t) \\ y'(t) \end{bmatrix} + \frac{1}{\sqrt{S}} \begin{bmatrix} y'(t) \\ -x'(t) \end{bmatrix} \frac{1}{\sqrt{S}} \begin{bmatrix} y'(t) \\ -x'(t) \end{bmatrix} \begin{bmatrix} x''(t) \\ y''(t) \end{bmatrix} \cdot 1 \cdot 1$$

$$\boldsymbol{A} = \frac{x'(t) \cdot x''(t) + y'(t) \cdot y''(t)}{x'(t)^2 + y'(t)^2} \cdot \begin{bmatrix} x'(t) \\ y'(t) \end{bmatrix} + \frac{y'(t) \cdot x''(t) - x'(t) \cdot y''(t)}{x'(t)^2 + y'(t)^2} \cdot \begin{bmatrix} y'(t) \\ -x'(t) \end{bmatrix} \quad \text{(A.31)}$$

The individual components of tangential and radial acceleration expressed in Cartesian x and y components of the ambient system are:

$$A_{tan}x = \frac{x'(t) \cdot x''(t) + y'(t) \cdot y''(t)}{x'(t)^2 + y'(t)^2} \cdot x'(t)$$

$$A_{tan}y = \frac{x'(t) \cdot x''(t) + y'(t) \cdot y''(t)}{x'(t)^2 + y'(t)^2} \cdot y'(t)$$

$$A_{rad}x = \frac{y'(t) \cdot x''(t) - x'(t) \cdot y''(t)}{x'(t)^2 + y'(t)^2} \cdot y'(t)$$

$$A_{rad}y = -\frac{y'(t) \cdot x''(t) - x'(t) \cdot y''(t)}{x'(t)^2 + y'(t)^2} \cdot x'(t)$$

For uniform on-center rotation with rotational speed ω and radius R, positions x and y are given by $x = \mathrm{R}\cos(\omega t)$ and $y = R\sin(\omega t)$. Plugging positions x and y and their derivatives into Eq. A.31, it simplifies to

$$\boldsymbol{A} = \left[\frac{0}{\omega^2} + \frac{-\mathrm{R}^2\omega^3\cos^2(\omega t) - \mathrm{R}^2\omega^3\sin^2(\omega t)}{R^2\omega^2}\right] \cdot \begin{bmatrix} -\mathrm{R}\,\omega\sin(\omega t) \\ \mathrm{R}\,\omega\cos(\omega t) \end{bmatrix}$$

$$= -\omega \cdot \begin{bmatrix} -\mathrm{R}\,\omega\sin(\omega t) \\ \mathrm{R}\,\omega\cos(\omega t) \end{bmatrix} = -R\omega^2,$$

where the result $R\omega^2$ is the familiar centripetal acceleration for uniform circular motion. In this case, as expected for uniform circular motion, the tangential acceleration is 0.

A.3 Modeled HFTO Signal

This work mainly focuses on the kinematics of the whirling pipe in the borehole. Here we show the expected radial and tangential accelerations for the hypothetical kinematics of high-frequency torsional oscillations. This should give even more evidence that HFTOs are unsuitable to explain the high frequency fluctuations in the field data. The center of rotation, in this case, is perfectly aligned with the center of the pipe, while the input rotary speed signal varies sinusoidally from 0 to 200 RPM with a frequency of 20 Hz (**Fig. 73**, left). The expected tangential acceleration signal of a sensor capturing such movement is in turn a sinusoidal signal with the same frequency content as the input signal

(Fig. 73, middle). The expected radial accelerations show an additional overtone of twice the input frequency (Fig. 73, right). Note that for HFTOs, we expect the absolute value of radial accelerations to greatly exceed the absolute value of tangential accelerations. Eq. 4 in Chapter 2 already predicts these results. Therefore, the multiple signal overtones found in field data cannot be explained by a sinusoidally oscillating pipe rotational speed alone.

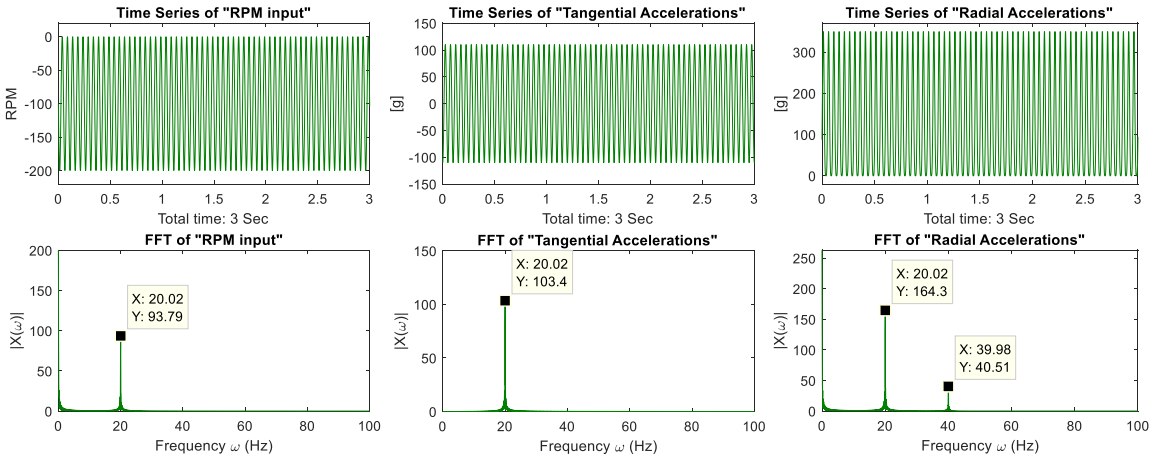

Fig. 73—Simulations of tangential and radial acceleration based on a sinusoidal high-frequency RPM variations.

A.4 Applied Whirl Correction Methodology

According to Hoffman et al. (2012), MWD tools usually are equipped with a methodology to correct for whirl: Data is recorded from multiple accelerometers, they are then combined to offset the effects of eccentric rotations.

The whirl model described in Chapter 2 can be used to test the described methodology. **Fig. 74** shows the simulation of two tangential accelerometers mounted on the tool with a 180-degree phase shift. In standard MWD setups, resulting tangential

acceleration from such a setup is calculated by combining values from both sensors (Mayer, 2007):

$$a_{tan} = \frac{1}{2}(a_{tan,S2} - a_{tan,S1}) \tag{A.32}$$

$$a_{rad} = \frac{1}{2}(a_{rad,S2} + a_{rad,S1}) \tag{A.33}$$

Fig. 74 demonstrates for tangential accelerations that applying these formulas to the simulated data does not reduce the high-frequency fluctuations of the data. The same procedure for radial acceleration yields comparable results. We therefore can conclude that the whirl correction procedures in MWD and other downhole measurement devices are not sufficient to remove fictious forces on the sensor because of off-center rotation.

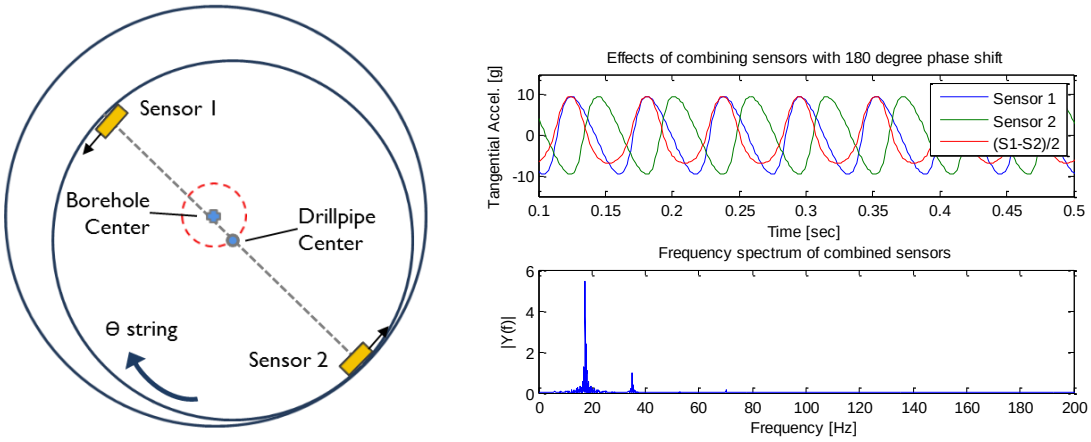

Fig. 74—Combined data from 2 sensors with a 180-degree phase shift still yields high-frequency fluctuations and overtones.

A.5 Graphical User Interface for Whirl Simulations

A graphical user interface (**Fig. 75**) was created to study the effect of different parameters on the sensor movement and the resulting velocities and accelerations, as seen by a sensor. The interface allows to adjust parameters in real-time, using the proposed numerical approach.

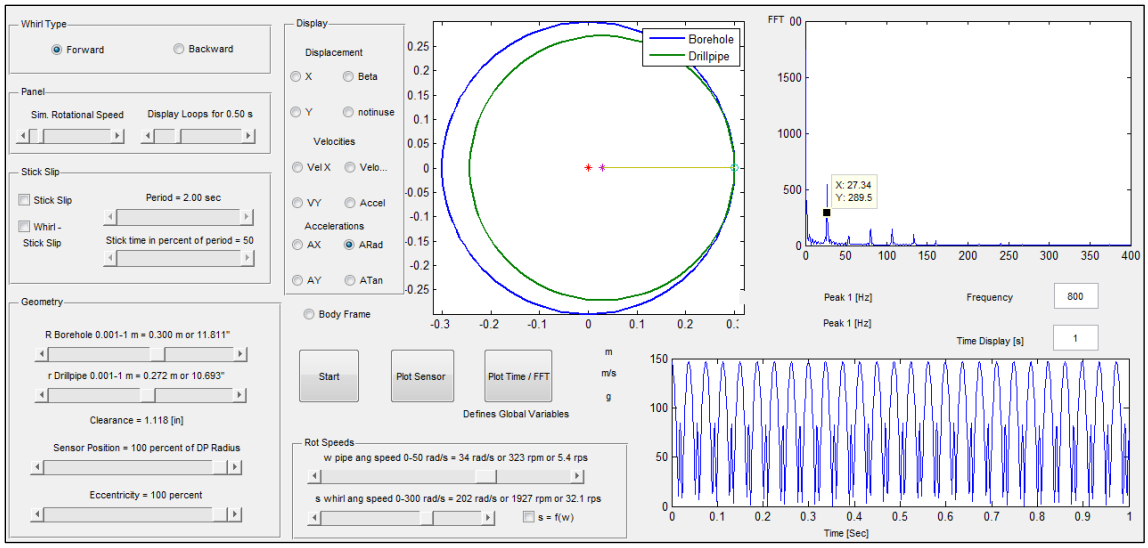

Fig. 75—Graphical user interface for whirl simulations.

APPENDIX B

B.1 Flow Charts of Correction Algorithms

The following sections conceptualizes algorithms described in Chapter 4 using flow chats. **Fig. 76** illustrates the algorithm for accelerometer offset correction. **Fig. 77** illustrates the algorithm for WOB correctio. **Fig. 78**, **Fig. 79** and **Fig. 80** illustrate the algorithm for downhole and surface alignment under consideration of latencies.

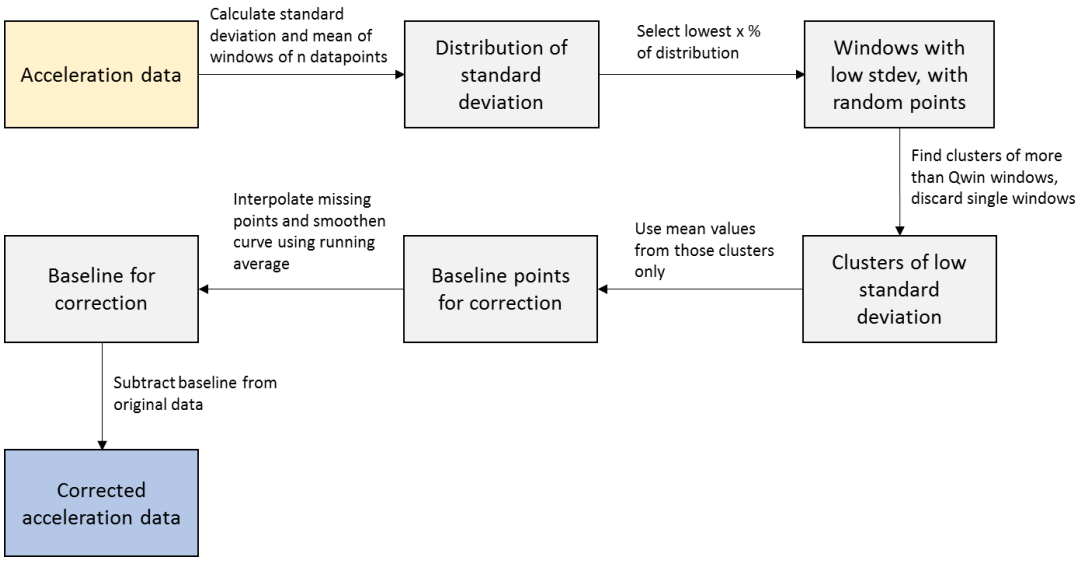

Fig. 76—Algorithm description for accelerometer offset correction.

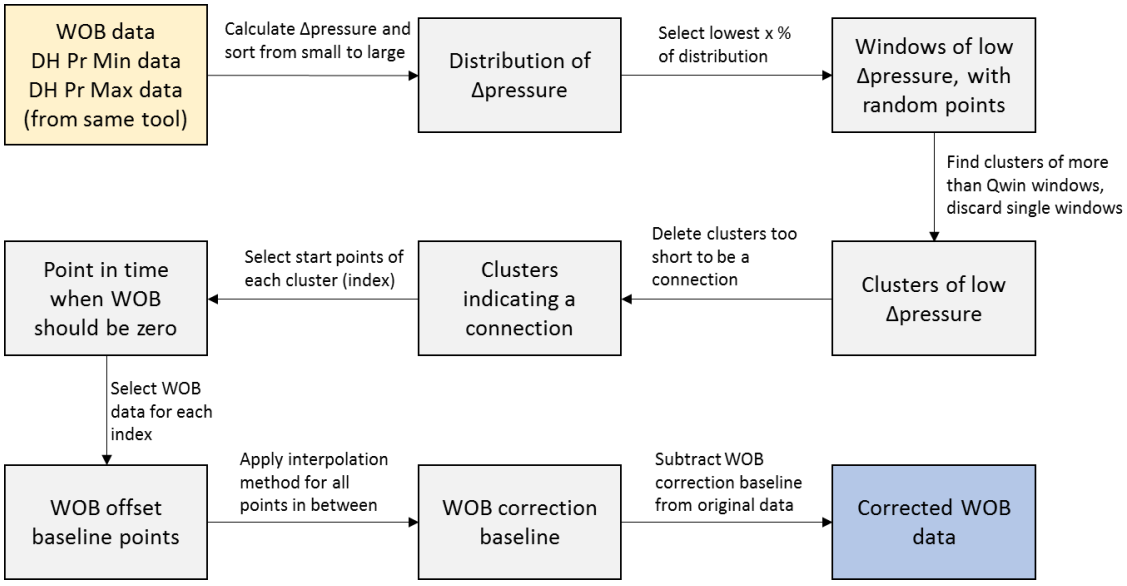

Fig. 77—Algorithm description for WOB drift correction

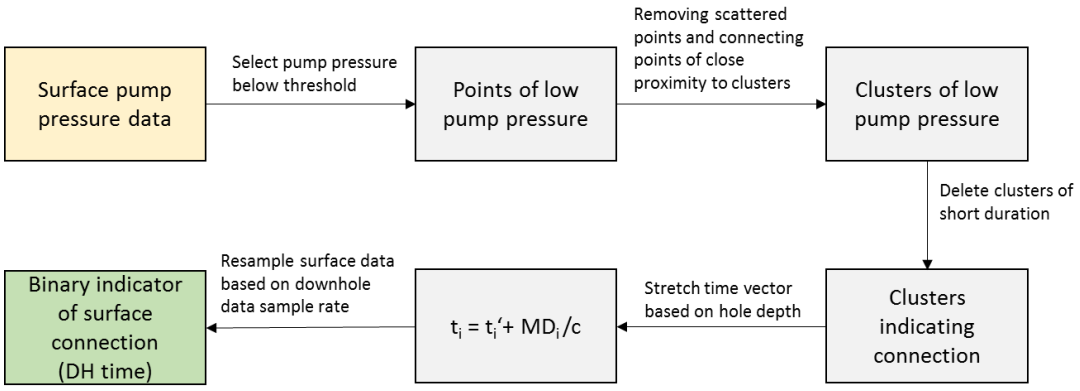

Fig. 78—Algorithm description for surface-downhole alignment – surface data processing.

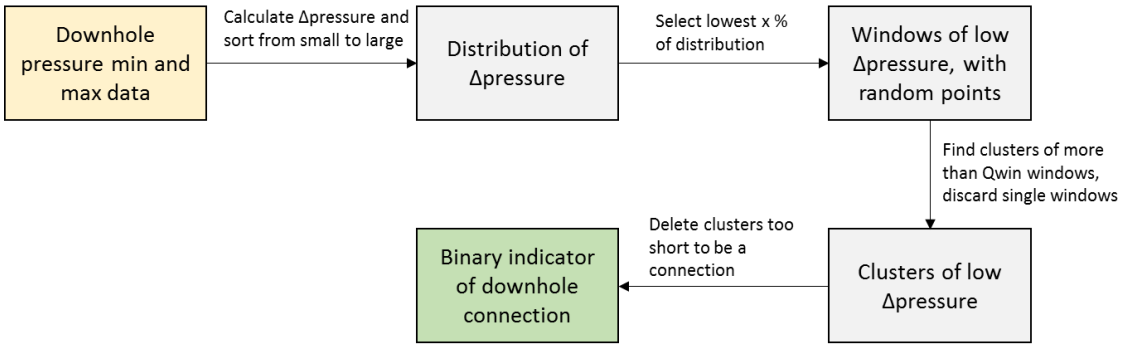

Fig. 79—Algorithm description for surface-downhole alignment – downhole data processing

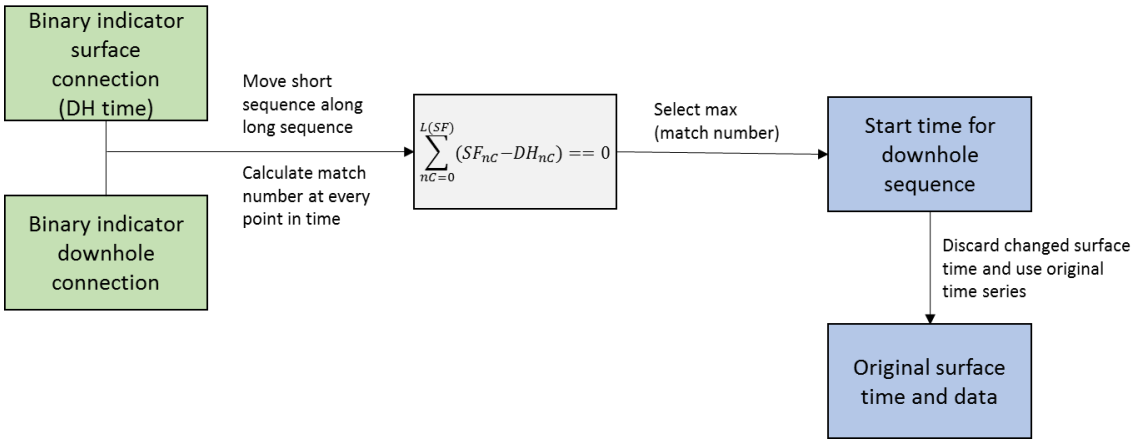

Fig. 80—Algorithm description for surface-downhole alignment – finding match time.

B.2 Naïve Bayes Classifier

The Naïve Bayes classifier is an approach of supervised machine learning. These types of models are probably the most common Bayesian models used in machine learning (Russell et al., 2010). This model consists of the class variable, which in this case is the "stick-slip" or "no-stick-slip" tag for each observation, as well as 15 predictor or attribute variables. The model is called "naïve" because it assumes that the attributes are conditionally independent of each other, given the class.

The prior probabilities for each class are directly estimated from the data. Kernel distributions were used for fitting the continuous attributes. A kernel is a nonparametric representation of the probability density function of random variables. Although the assumption of conditional independence of the predictor variables given the class might not be valid here, this approach has been chosen for its simplicity. Russell et al. (2010) states: "In practice, Naïve Bayes systems can work surprisingly well, even when the conditional independence assumption is not true."

Fig. 81 illustrates the input for the classifier algorithms. For each row, 15 predictor variables were extracted from the high-frequency data snippet.

	Predictor Variables / Attributes															Classifiers	
Index	TimeHrs	Min	Max	Diff	Std	Var	Avgmin	Avgmax	AvgDiff	Avg	FrquPeak1	PeakAmp1	FrquPeak2	PeakAmp2	PeakDist	Stick Slip	Whirl
113	43.20	1.50	2.59	1.10	0.09	0.01	2.01	2.04	0.03	2.02	0.00	0.00	0.00	0.00	0.00	0	0
114	43.55	1.50	2.32	0.82	0.09	0.01	2.00	2.07	0.07	2.02	0.00	0.00	0.00	0.00	0.00	0	0
115	43.90	1.50	2.59	1.10	0.09	0.01	1.99	2.05	0.06	2.03	0.00	0.00	0.00	0.00	0.00	0	0
116	44.25	1.50	2.59	1.10	0.08	0.01	1.95	2.04	0.09	2.03	0.00	0.00	0.00	0.00	0.00	0	0
117	44.60	1.50	2.32	0.82	0.08	0.01	1.95	2.04	0.09	2.03	0.00	0.00	0.00	0.00	0.00	0	0
118	44.95	1.50	2.32	0.82	0.14	0.02	1.77	2.04	0.27	1.94	0.00	0.00	0.00	0.00	0.00	0	0
119	45.30	1.50	2.59	1.10	0.12	0.01	2.04	2.32	0.27	2.27	0.00	0.00	0.00	0.00	0.00	0	0
120	45.65	1.50	2.59	1.10	0.09	0.01	2.01	2.07	0.06	2.06	0.00	0.00	0.00	0.00	0.00	0	0
121	46.00	2.04	6.15	4.11	1.07	1.14	2.61	5.49	2.89	3.90	0.00	0.00	0.00	0.00	0.00	1	0
122	46.35	2.59	4.78	2.19	0.36	0.13	3.17	3.99	0.82	3.57	0.68	0.22	0.00	0.00	0.00	1	0
123	46.70	2.32	5.33	3.01	0.64	0.41	2.75	4.43	1.68	3.51	0.00	0.00	0.00	0.00	0.00	1	0
124	47.05	2.32	5.06	2.74	0.56	0.31	2.93	4.31	1.38	3.58	0.00	0.00	0.00	0.00	0.00	1	0
125	47.40	2.04	6.43	4.38	1.23	1.51	2.53	5.76	3.24	4.00	0.29	0.47	0.00	0.00	0.00	1	0
126	47.75	2.04	6.15	4.11	1.04	1.07	2.58	5.33	2.75	3.84	0.00	0.00	0.00	0.00	0.00	1	0
127	48.10	2.04	6.15	4.11	1.12	1.26	2.44	5.21	2.77	3.56	0.00	0.00	0.00	0.00	0.00	1	0
128	48.45	2.04	6.15	4.11	1.06	1.13	2.56	5.20	2.64	3.70	0.00	0.00	0.00	0.00	0.00	1	0
129	48.80	2.32	4.51	2.19	0.22	0.05	3.45	3.96	0.51	3.62	0.00	0.00	0.00	0.00	0.00	0	0
130	49.15	1.50	5.33	3.83	0.44	0.19	3.41	4.24	0.82	3.59	0.00	0.00	0.00	0.00	0.00	0	0
131	49.50	1.77	2.59	0.82	0.09	0.01	2.23	2.37	0.15	2.32	0.00	0.00	0.00	0.00	0.00	0	0
132					0.97	0.95	2.62				0.00	0.00		0.00			

Fig. 81—Dataset with attributes and classifiers as input for the Naïve Bayes classifier.

APPENDIX C: MDTS FILE ILLUSTRATION

```
~File Information Block
#TAG                    Data                    Unit    Description
#--------- ----------------------------------  ------  ------------------------------------------------------------
 Version                                1.00:           Memory Data Transfer Standard-Version 1.00
 Wrap                                     NO:           One line per time step
 FileGenDate                  01-OCT-2015:              Date this MDTS file was generated
 FileGenName            Theresa Baumgartner:            Person who generated this MDTS file
 FileGenAffil       The University of Texas:            Affiliation of person who generated this MDTS file

~Well Information Block
#TAG                    Data                    Unit    Description
#--------- ----------------------------------  ------  ------------------------------------------------------------
 WellName                       Rapid-1-2H:             Descriptive name of well
 WellUID                42-501-20130-03-00:             Unique well identifier
 Wellbore                      Sidetrack 2:             Identification of borehole
 OperatorName                   OilCompany:             Operating company
 ContractorName           FastDrillers Inc:             Ending Depth
 ServicCompanyName         DrillQuants Inc:             Drilling contractor company
 SpudDate                 11:11:2015 18:30:             Spud date
 Field                       HighPerm East:             Name of field
 State                              Texas:               State
 Country                              USA:               Country
 Latitude                      30.290191:                Wellhead position latitude (north is positive)
 Longitude                    -97.736534:                Wellhead position longitude (east is positive)

~Run Information Block
#TAG                    Data                    Unit    Description
#--------- ----------------------------------  -----   ------------------------------------------------------------

 numBitRun                              2:              Bit run number
 numStringRun                           2:              The BHA (drilling string) run number
 RunStartTime          15:11:2015 04:31:                Date and time that activities started
 RunEndTime            16:11:2015 16:09:                Date and time that activities stopped
 StartDepth                     9,232: ft               Depth of data recording start
 EndDepth                      10,123: ft               Depth of data recording end
 WellType                    vertical:                  Wellbore trajectory shape (vertical,curve,horizontal,tangent,...)
 BitSize                        8.5: in                 Diameter of drilled hole
 BitType                        PDC:                    Type of bit
 SurfaceDataReference        Amphion:                   Surface data collection system/company (e.g. Amphion, Pason,etc.)
 TimeCorrection   (dh-0.00342)*1.00043: sec             Time lag compared to surface data, both shift and stretch of dh data
 OperationsComments     Sensor 3 failed:                Irregular operational event occurring in this run

~Device Information Block
#TAG                    Data                    Unit    Description
#--------- ----------------------------------  -----   ------------------------------------------------------------

 DeviceName                   BlackBox:                 Commercial name of device
 DeviceVendor                    NOV:                   Unique identifier for data service company (e.g. stock code)
 VendorContactName  Firstname Lastname:                 Contact person within data service company
 NullValue                    -999.25:                  Invalid number indicator
 Transmission                 Memory:                   Type of data transmission system (memory, mud pulse, wired drillpipe)
 MemorySize                        1: GB                Size of downhole data storage (if applicable)
 RealTimeRate                      0: bits/sec          Data rate for real time submission (if applicable)
 NoofSensors                       4:                   Number of sensors in device
 DeviceLocation                  BHA:                   BIT, BHA, ASM, SUB, RIG, BSL - descriptive location
 Axial Position                 23.3: ft                Distance from bit (ref: lower end of device)
```

Fig. 82—Example MDTS File part 1 (illustrative).

```
~Sensor Information Block
#TAG                    Data                      Unit     Description
#--------- ------------------------------------  -----    ------------------------------------------------------------

 ~S1                                      1:              Sensor number (S1,S2,S3,Ö)
 SensorName                      Accelerometer:           Commonly used sensor description or name
 SensorType          Tangential accelerometer:           Technical sensor name
 SensorCategory                   Acceleration:          Acceleration, Velocity, Displacement, Force,...
 relAxialPosition                          3.5: ft        Distance from lower end of device
 relLateralPosition                       4.12: in        Distance from device axial center
 SamplingRate                              800: 1/sec     Sensor sampling rate
 LastCalibrationDate          10:11:2015 20:15:           Date and time of last sensor calibration
 LastCalibrationType                   offsite:           Offsite,onsite manual,onsite semi-automatic,onsite automatic
 MinValueRange                             -100: g        Lower limit of sensor measurement
 MaxValueRange                             +100: g        Upper limit of sensor measurement
 Accuracy                                0.005: +/-%FS    Estimated field accuracy
 Precision                               0.005: g         Repeatability of measurement
 DigitalResolution                       0.005: g         Measurement increments
 Filter                                     y: (y/n)      Signal goes through filtering process
 High Cut-Off Amplitude                    -72: dB        Filter description details
 High Cut-Off Frequency                     45: 1/sec     Filter description details
 High Roll-Off Amplitude                    -3: dB        Filter description details
 High Roll-Off Frequency                    35: 1/sec     Filter description details
 Low Cut-Off Amplitude                       0: dB        Filter description details
 Low Cut-Off Frequency                       0: 1/sec     Filter description details
 Low Roll-Off Amplitude                      0: dB        Filter description details
 Low Roll-Off Frequency                      0: 1/sec     Filter description details

 ~S2                                      2:              Sensor number (S1,S2,S3,Ö)
 SensorName                       downhole WOB:           Commonly used sensor description or name
 ...                                     ...:             ...

~Measurement Information Block
#TAG                    Column Nr.                Unit     Description
#--------- ------------------------------------  -----    ------------------------------------------------------------

 Time                                     1:              Time and date in standard format
 Elapsed Time                             2: s            Zero value = start of bit run
 Acceleration                             3: g            Radial acceleration
 RPM                                      4: RPM          Calculated value from radial acceleration
 RMS                                      5: g            Desrciption of calculation - average

~Measurement Information Block
#TAG                    Column Nr.                Unit     Description
#--------- ------------------------------------  -----    ------------------------------------------------------------

 ~C1                                      1:              Channel number (C1, C2, C3,Ö)
 Sensors                                1,4:              Sensor or sensors used for this measurement
 OutputRate                             0.4: 1/sec        Channel data rate
 MeasurementCharacter                     n: (y/n)        None, average, standard deviation, minimum, maximum, RMS, etc.
 MovingAverage                            y: (y/n)        Average calculated in moving window vs. fixed WINDOW
 WindowLength                            10: sec          Window length of statistics
 DerivedValue                             y: (y/n)        Output other than direct measurement or statistics
 DerivationDetails                    S1+S2:              Description of derivation
 Continous                                n: (y/n)        Continuous data stream over the entire run vs sequences
 SequenceLength                           5: sec          Window length of one high frequency sequence
 SequenceGap                             20: min          Time distance between two windows
 SequenceTriggering                      no: (y/n)        Start of data collection after triggering measurement value
 Correction                               y: (y/n)        Post retrieval data correction
 CorrectionProcedure                 Manual:              Description of algorithm or procedure for data correction
 Classification                           y: (y/n)        Classification of measurement into severities or types
 Class1                  mild vibs(0/5):                  Name of classification type and upper and lower limits
 Class2                severe vibs(5/inf):                Name of classification type and upper and lower limits
 Channel comments                                         Irregular measurement observations

 ~C2                                      2:              Channel number (C1, C2, C3,Ö)
 Sensors                                  2:              Sensor or sensors used for this measurement
  ...                                    ...:             ...

~DATA

 2015-11-15T03:31:57.8860000     0.000000      5.592454246     96.42046189     77.13636951
 2015-11-15T03:31:57.8872500     0.001250      4.838110207     109.4702876     87.57623009
 2015-11-15T03:31:57.8885000     0.002500      8.873063461     94.54559966     75.63647973
 2015-11-15T03:31:57.8897500     0.003750      8.264953178     104.9712956     83.97703648
 2015-11-15T03:31:57.8910000     0.005000      4.860732869     98.58256063     78.86604850
 2015-11-15T03:31:57.8922500     0.006250      6.356496846     98.83569805     79.06855844
 2015-11-15T03:31:57.8935000     0.007500      5.298730096     91.78874146     73.43099317
 2015-11-15T03:31:57.8947500     0.008750      6.639808854     92.51589572     74.01271658
 2015-11-15T03:31:57.8960000     0.010000      5.050072132     93.83846794     75.07077435
 2015-11-15T03:31:57.8972500     0.011250      6.008001400     109.2973631     87.43789050
 2015-11-15T03:31:57.8985000     0.012500      5.132832560     107.3479382     85.87835057
```

Fig. 83—Example MDTS File part 2 (illustrative).

APPENDIX D: A JOINT INDUSTRY PROJECT TO COMBINE DRILLING DATA AND EDUCATION[11]

D.1 Introduction

On their continuous quest to improve drilling efficiency, operators are reaching more and more towards sensor and data-streaming technologies and their powerful data analytics capabilities. For this project, an operator partnered with the drilling automation research group at the University of Texas at Austin to develop a workflow for big data analysis and visualization. The objectives were to maximize the value derived from data, establish an analysis toolkit, and train students on data analytics—a necessary job function of any future drilling engineer. The operator provided data sets, business and technical objectives, and guidance for the project, while a multi-disciplinary group of undergraduate and graduate students piloted an analysis workflow. The students developed methods to: 1) understand and clean the data; 2) structure, combine, and condense information; 3) visualize, benchmark, and interpret the data, as well as derive key performance indicators (KPI); and 4) automate these processes.

The operator provided data collected from drilling 16 wells in an US unconventional play. The large data sets comprised of unorganized time and depth based information from surface and downhole sensors, daily drilling reports, geological information, etc. Students were trained on specialized software and subsequently curated data into smaller sizes and standard formats.

[11] Chapter based on: Zhou, Y., Baumgartner, T., Saini, G., Ashok, P., van Oort, E., Isbell, M. R., & Trichel, D. K. (2017, March 14). Future Workforce Education through Big Data Analysis for Drilling Optimization. Society of Petroleum Engineers. doi:10.2118/184739-MS. Zhou, Y., Baumgartner, T. and Saini, G. contributed in equal shares to the content and text of the paper. Ashok, P supervised the project that the paper is based on and contributed to the paper in a supervisory role. van Oort, E. initiated the project and supervised the composition of the paper.

Students investigated bottom hole assembly (BHA) and directional drilling performance using a combination of auto-generated conventional visuals (e.g. BHA designs, annotated time vs. depth curves) and newly developed tools (e.g. tortuosity, 3D well trajectory plots combined with operational data). Methods for "push a button" investigations of mechanical specific energy (MSE), vibration, torque and drag were also developed by calculating specific KPIs from the raw data. The analysis work itself coupled with the attempt to improve the workflow processes served as a meaningful and highly effective way to educate students and prepare them to be the "drilling engineers of the future" with proficiency in data analytics.

Drilling Data Analysis

The oil and gas industry is undergoing a transformation to drive waste out of the business of safely delivering hydrocarbons to consumers. The societal, technological, and political environment in which petroleum producers operate continues to elevate future requirements (Handscomb et al., 2016):

- Sustained resource abundance and the possibility of moderate oil prices require companies to focus on production maximization with efficiency and speed.
- Technological advances in the areas of digitization, data analytics and automation may enable step changes in productivity when the industry takes on the challenge.
- Demographic changes with an entire generation going into retirement leaves room for millennials[12] as the "digital natives" to become technical experts and take on leadership roles.

[12] Millennials are individuals with starting birth years as early as 1980's and ending birth years as late as the 2000's

Companies across the oil and gas industry face fierce pressures to make effective decisions and execute them safely and efficiently while struggling to remain profitable in a time of lower oil and gas prices. The people completing this work use their experience, work processes, and tools to guide business operations. The measurements and records from these activities are increasingly being captured in the form of digital data. Efforts are underway to combine this data in innovative ways to safely increase the rate of improvement in well delivery in terms of reduced cycle time and cost.

Analysis of historical data has always been used to characterize performance in well delivery. Our specific focus in this chapter is on drilling performance. Technological advances offer the right tools: big data analysis to derive meaningful insights, machine intelligence and mechanization to carry out tasks in as efficient a manner as possible. Exploration and production companies can adapt the way they hire and train their employees and encourage collaboration to fully take advantage of these new methods as they seek to create and protect more value from their existing business data.

Soon, every sensor or measurement device at a rig could be connected in real-time – with each other and to the office. Operations of the future will have an increased level of complexity in such a multi-connected environment. Engineers will only be able to master a small portion of a project, and will need to consult other specialists. Collaboration, sharing knowledge, structuring tasks, and explaining complicated material in simple terms to business stakeholders will become ever more important.

In addition to being able to work effectively in teams, mastering digitization (being technology savvy, recognizing the potential of data and automation in processes and workflows, making best use of software and programming, comfortably handling large amounts of data, etc.) could be the most sought-after skillset of a future drilling engineer.

Data-savvy drilling engineers will prepare real-time data from drilling operations for more senior colleagues to make informed and effective decisions. Repetitive tasks will be taken over by machines, allowing engineers to test creative solutions and to focus on solving unfamiliar problems. The drilling engineer of the future will need to develop machine intelligence, the ability to use machine to automate day-to-day processes, and will need to work closely with data science currently considered in the information technology domain.

Universities are still somewhat disconnected from industry pressures and objectives. The current educational systems value competition over collaboration, individual effort over team work, single-number answers over uncertainty, and strict assumptions over understanding fuzzy complexities. In general, they need to start doing a better job of preparing a new generation of engineers for success in industry. This requires effectively addressing disconnects in current curricula.

At the University of Texas at Austin (UT Austin), a Real-Time Collaboration Center (RTCC) was built in 2014 to facilitate the receipt and use of data by students. Real-time and historical drilling data can be streamed, visualized, and analyzed. Students are provided with several multi-screen working stations and a variety of data analysis software. Data security precautions are in place to ensure integrity and security of the data.

UT Austin collaborated with an independent operator to involve undergraduate and graduate students in analyzing large sets of unconventional shale drilling data over the course of an entire year. This project is helping to address some of the gaps between the current educational system and the challenges in a rapidly transforming industry, while making effective use of the unique research capabilities at UT Austin.

D.2 Project Overview

Objectives

The project stakeholders agreed on three main objectives:

- Foremost, *maximize the value* from the tens of gigabytes of data gathered during drilling operations. Several work streams were selected to help identify key drilling performance limiters and cost saving opportunities. These work streams include assessment of the bottom hole assembly and directional drilling performance, by using measures such as wellbore tortuosity, time-based vibration data, and other well information to create meaningful visualizations and implement standardized data structures.
- Establish a standardized *data analysis toolkit*. The steps towards such a toolkit were to 1) identify, streamline, and document the working process to establish workflows, and 2) build software tools that automate these workflows (i.e. perform analysis and/or visualization of the data).
- Help *educate undergraduate students* and equip them with skill sets necessary to tackle problems in a big data world. By working on the project, the students would familiarize themselves with in-depth drilling processes and drilling jargon, i.e. learn drilling in an entirely different (but very relevant and hands-on) way from the usual university curriculum, and acquire a data analysis skill set at the same time.

Data Sets

The data available for this project covered four pads, sixteen wells, in the Bakken formation that were drilled from 2014 to 2015 for a total of 256 active rig days. The data was a product of a drilling automation pilot project previously published by the operator (Trichel et al., 2016). The data set for each well was comprehensive and included well

planning reports (well plan, drilling schedule), geology information (formation tops, log, compressive strength), surface sensor data, directional surveys, daily drilling reports (DDR) and extensive measurement/logging while drilling (MWD/LWD) and other downhole data. Raw file formats included pdf, text, spreadsheets, and presentations. Their size varied from a few hundred KB to more than 5 GB each. In total, there were more than 50 individual files, amounting to over 100 GB of data with more than 20 million rows of information.

D.3 Deliverables

To accomplish the first two objectives noted above, the students decided they would work towards interactive visualizations using available drilling data, to quickly assess a well's drilling performance. Three main deliverables formed the basis for the data analysis toolkit (**Fig. 84**):

1. *Data curation*: assure data quality and organize data into a more cohesive, consistent, and accessible format. Effective analytical approaches could only be applied once the data was classified and cleaned. Note that a significant amount of time was spent on data preparation for analysis.
2. *Data visualization*: analyze and visualize key information in the form of interactive and informative graphics.
3. *Storyboard*: Develop a workflow that guides the user through different visualizations from an overview to a highly-detailed level, in order to illustrate and quantify key elements of the drilling performance related to the drilling systems and well delivery requirements.

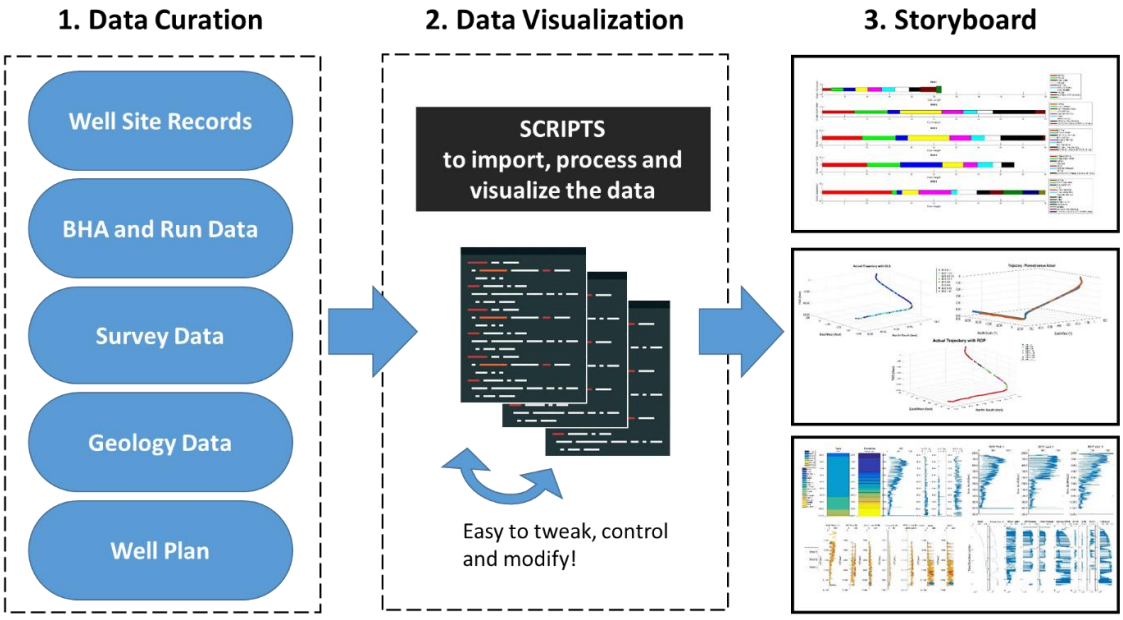

Fig. 84—Key components in delivering value from big data.

Data Security

Sharing critical data with third parties raises evident security concerns. Traditionally, geological, and geophysical data giving insight into the properties of hydrocarbon reservoirs is the most sensitive information to oil and gas companies, for reasons of investment decisions and competitive intelligence. However, even drilling tool selection and operational practices can give companies a competitive advantage and allow them to develop certain plays more successfully than others. For these reasons, companies do not want their data to be used by unauthorized people or for unauthorized purposes.

Legal agreements between the university and the operator prevent students from sharing data, storing it on their personal machines, keeping files beyond the project, or using data in unintended ways. To create data security barriers, UT Austin's RTCC is equipped with modern security systems, such as access control with door badge systems to ensure only students with the required permission can physically enter the RTCC, where

computers and servers are located. Access to the data, stored on protected servers, is granted only to individuals working on the projects. This is an essential step that educational institutes working with business data must take to address their project partner's data security concerns.

Data Curation

Efficient data transfer from the data service provider to the operator seems to be one of the greatest challenges that is currently preventing the industry from using data to its full potential. In this case, the operator received drilling operation data recorded at the rig site and downhole through different data service providers using multiple measurement systems.

One of the other big challenges in this project was associated with data dumps that were too large to open. The size of files with 1-2 million rows and almost 600 data columns (i.e. channels for individual measurements) exceeded the capabilities of standard data processing software. Several iterations were required to establish a successful workflow to overcome these difficulties. The students spent some time identifying tools13 for processing large data sets:

A software tool called "Delimit" was used to slice the large CSV files into smaller files, then process the smaller files in either Microsoft Excel (2016) for visual inspection or in MATLAB (2015b) for a more in depth analysis and visualization. A more unified method to process the data replaced it in the second step.

Next, MATLAB scripts imported pre-selected channels for targeted analysis. After importing those channels, many of them were identified as completely empty or had too many invalid data points.

[13] The mentioned software tools are generally available in a university setting.

Data quality checks were performed. This step successfully reduced the data size by ~30-50% in most cases. The files were cut into individual sections by either casing strings or BHA run, which further reduced the file sizes.

A database was created as a last step to upload and store processed and good quality data for all wells in a structured format. Specific channels (measurements) at a given time/depth interval for each well could now be downloaded and used for further analysis.

As mentioned above, the quality of the data provided a challenge. The largest data files contained time-series data with a sample rate of 1 Hz. Many columns consisted of null data (e.g. were completely empty, contained an invalid dummy value). The column names were the only hint to the nature of the measurements. Other channels were used to store "static" data (i.e. bit size with the same value at every time step), unnecessarily adding to the file sizes. The quality and nature of each channel was quantified by automatically calculating certain statistics for each data column, as shown in **Fig. 85.**

	A	B	C	D	E	F
1	channel	unique count	min	med	mean	max
2	AD.DP.ENABLED	1	1	1	1	1
3	AD.WOB.ENBLED	1	1	1	1	1
4	Batt.Stat.2	1	1536	1536	1536	1536
5	Bit.Position	1	1	1	1	1
6	Bit.TVD	1	-999.25	1	-99.025	1
7	Bit.TVD...WITS	1	-999.25	-999.25	-999.25	-999.25
8	Bit.Weight	1	142	142.2	142.185	142.3
9	Block.Height	1	54.16	54.16	54.16	54.16
10	Bttm.Pipe.Temp	1	-999.25	-999.25	-999.25	-999.25
11	Choke.Position.1	1	100	101	100.95	101
12	Co..Man.G.L	1	41	41	41	41

Fig. 85—A summary report of some channels with one unique value.

For example, channels that had only one unique value (either 0 or -999.25 as a dummy value) were classified to be either empty or invalid. Out of more than one million

rows, any channel with less than a dozen unique values was considered to be static. In general, one third of the 588 listed channels in all wells had less than 10 unique values, hence could not be considered time-based data.

Then, there was the challenge of missing contextual data. The large data file initially had 588 data channels without any additional documentation or description. Chapter 5 proposes a data transfer structure that could help preserve important contextual information during data transfers.

After a series of requests to the service company, multiple documents were received; each described a small subset of channels listed in the raw data file. In a time-consuming, manual process, the descriptions were matched to the files column names. However, only ~20% of the channels could be matched with its contextual information. It is worth noting that some channels with potentially useful information, such as "Rig Activity Code" and "Bit Status", were rendered useless because of the lack of associated decoding information.

Visualization

Drilling is a complex process. Often, one single measurement does not provide enough insight to evaluate performance or to even determine the current rig activity. Only a combination of multiple measurement streams and static data allows the analysis of drilling operations. Structured visualizations organically combine the data and provide insights. Several KPIs allow an engineer to quickly evaluate a well's performance. The students designed a variety of such visualizations and KPIs, and then wrote scripts to automatically extract, process, and display the data and calculate KPIs.

Much useful information in drilling today is still stored in unstructured formats such as written text, PDFs, or scanned images. For example, daily drilling reports or tool

specifications contain essential information that is hard to automatically extract. Sidahmed et al. (2015) described various methods and workflows of transforming such files into a more accessible format. In this project, undergraduate students read unstructured data (DDRs), then manually extracted and reformatted various streams of information into a new format. This tedious process helped the students to familiarize themselves with drilling jargon and the various operational processes, and gave them a good overview of the wells.

In future work, an automated process could leverage natural language processing capabilities for handling this task. **Fig. 86** illustrates the three-step workflow to creating easily interpretable visuals from unstructured data. First, information was extracted from DDRs. Second, students classified the text and compiled data tables. Third, the data tables served as input for automated visualizations. For example, a list of categorized BHA components could be automatically plotted and was used to compare multiple BHA designs at a quick glance. In a different visualization, the students could augment a time vs. depth curve with descriptions of notable events.

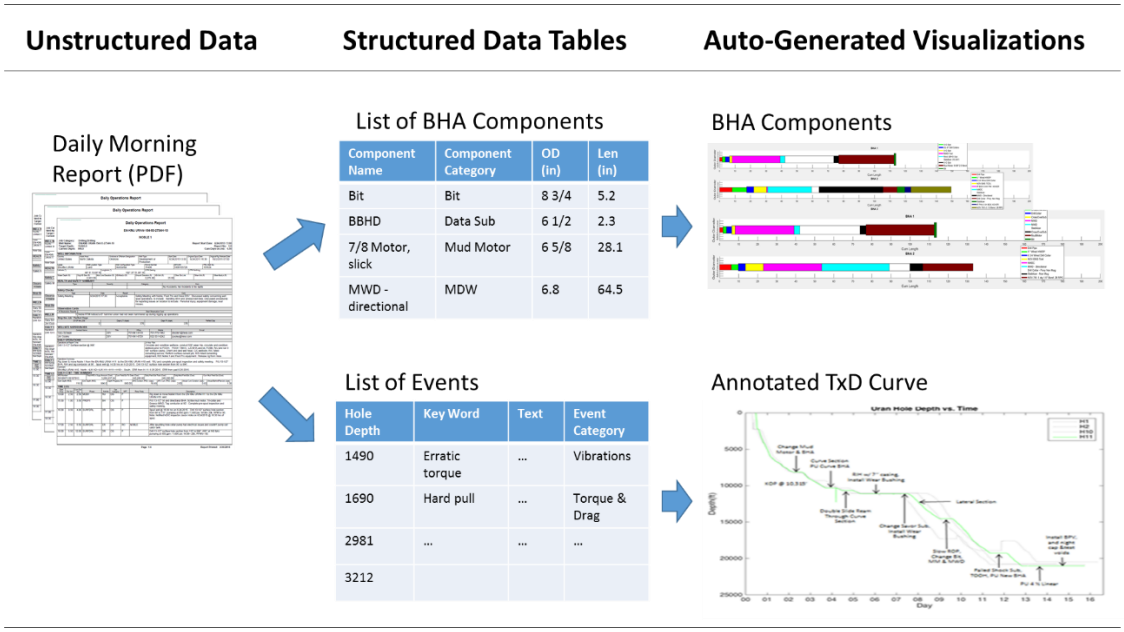

Fig. 86—Visualization process for unstructured data.

To quickly assess essential information (e.g. directional performance, BHA performance, vibration severity), the students developed analysis toolkits that produced a variety of 2D and 3D visualizations. These provide clear and intuitive assessments of aspects of an individual well as also for multiple wells in each pad. Visualizations can cover either a single well or all wells on an entire well pad. They can extend from a high-level overview, such as pad specific multi-well rate of penetration (ROP) comparison and annotated time vs. depth graph, to detailed assessments such as BHA component visualization and downhole vibrations.

For example, the planned vs. actual directional performance visualization illustrated in **Fig. 87** combined 3D and 2D well profile visualizations. Key parameters displayed alongside in strip charts help compare the well's actual to the planned well path. Users can trace root causes of anomalies by making use of additional visualizations of BHA components and/or directional performance per BHA design and per formation.

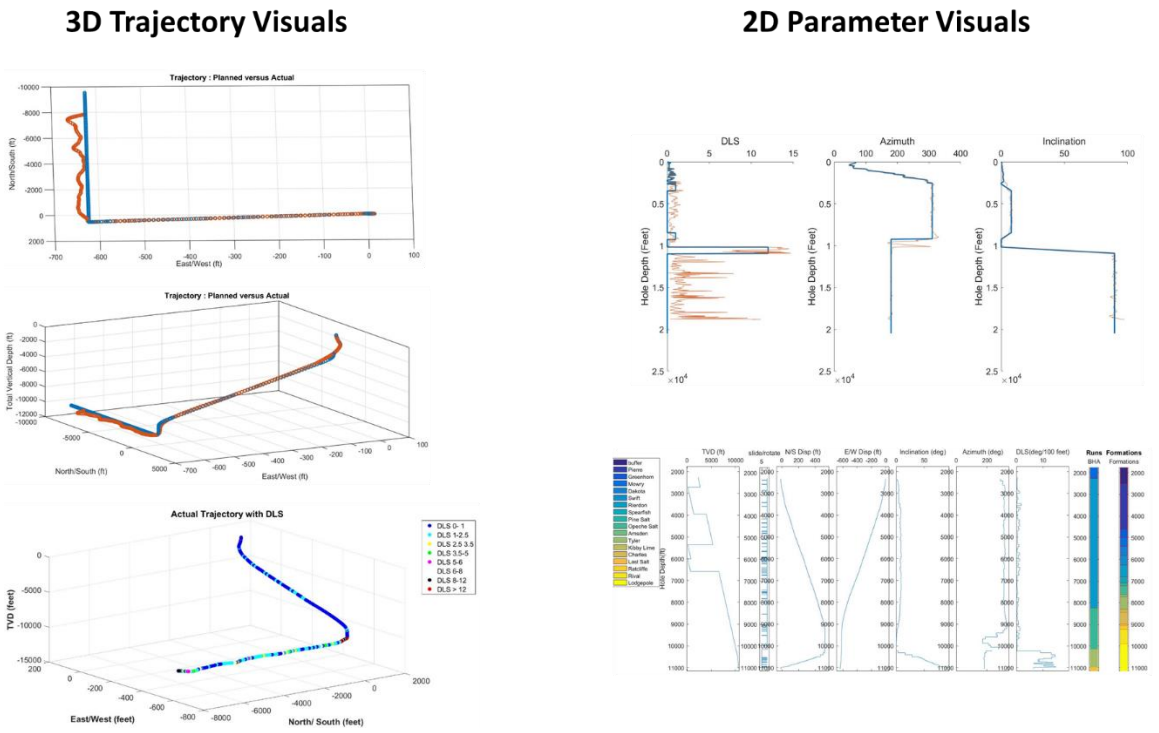

Fig. 87—Visualizations for directional performance.

The students developed scripts to automatically perform the analysis and generate associated visualizations with minimum user effort. The script would prompt the user at various points of execution, asking for input data files when the user executed the master script. The scripts would then process the data and generate multiple one page visualizations. The modular nature of the scripts also made them robust and easy to modify and maintain.

Storyboard

Multiple individual visuals were generated for each well, and several more for each well pad because of the large amount of available data and the automated process. The team developed a storyboarding concept, where sets of visuals provided the required

context for various drilling system performance aspects. As the name suggests, it organized the visualizations in different threads and layers to tell the story of the well. A drilling engineer or a trained user can follow a storyline to gain an in-depth understanding of a particular element of well performance, and to extract clues to potential drilling performance optimization.

Pre-set visualizations were selected to address commonly asked questions about drilling performance. Visualizations were then grouped together to form a storyline that the user follows in a specific order. **Fig. 88** illustrates a sample storyboard. For instance, to answer "How did the BHA perform?", the user is presented with a storyline of four visualizations. The user first looks at the comparison of the planned and actual well path, which illustrates the directional execution of the well. Next, the user is shown the ROP distribution information along different sections of the well. Then, the user is shown the BHA run and formation top information, alongside with inclination, azimuth, dogleg severity, and tortuosity index in vertical strip charts. Finally, the user is presented with vibration and other downhole measurements associated with different BHAs at different formations. By following the story line, the user develops a thorough understanding of information relevant to the posed question(s), and is equipped to draw conclusions from the information presented.

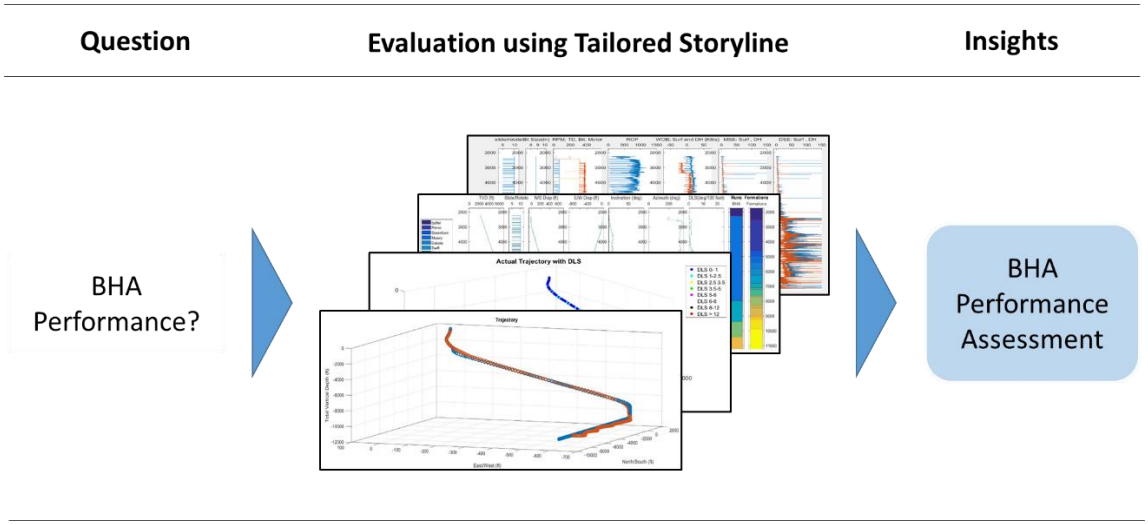

Fig. 88—Storyboard application example.

D.4 Student Learning

As mentioned, one key objective of this project was to further educate, train, and develop students' data analytics skills and offer them real industry experience. Traditionally, petroleum engineering degrees are not very industry oriented, with internship(s) as the only opportunity to learn more about industry operations. Moreover, the cyclical business environment can take a toll on newly graduating students and reduces the options for internships and other industry involvement. Students themselves are generally keen to keep up with trends in the industry, constantly learning new skills not covered in class curricula. The present project presented a useful opportunity to acquaint themselves with industry jargon and learn relevant skills. Over the course of a year, three groups of undergraduate students were recruited and trained for participation in this project. Students gained valuable experience learning and applying problem solving tools with messy real data, as described below.

Project Management and Ownership

During the course of the project, the undergraduate students formed separate groups and worked on separate sub-projects. This encouraged students to establish ownership for different parts of the project and to deliver results on a strict timeline. Weekly meetings and regular individual deliverables helped students to document their progress, discuss their road blocks, and plan their future work. At the same time, their reports were used as the basis for reporting to the operator. This workflow seemed to incentivize undergraduate students to effectively manage their own progress, and also allowed the graduate student leaders to better support the students in achieving their goals.

Problem Solving Skills

Shifting the focus from the path or method towards the goal itself was an important lesson the students took away from this project. During this project, we noticed that the undergraduate students could be easily discouraged if some parts of the puzzle needed to solve a problem weren't readily available. For instance, unavailable or faulty data constituted the end of the task for some. If the right data is missing, or equations are wrong in a homework problem, the task is dropped. However, real life tasks are not structured that way. Solving real life problems meant utilizing any tool available and finding resources when the path forward was not clear.

Team Building

The students experienced a mix of individually assigned problems and collaboration tasks within groups. They participated in brainstorming sessions, where they became more comfortable speaking up and sharing their ideas as the project progressed in time. We believe that such group sessions not only produced excellent ideas, but also made students feel like they were equal stakeholders in the project.

Time Management and Prioritization

The students committed to a certain number of hours on the project each week, and were held accountable to fulfill the set expectations. Exceptions for exams and other situations needed to be communicated and approved ahead of time, and the students were encouraged to make their own arrangements to ensure the completion of their tasks. In this process, the students encountered different time management and prioritization requirements. Most of them attended every weekly meeting, delivered on their tasks, and sent their progress reports on time.

Presentation Skills

Through monthly presentations, the project team kept the operator apprised of progress in the project, providing students timely feedback for their current and future work. The presentation deck reflected a seamless integration of everyone's work. To that effect, the students made sure that their final set of slides fit into the overall goal of the team's presentation, and that they complemented each other's work. During those meetings, individual students were given the opportunity to present their own work. This helped them advance their presentation skills, and a marked improvement was seen over the course of this project.

Technical Competency

Perhaps more than anything else, this project developed students' abilities on the technical front:

The students gained a thorough and in-depth understanding of multi-well pad drilling. Working with data such as the daily drilling reports, formation information and surveys helped them make sense of the drilling jargon and understand the drilling processes

better. The students acquired data analysis techniques by working with large amounts of drilling data, conducting data processing, analysis, and visualization.

Interactions and brainstorming sessions with graduate students and feedback from supervising professors and operators helped the students gain insight in solving drilling problems. The students were exposed to advanced drilling engineering research and concepts by reading papers on BHA analysis, mechanical specific energy (MSE), drilling specific energy (DSE), and drilling dysfunction such as torsional (stick-slip) and lateral (whirl) vibrations.

Leadership Skills

The PhD students co-leading the project also gained leadership training. This managerial and mentoring task presented a perfect learning opportunity for them. Typically, PhD students are expected to join the industry with higher responsibility, but leadership training or exposure is rarely offered at school or during internships. Coaching, leading and mentoring undergraduate students provided them with an opportunity to work on their leadership skills. In this project, the graduate student co-leaders faced many challenges a typical manager would encounter: How to deliver strong results? How to motivate the undergraduate students and guide them to stay on course? How to prioritize, and stay focused on the project? How to maintain productive and high-quality work?

D.5 Conclusions

This joint project between the University of Texas at Austin and an independent operator provided an exciting glimpse of an automated future state where data is proactively used while drilling a well and re-used to find limiting factors and improved

practices to advance efficiency. The work has benefitted the parties involved in the following ways:

The Operator

- Improved value extracted from data collected for an in-depth data study. Many files would otherwise never have been further analyzed.
- Gained insights into data quality will improve data standards and service agreements between the data service provider and the operator in the future.
- Realized quick cost savings from operational, BHA and well design changes identified by observations in the data.
- Improved standardization and use of drilling data for visualizations.
- Tested new visualization concepts, such as the storyboards, to increase the efficiency of dealing with large amounts of data and several types of measurements.
- Utilized an inexpensive yet well qualified research workforce at an educational institute.
- Educated and supported the training of future drilling engineers, i.e. their future workforce.

The Students

- Acquired a variety of important soft skills and real world drilling knowledge, improving their ability to successfully compete in the marketplace for future industry jobs.
- Gained an understanding of the benefits of data analysis and structured problem solving for moving towards more efficient drilling.

- Learned various tools and methods for analyzing large data sets containing information from multiple systems and representing complex engineering problems.
- Benefitted from the monetary compensation while at school.
- Made contacts with a potential future employer.

The University

- Provided a competitive advantage for their students in landing a position in the industry.
- Showcased the beneficial applied use of research funding.
- Demonstrated its flexibility to adapt teaching strategies to a changing environment.
- Contributed in innovative ways to solve new industry problems.
- Differentiated itself by quickly adapting to new industry needs and trends.

The project showed that process automation is the key to success in data analysis exercises such as these; the amount of data analyzed was too much to handle manually. It is essential to define a set of KPIs, analysis methods, and visualizations, and then automate their generation and deployment, such that any insights revealed by them can become available in a timely manner for multiple data sets.

Process automation requires a standardized and structured data input. The process of gathering the data from an unstructured, undocumented, and faulty state into a standardized one was the most challenging and time-consuming task of the entire project. Structured, standardized and transparently formatted data is essential for stakeholders to derive maximum timely value from any data gathered.

Applying information technology to engineering problems is a key challenge to future engineers, and it therefore is essential that they become proficient in information technology methods. Every task in this project required coding skills in one way or another. Students that had some prior coding experience could leverage these skills to solve problems faster or even augment tasks that were traditionally performed manually (e.g. screening daily drilling reports for key words). This clearly shows that learning at least one commonly used programming language early is a prerequisite to become an effective future petroleum engineer. Drilling engineering graduates with coding skills are capable of quickly prototyping tailored tools to solve specific drilling problems; these tools can then be developed into user friendly software by company's IT departments or outside resources.

D.6 Future Work

The project demonstrated what is possible in using new capabilities in data handling and analysis methods. Future projects will further drive drilling performance and innovation. Formalizing this problem-solving approach and offering students a class on various aspects of drilling data analysis is a key goal for the research and education program.

This drilling data analytics project constitutes the first of hopefully many such initiatives in the future. By communicating the benefits for all parties and eliminating concerns about data security, we hope that more companies will be willing to share their data and be open to sharing their analyses to enable the entire industry to drill faster and safer wells.

Glossary

ADC	Analog to Digital Converter
API	American Petroleum Institute
ASCII	American Standard Code for Information Interchange
ATCE	Annular Technical Conference and Exhibition
BHA	Bottom Hole Assembly
CSV	Comma Separated Value
DDR	Daily Drilling Reports
DLIS	Digital Log Interchange Standard
DSATS	Drilling Systems Automation Technical Session
DSE	Drilling Specific Energy
ECD	Equivalent Circulating Density
EIA	Energy Information Administration
FFT	Fast Fourier transform
FIT	Formation Integrity Tests
GB	Gigabytes
HFTO	High-Frequency Torsional Oscillations
HMI	Human Machine Interface
HWDP	Heavy Weight Drill Pipe
IPTC	International Petroleum Technical Conference
ISCWSA	Industry Steering Committee on Wellbore Survey Accuracy
KB	Kilobytes
KPI	Key Performance Indicators
LAS	Log ACSII Standard

LIS	Log Information Standard
LWD	Logging While Drilling
MD	Measured Depth
MDTS	Memory Data Transfer Standard
MEMS	Microelectromechanical
MPD	Managed Pressure Drilling
MSE	Mechanical Specific Energy
MWD	Measurement While Drilling
NEMS	Nanoelectromechanical
NOV	National Oilwell Varco
NPT	Non-Productive Time
OPC-UA	Open Platform Communications Unified Architecture
PAA	Piecewise Aggregate Approximation
PDC	Polycrystalline Diamond Compact
PWD	Pressure While Drilling
QRI	Quantum Reservoir Impact
RMS	Root Mean Square
ROP	Rate of Penetration
RPM	Revolutions Per Minute
RSS	Rotary Steerable System
RTCC	Real-Time Collaboration Center
SAX	Symbolic Aggregate approXimation
SPE	Society of Petroleum Engineers
TD	Total Depth

TOB	Torque on Bit
TVD	Total Vertical Depth
UT	The University of Texas
WITSML	Wellsite Information Transfer Standard Markup Language
WOB	Weight on Bit

References

Al-Farisi, O., Dajani, N., Boyd, D., & Al-Felasi, A. (2002, January 1). Data Management and Quality Control in the Petrophysical Environment. Society of Petroleum Engineers. doi:10.2118/78524-MS

Ali, T. H., Sas, M., Hood, J. A., Lemke, S. R., Srinivasan, A., McKay, J., Reeves, M. (2008, January 1). High Speed Telemetry Drill Pipe Network Optimizes Drilling Dynamics And Wellbore Placement. Society of Petroleum Engineers. doi:10.2118/112636-MS

Allan, M. E., Beaschler, T. D., & Lalicata, J. J. (2012, June 16). Too Much Petrophysical Data - a Dream Or a Nightmare. Society of Petrophysicists and Well-Log Analysts.

Ambrus, A., Ashok, P., & van Oort, E. (2013, September 30). Drilling Rig Sensor Data Validation in the Presence of Real-Time Process Variations. Society of Petroleum Engineers. doi:10.2118/166387-MS

Arnaout, A., Zoellner, P., Thonhauser, G., & Johnstone, N. (2013, October 28). Intelligent Data Quality Control of Real-time Rig Data. Society of Petroleum Engineers. doi:10.2118/167437-MS

Ashok, P., Ambrus, A., Ramos, D., Lutteringer, J., Behounek, M., Yang, Y. L., Weaver, T. (2016, September 6). A Step by Step Approach to Improving Data Quality in Drilling Operations: Field Trials in North America. Society of Petroleum Engineers. doi:10.2118/181076-MS

Ashok, P., van Oort, E., & Ambrus, A. (2013, March 5). Automatic Sensor Data Validation: Improving the Quality and Reliability of Rig Data. Society of Petroleum Engineers. doi:10.2118/163726-MS

Bang, J., Jegbefume, O., Ledroz, A., Weston, J., & Thompson, J. (2016, March 1). Analysis and Quantification of Wellbore Tortuosity. Society of Petroleum Engineers. doi:10.2118/173103-PA

Bataee, M., Kamyab, M., & Ashena, R. (2010, January 1). Investigation of Various ROP Models and Optimization of Drilling Parameters for PDC and Roller-cone Bits in Shadegan Oil Field. Society of Petroleum Engineers. doi:10.2118/130932-MS

Baumgartner, T., & van Oort, E. (2015, September 28). Maximizing Drilling Sensor Value through Optimized Frequency Selection and Data Processing. Society of Petroleum Engineers. doi:10.2118/174986-MS

Baumgartner, T., & van Oort, E. (2014, October 27). Pure and Coupled Drill String Vibration Pattern Recognition in High Frequency Downhole Data. Society of Petroleum Engineers. doi:10.2118/170955-MS

Baumgartner, T., Zhou, Y., & van Oort, E. (2016, March 1). Efficiently Transferring and Sharing Drilling Data from Downhole Sensors. Society of Petroleum Engineers. doi:10.2118/178900-MS

Belaskie, J. P., Dunn, M. D., & Choo, D. K. (1993, June 1). Distinct Applications of MWD, Weight on Bit, and Torque. Society of Petroleum Engineers. doi:10.2118/19968-PA

Bond, D. F., Scott, P. W., Page, P. E., & Windham, T. M. (1998, September 1). Applying Technical Limit Methodology for Step Change in Understanding and Performance. *SPE Drilling & Completio*n doi:10.2118/51181-PA

Bowler, A., Harmer, R., Logesparan, L., Sugiura, J., Jeffryes, B., & Ignova, M. (2016, May 1). Continuous High-Frequency Measurements of the Drilling Process Provide New Insights Into Drilling-System Response and Transitions Between Vibration Modes. Society of Petroleum Engineers. *SPE Drilling & Completion*. doi:10.2118/170713-PA

Brett, J. F., Warren, T. M., & Behr, S. M. (1989, January 1). Bit Whirl: A New Theory of PDC Bit Failure. Society of Petroleum Engineers. doi:10.2118/19571-MS

Cardy, N., Hjortland, F., Jeffrey, C., Wilde, S., Muecke, N., & Wroth, A. (2016, March 1). Along String Dynamics Measurements Reveal Isolated Potentially Damaging Upper String Vibration Environments. Society of Petroleum Engineers. doi:10.2118/178872-MS

Cavazos, C. (2014, April 1). Data Security Promotes Improved Intelligent Drilling. Society of Petroleum Engineers. doi:10.2118/167904-MS

Cayeux, E., Daireaux, B., & Dvergsnes, E. (2011, December 1). Automation of Drawworks and Topdrive Management To Minimize Swab/Surge and Poor-Downhole-Condition Effect. Society of Petroleum Engineers. doi:10.2118/128286-PA

Cayeux, E., Daireaux, B., Dvergsnes, E. W., & Florence, F. (2013, March 5). Toward Drilling Automation: On the Necessity of Using Sensors That Relate to Physical Models. Society of Petroleum Engineers. doi:10.2118/163440-MS

Chen, S. L., Blackwood, K., & Lamine, E. (2002, March 1). Field Investigation of the Effects of Stick-Slip, Lateral, and Whirl Vibrations on Roller-Cone Bit Performance. Society of Petroleum Engineers. *SPE Drilling & Completion.* doi:10.2118/76811-PA

Close, D. A., Owens, S. C., & MacPherson, J. D. (1988, January 1). Measurement of BHA Vibration Using MWD. Society of Petroleum Engineers. doi:10.2118/17273-MS

Coley, C. J., & Edwards, S. T. (2013, March 5). The Use of Along String Annular Pressure Measurements to Monitor Solids Transport and Hole Cleaning. Society of Petroleum Engineers. doi:10.2118/163567-MS

Collier, P. 2012. A Most Incomprehensible Thing: Notes Towards a Very Gentle Introduction to the Mathematics of Relativity. 2nd Edition. Incomprehensible Books. ISBN 978-0-9573894-5-8.

Cunningham. R.A. (1968). Analysis of Downhole Measurements of Drill String Forces and Motions. J. Manuf. Sci. Eng. 90(2), 208-216. doi:10.1115/1.3604616

D'Ambrosio, P., Bouska, R., Clarke, A. J., Laird, J. L., Mckay, J. E., & Edwards, S. T. (2012, January 1). Distributed Dynamics Feasibility Study. Society of Petroleum Engineers. doi:10.2118/151477-MS

David, R. M. (2016, September 26). Accelerating the Learning Curve of Next Generation Exploration and Production Workforce through Smart Data and Knowledge Environment. Society of Petroleum Engineers. doi:10.2118/181594-MS

Deily, F.H., Dareing, D.W., Paff, G.F., Ortloff, J.E. and Lynn, R.D. (1968). Downhole Measurements of Drill-String Forces and Motions. J. of Engineering for Industry, 90 (2). pp. 217-226.

Dykstra, M. (1996). Downhole Measurement Interpretation. PhD thesis, University of Tulsa, OK, Appendix D.

Einstein, A. (1915). Relativity: The Special and the General Theory. Part III: Considerations of the Universe as a Whole. Methuen & Co Ltd. ISBN 0-517-029618 (Project Gutenberg)

Emmerich, W., Akimov, O., Brahim, I. B., & Greten, A. (2015, March 17). Reliable High-speed Mud Pulse Telemetry. Society of Petroleum Engineers. doi:10.2118/173032-MS

Energy Information Administration, Drilling Productivity Report, https://www.eia.gov/petroleum/drilling/archive/2017/01/ retrieved January 21, 2017.

Ertas, D., Bailey, J. R., Wang, L., & Pastusek, P. E. (2013, March 5). Drillstring Mechanics Model for Surveillance, Root Cause Analysis, and Mitigation of Torsional and Axial Vibrations. Society of Petroleum Engineers. doi:10.2118/163420-MS

Evangelatos, G. I., & Payne, M. L. (2016, March 1). Advanced BHA-ROP Modeling Including Neural Network Analysis of Drilling Performance Data. Society of Petroleum Engineers. doi:10.2118/178852-MS

Florence, F., Chapman, C., Macpherson, J., & Cavanaugh, M. (2015, September 28). Implementation of Drilling Systems Automation - Halifax Workshop Summary: Industry Standards, Business Models and Next Steps. Society of Petroleum Engineers. doi:10.2118/174779-MS

Fredd, C. N., Daniels, J. L., & Baihly, J. D. (2015, January 26). $40 Billion Learning Curve: Leveraging Lessons Learned to Minimize the Overall Investment in Unconventional Plays. Society of Petroleum Engineers. doi:10.2118/172973-MS

Gao, G., & Miska, S. (2010, September 1). Dynamic Buckling and Snaking Motion of Rotating Drilling Pipe in a Horizontal Well. Society of Petroleum Engineers. *SPE Journal*. doi:10.2118/113883-PA

Gidh, Y. K., Purwanto, A., & Ibrahim, H. (2012, January 1). Artificial Neural Network Drilling Parameter Optimization System Improves ROP by Predicting/Managing Bit Wear. Society of Petroleum Engineers. doi:10.2118/149801-MS

Gravdal, J. E. (2009, January 1). Real-Time Evaluation of Kick during Managed Pressure Drilling based on Wired Drill Pipe Telemetry. International Petroleum Technology Conference. doi:10.2523/IPTC-13959-MS

Grinfeld, P. (2013). Introduction to Tensor Analysis and the Calculus of Moving Surfaces. Springer-Verlag New York. DOI: 10.1007/978-1-4614-7867-6

Grosso, D. S., Raynal, J. C., & Rader, D. (1983, May 1). Report on MWD Experimental Downhole Sensors. Society of Petroleum Engineers. doi:10.2118/10058-PA

Guidry, T. F., & Scego, J. F. (1986, January 1). Improve Drilling Results Using a Real-Time Data Center. Society of Petroleum Engineers. doi:10.2118/14069-MS

Guo, B., & Hareland, G. (1994, January 1). Bit Wobble: A Kinetic Interpretation of PDC Bit Failure. Society of Petroleum Engineers. doi:10.2118/28313-MS

Halsey, G. W., Kyllingstad, A., & Kylling, A. (1988, January 1). Torque Feedback Used to Cure Slip-Stick Motion. Society of Petroleum Engineers. doi:10.2118/18049-MS

Handscomb, C., Sharabura, S., Woxholth, J. (2016). The Oil and Gas Organization of the Future. McKinsey Oil & Gas, September 2016, http://www.mckinsey.com/industries/oil-and-gas/our-insights/the-oil-and-gas-organization-of-the-future.

Heisig, G., Sancho, J., & Macpherson, J. D. (1998, January 1). Downhole Diagnosis of Drilling Dynamics Data Provides New Level Drilling Process Control to Driller. Society of Petroleum Engineers. doi:10.2118/49206-MS

Hill, A. D., & Holditch, S. A. (2013, June 1). Deja vu All Over Again? Society of Petroleum Engineers. *Journal of Petroleum Technology*. doi:10.2118/0613-0018-JPT

Hinton, G. (2014). Where Do Features Come From?, *Cognitive Science*, 38 (6): 1078–1101.

Hoffmann, O.J., Jain, J.R., Spencer, R.W., et al. (2012). Drilling Dynamics Measurements at the Drill Bit to Address Today's Challenges. IEEE I2MTC

Hohl, A., Tergeist, M., Oueslati, H., Herbig, C., Ichaoui, M., Ostermeyer, G.-P., & Reckmann, H. (2016, March 1). Prediction and Mitigation of Torsional Vibrations in Drilling Systems. Society of Petroleum Engineers. doi:10.2118/178874-MS

Hutchinson, M., & Rezmer-Cooper, I. (1998, January 1). Using Downhole Annular Pressure Measurements to Anticipate Drilling Problems. Society of Petroleum Engineers. doi:10.2118/49114-MS

Isaacs, W. R., & Bobo, J. E. (1984, January 1). Design and Impact of a Real-Time Drilling Data Center. Society of Petroleum Engineers. doi:10.2118/13109-MS

Iversen, F. P., Cayeux, E., Dvergsnes, E. W., Gravdal, J. E., Vefring, E. H., Mykletun, B., Merlo, A. (2006, January 1). Monitoring and Control of Drilling Utilizing Continuously Updated Process Models. Society of Petroleum Engineers. doi:10.2118/99207-MS

Jain, J. R., Oueslati, H., Hohl, A., Reckmann, H., Ledgerwood III, L. W., Tergeist, M., Ostermeyer, G. P. (2014, March 4). High-Frequency Torsional Dynamics of Drilling Systems: An Analysis of the Bit-System Interaction. Society of Petroleum Engineers. doi:10.2118/167968-MS

Jamieson, A. (2012). *Introduction to Wellbore Positioning*. University of the Highlands & Islands Retrieved from: http://www.uhi.ac.uk/en/research-enterprise/energy/wellbore-positioning-download

Jamieson, G. A., Wang, L., Neyedli, H. F. (2008). Developing Human-Machine Interfaces to Support Appropriate Trust and Reliance on Automated Combat Identification Systems. Contract report prepared by Cognitive Engineering Laboratory, University of Toronto

Jansen, J. D. (1992, June 1). Whirl and Chaotic Motion of Stabilized Drill Collars. Society of Petroleum Engineers. *SPE Drilling Engineering*. doi:10.2118/20930-PA

Jardine, S. I., Johnson, A. B., White, D. B., & Stibbs, W. (1993, January 1). Hard or Soft Shut-in: Which Is the Best Approach? Society of Petroleum Engineers. doi:10.2118/25712-MS

Jiang, W., & Samuel, R. (2016, March 1). Optimization of Rate of Penetration in a Convoluted Drilling Framework using Ant Colony Optimization. Society of Petroleum Engineers. doi:10.2118/178847-MS

Kendall, H. A., & Goins, W. C. (1960, January 1). Design and Operation of Jet-Bit Programs For Maximum Hydraulic Horsepower, Impact Force or Jet Velocity. Society of Petroleum Engineers.

Keogh, E., Lin, J. and Fu, A. (2005). HOT SAX: Efficiently Finding the Most Unusual Time Series Subsequence. In Proc. of the 5th IEEE International Conference on Data Mining (ICDM 2005), pp. 226 - 233., Houston, Texas, Nov 27-30.

Leine, R. I., van Campen, D. H., Keultjes, W.J.G. (2002). Stick-slip Whirl Interaction in Drillstring Dynamics. J. Vib. Acoust. 124(2), 209-220 March. doi:10.1115/1.1452745

Lesso, W. G., Ignova, M., Zeineddine, F., Burks, J. M., & Welch, J. B. (2011, January 1). Testing the Combination of High Frequency Surface and Downhole Drilling Mechanics and Dynamics Data Under a Variety of Drilling Conditions. Society of Petroleum Engineers. doi:10.2118/140347-MS

Lin, J., Williamson, S., Borne, K. D., et al. (2012). Pattern Recognition in Time Series. Advances in Machine Learning and Data Mining for Astronomy. M. Way, J. Scargle, K. Ali, and A. Srivastava, Eds. New York, NY: Chapman and Hall.

Lines, L. A., Stroud, D. R. H., & Coveney, V. A. (2013, March 5). Torsional Resonance - An Understanding Based on Field and Laboratory Tests with Latest Generation Point-the-Bit Rotary Steerable System. Society of Petroleum Engineers. doi:10.2118/163428-MS

Liu, X., Nair, S. D., Cowan, M., & van Oort, E. (2015, April 13). A Novel Method to Evaluate Cement-Shale Bond Strength. Society of Petroleum Engineers. doi:10.2118/173802-MS

Lund, H., & Martel, K. (2013, September 30). Identifying And Addressing Drilling Dysfunctions In Long Horizontal Wells. Society of Petroleum Engineers. doi:10.2118/166155-MS

Macpherson, J. D., Paul, P., Behounek, M., & Harmer, R. (2015, September 28). A Framework for Transparency in Drilling Mechanics and Dynamics Measurements. Present at SPE Annual Technical Conference and Exhibition, Houston, Texas, 28-30 September. SPE-174874-MS. http://dx.doi.org/10.2118/174874-MS

Makkar, N., Sullivan, E., & Habernal, J. (2014, March 25). Coupling Between Lateral and Torsional Vibrations: A New Insight into PDC Bit Drilling Inefficiencies. Offshore Technology Conference. doi:10.4043/25056-MS

Mallary, C. R., Varco, M., & Quinn, D. (1999, January 1). Using Pressure-While-Drilling Measurements To Solve Extended-Reach Drilling Problems on Alaska's North Slope. Society of Petroleum Engineers. doi:10.2118/54592-MS

Mathis, W., & Thonhauser, G. (2007, January 1). Mastering Real-Time Data Quality Control - How to Measure and Manage the Quality of (Rig) Sensor Data. Society of Petroleum Engineers. doi:10.2118/107567-MS

Mathis, W., Thonhauser, G., Wallnoefer, G., & Ettl, J. (2007, September 1). Use of Real-Time Rig-Sensor Data To Improve Daily Drilling Reporting, Benchmarking, and Planning—A Case Study. Society of Petroleum Engineers. doi:10.2118/99880-PA

Minett-smith, D. J., Stroud, D. R. H., & Pagett, J. (2010, January 1). Real-Time Whirl Detector Aids Drilling Optimization. Society of Petroleum Engineers. doi:10.2118/135110-MS

Mitchell, R. F., Miska, S. Z. (2010). *Fundamentals of Drilling Engineering*. Richardson, US: Society of Petroleum Engineers. p. 5.

Osnes, S. M., Amundsen, P. A., Weltzin, T., Nyrnes, E., & Grindhaug, G. (2009, January 1). Vibration Measurements: A Time for Standardisation. Society of Petroleum Engineers. doi:10.2118/119877-MS

Otalvora, W. C., AlKhudiri, M., Alsanie, F., & Mathew, B. (2016, September 26). A Comprehensive Approach to Measure the RealTime Data Quality Using Key Performance Indicators. Society of Petroleum Engineers. doi:10.2118/181315-MS

Oueslati, H., Jain, J. R., Reckmann, H., Ledgerwood, L. W., Pessier, R., & Chandrasekaran, S. (2013, September 30). New Insights Into Drilling Dynamics Through High-Frequency Vibration Measurement and Modeling. Society of Petroleum Engineers. doi:10.2118/166212-MS

Pastusek, P. E., Sullivan, E., & Harris, T. M. (2007, January 1). Development and Utilization of a Bit Based Data Acquisition System in Hard Rock PDC Applications. Society of Petroleum Engineers. doi:10.2118/105017-MS

Pickering, J. G., Kreijger, J., Grovik, L. O., Franssens, D., Deeks, N. R., Doniger, A., & Schey, J. (2009, January 1). WITSML "Comes of Age" for the Global Drilling and Completions Industry. Society of Petroleum Engineers. doi:10.2118/124347-MS

Pickering, J. G., Shields, J. A., Gidh, Y. K., Johnson, D., Al Shehry, M. A., Khudiri, M., Schey, J. (2012, January 1). WITSML: Laying the Foundation for Increasing Efficiency of Intelligent Wellsite Communications. Society of Petroleum Engineers. doi:10.2118/150278-MS

Pink, A. P., Kverneland, H., Bruce, A., & Applewhite, J. B. (2012, January 1). Building an Automated Drilling System Where the Surface Machines are Controlled by Downhole and Surface Data to Optimize the Well Construction Process. Society of Petroleum Engineers. doi:10.2118/150973-MS

Pink, T., Coit, A., Smith, J., & Nieto, J. (2015, March 17). Testing the Performance Impact of Automation Applications on Different Drive Systems in Unconventional Well Development. Society of Petroleum Engineers. doi:10.2118/173159-MS

Plaksina, T., & Gildin, E. (2015, September 28). Theory of Petroleum Engineering Education: Big Bounce, Big Crunch, or Big Freeze? Society of Petroleum Engineers. doi:10.2118/174742-MS

Poletto, F., Miranda, F. 2004. Seismic while drilling: Fundamentals of drill-bit seismic for exploration. Handbook of geophysical exploration. Section 1, Seismic exploration, ISBN 0080439284, Volume 35, xxvi, 520.

Quay, B. K. (1986, January 1). Daily Drilling Reporting System: Design/Usage. Society of Petroleum Engineers. doi:10.2118/15283-MS

Raap, C., Craig, A. D., & Perez Garcia, D. (2011, January 1). Understanding and Eliminating Drill String Twist-Offs by the Collection of High Frequency Dynamics Data. Society of Petroleum Engineers. doi:10.2118/148445-MS

Randell, C., Djiallis, C., Henk Muller, H. (2003). Personal Position Measurement Using Dead Reckoning. *Proceedings of the 7th IEEE International Symposium on Wearable Computers*. IEEE Computer Society, Washington, DC, USA.

Ramsey, M. S., Miller, J. F., & Morrison, M. E. (1983, January 1). Bottomhole Pressures Measured While Drilling. Society of Petroleum Engineers. doi:10.2118/11413-MS

Reinicke, K. M., Ganzer, L., & Teodoriu, C. (2011, January 1). New Ways in Research and Education: The Effect of Real Field Data on Multi-Disciplinary Student Projects in Petroleum Engineering. Society of Petroleum Engineers. doi:10.2118/145421-MS

Rezmer-Cooper, I. M., Rambow, F. H. K., Arasteh, M., Hashem, M. N., Swanson, B., & Gzara, K. (2000, January 1). Real-Time Formation Integrity Tests Using Downhole Data. Society of Petroleum Engineers. doi:10.2118/59123-MS

Runia, D. J., Dwars, S., & Stulemeijer, I. P. J. M. (2013, March 5). A brief history of the Shell "Soft Torque Rotary System" and some recent case studies. Society of Petroleum Engineers. doi:10.2118/163548-MS

Sadlier, A. G., Laing, M. L., & Shields, J. A. (2012, January 1). Data Aggregation and Drilling Automation: Connecting the Interoperability Bridge between Acquisition, Monitoring, Evaluation, and Control. Society of Petroleum Engineers. doi:10.2118/151412-MS

Saputelli, L., Economides, M., Nikolaou, M., & Kelessidis, V. (2003, January 1). Real-Time Decision-making for Value Creation while Drilling. Society of Petroleum Engineers. doi:10.2118/85314-MS

Schen, A. E., Snell, A. D., & Stanes, B. H. (2005, January 1). Optimization of Bit Drilling Performance Using a New Small Vibration Logging Tool. Society of Petroleum Engineers. doi:10.2118/92336-MS

Schultz, H., Schenck, D., Purdy, C., & Wallace, G. (2000, January 1). Wellogml: A Proposed Standard For Web-Based Exchange Of Digital Well Log Data. Society of Petrophysicists and Well-Log Analysts.

Shor, R. J. (2016). The effect of well path, tortuosity and drillstring design on the transmission of axial and torsional vibrations from the bit and mitigation control strategies. PhD Thesis, UT Austin.

Shor, R. J., Pryor, M., van Oort, E. (2014). Drillstring vibration observation, modeling and prevention in the oil and gas industry. DSCC2014-6147

Sidahmed, M., Coley, C. J., & Shirzadi, S. (2015, March 3). Augmenting Operations Monitoring by Mining Unstructured Drilling Reports. Society of Petroleum Engineers. doi:10.2118/173429-MS

Skalle, P. Toverud, T., Stein Tore Johansen, S. T., (2014, October). Attenuation of pump pressure in long wellbores (v02), *Journal of Petroleum Science and Engineering*, Volume 122, Pages 159-165, ISSN 0920-4105, http://dx.doi.org/10.1016/j.petrol.2014.07.005

Stockhausen, E. J., & Lesso, W. G. (2003, January 1). Continuous Direction and Inclination Measurements Lead to an Improvement in Wellbore Positioning. Society of Petroleum Engineers. doi:10.2118/79917-MS

Stroud, D. R. H., Lines, L. A., & Minett-smith, D. J. (2011, January 1). Analytical and experimental backward whirl simulations for Rotary Steerable bottom hole assemblies. Society of Petroleum Engineers. doi:10.2118/140011-MS

Sugiura, J., Samuel, R., Oppelt, J., Ostermeyer, G. P., Hedengren, J., & Pastusek, P. (2015, March 17). Drilling Modeling and Simulation: Current State and Future Goals. Society of Petroleum Engineers. doi:10.2118/173045-MS

Sutcliffe, B., Sim, D. (1991). Drilling Optimized by Monitoring BHA Dynamics with MWD. *Oil & Gas Journal*

Svensson, I., Saeverhagen, E., & Bouillouta, F. M. (2015, March 3). Driving Rig Performance through Real-Time Data Analysis, Benchmarking, Dashboards and Developed Key Performance Indicators. Society of Petroleum Engineers. doi:10.2118/173413-MS

Theys, P., Roque, T., Constable, M. V., Williams, J., & Storey, M. (2014, September 16). Current Status of Well Logging Data Deliverables and a Vision Forward. Society of Petrophysicists and Well-Log Analysts. SPWLA-2014-DD.

Thonhauser, G. (2004). Using Real-Time Data for Automated Drilling Performance Analysis, *OIL GAS European Magazine*, 4, 2004

Tikhonov, V. S., & Bukashkina, O. S. (2014, December 10). A New Model of High-Frequency Torsional Oscillations (HFTO) of Drillstring in 3-D Wells. International Petroleum Technology Conference. doi:10.2523/IPTC-17958-MS

Trichel, D. K., Isbell, M., Brown, B., Flash, M., McRay, M., Nieto, J., & Fonseca, I. (2016, March 1). Using Wired Drill Pipe, High-Speed Downhole Data, and Closed Loop Drilling Automation Technology to Drive Performance Improvement Across Multiple Wells in the Bakken. Society of Petroleum Engineers. doi:10.2118/178870-MS

Vajargah, A. K., & van Oort, E.(2015, March 17). Automated Drilling Fluid Rheology Characterization with Downhole Pressure Sensor Data. Society of Petroleum Engineers. doi:10.2118/173085-MS

Van Oort, E., & Vargo, R. F. (2008, September 1). Improving Formation-Strength Tests and Their Interpretation. Society of Petroleum Engineers. *SPE Drilling and Completion*. doi:10.2118/105193-PA

Vandiver, J. K., Nicholson, J. W., & Shyu, R.-J. (1989, January 1). Case Studies of the Bending Vibration and Whirling Motion of Drill Collars. Society of Petroleum Engineers. doi:10.2118/18652-MS

Vandiver, K. J., Nicholson, J. W., & Shyu, R.-J. (1990, December 1). Case Studies of the Bending Vibration and whirling Motion of Drill Collars. Society of Petroleum Engineers. *SPE Drilling Engineering*. doi:10.2118/18652-PA

Vandiver, K.J. Engineering Dynamics (2011). Lecture 3: Motion of Center of Mass; Acceleration in Rotating Ref. Frames. MIT OpenCourseWare. Massachusetts, Fall 2011. Lecture.

Vogel, S. K., & Asker, J. (2010, January 1). Real Time Data Management And Information Transfer As An Effective Drilling Technique. Society of Petroleum Engineers. doi:10.2118/136296-MS

Warren, T. M., & Oster, J. H. (1998, January 1). Torsional Resonance of Drill Collars with PDC Bits in Hard Rock. Society of Petroleum Engineers. doi:10.2118/49204-MS

Whitfield, S. (2017, February 23). Artificial Intelligence Holds Promise for Seismic and Drilling Data. Journal of Petroleum Technology. Volume: 69,4.

Wolf, S. F., Zacksenhouse, M., & Arian, A. (1985, January 1). Field Measurements of Downhole Drillstring Vibrations. Society of Petroleum Engineers. doi:10.2118/14330-MS

Wu, A., & Hareland, G. (2012, January 1). Calculation of Friction Coefficient And Downhole Weight On Bit With Finite Element Analysis of Drillstring. American Rock Mechanics Association.

Zenero, N., and Behounek, M. (2016). Drilling to the limit: Operators Group for Data Quality aims to create common specifications. Drilling Contractor, May/June.

Zenero, N., Koneti, S., & Schnieder, W. (2016, March 1). Iron Roughneck Make Up Torque–It's Not What You Think! Society of Petroleum Engineers. doi:10.2118/178776-MS

Zhou, Y., Baumgartner, T., Saini, G., Ashok, P., van Oort, E., Isbell, M. R., & Trichel, D. K. (2017, March 14). Future Workforce Education through Big Data Analysis for Drilling Optimization. Society of Petroleum Engineers. doi:10.2118/184739-MS

Zhou, Y., Zheng, D., Ashok, P., & van Oort, E. (2016, March 1). Improved Wellbore Quality Using a Novel Real-Time Tortuosity Index. Society of Petroleum Engineers. doi:10.2118/178869-MS